



Publicly Accessible Penn Dissertations

---


Spring 2010

## Hydrogen Release From Ammonia Borane

Daniel W. Himmelberger

University of Pennsylvania, [hidaniel@sas.upenn.edu](mailto:hidaniel@sas.upenn.edu)

Follow this and additional works at: <https://repository.upenn.edu/edissertations>

 Part of the [Inorganic Chemistry Commons](#), [Oil, Gas, and Energy Commons](#), and the [Sustainability Commons](#)

---

### Recommended Citation

Himmelberger, Daniel W., "Hydrogen Release From Ammonia Borane" (2010). *Publicly Accessible Penn Dissertations*. 158.

<https://repository.upenn.edu/edissertations/158>

This paper is posted at ScholarlyCommons. <https://repository.upenn.edu/edissertations/158>  
For more information, please contact [repository@pobox.upenn.edu](mailto:repository@pobox.upenn.edu).

---

# Hydrogen Release From Ammonia Borane

## Abstract

Development of a safe and efficient storage medium for hydrogen is integral to its use as an alternative energy source. The overall goal of the studies described in this dissertation was to investigate the use of a chemical hydride, ammonia borane (AB (19.6 wt% H<sub>2</sub>)), as a potentially efficient material for hydrogen storage. The specific goals of this study were both to develop new efficient methods for increasing the rate and extent of H<sub>2</sub>-release from AB and to elucidate the important mechanistic pathways and intermediates in these reactions. Significant achievements that resulted from this work are that AB H<sub>2</sub>-release is activated in the presence of either ionic liquids or bases. For example, an AB H<sub>2</sub>-release reaction carried out at 110 °C in 50 wt% ionic liquid liberated over 2 equivalents H<sub>2</sub> in 15 minutes. Reducing ionic liquid loading to 20 wt% at 110 °C yielded a higher materials weight percent (11.4 mat wt%), while still having fast release rates: 2 equivalents in ~2.5 hours. The addition of the strong nitrogen base 1,8-bis(dimethylamino)naphthalene, Proton Sponge™, to ionic liquid solutions of AB increased the AB H<sub>2</sub>-release rate at 85 °C, with over 2 equivalents of H<sub>2</sub> achieved within 3 h. Additional Proton Sponge increased the rate of release; however, the mat wt% of H<sub>2</sub> decreased since the Proton Sponge added significant weight to the system. Solid state and solution <sup>11</sup>B NMR and DSC studies of reactions in progress allowed the identification of initial and final products in the H<sub>2</sub>-release reactions and helped elucidate the overall reaction pathway. The initial formation of diammoniate of diborane, the key intermediate in dehydropolymerization of ammonia borane, was promoted by the addition of ionic liquids. Subsequent H<sub>2</sub>-release resulted in the formation of polyaminoborane then polyborazylene. Proton Sponge increased the release rate of the second equivalent of H<sub>2</sub> by a newly proposed anionic polymerization mechanism. The final product was identified by solid-state <sup>11</sup>B NMR and proved to be a sp<sup>2</sup>-framework of polyborazylene which formed regardless of base additive or amount/type of ionic liquid.

## Degree Type

Dissertation

## Degree Name

Doctor of Philosophy (PhD)

## Graduate Group

Chemistry

## First Advisor

Dr. Larry G. Sneddon

## Keywords

ammonia borane, hydrogen, energy, fuel cell

## Subject Categories

Inorganic Chemistry | Oil, Gas, and Energy | Sustainability

# HYDROGEN RELEASE FROM AMMONIA BORANE

Daniel W. Himmelberger

A DISSERTATION

in

Chemistry

Presented to the Faculties of the University of Pennsylvania

in

Partial Fulfillment of the Requirements for the

Degree of Doctor of Philosophy

2010

Supervisor of Dissertation

---

Professor Larry G. Sneddon, Blanchard Professor of Chemistry

Graduate Group Chairperson

---

Professor Gary A. Molander, Hirschmann-Makineni Professor of Chemistry

Dissertation Committee

Professor Christopher B. Murray, Richard Perry University Professor of Chemistry

Professor So-Jung Park, Assistant Professor of Chemistry

Professor Bradford B. Wayland, Professor of Chemistry, Temple Univeristy

# ABSTRACT

## HYDROGEN RELEASE FROM AMMONIA BORANE

**Daniel W. Himmelberger**

Supervisor: Professor Larry G. Sneddon

Development of a safe and efficient storage medium for hydrogen is integral to its use as an alternative energy source. The overall goal of the studies described in this dissertation was to investigate the use of a chemical hydride, ammonia borane (AB (19.6 wt% H<sub>2</sub>)), as a potentially efficient material for hydrogen storage. The specific goals of this study were both to develop new efficient methods for increasing the rate and extent of H<sub>2</sub>-release from AB and to elucidate the important mechanistic pathways and intermediates in these reactions. Significant achievements that resulted from this work are that AB H<sub>2</sub>-release is activated in the presence of either ionic liquids or bases. For example, an AB H<sub>2</sub>-release reaction carried out at 110 °C in 50 wt% ionic liquid liberated over 2 equivalents H<sub>2</sub> in 15 minutes. Reducing ionic liquid loading to 20 wt% at 110 °C yielded a higher materials weight percent (11.4 mat-wt%), while still having fast release rates: 2 equivalents in ~2.5 hours. The addition of the strong nitrogen base 1,8-bis(dimethylamino)naphthalene, Proton Sponge™, to ionic liquid solutions of AB increased the AB H<sub>2</sub>-release rate at 85 °C, with over 2 equivalents of H<sub>2</sub> achieved within 3 h. Additional Proton Sponge increased the rate of release; however, the mat-wt% of H<sub>2</sub> decreased since the Proton Sponge added significant weight to the system. Solid state

and solution  $^{11}\text{B}$  NMR and DSC studies of reactions in progress allowed the identification of initial and final products in the  $\text{H}_2$ -release reactions and helped elucidate the overall reaction pathway. The initial formation of diammoniate of diborane, the key intermediate in dehydropolymerization of ammonia borane, was promoted by the addition of ionic liquids. Subsequent  $\text{H}_2$ -release resulted in the formation of polyaminoborane then polyborazylene. Proton Sponge increased the release rate of the second equivalent of  $\text{H}_2$  by a newly proposed anionic polymerization mechanism. The final product was identified by solid-state  $^{11}\text{B}$  NMR and proved to be a  $\text{sp}^2$ -framework of polyborazylene which formed regardless of base additive or amount/type of ionic liquid.

## Table of Contents

<b>Title Page</b>	i
<b>Abstract</b>	ii
<b>Table of Contents</b>	iv
<b>List of Tables</b>	ix
<b>List of Figures</b>	xi
<b>List of Equations</b>	xvi
<b>Chapter 1. The Hydrogen Economy: Benefits, Problems, and Possible Solutions</b>	
Summary	1
<b>1.1 We Use More than We Make!</b>	2
<b>1.2 Push for a Hydrogen Economy</b>	4
<b>1.2.1 Why Do We Need a Hydrogen Economy?</b>	4
<b>1.2.2 What are the Barriers to a Hydrogen Economy?</b>	5
<b>1.2.2.1 Hydrogen Production</b>	6
<b>1.2.2.2 Hydrogen Delivery</b>	6
<b>1.2.2.3 Hydrogen Storage</b>	7
<b>1.2.3 The Chemical Hydrogen Storage Center of Excellence</b>	9
<b>1.3 What is Ammonia Borane?</b>	11
<b>1.3.1 How to Release Hydrogen from Ammonia Borane?</b>	17
<b>1.3.1.1 Utilizing Hydrolysis to Release Hydrogen.</b>	18

<b>1.3.1.2</b>	The Better Hydrogen Release Method: Thermolysis.	18
<b>1.3.2</b>	Ammonia Borane Solid-State H <sub>2</sub> -Release	19
<b>1.3.3</b>	Activated AB H <sub>2</sub> -Release from AB	23
<b>1.3.3.1</b>	Mesoporous Scaffolds Aid in Solid-State H <sub>2</sub> -Release	23
<b>1.3.3.2</b>	Acid Catalyzed Hydrogen Release Reactions	24
<b>1.3.3.3</b>	Using Transition-Metal Catalysis to Enhance Release Rate and Extent.	26
<b>1.3.3.3.1</b>	Heterogeneous Transition-Metal Catalysts	26
<b>1.3.3.3.2</b>	Homogeneous Transition-Metal Catalysts	28
<b>1.3.3.3.2.1</b>	Iridium Pincer Catalyst	28
<b>1.3.3.3.2.2</b>	Nickel Carbene Catalyst	31
<b>1.3.3.3.2.3</b>	Titanocene Catalyst	35
<b>1.3.3.3.2.4</b>	Transition-Metal Catalysis in Hydrolysis/Methanolysis	37
<b>1.3.4</b>	Large Scale Preparations of Ammonia Borane.	38
<b>1.3.5</b>	Recycling the AB Fuel Source.	39
<b>1.3.6</b>	Hybrid Materials Try to Bridge the Gap Between AB and Metal Hydrides.	40
<b>1.4</b>	Conclusions	42
<b>1.5</b>	References	43

## Chapter 2. Ammonia Borane Hydrogen Release in Ionic Liquids

Summary	51
2.1 Introduction	52
2.2 Experimental Section	53
2.2.1 Materials	53
2.2.2 Physical Measurements	53
2.2.2.1 H <sub>2</sub> -Release Measured On a Toepler Pump	53
2.2.2.2 H <sub>2</sub> -Release Measured On an Automated Gas Burette	54
2.2.2.3 Procedures for <sup>11</sup> B NMR Studies of Reaction Products	76
2.3 Results and Discussion	77
2.3.1 Why Use Ionic Liquids?	77
2.3.2 Procedures for AB H <sub>2</sub> -release reactions	80
2.3.3 Solid-State vs. Ionic Liquid H <sub>2</sub> -Release	81
2.3.4 <sup>11</sup> B NMR Characterization of Reaction Products and Pathways	93
2.3.4.1 <sup>11</sup> B NMR of Pyridine Extracts from Reaction Products	93
2.3.4.2 Solid-State <sup>11</sup> B NMR Studies	96
2.3.4.3 <i>In Situ</i> <sup>11</sup> B NMR Studies in Ionic Liquids	96
2.3.6 Why do Ionic Liquids Accelerate AB H <sub>2</sub> -release? What is the Role of DADB?	103



<b>2.3.7</b> H <sub>2</sub> -Release Reactions in Tetraglyme	108
<b>2.4</b> Conclusions	111
<b>2.5</b> References	112
<b>Chapter 3.</b> Base Promoted Ammonia Borane Hydrogen Release	
Summary	116
<b>3.1</b> Introduction	117
<b>3.2</b> Experimental Section	119
<b>3.2.1</b> Materials	119
<b>3.2.2</b> Physical Measurements	119
<b>3.2.3</b> Procedures for AB H <sub>2</sub> -Release Reactions	121
<b>3.2.4</b> Computational Methods	122
<b>3.3</b> Results and Discussion	126
<b>3.3.1</b> H <sub>2</sub> -Release from AB/PS Solid-State Reactions	126
<b>3.3.2</b> H <sub>2</sub> -Release from AB/PS Solution Reactions	132
<b>3.3.2.1</b> Initial Reactions Measured with the Toepler Pump	132
<b>3.3.2.2</b> H <sub>2</sub> -Release Reactions Measured with the Automated Gas Burette	136
<b>3.3.3</b> <sup>11</sup> B NMR Studies of Reaction Pathways and Intermediates	141
<b>3.3.3.1</b> Solid-State <sup>11</sup> B NMR Studies	141
<b>3.3.3.2</b> <i>In Situ</i> <sup>11</sup> B NMR Studies of Reaction Progress in Ionic Liquids	144

<b>3.3.4</b>	<b>Proton Sponge Reduces Foaming During AB Thermolysis</b>	146
<b>3.3.5</b>	<b>H<sub>2</sub>-Release in Other Ionic Liquids and Tetraglyme</b>	147
<b>3.3.6</b>	<b>Why Does Proton Sponge Induce H<sub>2</sub>-Release from AB?</b>	151
<b>3.4</b>	<b>Conclusions</b>	158
<b>3.5</b>	<b>References</b>	159

## List of Tables

### Chapter 2

<b>Table 2.1</b> AB H <sub>2</sub> -Release Data Collected on the Automated Gas Burette from the H <sub>2</sub> -Release Reaction of a Solid-State AB Sample at 85 °C	57
<b>Table 2.2</b> Times to Selected Equivalent Points of H <sub>2</sub> -Release (Gas Burette) of Ionic Liquid and Solid-State Reactions at 85 °C	83
<b>Table 2.3</b> Times to Selected Equivalent Points of H <sub>2</sub> -Release (Gas Burette) of 50-wt% AB (150 mg) in BmimCl (150 mg) at Different Temperatures	85
<b>Table 2.4</b> Times to Selected Equivalent Points of H <sub>2</sub> -Release (Gas Burette) of AB (150 mg) in 20.2-wt% BmimCl (38 mg) at Different Temperatures	87
<b>Table 2.5</b> H <sub>2</sub> -Release Data (Toepler pump) for AB/Ionic-Liquid (50-wt%) Reactions at 85 °C	88
<b>Table 2.6</b> H <sub>2</sub> -Release Data (Toepler pump) for AB/Ionic-Liquid (50-wt%) Reactions at 65 and 45 °C	91
<b>Table 2.7</b> Times to Selected Equivalent Points of H <sub>2</sub> -Release (Gas Burette) of bmimOTf (450 mg) and 10-wt% (50 mg) each of: (A) DADB and (B) AB at 85 °C	105
<b>Table 2.8</b> Times to Selected Equivalent Points of H <sub>2</sub> -Release (Gas Burette) of 50-wt% AB (150 mg) in Tetraglyme (150 mg) at Different Temperatures	109

### Chapter 3

<b>Table 3.1</b> Cartesian Coordinates for [H <sub>3</sub> BNH <sub>2</sub> ] <sup>-</sup>	123
<b>Table 3.2</b> Cartesian Coordinates for Straight Chain [H <sub>3</sub> BNH <sub>2</sub> BH <sub>2</sub> NH <sub>2</sub> BH <sub>2</sub> NH <sub>2</sub> BH <sub>2</sub> NH <sub>2</sub> ] <sup>-</sup>	123

<b>Table 3.3</b> Cartesian Coordinates for Branched Chain	124
$[\text{HB}(\text{NH}_2\text{BH}_3)_2\text{NH}_2\text{BH}_2\text{NH}_2]^-$	
<b>Table 3.4</b> Cartesian Coordinates for Branched Chain	125
$[\text{H}_3\text{BNH}_2\text{BH}_2(\text{BH}_2\text{NH}_3)\text{NHBH}_2\text{NH}_2]^-$	
<b>Table 3.5</b> Cartesian Coordinates for $[\text{H}_3\text{BNH}_2\text{BH}_2\text{NH}_2\text{BEt}_3]^-$	125
<b>Table 3.6</b> H <sub>2</sub> -Release Data (Toepler pump) for AB/PS Solid-State Reactions at 85 °C	129
<b>Table 3.7</b> H <sub>2</sub> -Release Data (gas burette) for AB/PS Solid-State Reactions at 85 °C	129
<b>Table 3.8</b> H <sub>2</sub> -Release Data (Toepler pump) for AB/BmimCl/PS Reactions at 85 °C	133
<b>Table 3.9</b> H <sub>2</sub> -Release Data (gas burette) for AB/bmimCl/PS Reactions	137
<b>Table 3.10</b> H <sub>2</sub> -Release (Toepler pump) Data for Partially Dehydrogenated AB	140
<b>Table 3.11</b> H <sub>2</sub> -Release Data (Toepler pump) for AB/Ionic-Liquid/PS Reactions at 85 °C	148
<b>Table 3.12</b> H <sub>2</sub> -Release Data (gas burette) for AB/Tetraglyme/PS Reactions at 85 °C	149

## List of Figures

### Chapter 1

<b>Figure 1.1</b>	Energy demand by sector and supply by source for 2008.	3
<b>Figure 1.2</b>	Simple schematic diagram of a PEM fuel cell.	4
<b>Figure 1.3</b>	Total system targets from DOE Center of Excellence.	9
<b>Figure 1.4</b>	Select amine boranes discussed in the following Chapters.	11
<b>Figure 1.5</b>	Low temperature (orthorhombic) crystal structure of AB. Nitrogen, boron, and hydrogen atoms are depicted in blue, purple, and gray, respectively.	12
<b>Figure 1.6</b>	Schematic energy profile of the conversion of 2 AB to DADB.	15
<b>Figure 1.7</b>	Schematic energy profile of the dehydrogenation of DADB.	17
<b>Figure 1.8</b>	Comparison of thermogravimetric and volumetric data at 5 K/min of AB thermolysis.	20
<b>Figure 1.9</b>	Solid-State hydrogen release data for AB at 85 and 95 °C.	20
<b>Figure 1.10</b>	$^{11}\text{B}$ NMR (128.4 MHz) spectra recorded at 20 °C. Pyridine extract of a solid-state AB reaction at 85 °C after 19 h with 0.83 equivalents of $\text{H}_2$ -released.	22
<b>Figure 1.11</b>	DFT/GIAO calculated $^{11}\text{B}$ NMR shifts for possible dehydropolymerization products.	23
<b>Figure 1.12</b>	Baker's nickel carbene catalyst with $^{11}\text{B}$ NMR showing final products.	32
<b>Figure 1.13</b>	Schematic energy profile of the nickel carbene catalyst using the carbene as a proton abstractor.	33
<b>Figure 1.14</b>	Schematic energy profile for free carbene abstracting $\text{H}_2$ from AB.	34

## Chapter 2

- Figure 2.1** Toepler pump system used for H<sub>2</sub>-release measurements. 54
- Figure 2.2** Automated gas burette used for H<sub>2</sub>-release measurements. 55
- Figure 2.3** Structures of ionic liquids used in these studies. 80
- Figure 2.4** H<sub>2</sub>-release measurements (gas burette) at 85 °C of: (A) 50-wt% AB (150 mg) in bmimCl (150 mg,) and (B) solid-state AB (150 mg). 82
- Figure 2.5** H<sub>2</sub>-release measurements (gas burette) of 50-wt% AB (150 mg) in bmimCl (150 mg) at various temperatures. 85
- Figure 2.6** H<sub>2</sub>-release measurements (gas burette) of AB (150 mg) in 20.2-wt% bmimCl (38 mg) at various temperatures. 86
- Figure 2.7** H<sub>2</sub>-release measurements (Toepler pump) of the reaction of 50-wt% AB (250 mg) at 85 °C in 250 mg of with various ionic liquids. 88
- Figure 2.8** H<sub>2</sub>-release measurements (Toepler pump) of the reaction of 50-wt% AB (250 mg) in 250 mg of various ionic liquids at (a) 65 °C and (b) 45 °C. 90
- Figure 2.9** Above: Solution <sup>11</sup>B NMR (128.4 MHz) spectra of the residues (extracted in pyridine) of the 85 °C reaction of solid-state and ionic liquids with AB. 94
- Figure 2.10** Solid-state <sup>11</sup>B NMR (240 MHz) spectra recorded at 25 °C of the reaction of 50-wt% AB (150 mg) in bmimCl (150 mg) at 110 °C. 95
- Figure 2.11** Solution <sup>11</sup>B NMR (128.4 MHz) spectra recorded at 25 °C of the reaction of 10-wt% AB (50 mg) in bmimOTf (450 mg) at 85 °C. 98

<b>Figure 2.12</b> 1,3-dimethylimidazolium hexafluorophosphate with 0.5 mol benzene included as a clathrate.	99
<b>Figure 2.13</b> Solution $^{11}\text{B}$ NMR (128.4 MHz) of the reaction of 10-wt% AB (50 mg) in bmimOTf (450 mg) at 85 °C for 6 h at various temperatures	101
<b>Figure 2.14</b> Solution $^{11}\text{B}$ NMR (128.4 MHz) spectra recorded at 25 °C of 10-wt% borazine (50 mg) in bmimI (450 mg) after at various times.	102
<b>Figure 2.15</b> $\text{H}_2$ -release measurements (gas burette) of bmimOTf (450 mg) and 10-wt% (50 mg) of DADB and AB.	105
<b>Figure 2.16</b> Solution $^{11}\text{B}$ NMR (128.4 MHz) spectra recorded at 25 °C of the reaction of 10-wt% DADB (50 mg) in bmimOTf (450 mg) at 85 °C.	106
<b>Figure 2.17</b> Possible pathway for ionic-liquid promoted $\text{H}_2$ -release from AB.	107
<b>Figure 2.18</b> $\text{H}_2$ -release measurements (gas burette) of 50-wt% AB (150 mg) in tetraglyme (150 mg) at various temperatures.	109
<b>Figure 2.19</b> Solution $^{11}\text{B}\{^1\text{H}\}$ NMR (128 MHz) spectra recorded at 80 °C of the reaction of 10-wt% AB (50 mg) in tetraglyme (450 mg) at 85 °C.	110
<b>Chapter 3</b>	
<b>Figure 3.1</b> $\text{H}_2$ -release measurements for solid state AB reactions with Proton Sponge at 85 °C using the Toepler pump and gas burette.	128
<b>Figure 3.2</b> $^{11}\text{B}\{^1\text{H}\}$ NMR (128.4 MHz) spectra recorded at 25 °C of the glyme extract of the reaction of solid-state AB with and without Proton Sponge.	130

<b>Figure 3.3</b> Solid-state $^{11}\text{B}$ NMR (240 MHz) spectra recorded at 25 °C of the reaction of solid-state AB reactions with and without Proton Sponge after 1 equivalent was released.	131
<b>Figure 3.4</b> $\text{H}_2$ -release measurements (Toepler pump) of the reaction of AB in bmimCl with Proton Sponge at 85 °C.	132
<b>Figure 3.5</b> Differential Scanning Calorimetry analyses of the reactions of AB in bmimCl with Proton Sponge at various temperatures.	135
<b>Figure 3.6</b> $\text{H}_2$ -release measurements (gas burette) of the reaction of AB in bmimCl with Proton Sponge at various temperatures.	138
<b>Figure 3.7</b> $\text{H}_2$ -release measurements (gas burette) of partially dehydrogenated AB where 1 $\text{H}_2$ -equivalent was initially released at 85 °C, then bmimCl and bmimCl/Proton Sponge were added to separate samples and heating resumed at 85 °C.	139
<b>Figure 3.8</b> Solid-state $^{11}\text{B}$ NMR (240 MHz) spectra recorded at 25 °C of the reaction of AB and Proton Sponge in bmimCl at 85 °C.	142
<b>Figure 3.9</b> DFT optimized geometries (B3LYP/6-31G(d)) and GIAO calculated (B3LYP/6-311G(d)) $^{11}\text{B}$ NMR chemical shifts.	143
<b>Figure 3.10</b> Solid-state $^{11}\text{B}$ NMR (240 MHz) spectrum recorded at 25 °C of the reaction of AB and Proton Sponge in bmimCl at 85 °C for 23 h.	144
<b>Figure 3.11</b> Solution $^{11}\text{B}$ NMR (128 MHz) spectra recorded at 25 °C of the reaction of AB in mmimMeSO <sub>4</sub> at 85 °C with and without Proton Sponge.	145



<b>Figure 3.12</b>	Foaming resulting from the reaction of 250 mg AB in 250 mg bmimCl after 1 h at 100 °C with and without Proton Sponge.	146
<b>Figure 3.13</b>	H <sub>2</sub> -release measurements (Toepler pump) of the reaction of AB in ionic liquids or tetraglyme with Proton Sponge at 85 °C.	147
<b>Figure 3.14</b>	Solution <sup>11</sup> B{ <sup>1</sup> H} NMR (128 MHz) spectra recorded at 80 °C of the reaction of AB and Proton Sponge in tetraglyme at 85 °C.	150
<b>Figure 3.15</b>	Selected bond distances (Å) and angles (°) for [Et <sub>3</sub> BNH <sub>2</sub> BH <sub>3</sub> ] <sup>-</sup> K <sup>+</sup> •18-crown-6.	153
<b>Figure 3.16</b>	Possible anionic polymerization pathway for PS-promoted H <sub>2</sub> -release from AB.	155
<b>Figure 3.17</b>	DFT (B3LYP/6-31G(d)) optimized geometry and GIAO (B3LYP/6-311G(d)) calculated <sup>11</sup> B NMR shifts for [Et <sub>3</sub> BNH <sub>2</sub> BH <sub>2</sub> NH <sub>2</sub> BH <sub>3</sub> ] <sup>-</sup> .	157

## List of Equations

### Chapter 1

1.1 Fuel cell half reactions	5
1.2 Methane reforming for H <sub>2</sub> production	6
1.3 Ammonia borane hydrolysis	18
1.4 Ammonia triborane hydrolysis	18
1.5 Ammonia borane thermolysis	19
1.6 Acid catalyzed AB H <sub>2</sub> -release mechanism	25
1.7 Colloidal rhodium catalyzed AB H <sub>2</sub> -release mechanism	27
1.8 Generic homogeneous catalyzed AB H <sub>2</sub> -release mechanism	29
1.9 Iridium pincer catalyzed AB H <sub>2</sub> -release using 16 e <sup>-</sup> mechanism	30
1.10 Difference between iridium and other homogenous catalyst mechanisms	31
1.11 Nickel carbene catalyzed AB H <sub>2</sub> -release mechanism	35
1.12 Calculated titanocene catalyzed AB H <sub>2</sub> -release mechanism	36
1.13 Experimentally predicted Titanocene catalyzed AB H <sub>2</sub> -release mechanism	37
1.14 Ammonia borane production from NaBH <sub>4</sub> and (NH <sub>4</sub> ) <sub>2</sub> SO <sub>4</sub>	38
1.15 Ammonium borohydride production from NaBH <sub>4</sub> and NH <sub>4</sub> Cl	38
1.16 Decomposition ammonium borohydride to form ammonia borane	38
1.17 Spent fuel regeneration scheme	39

### Chapter 2

2.1 Ammonia borane thermolysis	52
2.2 Ammonia borane dimerization into ionic intermediate the diammoniate of	103

diborane	
<b>2.3</b> Thermolytic H <sub>2</sub> -release from diammoniate of diborane	103
<b>Chapter 3</b>	
<b>3.1</b> Ammonia borane dehydrogenated with lithium amide	117
<b>3.2</b> Ammonia borane dehydrogenated with lithium hydride	117
<b>3.3</b> Lithium amidoborane undergoing dehydropolymerization with ammonia borane	118
<b>3.4</b> Lithium amidoborane decomposition into aminoborane	118
<b>3.5</b> Formation of side-product lithium borohydride	118
<b>3.6</b> Proton Sponge protonation	151
<b>3.7</b> Ammonia borane studies with lithium and potassium triethylborohydride	152
<b>3.8</b> Ammonia borane chain growth studies with lithium and potassium triethylborohydride	156

## Chapter 1

### The Hydrogen Economy: Benefits, Problems, and Possible Solutions

#### Summary

The overall goal of the studies described in this dissertation was to investigate the use of a chemical hydride, ammonia borane (AB), as a potentially efficient material for hydrogen storage. The specific goals of this study were both to develop new efficient methods for increasing the rate and extent of H<sub>2</sub>-release from AB and to elucidate the important mechanistic pathways and intermediates in these reactions. **Chapter 1** discusses the need for a chemical hydrogen storage system, and more generally, the need for a paradigm shift from hydrocarbons to a hydrogen economy. **Chapter 2** demonstrates that AB/ionic liquid based H<sub>2</sub>-release systems show increased activity for H<sub>2</sub>-release compared to neat AB. Furthermore, it is also shown that these reactions can be tuned by using various ionic liquids, temperatures, and loading ratios. In **Chapter 3**, base catalyzed reactions, using primarily 1,8-bis(dimethylamino)naphthalene, Proton Sponge (PS), are also shown to enhance release rates and reduce reaction foaming (a common AB thermolysis problem) in both solid state and systems solvated by ionic liquids.

## 1.1 We Use More than We Make!

As discussed in the 2008 Annual Energy Review generated by the Department of Energy,<sup>1</sup> worldwide consumption of energy continues to rise while global production of energy struggles to keep pace. In the United States, most of the energy consumed is used in the form of electric power. However, the second largest consumption sector is transportation at 27.8% in 2008. Energy sources used for transportation include, petroleum, natural gas, and biofuels, but 95% of the consumed energy is from petroleum. Domestic production has not been able to keep up with demand for decades; production of crude oil has slowly declined since its peak in 1970. Therefore, importation of petroleum has increased to keep pace with consumption demands. The United States currently imports (12.9 million barrels per day) twice the petroleum it produces (6.7 million barrels per day).

Looking at the breakdown of petroleum consumption in the United States, most is used in the transportation sector (71%, **Figure 1.1**), and of that most petroleum is used for light vehicles (i.e. cars and light trucks).<sup>1</sup> Oil reserves will inevitably run out and fuel prices will continue to rise. To match current and future energy needs, a new energy carrier is needed. Additional reasons for phasing out the use of petroleum as a transportation energy carrier are the negative effects of global warming caused by the CO<sub>2</sub> produced by petroleum combustion and the danger to United States national security caused by having an unstable foreign energy supply. As discussed in the next section, utilization of hydrogen as a substitute for petroleum has many benefits particularly when used with fuel cells, a rapidly developing technology.

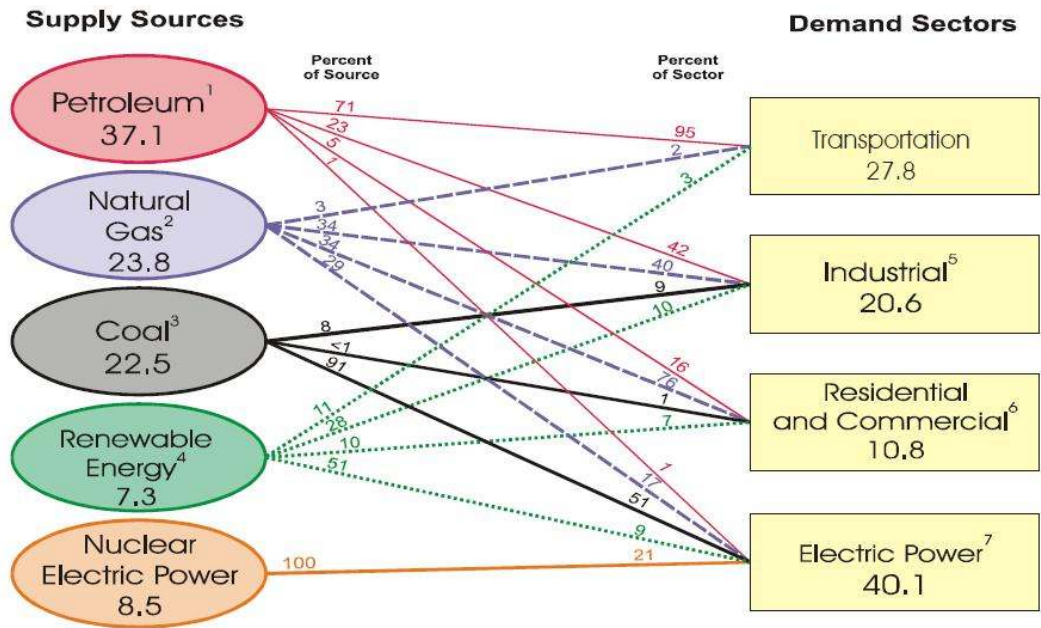


**Figure 1.1** Energy demand by sector and supply by source for 2008.<sup>1</sup>

## 1.2 Push for a Hydrogen Economy

### 1.2.1 Why Do We Need a Hydrogen Economy?

In 2003, President George W. Bush announced the hydrogen fuel initiative that had as its goals the development of new technology for the production, storage, and distribution of hydrogen. The ultimate goal was to make fuel cell powered cars competitive by 2020. In order to accomplish this goal, the hydrogen economy must be as good, if not better, than the current hydrocarbon based energy economy. Hydrogen as an energy carrier has many benefits, the biggest being as a fuel source for fuel cells.

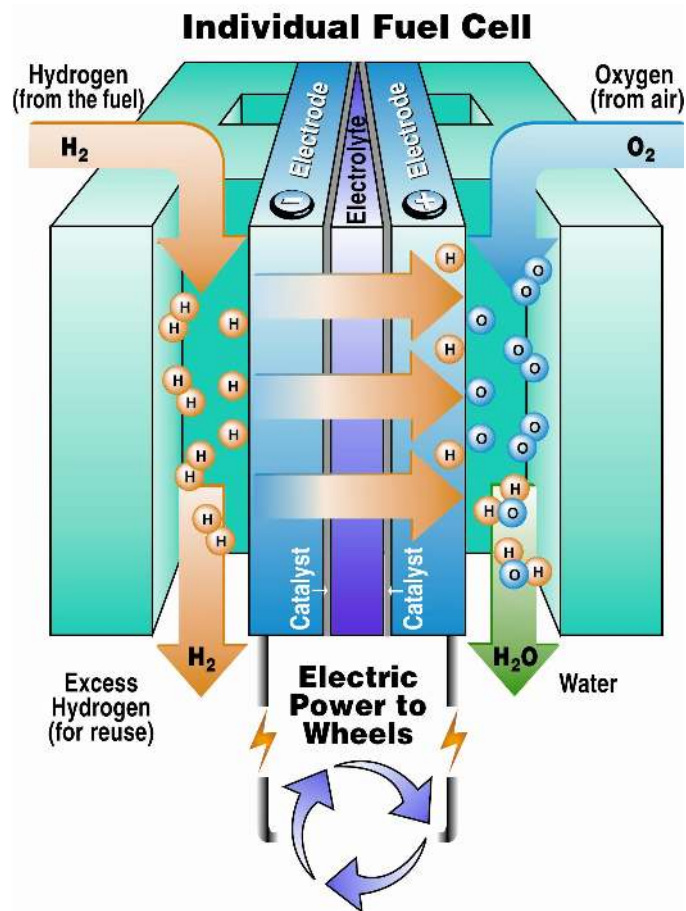
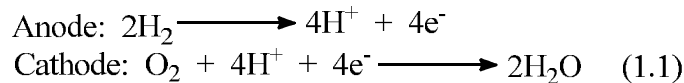


**Figure 1.2** Simple schematic diagram of a PEM fuel cell.<sup>2</sup>

A Proton Exchange Membrane (PEM) fuel cell (**Figure 1.2**) operates by oxidizing molecular hydrogen and allowing the protons to migrate through the membrane while the electrons are shuttled out to do work by the catalytic electrodes. The protons recombine on the other side of the membrane with reduced molecular oxygen, typically from the air, to form water,<sup>3</sup> as shown in the half reactions in **Equation 1.1**.



Fuel cells have two to three times the efficiency of internal combustion engines and can be designed to power a broad spectrum of sizes of applications from a watch to a building. Additionally, the only product from fuel cells when using hydrogen as a fuel is water.

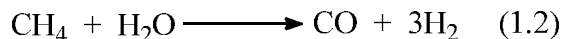
### **1.2.2 What are the Barriers to a Hydrogen Economy?**

There are many barriers to implementing a hydrogen economy. The biggest overarching difficulty is in replacing an energy system that has been in place for one hundred years. Gasoline is an excellent energy carrier. It has a high energy density, it is easy to transport and handle, and is inexpensive for now. Gasoline has the added benefit of one hundred years of optimization and infrastructure that hydrogen will have to overcome. It is difficult to expect hydrogen to replace this type of system in a short period of time (a few decades), but that is exactly what is expected. The difficulties in implementing a hydrogen economy can be broken down into three areas: hydrogen production, hydrogen delivery, and hydrogen storage.



### 1.2.2.1 Hydrogen Production

Most hydrogen (95%) is currently produced from natural gas reforming via high temperature steam. The generic reaction is given in **Equation 1.2** where steam at temperatures from 700 °C to 1000 °C is used to split the methane into carbon monoxide and hydrogen.<sup>4</sup>



If hydrogen is produced from hydrocarbons or other fossil fuels like coal, then we are still: relying on foreign sources, quickly depleting hydrocarbon fuel sources, and producing large amounts of carbon monoxide. Other production methods are necessary in order to create an environmentally friendly, secure hydrogen energy supply. Biomass or water electrolysis using electricity from nuclear or renewable sources, such as wind and photovoltaics, must be employed to efficiently produce the hydrogen to make the hydrogen economy viable. While these sources are still being developed, a great deal of progress has recently been made especially in the area of water splitting. The Nocera lab has been a leader in developing self-regenerative water-splitting catalysts.<sup>5</sup> These types of new technologies are necessary to make the implementation of a hydrogen economy possible.

### 1.2.2.2 Hydrogen Delivery

The problems with delivery center around what sort of infrastructure for hydrogen delivery would be needed. The existing pipelines used for moving petroleum do not work for gases. In theory, with renewable sources producing hydrogen, local fuel stations or even individuals could produce their own hydrogen. However, depending on the hydrogen storage method used in vehicles, central processing plants maybe needed

and therefore transportation of gas or solid fuels would be necessary. The type of delivery system is heavily dependent on the storage method used.

### **1.2.2.3 Hydrogen Storage**

The Department of Energy (DOE) originally setup a series of metrics<sup>2</sup> that hydrogen would have to meet or exceed for it to become economically viable as a gasoline equivalent. These goals included the need for the fuel cell vehicle to have greater than a 300 mile range, with the fuel delivered at an equivalent cost to gasoline, as well as durability of the fuel cell and the over all system. Important requirements for hydrogen-based systems are that they operate over the wide variety of environments in which gasoline operates. Fuel cell systems must work in -20 °C temperatures and survive -40 °C, while not breaking down at temperatures that exceed 50 °C.

There are three main methods currently being explored for storing hydrogen for transportation purposes. The first utilizes high pressure storage tanks. Tanks have a large number of benefits. Simplicity in the overall system is the biggest benefit. Using a high pressure tank delivery system in the vehicle is much simpler since the fuel is stored in the form in which it is ultimately consumed and the fuel can be transferred in the same form. There are of course drawbacks to this approach mainly due to the pressure required to make these tanks practical. For instance, a 5000 psi fuel tank holding 3.92 kg of hydrogen only gives the Honda Clarity a 240 mile range,<sup>6</sup> which is well short of the goal set by the DOE and much worse than comparable gasoline vehicles. Higher ranges are possible only with higher pressures because hydrogen gas has a low energy density. This creates a problem with current tank design and has a direct impact on safety of these

systems. The higher the pressure being stored, the more dangerous tank imperfections are. Likewise the durability of the tanks in vehicular collisions is a real danger.

A second method for storing hydrogen is in the liquid phase which gives much lower pressures for storage, as well as a higher energy density. To compare compressed gas versus liquid hydrogen; a 10,000 psi tank of compressed hydrogen has a hydrogen density of  $\sim 56 \text{ kg/m}^3$ , whereas the same volume tank of liquid hydrogen would only be  $\sim 670 \text{ psi}$  with a density of  $\sim 68 \text{ kg/m}^3$ . However, this technology is impractical due to the higher energy costs necessary to liquefy hydrogen and the cryogenic tanks necessary to maintain it as a liquid. For these reasons, the energy input is greater than the efficiency gained by a higher energy density.

The third storage method is to utilize materials and compounds, that is, chemical hydrides, for storage. Chemical hydrides can have a higher energy density for  $\text{H}_2$  storage than can be achieved by either gas or liquid hydrogen tank systems to store the hydrogen. Under this umbrella term 'materials' there are three subcategories; reversible metal hydrides, carbon adsorption materials, and chemical hydrogen storage. Some examples of metal hydrides include materials such as lithium aluminum hydride and lithium hydride.<sup>7-18</sup> Carbon nanotubes and metal-organic frameworks have been the focal points of carbon-based storage systems.<sup>19-29</sup> Because of their high material weight percents, chemical hydrogen storage has focused mainly on boron hydrides, including compounds such as sodium borohydride, ammonium borohydride, and ammonia borane (AB).

### 1.2.3 The Chemical Hydrogen Storage Center of Excellence

In order to comprehensively investigate the three materials-based storage methods, the DOE setup Centers' of Excellence to work on each of these materials. As summarized in **Figure 1.3**, the DOE set specific goals, the main one being total system weight percent of 9.0 % by 2015.<sup>2</sup> To clarify, the **total system weight percent** is the weight of hydrogen produced, divided by the weight of the fuel system including tanks, heaters, tubing, release compound and solvents. On the other hand, **materials weight percent**, is just the weight of hydrogen released divided by the weight of the compound system (including possible solvent and catalyst) doing the release. To achieve a target total system weight percent, the material weight percent must be much higher so that additional weight for tanks, etc. can be factored in. Other goals such as volumetric density, flow rate, and initial rate also have metrics set by the DOE. All of these goals were set based on the needs of fuel cells powering a vehicle for a 300 mile range and that the H<sub>2</sub>-storage container should not be significantly larger than the existing gasoline tank.

Target	2015
	<i>old</i>
System Gravimetric Density [wt.%] (kWh/kg)	[9] (3.0)
System Volumetric Density [g/L] (kWh/L)	[81] (2.7)
System fill time for 5-kg fill [min] (kgH <sub>2</sub> /min)	[2.5] (2.0)
System cost [\$/kgH <sub>2</sub> ] (\$/kWh <sub>net</sub> )	[67] (2)

**Figure 1.3** Total system targets from DOE Center of Excellence.<sup>2</sup>

To achieve these goals, the Center for Chemical Hydrogen Storage brought together a diverse group of partners. The Center combined computational and synthetic expertise from academics: UCLA, Univ. of Pennsylvania, Univ. of Alabama, Univ. of Washington, Penn State, UC Davis, and Northern Arizona University. Analytical and computational resources were drawn from national labs such as Pacific Northwest National Laboratories and Los Alamos National Laboratories. Scale up and economic experience was taken from industrial companies Borax, Millennium Cell, Rohm and Haas, and Intematix. Therefore, the Center as a whole had a wide range of technical expertise. Conference calls and collaborations as well as periodic progress reports and an annual review provided the coordination of the efforts.

### 1.3 What is Ammonia Borane?

After the initial 2003 Hydrogen initiative was announced, amine boranes were identified as an excellent hydrogen storage material candidate. Amine boranes' high hydrogen densities, for example 24.5 materials weight percent (mat. wt.%) for ammonium borohydride, 19.6 mat. wt% for AB, and 17.8 mat. wt.% for ammonia triborane, were the primary attribute that made these materials attractive. The structures and abbreviations of the compounds are shown in **Figure 1.4**. The other attractive property of amine boranes comes from the different electronegativities of B(2.04) and N(3.04) that result in protonic N-H and hydridic B-H hydrogens. Thus, the elimination of H<sub>2</sub> by the reaction of B-H<sup>-</sup> and N-H<sup>+</sup> is favorable.

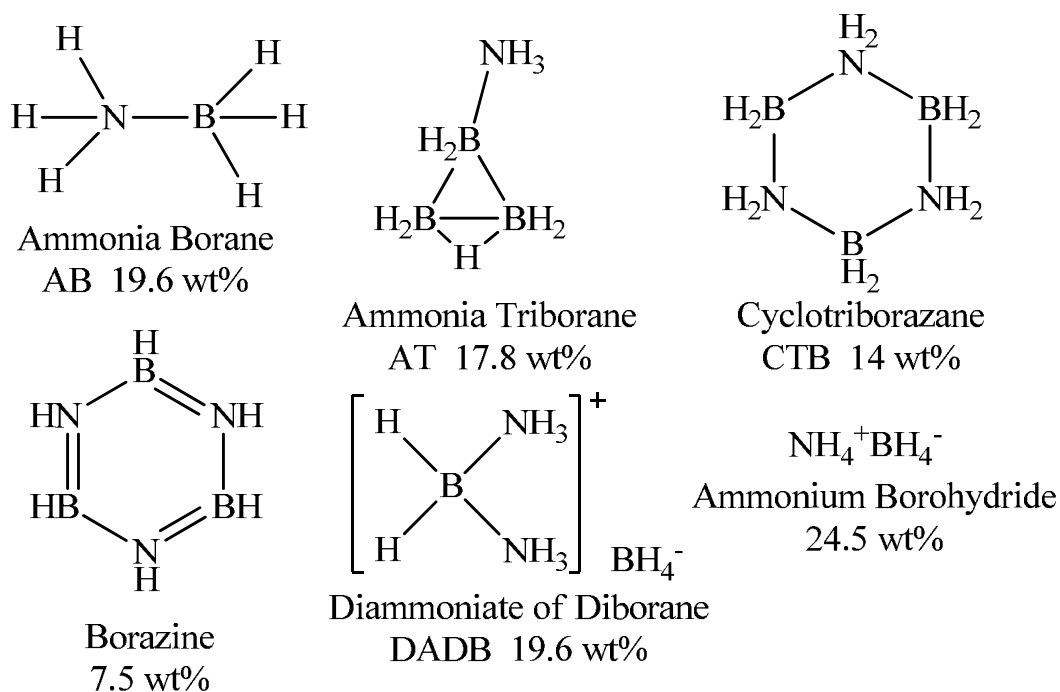


**Figure 1.4** Select amine boranes discussed in the following **Chapters**.

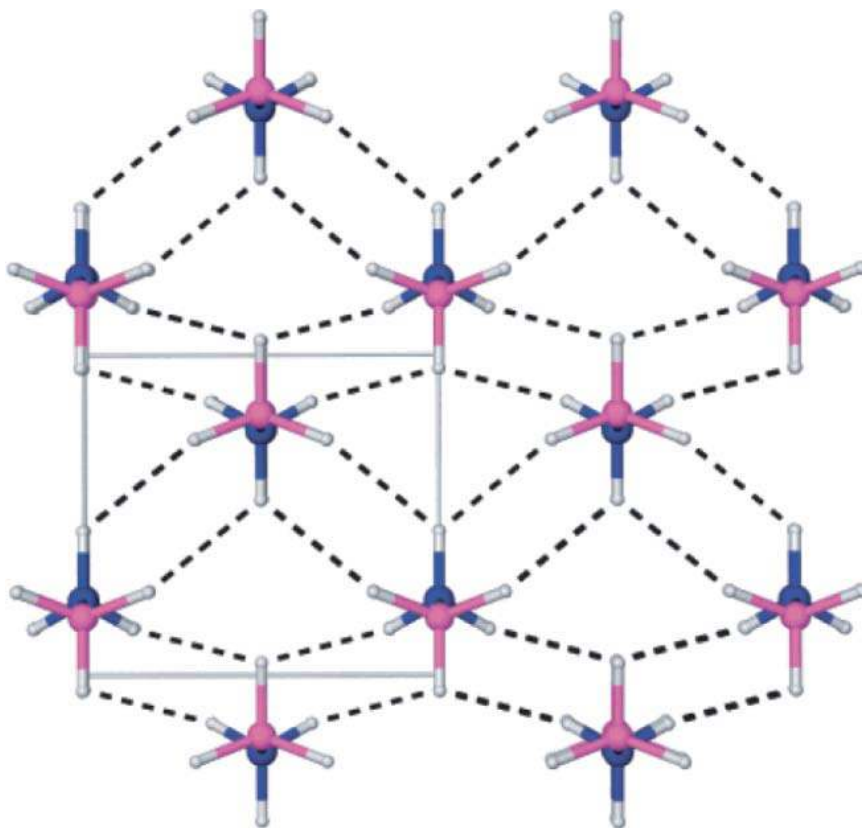


**Figure 1.5** Low temperature (orthorhombic) crystal structure of AB. Nitrogen, boron, and hydrogen atoms are depicted in blue, purple, and gray, respectively.<sup>30</sup>

Within the amine borane class of compounds, AB was quickly identified as the best overall candidate due to its high materials weight percent (19.6 %), as well as its stability and non-toxicity. The first group to work on ammonia borane and the ionic dimer diammoniate of diborane (DADB) was Alfred Stock, who reported the formation of these compounds in 1925.<sup>31</sup> The Schlesinger group in the 1930s initially proposed incorrect structures for DADB and AB based on incorrect molecular weight measurements.<sup>13</sup> Crystalline AB was synthesized by Parry and Shore in 1955 and purified from DADB using AB's ether solubility. They also collected the first definite

X-ray powder diffraction of AB.<sup>32</sup> The correct structures of AB and DADB were elucidated in a series of papers by Parry and Shore in 1958.<sup>33</sup> Work continued in these groups through the 1960s further defining the properties.

Ammonia borane is a colorless solid that melts at 110 °C – 114 °C, but is stable at room temperature. There are several methods of producing AB that will be discussed in section 1.3.4. It is soluble in a variety of polar solvents, including ammonia (260 g/ 100 g solvent), water (33.6 g/ 100 g solvent), and tetrahydrofuran (25 g/ 100 g solvent). Both X-ray and neutron diffraction studies have been used to determine the solid-state structure of AB. AB has a staggered conformation with a B-N bond distance of 1.564(6) Å. The gas phase calculations determined the B-N bond distance to be 1.6722(5) Å. Solid-state AB shows close BH---HN distances of 2.02 Å on adjacent molecules which is inside the Van der Waals distance of 2.4 Å indicating strong dihydrogen bonds (**Figure 1.5**). Due to the dihydrogen bonding, a stabilization energy of 90.4 kJ/mol is added making AB a solid.<sup>34</sup> This gives AB a much higher volumetric density than ethane, its isoelectronic carbon analogue.

The diammoniate of diborane (DADB,  $[\text{BH}_2(\text{NH}_3)_2]^+\text{BH}_4^-$ ) is the ionic dimer of AB where the cation is comprised of a NBN motif with the terminal ammonia groups forming dative bonds with the  $\text{BH}_2^+$  unit while the anion is a borohydride group. DADB does not have a melting point, but decomposes at 80 °C to give similar decomposition products, in general, as AB. DADB is insoluble in ethers and hydrolyzes readily in water and will slowly split off hydrogen at room temperature. Shultz, Parry, and Shore were the first to correctly identify<sup>33</sup> the structure of DADB as  $[\text{H}_3\text{NBH}_2\text{NH}_3]^+[\text{BH}_4]^-$  and not  $[\text{NH}_4]^+[\text{H}_3\text{BNH}_2\text{BH}_3]^-$ <sup>35</sup> or  $\text{NH}_4(\text{H}_2\text{BNH}_2)\text{BH}_4$ <sup>36</sup> through a series of reactivity studies.



The first reactions were with sodium which, when reacted with DADB, formed sodium borohydride and not the complex salt  $\text{Na}[\text{H}_3\text{BNH}_2\text{BH}_3]$ .

Another interesting property of DADB is the stabilizing effect of the cation on the borohydride anion. Lithium borohydride salts reacts vigorously with water, whereas the DADB reaction is not nearly as violent. Reaction of DADB with lithium halide salts increased the proton sensitivity on the borohydride as evidenced by increased  $\text{H}_2$ -release.<sup>33</sup> The standard DADB preparation is to bubble diborane through liquid ammonia held at  $-78\text{ }^\circ\text{C}$ . DADB can also be made in organic solvents; however, the yields are reduced. Regardless of the solvent used, the reaction is highly temperature sensitive and if the solvent is warmer, the product ratio shifts towards the side product, AB.<sup>37</sup> If pure DADB is placed in complex ethers such as glyme, it will slowly convert to AB almost cleanly.<sup>38</sup> The IR spectrum of DADB has also been tentatively assigned.<sup>39</sup>

AB dehydrogenation is exothermic. The Dixon group and collaborators have calculated detailed reaction pathways starting from 2 AB molecules through the formation of DADB and subsequent hydrogen loss from DADB.<sup>40</sup> They also used coupled cluster (CCSD(T)) level calculations to show that breaking the B-N bond is the easiest AB decomposition method. This had serious implications for a reaction mechanism where the easiest bond breakage formed free ammonia and borane moieties.<sup>41</sup>

**Figure 1.6** shows an energy profile calculated by the Dixon group. Starting with two AB, one of the two AB units dissociates into borane and ammonia with the borane associated with both the hydridic B-H from the other AB and the ammonia forming a transition state which is 12.4 kcal/mol above the two free AB. This then forms a bridging hydrogen with ammonia dissociation dropping the energy by 4.3 kcal/mol. If the free

ammonia associates with the protonic N-H of the other AB the energy drops 0.3 kcal/mol below the starting point. The second transition state involves abstraction of the hydride by the free borane and association of the free ammonia with the now positively charged borane. This transition state lays 27.8 kcal/mol above the starting point. The ionic dimer of AB, DADB, forms from this transition state and is 3.3 kcal/mol more stable than the two starting AB molecules.

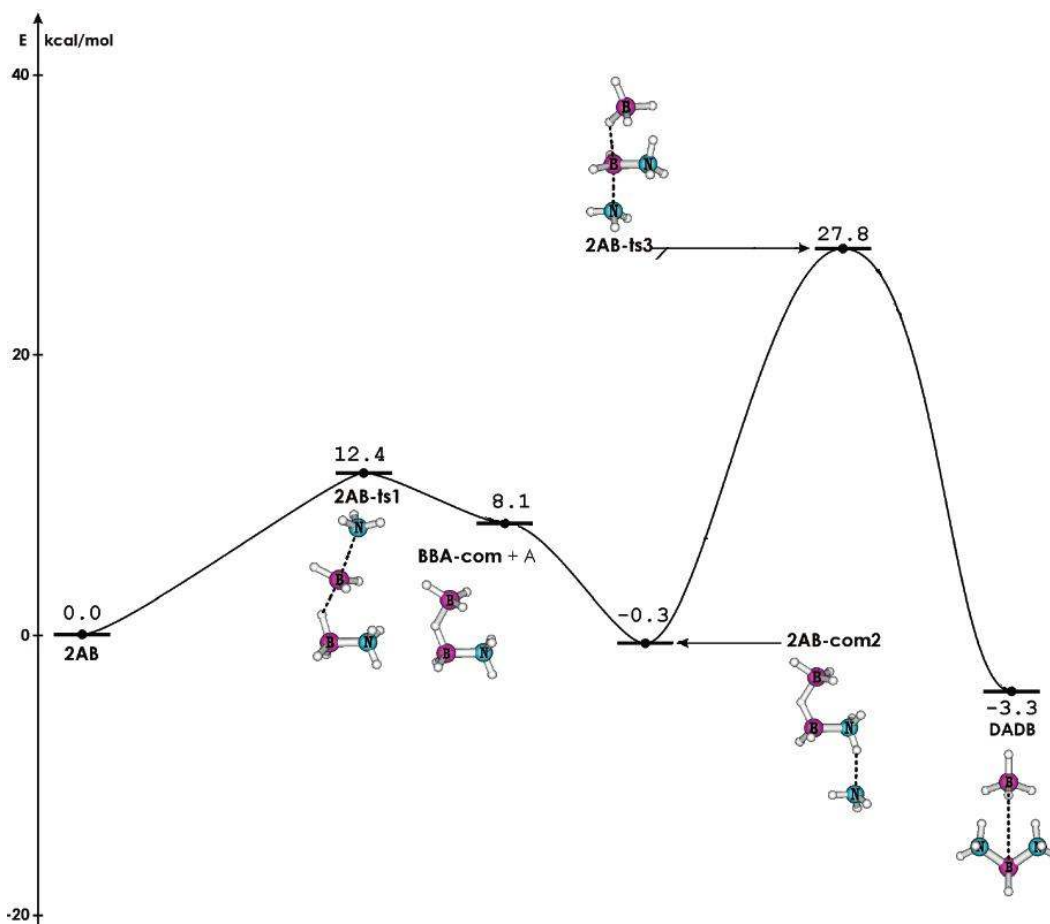


**Figure 1.6** Schematic energy profile of the conversion of 2 AB to DADB.<sup>40</sup>

To then release hydrogen from DADB, the Dixon group calculated the energy profile, **Figure 1.7**, where the boron and hydride from the borohydride associates with the protonic N-H with concomitant H<sub>2</sub>-release and formation of the B-N bond. They then calculated that the most favorable conformation is cis so that the boron and nitrogen can associate. Further monomer addition and dehydrogenation yield products such as CTB ( $\Delta H_f^\circ = -120.5$  kcal/mol (solid)) and borazine ( $\Delta H_f^\circ = -122.6$  kcal/mol (liquid)).<sup>42</sup> The  $\Delta H$  of the reaction of three AB going to form CTB with the release of three H<sub>2</sub> was calculated to be -55.9 kcal/mol at 298 K. The subsequent release of another three H<sub>2</sub> to form borazine was calculated to be -18.9 kcal/mol at 298 K.<sup>42</sup> Nguyen also calculated a reaction plot using free borane as a catalyst where the products were H<sub>2</sub>, borane (which continued catalyzing the reaction), and aminoborane. Aminoborane is a highly reactive species that was implicated by others in the overall AB reaction scheme.<sup>41</sup> These proposed mechanisms explain the reason a significant amount of ammonia is released during solid-state AB reactions.

The abstraction of a proton from AB to form the H<sub>3</sub>BNH<sub>2</sub><sup>-</sup> anion was calculated to be 357 kcal/mol at 298 K. This is a gas phase calculation and is based mainly on the enthalpic contribution which is mostly from the stability of the anion.<sup>43</sup> The difficulty of removing a proton in a solvent environment should be dramatically less.

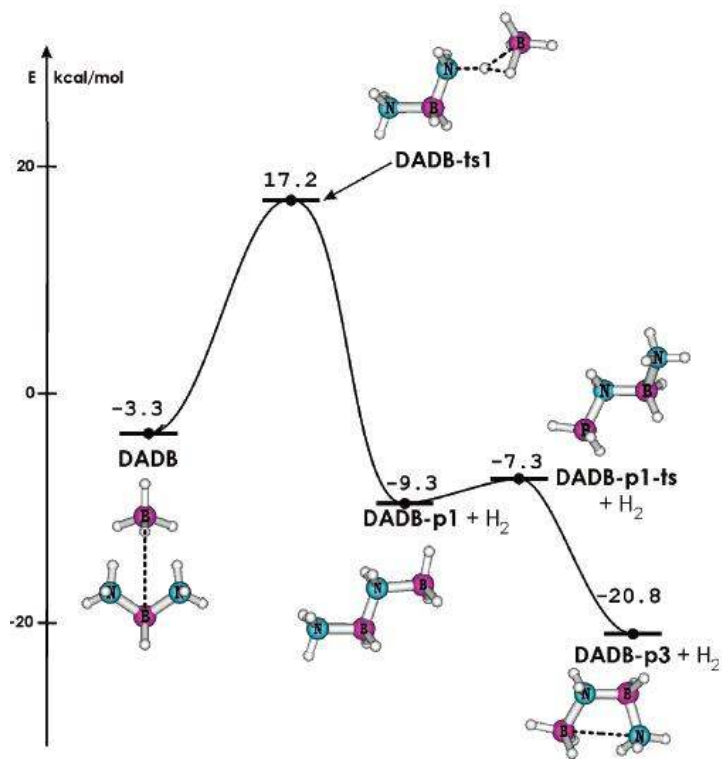


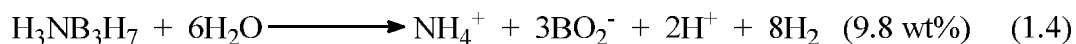
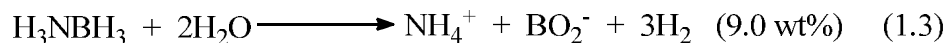
**Figure 1.7** Schematic energy profile of the dehydrogenation of DADB.<sup>40</sup>

### 1.3.1 How to Release Hydrogen from Ammonia Borane?

There are two main methods to release hydrogen from a chemical hydride; hydrolytically and thermolytically. The requirements for hydrogen release for utilization in vehicles powered by fuel cells are fast, controlled, and complete release. The hydrogen needs to be fast enough to power fuel cells in times of acceleration when more energy is needed. The H<sub>2</sub>-release also needs to be both controllable so that it can be turned off and have a consistent release rate so there are no spikes of hydrogen when it is not needed. Lastly, in order to achieve a high materials weight percent, most of the hydrogen needs to be released or the hydrogen yield will be very low.

### 1.3.1.1 Utilizing Hydrolysis to Release Hydrogen.

The area that received the most attention early was AB hydrolysis. General reactions for amine borane hydrolysis are given in **Equations 1.3** and **1.4**.

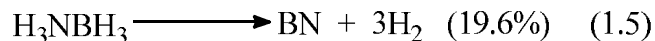


Ammonia borane will undergo hydrolysis only very slowly at room temperature in basic water, but the rate is accelerated by lowering the pH or increasing the temperature. Most of the research in this area has focused on the search for transition-metal catalysts to increase the rate of AB-hydrolysis. Utilization of catalysis<sup>44-64</sup> can lower the H<sub>2</sub>-release temperature to room temperature. Metal catalyzed hydrolysis can give ultra-fast hydrogen release, often in seconds, with very controllable rates. This method also drives the dehydrogenation of AB to near completion, with ~3 equivalents released. Nonetheless, the use of hydrolysis as a method for hydrogen delivery in a fuel cell powered car is impractical for several reasons. AB is only moderately soluble in water and consumes 2 waters per AB so that despite a theoretical materials weight percent of 9 %, only ~5 % materials weight percent is possible. Regeneration of the spent fuel is another reason hydrolytic hydrogen release is not going to be used in vehicle fuel cells due to the difficulty of reducing B-O bonds. More about fuel regeneration will be discussed later. While this technology has great promise in certain areas such as emergency power backup, it is too inefficient to work in the transportation sector.

### 1.3.1.2 The Better Hydrogen Release Method: Thermolysis.

The simplest hydrogen release method is to just heat it up. Thermolysis offers several benefits over hydrolysis, with the main advantage being the system can achieve

much higher material weight percent, as shown in the general reaction for AB thermolysis given in **Equation 1.5**.



### 1.3.2 Ammonia Borane Solid-State H<sub>2</sub>-Release

Wolf<sup>65,66</sup> first showed that there are two exothermic H<sub>2</sub>-release events associated with the decomposition of AB. The first event starts at ~70 °C when heating at 1 K/min but ~100 °C at 5 K/min. The endotherm directly before the first exotherm centered at ~100 °C is attributed to the melting of AB. The second event is much broader and starts at ~130 °C before the first event is finished. Comparing volumetric H<sub>2</sub>-release and thermogravimetric analysis (**Figure 1.8**), the two release events become clear as does a disparity. The thermogravimetric curves indicate more mass loss than the volumetric curve. This is attributed to other volatile gases being formed besides H<sub>2</sub> and the gap increases as the heating rate increases.<sup>65</sup> According to Autrey, raising the temperature of reaction can release potentially all three equivalents from AB taking >500 °C.<sup>67</sup> Most research in AB hydrogen release has focused on increasing the extent of release as well as the rate.

While thermolysis is a simple system and hence has many benefits for engineering an end use system, there are a host of difficulties associated with solid-state reactions. There are four major problems with solid-state H<sub>2</sub>-release reactions illustrated in **Figure 1.9**.

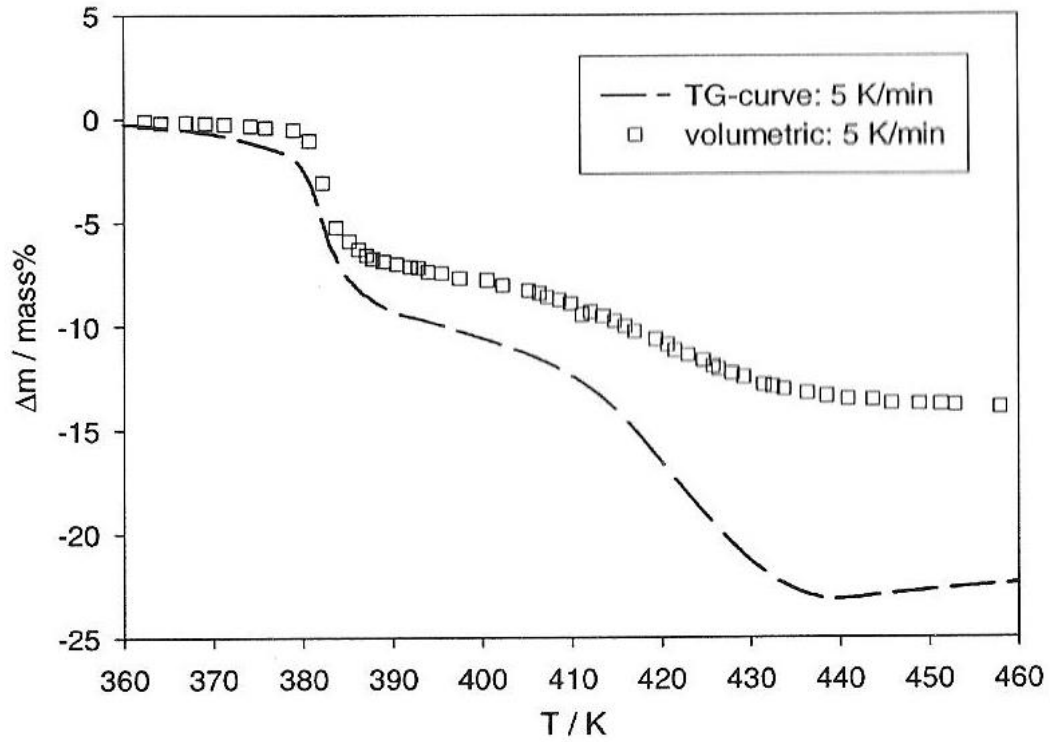


**Figure 1.8** Comparison of thermogravimetric and volumetric data at 5 K/min of AB thermolysis.<sup>65</sup>

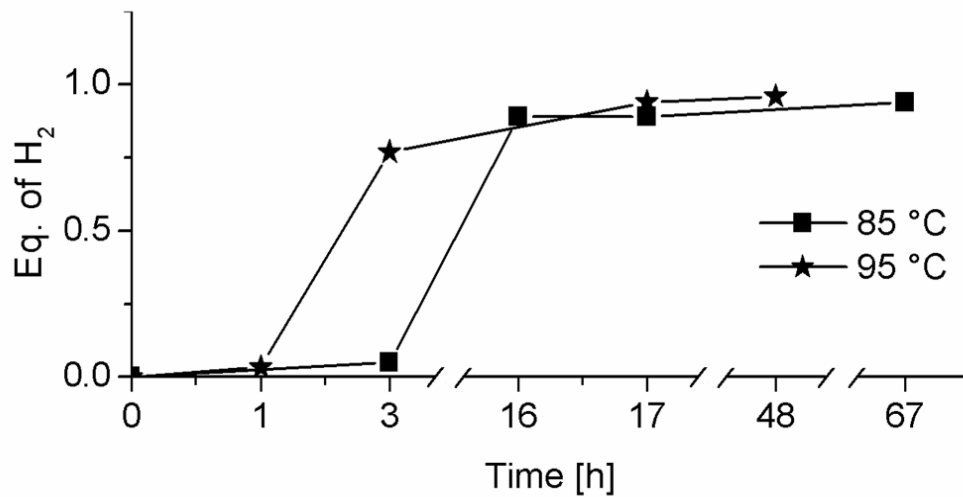


**Figure 1.9** Solid-State hydrogen release data for AB at 85 and 95 °C.

The first is an induction period where, it has been proposed,<sup>68</sup> the AB is slowly converting to the DADB, the active intermediate and ionic dimer of AB discussed in depth in **Chapter 2**, with H<sub>2</sub>-release not beginning until after 3 hours at 85 °C. The conversion of AB to DADB releases no hydrogen. The second major issue is the slow rate of H<sub>2</sub>-release. Once dehydrogenation starts, it takes hours to get to one equivalent. The third is, as discussed above, AB can release 3-H<sub>2</sub> when heated above 500 °C, but this would require heaters to raise the temperature thus adding weight and complexity to the system as well as requiring energy to power the heaters. A proton exchange membrane fuel cell's waste heat is ~85 °C, so to avoid the need for heaters, the most efficient systems for AB H<sub>2</sub>-release should be designed to operate near 85 °C. However, at 85 °C, less than one third (one equivalent) of the hydrogen is released from solid-state AB. These three problems seriously limit the practical uses of solid-state AB reactions for transportation since fast rates as well as high wt% H<sub>2</sub>-materials are needed. The fourth major issue is the products that form during the dehydrogenation reaction are diverse which can cause problems in regenerating the spent fuel.

In order to better understand the reaction pathways the products of these reactions were studied. The large product distribution coupled to the insolubility of some of the products made analysis difficult. Initially, pyridine extracts of reactions in progress were analyzed using <sup>11</sup>B NMR. A typical <sup>11</sup>B NMR spectrum for one of these extracts after the release of 1 equivalent is shown in **Figure 1.10**. At least 5 different resonances can be observed. Geanangel was the first to do comprehensive studies of the thermal decomposition of AB and proposed the formation of polyaminoboranes (NH<sub>2</sub>BH<sub>2</sub>)<sub>x</sub> as the initial product.<sup>69,70</sup> Indeed, DFT/GIAO calculations of linear (NH<sub>2</sub>BH<sub>2</sub>)<sub>x</sub> shown in



**Figure 1.11** indicate that the  $^{11}\text{B}$  shifts at -12 and -23 ppm correlate with the  $\text{BH}_2$  and  $\text{BH}_3$  of the linear polymer. The signal at -5 ppm is in good agreement with the calculated shift of the BH unit of a branched chain polyaminoborane (**Figure 1.11**). The -12 and -36 ppm signals correlate with the cation and anion of DADB respectively.<sup>33,71</sup> Lastly, the small signal at 30 ppm is characteristic of unsaturated B-N bonds and could be either unsaturated polyaminoborane (**Figure 1.11**) or borazine.<sup>72-74</sup> Poorly defined products made it difficult to determine the best catalyst to use to improve the rate and extent of  $\text{H}_2$ -release. The diverse product distribution has other ramifications, namely with the regeneration of spent fuel research, that will be discussed later in section 1.3.6.

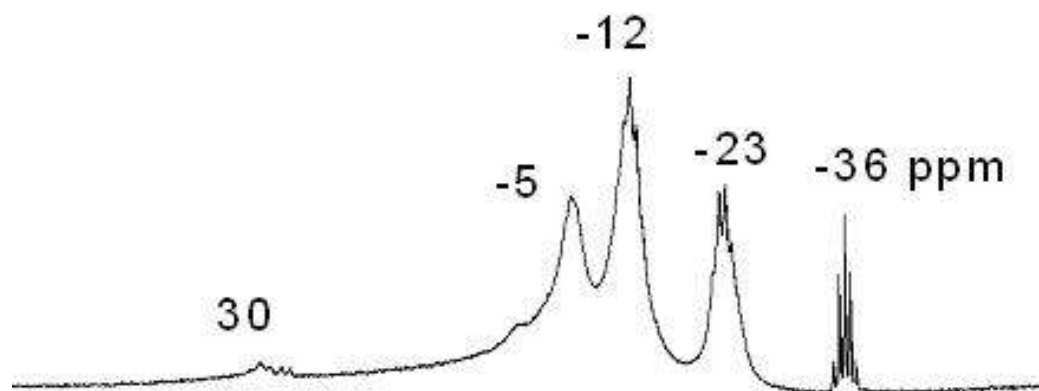


**Figure 1.10**  $^{11}\text{B}$  NMR (128.4 MHz) spectra recorded at 20 °C. Pyridine extract of a solid-state AB reaction at 85 °C after 19 h with 0.83 equivalents of  $\text{H}_2$ -released.

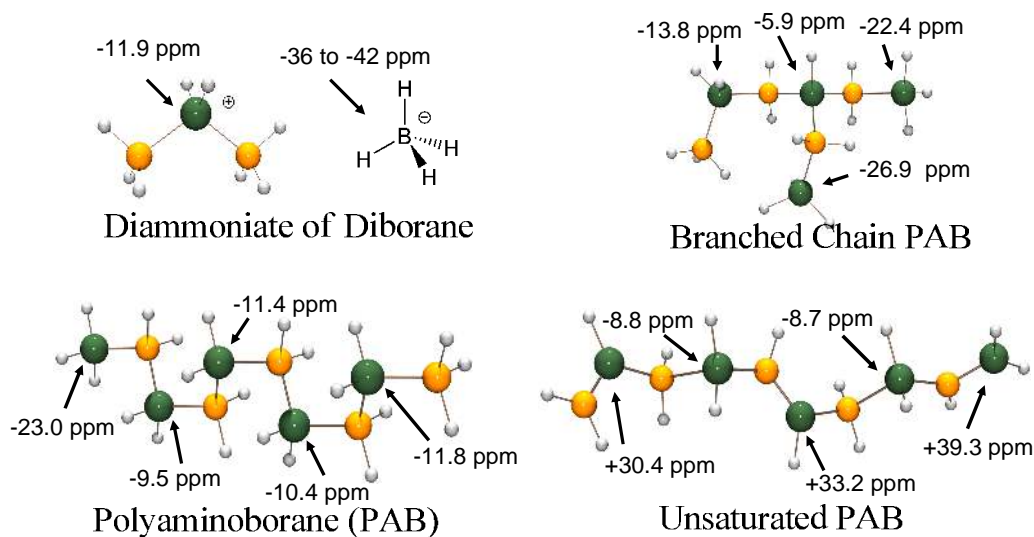


**Figure 1.11** DFT/GIAO calculated  $^{11}\text{B}$  NMR shifts for possible dehydropolymerization products.

### 1.3.3 Activated AB $\text{H}_2$ -Release from AB

#### 1.3.3.1 Mesoporous Scaffolds Aid in Solid-State $\text{H}_2$ -Release

Mesoporous scaffolds have been shown to activate AB  $\text{H}_2$ -release and have achieved faster release rates, lower  $\text{H}_2$ -release temperatures, and better product control. There are four main types of scaffolds: carbon cryogels,<sup>19,22,25-27</sup> mesoporous silica,<sup>20,21,24,28</sup> zeolites,<sup>29</sup> and metal-organic frameworks.<sup>23</sup> The carbon scaffolds were explored both with AB and AB/metals intercalated into them. One type of carbon scaffold, mesoporous carbon, is somewhat acidic and was shown to enhance reaction rates and lower temperatures due to the acidity or the proximity of another AB unit. It was also shown that the addition of lithium to this scaffold ‘scrubs’ the gas stream by removing  $\text{NH}_3$ ,<sup>22</sup> a potential fuel cell killer. All of the carbon based mesoporous scaffolds decrease the temperature needed for AB dehydrogenation. The efficiency is

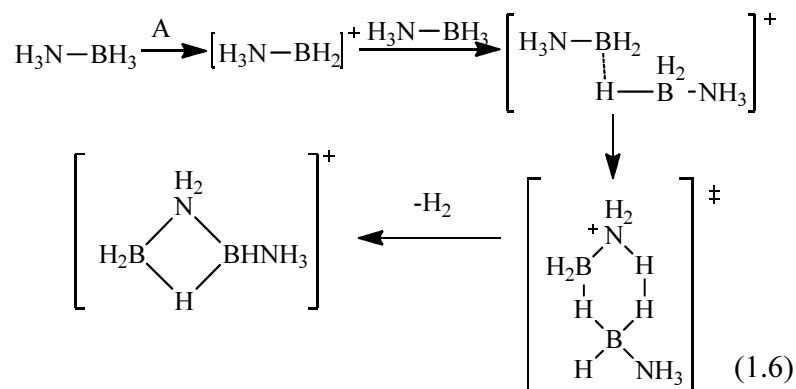
affected by pore size where the smaller the pore size, the lower the activation energy. Like the lithium doped scaffold that removed ammonia, non-metal doped AB-carbon scaffolds suppress the formation of borazine, another potential fuel cell killer.<sup>19,25-27</sup> Mesoporous silica showed similar reaction rates and volatile-elimination improvements as its carbon analogues.<sup>20,21,24,28</sup> Autrey *et al.* used SBA-15 and methanol to get a 1:1 ratio of AB and mesoporous silica. Subsequent reaction resulted in a 15 °C reduction in onset temperature for dehydrogenation.<sup>20</sup> Carbon cyrogels have the advantage of being slightly easier to synthesize. Unfortunately, thermolysis of these materials only lends ~7 materials weight percent due to the excessive weight of the scaffold.

The other two mesoporous materials, zeolites and metal-organic frameworks, were used differently than the carbon and silica scaffolds. In the case of zeolites, research focused on using them as supports for metal nanoclusters. Zahmakiran *et al.* showed that reduction of Rh(III) onto the zeolite backbone can significantly enhance the catalytic activity during hydrolysis.<sup>29</sup> Similarly, metal-organic frameworks perform well as hydrolysis catalysts.<sup>23</sup> The resiliency of these materials was far greater than normal heterogeneous catalysts in hydrolysis; however, as stated previously, hydrolysis cannot achieve the overall total system weight goals.

### **1.3.3.2 Acid Catalyzed Hydrogen Release Reactions**

Only limited research has gone into studying the acid catalyzed H<sub>2</sub>-release from AB. Work first focused on acids in ethereal solvents, such as tris(pentafluorophenyl)borane, since there was precedence for dehydrocoupling reactions with dihydrophenylphosphine borane.<sup>75</sup> While Manners showed that B(C<sub>6</sub>F<sub>6</sub>)<sub>3</sub> does not

catalyze the dehydrocoupling of  $\text{Me}_2\text{NHBH}_3$ ,<sup>76</sup> Stephens showed that it catalyzed  $\text{H}_2$ -releases from AB.<sup>77</sup>



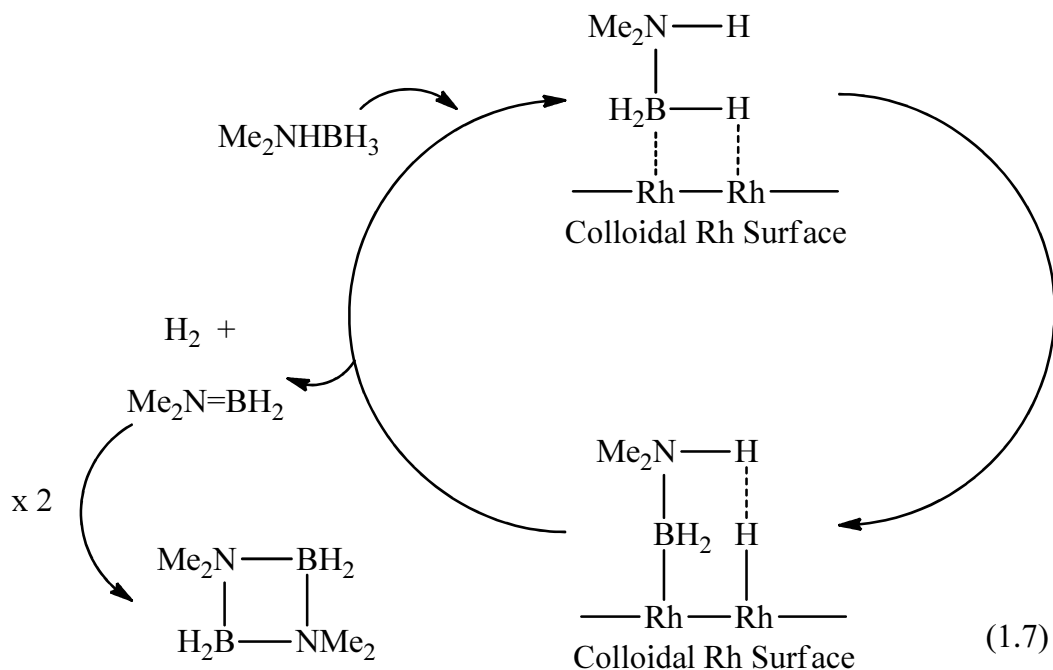
It was found that the amount of acid dramatically changed the reaction pathway. The proposed mechanism is cationic (**Equation 1.6**) and started with hydride abstraction followed by association of AB and subsequent  $\text{H}_2$ -release and formation of a cationic ammonia-substituted  $\mu$ -aminodiborane. With low acid concentration ( $\leq 1$  mol%), more hydrogen was released and cationic dehydropolymerization continued. However, at high acid loadings ( $>10$  mol%), a side reaction occurred where neutral  $\mu$ -aminodiborane was the main product and  $\text{H}_2$ -release stopped after only 0.6 equivalents. Stephens also showed that HCl in ethereal solvents can release 1.2 equivalents of hydrogen at 60 °C after 20 hours.  $\text{H}_2$ -release reactions were measured the on a manual gas burette setup.<sup>77</sup> The products of the low acid reactions tended to be cyclic species, such as borazine; however, this was most likely due to the use of organic solvents not as a result of acid catalysis. Ultimately, the slow reaction rates and low  $\text{H}_2$ -release amounts, as well as the use of volatile catalysts made this method less favorable than other activation methods.

### 1.3.3.3 Using Transition-Metal Catalysis to Enhance Release Rate and Extent.

Since AB is an ethane analogue, the use of transition-metal catalysis was a logical path to explore to activate AB for H<sub>2</sub>-release. Research has focused on both heterogeneous catalysis, mainly nanomaterials, and homogenous catalysts. These catalysts were used for both thermolysis and hydrolysis/methanolysis reactions. Transition-metal catalysts were also used to activate alkylated amine boranes.

#### 1.3.3.3.1 Heterogeneous Transition-Metal Catalysts

The Manners group spearheaded the chemistry of transition-metal catalysis of aminoboranes. From 2001 until 2006, the Manners group was the only group publishing on aminoborane catalysis.<sup>76,78-81</sup> The work in 2001 focused on rhodium complexes that cyclized alkylated aminoboranes. They found that the secondary amine borane adducts formed cyclodimers. On the other hand, the monomethylamine borane and parent AB, formed trimers, but with the parent borazine formed in only 10 % yield.<sup>78</sup> It was found that the original catalyst, [Rh(1,5-cod)(μ-Cl)]<sub>2</sub>, was the most active at Me<sub>2</sub>NHBH<sub>3</sub> dimerization achieving 100 % yield in 8 hours at room temperature. It was proposed at the time that based on TEM and Hg poisoning studies, the active catalyst was a heterogeneous colloidal Rh(0).<sup>76</sup> The proposed mechanism for colloid catalysis is shown in **Equation 1.7**.<sup>80</sup>



Others have used nanoclusters similar to those in the above experiments, which were formed *in situ* starting from the precatalyst  $[\text{Rh}(\text{COD})\text{Cl}]_2$ .<sup>79,82,83</sup> There has been controversy surrounding the size of the rhodium active catalyst and whether it was metallic or a ligated cluster. Chen *et al.* in 2005 showed that rhodium formed six atom clusters when used in toluene where amine boranes formed the ligands to the rhodium clusters.<sup>83</sup> A more complete study was published in 2007 by Fulton *et al.* where it was shown that the clusters were either four or six rhodium clusters, not metallic rhodium, though metallic rhodium was formed when the clusters were exposed to air.<sup>82</sup> Therefore, it was argued that these clusters are actually homogenous catalysts. Other work by Chang used nanoparticles as additives,<sup>84</sup> which could also be supported.<sup>85</sup> Work has also gone into the recovery of these nanoparticles. Zhang *et al.* designed shell-core particles that use iron as the core and platinum as the shell so they can be magnetically recovered.<sup>86</sup>

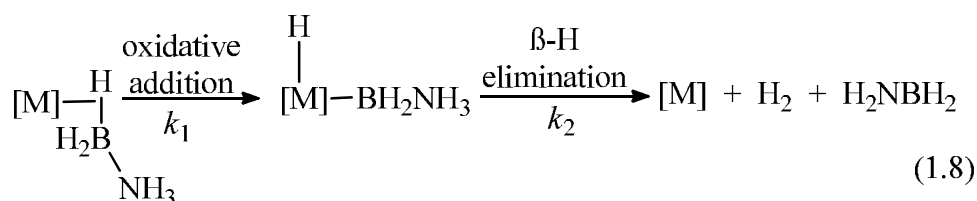
### 1.3.3.3.2 Homogeneous Transition-Metal Catalysts

Homogenous catalysis is another area of research using a range of first, second, and third row transition metals. One of the most exciting new catalysts was an iridium pincer catalysis, (*t*-BuPOCOP)Ir(H)<sub>2</sub>.<sup>87-90</sup> First row transition metal catalysis focused on nickel carbene chemistry, where both experimental<sup>90,91</sup> and theoretical<sup>92-94</sup> work showed activity in high extent of H<sub>2</sub>-release. Catalysis by early transition metals, such as titanocene, has been reported by Pun.<sup>95</sup> Three examples of transition-metal catalysts used to enhance AB H<sub>2</sub>-release will be discussed below.

#### 1.3.3.3.2.1 Iridium Pincer Catalyst

Heinekey and Goldberg first identified the iridium pincer ( $\kappa^3$ -1,3-(OP<sup>*t*</sup>Bu)<sub>2</sub>C<sub>6</sub>H<sub>3</sub>)Ir(H)<sub>2</sub> as an excellent catalyst for the dehydrogenation of AB. They found that at room temperature with only 0.5 mol% catalyst loading, the reaction went to one equivalent in 14 minutes and at 1 mol% it was complete in just 4 minutes. This makes the iridium catalyst the fastest dehydrogenation catalyst to date. The <sup>11</sup>B NMR spectra of the dehydrogenation products showed a broad signal at -18 ppm characteristic of tetracoordinate boron. The product of the iridium catalyzed reaction was identified as the AB pentamer, [H<sub>2</sub>NBH<sub>2</sub>]<sub>5</sub>, by IR and X-ray powder diffraction and was formed in near quantitative yields.<sup>87</sup> It was found that the catalyst was also active for methylamineborane and the product was soluble unlike the AB reaction products. The methylated products were not discrete pentamers like the previously reported<sup>87</sup> AB dehydrogenation products, but were a mixture of cyclic oligomers [MeNHBH<sub>2</sub>]<sub>*n*</sub> (*n* = 2 – 20) as well as acyclic oligomers. Heinekey and Goldberg then catalyzed mixtures of methylamineborane and AB to get a soluble product while increasing the hydrogen

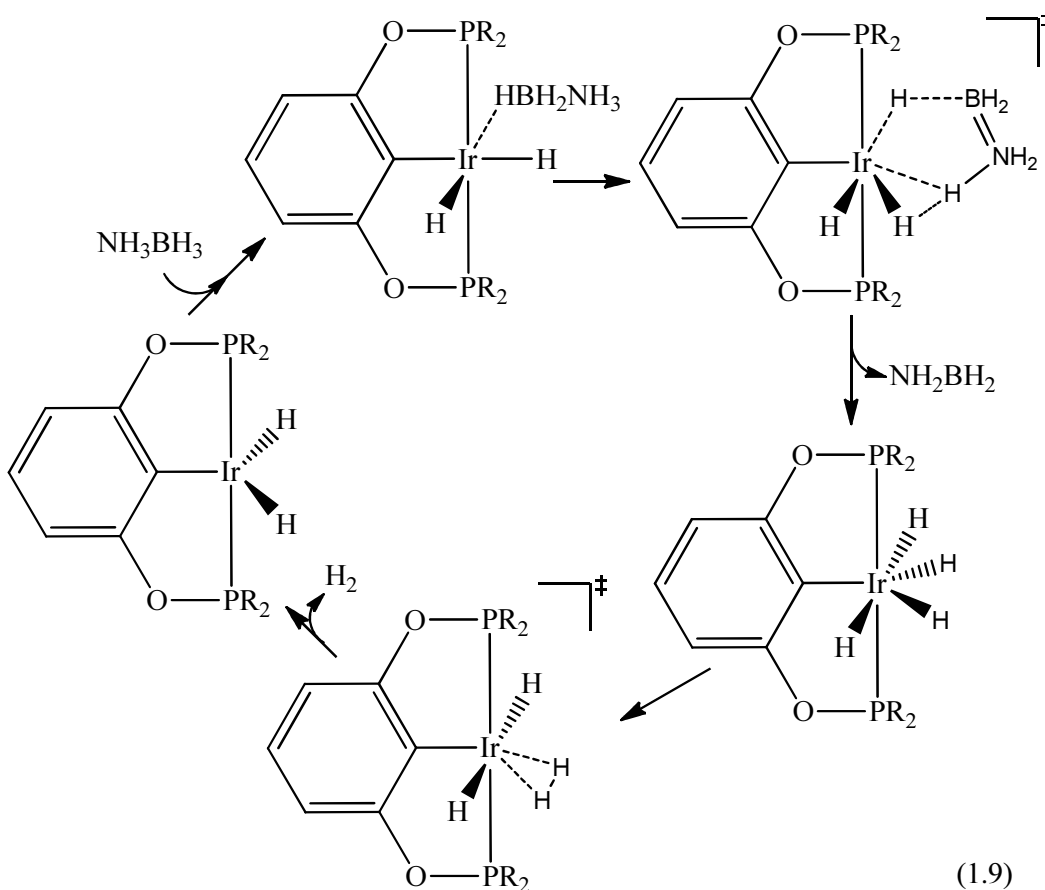
weight percent. The 1:1 ratio of methylamineborane : AB was still fast and made soluble products. Higher AB ratios produced insoluble products.<sup>88</sup> The iridium catalyst was also used by Manners to make discrete linear alkylated amine borane species.<sup>96</sup> In these studies the concentration of substrate (AB, MeNH<sub>2</sub>BH<sub>3</sub>, and *n*BuNH<sub>2</sub>BH<sub>3</sub>) was increased substantially from 0.5 M solution in the Heinekey/Goldberg reactions to 10 M. With only 0.3 mol% iridium catalyst at 0 °C, Manners was able to produce high molecular weight, soluble (MeNH<sub>2</sub>BH<sub>3</sub>) polyaminoboranes. These polymers were characterized through gel permeation chromatography and the MeNH<sub>2</sub>BH<sub>3</sub> based polymer showed a poly-dispersion index of only 2.9 with a molecular weight of 160,000.



The iridium pincer catalyst was initially used for alkane dehydrogenation. In these reactions it was proposed that C-H oxidative addition was the first step. Since AB has a heteroatomic backbone other reaction pathways are possible. It is generally believed that AB dehydrogenation with transition-metal catalysts follow **Equation 1.8**; however, theoretical studies have introduced the possibility of a much more complex mechanism.<sup>89</sup> Calculations showed that both a 14 e<sup>-</sup> and 16 e<sup>-</sup> iridium systems were possible although the 14 e<sup>-</sup> mechanism is higher in energy than the 16 e<sup>-</sup> system and too high for the reaction to occur at room temperature. The 16 e<sup>-</sup> system is shown in **Equation 1.9** and progresses through a 6 center transition state. The most stable species in this mechanistic pathway is the tetrahydroiridium center by 12.5 kcal/mol and

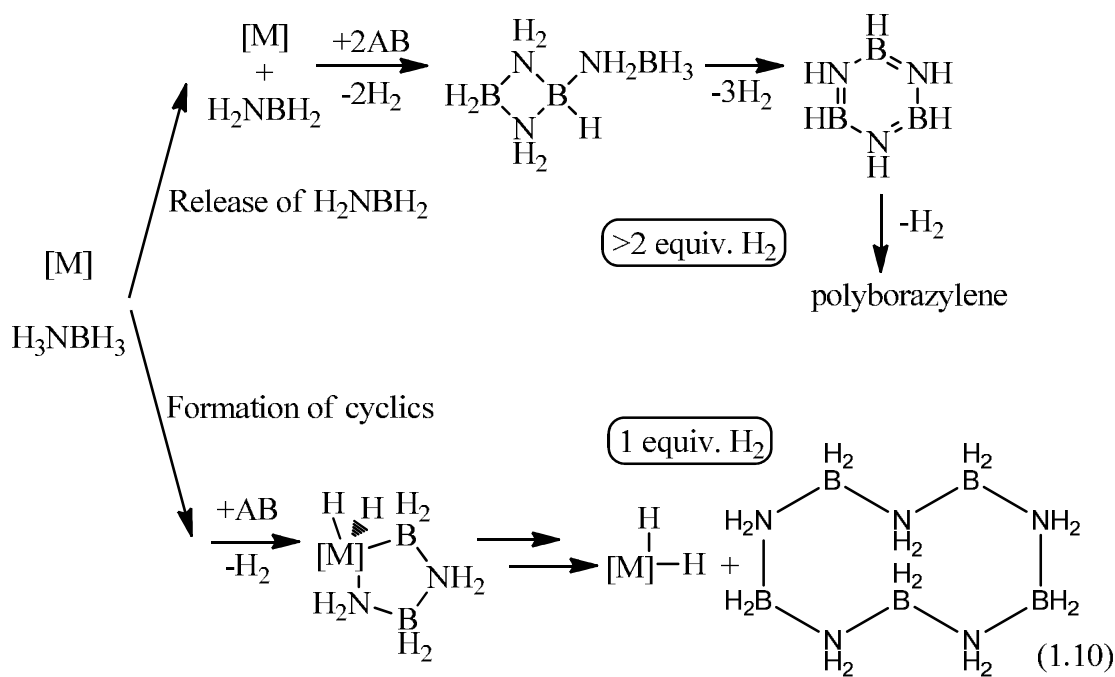


progresses to the parent species by loss of molecular hydrogen.<sup>89</sup> The catalyst kicks out aminoborane which is proposed to then polymerize in the solvent, THF.



The initially proposed reason for pentamer formation in AB dehydrogenation is based on the fact that the AB timer (CTB) is soluble in THF, but the pentamer is not and therefore the pentamer is isolated exclusively.<sup>89</sup> However, more recent trapping studies by Baker along with calculations by Dixon revealed that metal coordination of aminoborane ( $\text{H}_2\text{NBH}_2$ ) may be the important intermediate in the mechanism of these reactions. Baker and Dixon proposed that strong coordination to the iridium center with polymerization stopping at the pentamer was due to sterics (**Equation 1.10**) whereas non-iridium transition-metal catalysts released the aminoborane thus giving a much

different product distribution.<sup>90</sup> The dehydrogenation of  $\text{MeNH}_2\text{BH}_3$  that formed linear polymers found by Manners was at a higher concentration and cooler temperatures than previously reported by Heinekey and Goldberg. However, the Heinekey and Goldberg products were not well characterized and therefore no direct comparisons can be drawn. The catalyst is not implicated in further dehydrogenation or polymerization due to its steric bulk. Another reason for the iridium pincer catalyst stopping at one equivalent was poisoning of the iridium center with a borane moiety. It was then shown that the catalyst could be regenerated by placing it under  $\text{H}_2$  pressure.<sup>87,97</sup>



### 1.3.3.3.2.2 Nickel Carbene Catalyst

While the iridium catalyst is exceedingly fast, the reaction only reaches one equivalent. This is a problem for application to  $\text{H}_2$ -release systems but other recently reported catalysts can now achieve more extensive  $\text{H}_2$ -release. An example of a high extent of  $\text{H}_2$ -release catalyst is Baker's nickel carbene catalyst.<sup>91</sup> Baker explored N-

heterocyclic carbenes (NHC) as a more robust ligand system than phosphines and found that it gave unprecedented dehydrogenation, achieving 2.5 equivalents.<sup>91</sup> This system uses a Ni(cod)<sub>2</sub> precatalyst with 2 equivalents of NHC ligand to generate the active catalyst *in situ*. Enders' NHC (1,3,4-triphenyl-4,5-dihydro-1H-1,2,4-triazol-5-ylidene) was shown to exhibit the best activity releasing 18 wt% H<sub>2</sub> based on the amount of AB used. The reaction was run in diglyme at 60 °C and produced mainly polyborazylene type products, as well as some carbene-BH<sub>3</sub> side-product (**Figure 1.12**). The nickel carbene system is certainly not as fast as the iridium pincer, but the catalytic release of over 2 equivalents is unique to this catalyst.

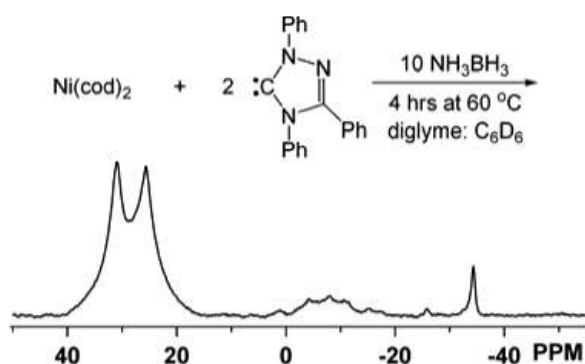


**Figure 1.12** Baker's nickel carbene catalyst with <sup>11</sup>B NMR showing final products.<sup>91</sup>

The initial overall reaction mechanism proposed for nickel, rhodium, and a few other catalysts is shown in **Equation 1.8**. The first step is association of AB with the metal center. The B-H bond then oxidatively adds to the metal center followed by a β-H elimination. Pons and Heinekey reported some experimental evidence for this reaction pathway by forming complexes where an amine borane is associated with a metal center. Using Cr(CO)<sub>5</sub> and dimethylamineborane they were able to form

[Cr(CO)<sub>5</sub>(η<sup>1</sup>-H<sub>3</sub>BNHMe<sub>2</sub>)] which decomposed within hours at 20 °C into (Me<sub>2</sub>NBH<sub>2</sub>)<sub>2</sub>. They also generated the AB adduct [Cr(CO)<sub>5</sub>(η<sup>1</sup>-H<sub>3</sub>BNH<sub>3</sub>)] which decomposed above -20 °C to form uncharacterized material.<sup>98</sup>

However, the side-product carbene-BH<sub>3</sub> along with the observed kinetic isotope effects and calculations have shown that for carbene catalysts, there is an unexpected proton transfer to the carbene rather than the B-H bond undergoing oxidative addition.<sup>99</sup> Hall calculated a reaction pathway where the boron coordinates to the nickel center while a proton from the nitrogen is abstracted by one of the carbene ligands (**Figure 1.13**). The proton then adds to the nickel center as well as a hydride. H<sub>2</sub> then reductively eliminates followed by loss of aminoborane.<sup>99</sup>

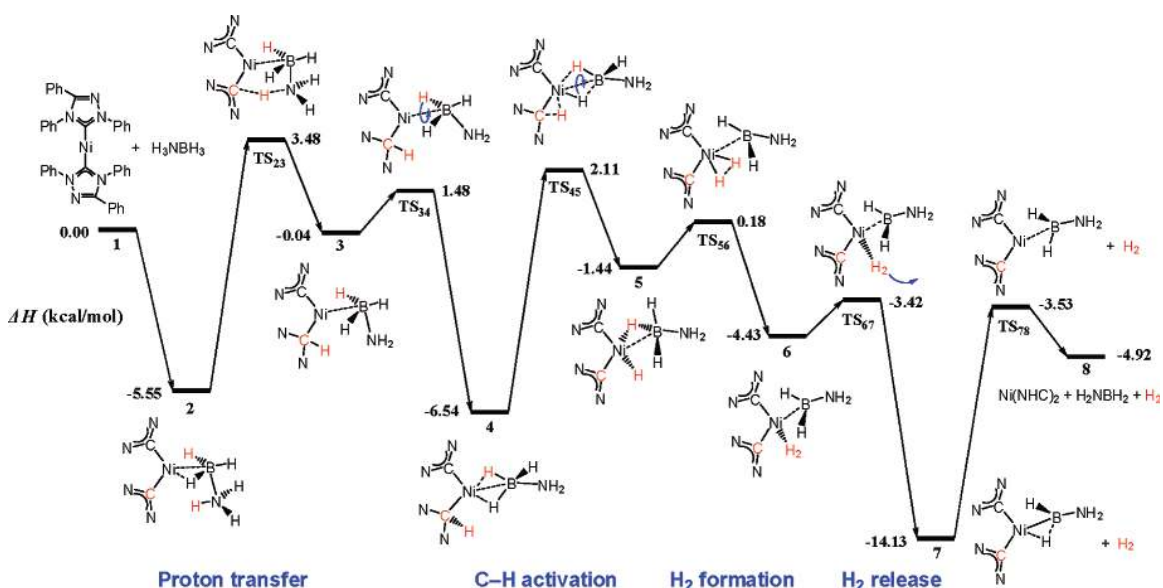


**Figure 1.13** Schematic energy profile of the nickel carbene catalyst using the carbene as a proton abstractor.<sup>99</sup>

This pathway does not explain the formation of carbene-BH<sub>3</sub> which requires a free carbene ligand. Kinetic isotope effect studies as well as additional calculations showed that AB replaces one of the NHC ligands so that the active catalyst is actually a Ni-NHC monoligated species.<sup>92,93</sup> In addition to the dehydrogenation reaction at the nickel center, the free carbene actively dehydrogenates AB so that there are two catalytic cycles operating in conjunction with each other. The free carbenes calculated AB H<sub>2</sub>-release mechanism is shown in **Figure 1.14**. As part of the catalytic cycle, the carbene reattaches to the nickel center through oxidative addition once the nickel's catalytic cycle has reached a point where a ligated aminoborane can assist in the dehydrogenation as shown in **Equation 1.11**.<sup>93</sup>

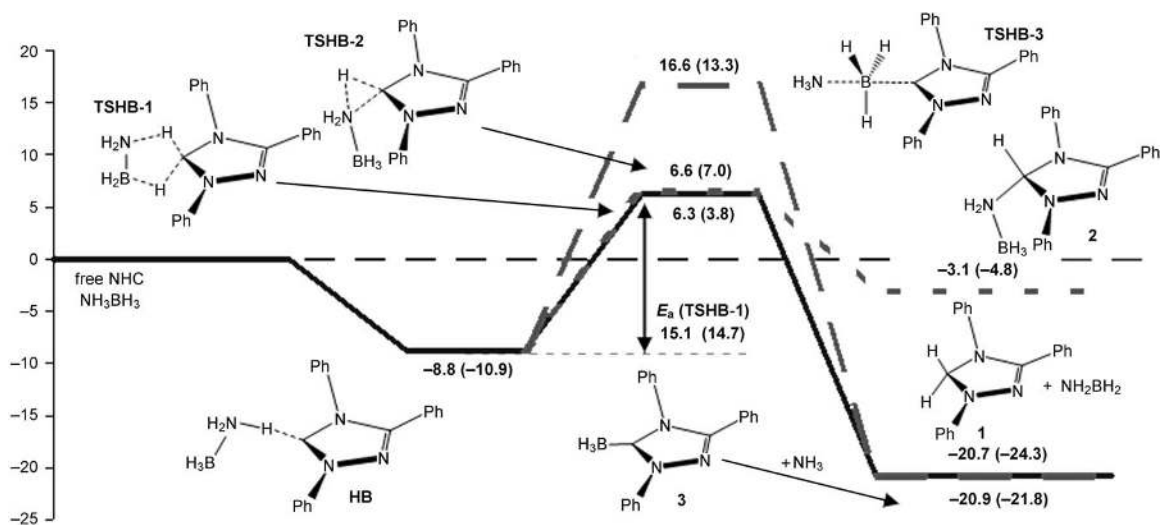
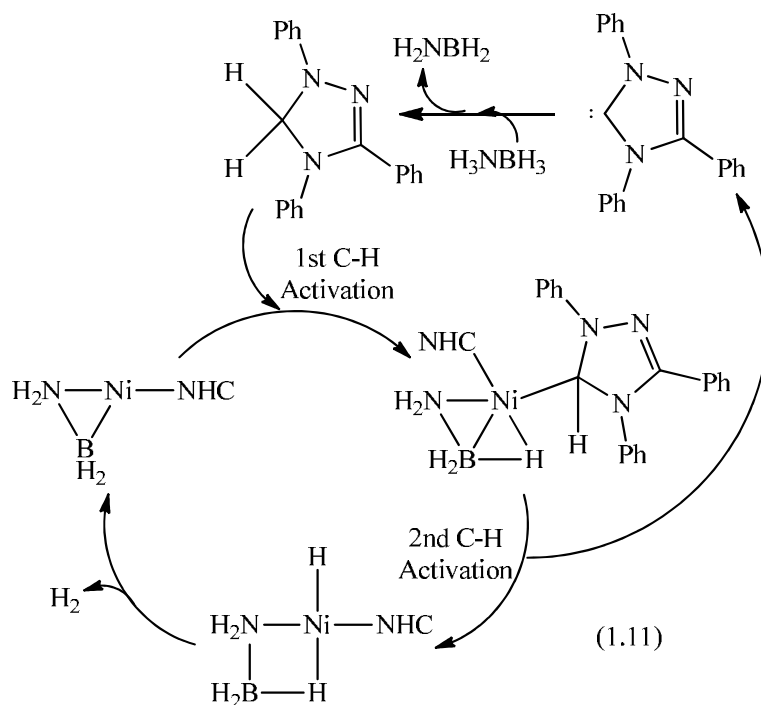


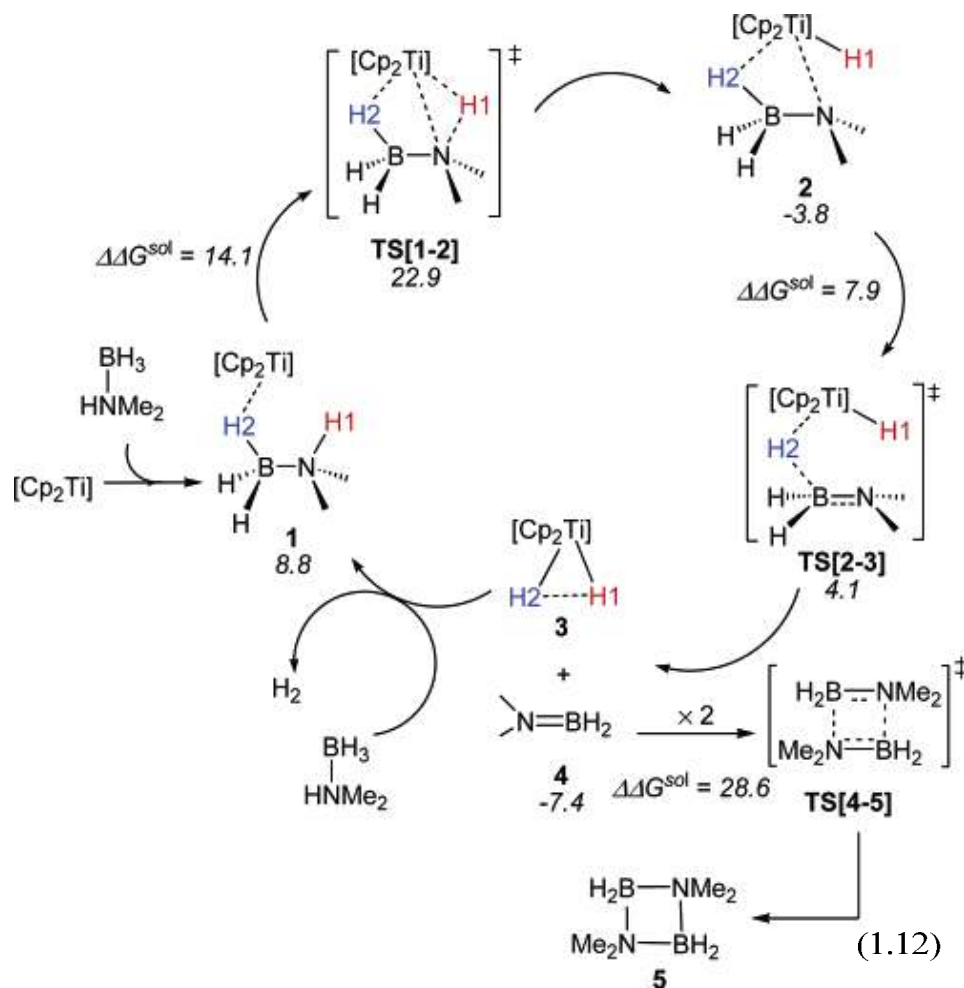
**Figure 1.14** Schematic energy profile for free carbene abstracting H<sub>2</sub> from AB.<sup>93</sup>

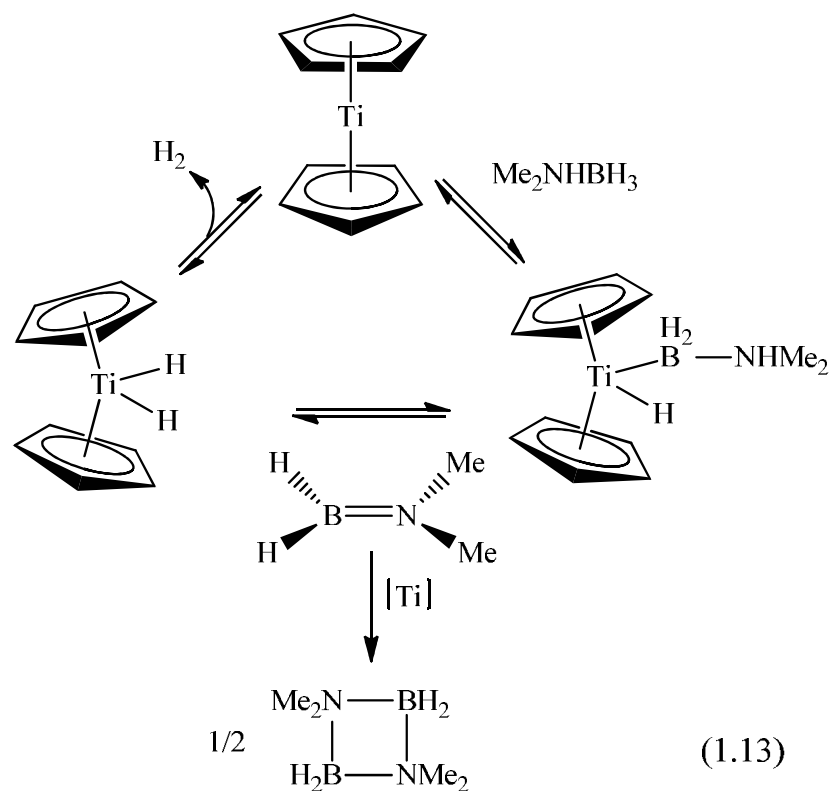


### 1.3.3.3.3 Titanocene Catalyst

Early transition-metal complexes have also been evaluated for AB dehydrogenation catalysts. Manners' screening of complexes for activity with  $\text{Me}_2\text{NHBH}_3$  showed that  $\text{Cp}_2\text{TiMe}_2$ , a Ti(IV), was inactive.<sup>76</sup> They later showed that  $\text{Cp}_2\text{Ti}$ , a Ti(II), which is made *in situ* using  $\text{Cp}_2\text{TiCl}_2$  and  $n\text{BuLi}$ . The Ti(II) catalyst was not studied with AB extensively and therefore no  $\text{H}_2$ -release data are available. The reaction was followed by  $^{11}\text{B}$  NMR and the initial product was cyclotriborazane which slowly converted to borazine with release of 2 equivalents of  $\text{H}_2$ .<sup>95</sup>  $\text{H}_2$ -release data collected for  $\text{Me}_2\text{NHBH}_3$  and the titanium catalyst showed 50 % conversion to the dimer in <50 minutes, whereas the heterogeneous Rh(0) catalyst took >400 minutes to reach the same conversion percentage.<sup>81</sup> The proposed mechanism for  $\text{H}_2$ -release and  $\text{Me}_2\text{NHBH}_3$  dimerization utilizing  $\text{Cp}_2\text{Ti}$  is shown in **Equation 1.12**. This calculation study by Luo and Ohno started with coordination and abstraction of a proton from the nitrogen in

Me<sub>2</sub>NHBH<sub>3</sub> followed by subsequent removal of the B-H hydride and Me<sub>2</sub>NBH<sub>2</sub> release to self-dimerize.<sup>100</sup> This study failed to take into account concurrent results by Chirik that showed in a similar catalyst the mechanistic cycle is reversible. This was shown by deuterium studies where (Cp\*<sub>2</sub>Ti)<sub>2</sub>N<sub>2</sub> was subjected to a D<sub>2</sub> atmosphere while dehydrogenating Me<sub>2</sub>NHBH<sub>3</sub>. Deuterium was found in the B-H position and HD was also detected.<sup>95</sup> This slightly alternative mechanism is shown in **Equation 1.13**.





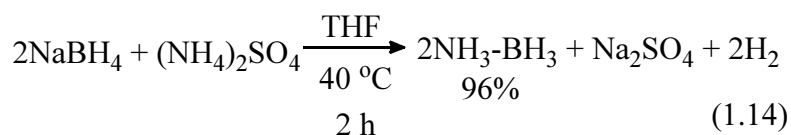
#### 1.3.3.3.2.4 Transition-Metal Catalysis in Hydrolysis/Methanolysis

Although hydrolysis/methanolysis cannot meet the DOE's total system targets as previously discussed, utilizing this technology in areas not as dependent on weight efficiency is possible. Therefore, research has continued in this area and developed a wide range of catalysts. Most of these catalysts are heterogeneous and on the nano-scale. Some, like work done by Umegaki and coworkers,<sup>60,61</sup> use supported nanoclusters, while the bulk of the hydrolysis catalysts are free nanoparticle/nanocluster. A majority of this work has used first-row transition metals such as cobalt, nickel and iron<sup>51,56-59,62,63,101</sup> and the rest use much more expensive noble metal nanoparticles.<sup>53-55,64</sup>

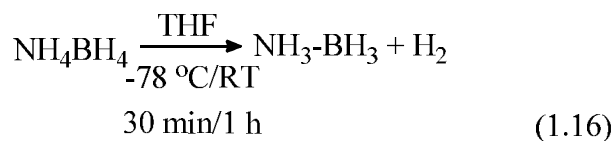
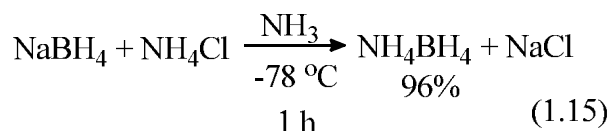


### 1.3.4 Large Scale Preparations of Ammonia Borane

In order to make the hydrogen economy work, a large scale synthesis of AB is needed. The traditional preparation of AB uses sodium borohydride and ammonium sulfate in an ethereal solvent.<sup>102,103</sup> Ramachandran et al. have reported a large scale preparation using tetrahydrofuran as the solvent. In their prep (**Equation 1.14**), ammonium sulfate was used in 50 % excess with the resulting AB yield being 96 % and



achieved in 98 % purity. In addition to ammonium sulfate, ammonium formate was used in dioxane with similar results.<sup>102</sup> While these preps show that the traditional methods can be scaled-up, other pathways will be needed if AB is to become a large scale energy carrier. To that end, Heldebrant et al.<sup>103</sup> showed that AB could be made from the decomposition of ammonium borohydride which was made *in situ* by the reaction of NaBH<sub>4</sub> and NH<sub>4</sub>Cl. In their preparation, liquid ammonia was used as the solvent with

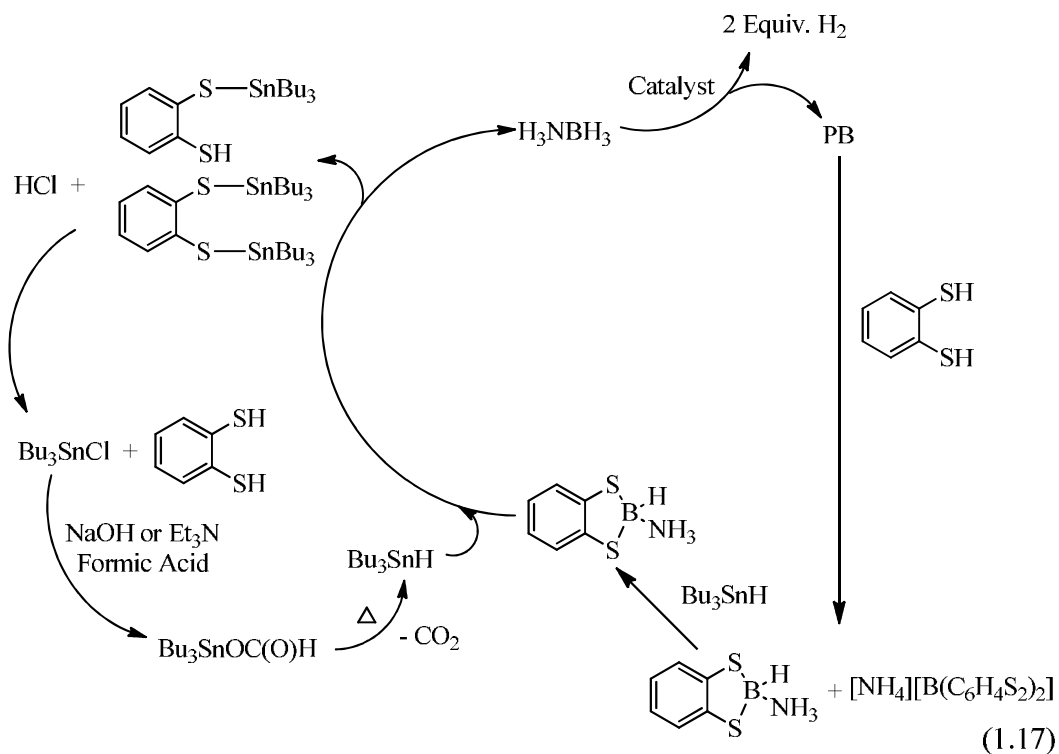


ammonium chloride and sodium borohydride forming the ammonium borohydride (**Equation 1.15**). Subsequent hydrogen loss and purification gave AB (**Equation 1.16**) in 99 % yield. All of these materials are available on large scales already; therefore scale-up should be straight forward.

### 1.3.5 Recycling the AB Fuel Source

Regeneration of the spent fuel is one of the most important aspects of a complete closed energy system. Most regeneration attempts focus on a two step system where the spent fuel is digested and the boron is converted into a B-X species which is then reduced to B-H bonds and coupled to ammonia. The best current approach for digestion uses *ortho*-benzenedithiol in THF which was refluxed for 12 hours to form the borane dithiol adduct. This adduct was then reduced using tributyltinhydride and the intermediate amine exchanged for ammonia (**Equation 1.17**).<sup>104</sup> Therefore, a regeneration scheme to turn the benzenedithiol-tributyltin adduct back into usable benzenedithiol and tributyltinhydride was designed. In this scheme, the adducts were replaced with chloride then oxidized using formic acid which was driven off with heat to recycle the tributyltinhydride.<sup>105</sup>

The production of large amounts of waste tributyltin in this process is a serious problem. In an effort to find an alternative to tin reducing agents, Mock et al. analyzed the hydride donor ability in acetonitrile of several transition-metal hydrides and compared them to the hydride affinities of several borane adducts such as B(OSiMe<sub>3</sub>)<sub>3</sub>, B(OPh)<sub>3</sub>, and BF<sub>3</sub>.<sup>106</sup> Utilizing this information, combinations of digestion agents and transition-metal hydride donors can be identified eliminating the need for hazardous, expensive stoichiometric reagents.



### 1.3.6 Hybrid Materials Try to Bridge the Gap Between AB and Metal Hydrides

Another class of amine boranes that has received attention is the metal amidoboranes. The progenitor of this class was sodium amidoborane ( $\text{Na}(\text{NH}_2\text{BH}_3)$ ), synthesized in 1938 by Schlesinger and Burg.<sup>13</sup> The lithium analogue was identified by Myers in 1996<sup>11</sup> and initially used as a powerful reductant. Metal amidoboranes have the potential to combine the high hydrogen content of amine boranes with the cleaner reaction pathways of metal borohydrides. Thermolytic release from lithium amidoborane can give 10.9 weight percent hydrogen while the sodium analogue is only 7.5 weight percent. These materials can be made through solid state ball milling of AB and the desired metal hydride/amide or similarly can be made in ethereal solvents such as tetrahydrofuran.<sup>7-11,13-18</sup> The range of compounds that can be synthesized is large and use alkali<sup>9-13,15-18</sup> and alkaline earth metals.<sup>7,8,14,15</sup> Lithium amidoborane can begin to release hydrogen at lower temperatures than even AB giving it a great advantage. As a class,

they also decompose cleaner than neat AB by not releasing borazine; however, they do release a good deal of ammonia. The ultimate goal of the use of metal amidoboranes is to achieve on-board regeneration of the spent fuel. As yet, none of the materials produced have shown the ability to uptake hydrogen at reasonable temperature for regeneration. The other drawbacks are lower hydrogen content due to the addition of the metal and additional synthetic steps.

## 1.4 Conclusions

As petroleum supplies run low and the need for an alternative energy carrier becomes evident, hydrogen has the potential to supplant petroleum as the United States' and the world's primary energy carrier. Ammonia borane is one of the most promising hydrogen storage materials due to its high materials weight percent and stability. While the solid-state reaction of AB is slow and incomplete, there are many methods being researched to enhance the rate and extent of H<sub>2</sub>-release from AB. There have been advances in the use of metals, carbon scaffold, and acid catalysis to achieve the DOE's targets; however none have solved the problems with AB H<sub>2</sub>-release either due to low extent and/or rate of H<sub>2</sub>-release or high cost. Now methods for activating AB dehydrogenation catalysis are needed to help AB become a solution for hydrogen storage. **Chapters 2 and 3** demonstrate two new complimentary ways of activating H<sub>2</sub>-release from AB.

## 1.5 References

1. Boyer, R., *et. al. Annual Energy Review*, Washington, 2008,  
<http://www.eia.doe.gov/emeu/aer/pdf/aer.pdf>.
2. Dillich, S. *2009 DOE Hydrogen Program & Vehicle Technologies Program*  
[http://www.hydrogen.energy.gov/pdfs/review09/st\\_0\\_dillich.pdf](http://www.hydrogen.energy.gov/pdfs/review09/st_0_dillich.pdf). DOE has recently lowered the 2015 gravimetric total system target to only 5.5 total system weight %.
3. Erlebacher, J.; Henry, E.; Frans, S., In *Solid State Physics*, Academic Press: Burlington, MA, 2009; Vol. 61, pp 77-141.
4. *Natural Gas Reforming*.  
[http://www1.eere.energy.gov/hydrogenandfuelcells/production/natural\\_gas.html](http://www1.eere.energy.gov/hydrogenandfuelcells/production/natural_gas.html).
5. Nocera, D. G. *Inorg. Chem.* **2009**, *48*, 10001-10017.
6. Honda *Honda FCX Clarity*. <http://automobiles.honda.com/fcx-clarity/>.
7. Chua, Y. S.; Wu, G.; Xiong, Z.; He, T.; Chen, P. *Chem. Mater.* **2009**, *21*, 4899-4904.
8. Diyabalanage, H. V. K.; Shrestha, R. P.; Semelsberger, T. A.; Scott, B. L.; Bowden, M. E.; Davis, B. L.; Burrell, A. K. *Angew. Chem. Int. Ed.* **2007**, *46*, 8995-8997.
9. Fijalkowski, K. J.; Grochala, W. *J. Mater. Chem.* **2009**, *19*, 2043-2050.
10. Lee, T. B.; McKee, M. L. *Inorg. Chem.* **2009**, *48*, 7564-7575.
11. Myers, A. G.; Yang, B. H.; David, K. J. *Tetrahedron Lett.* **1996**, *37*, 3623-3626.
12. Ramzan, M.; Silvearv, F.; Blomqvist, A.; Scheicher, R. H.; Lebegue, S.; Ahuja, R. *Phys. Rev. B: Condens. Matter. Mater. Phys.* **2009**, *79*, 132102-132104.

13. Schlesinger, H. I.; Burg, A. B. *J. Am. Chem. Soc.* **1938**, *60*, 290.
14. Spielmann, J.; Bolte, M.; Harder, S. *Chem. Comm.* **2009**, 6934-6936.
15. Wu, H.; Zhou, W.; Yildirim, T. *J. Am. Chem. Soc.* **2008**, *130*, 14834-14839.
16. Xiong, Z.; Chua, Y. S.; Wu, G.; W., X.; Chen, P.; Shaw, W. J.; Karkamkar, A.; Linehan, J. C.; Smurthwaite, T.; Autrey, T. *Chem. Comm.* **2008**, 5595-5597.
17. Xiong, Z.; Wu, G.; Chua, Y. S.; Hu, J.; He, T.; Xu, W.; Chen, P. *Energy Environ. Sci.* **2008**, *1*, 360-363.
18. Xiong, Z.; Yong, C. K.; Wu, G.; Chen, P.; Shaw, W. J.; Karkamkar, A.; Autrey, T.; Jones, M. O.; Johnson, S. R.; Edwards, P. P.; David, W. I. F. *Nat. Mater.* **2008**, *7*, 138-141.
19. Feaver, A.; Sepehri, S.; Shamberger, P.; Stowe, A.; Autrey, T.; Cao, G. *J. Phys. Chem. B* **2007**, *111*, 7469-7472.
20. Gutowska, A.; Li, L.; Shin, Y.; Wang, C. M.; Li, X. S.; Linehan, J. C.; Smith, R. S.; Kay, B. D.; Schmid, B.; Shaw, W. J.; Gutowski, M.; Autrey, T. *Angew. Chem. Int. Ed.* **2005**, *44*, 3578-3582.
21. Kim, H.; Karkamkar, A.; Autrey, T.; Chupas, P.; Proffen, T. *J. Am. Chem. Soc.* **2009**, *131*, 13749-13755.
22. Li, L.; Yao, X.; Sun, C.; Du, A.; Cheng, L.; Zhu, Z.; Yu, C.; Zou, J.; Smith, S. C.; Wang, P.; Cheng, H.-M.; Frost, R. L.; Lu, G. Q. *Adv. Funct. Mater.* **2009**, *19*, 265-271.
23. Li, Y.; Xie, L.; Li, Y.; Zheng, J.; Li, X. *Chem. Eur. J.* **2009**, *15*, 8951-8954.
24. Paolone, A.; Palumbo, O.; Rispoli, P.; Cantelli, R.; Autrey, T.; Karkamkar, A. *J. Phys. Chem. C* **2009**, *113*, 10319-10321.

25. Sepehri, S.; Feaver, A.; Shaw, W. J.; Howard, C. J.; Zhang, Q.; Autrey, T.; Cao, G. *J. Phys. Chem. B* **2007**, *111*, 14285-14289.
26. Sepehri, S.; Garcia, B. B.; Cao, G. *J. Mater. Chem.* **2008**, *18*, 4034-4037.
27. Sepehri, S.; García, B. B.; Cao, G. *Eur. J. Inorg. Chem.* **2009**, 599-603.
28. Wang, L.-Q.; Karkamkar, A.; Autrey, T.; Exarhos, G. J. *J. Phys. Chem. C* **2009**, *113*, 6485-6490.
29. ZahmakIran, M.; Özkar, S. *Appl. Catal., B* **2009**, *89*, 104-110.
30. Custelcean, R.; Dreger, Z. A. *J. Phys. Chem. B* **2003**, *107*, 9231-9235.
31. Stock, A.; Pohland, E. *Ber.* **1925**, *58*, 657.
32. Shore, S. G.; Parry, R. W. *J. Am. Chem. Soc.* **1955**, *77*, 6084-6085.
33. Shore, S. G.; Parry, R. W. *J. Am. Chem. Soc.* **1958**, *80*, 20-24 and preceding papers in this issue.
34. Stephens, F. H.; Pons, V.; Baker, R. T. *Dalton Trans.* **2007**, *25*, 2613-2626.
35. Schlesinger, H. I.; Burg, A. B. *J. Am. Chem. Soc.* **1938**, *60*, 290-299.
36. Schaeffer, G. W.; Adams, M. D.; Koenig, F. J.; Koenig, S. J. *J. Am. Chem. Soc.* **1956**, *78*, 725-728.
37. Mayer, E. *Inorg. Chem.* **1972**, *11*, 866-869.
38. Mayer, E. *inorg. Chem.* **1973**, *12*, 1954-1955.
39. Carpenter, J. D.; Ault, B. S. *J. Phys. Chem.* **1991**, *95*, 3502-3506.
40. Nguyen, V. S.; Matus, M. H.; Grant, D. J.; Nguyen, M. T.; Dixon, D. A. *J. Phys. Chem. A* **2007**, *111*, 8844-8856.
41. Nguyen, M. T.; Nguyen, V. S.; Matus, M. H.; Gopakumar, G.; Dixon, D. A. *J. Phys. Chem. A* **2007**, *111*, 679-690.



42. Matus, M. H.; Anderson, K. D.; Camaioni, D. M.; Autrey, S. T.; Dixon, D. A. *J. Phys. Chem. A* **2007**, *111*, 4411-4421.
43. Matus, M. H.; Grant, D. J.; Nguyen, M. T.; Dixon, D. A. *J. Phys. Chem. C* **2009**, *113*, 16553-16560.
44. Basu, S.; Brockman, A.; Gagare, P.; Zheng, Y.; Ramachandran, P. V.; Delgass, W. N.; Gore, J. P. *J. Power Sources* **2009**, *188*, 238-243.
45. Basu, S.; Zheng, Y.; Varma, A.; Delgass, W. N.; Gore, J. P. *J. Power Sources* **2010**, *195*, 1957-1963.
46. Chandra, M.; Xu, Q. *J. Power Sources* **2007**, *168*, 135-142.
47. Clark, T. J.; Whittell, G. R.; Manners, I. *Inorg. Chem.* **2007**, *46*, 7522-7527.
48. Metin, O.; Ozkar, S. *Energy Fuels* **2009**, *23*, 3517-3526.
49. Metin, Ö.; Sahin, S.; Özkar, S. *Int. J. Hydrogen Energy* **2009**, *34*, 6304-6313.
50. Mohajeri, N.; T-Raissi, A.; Adebiiyi, O. *J. Power Sources* **2007**, *167*, 482-485.
51. Yan, J.-M.; Zhang, X.-B.; Shioyama, H.; Xu, Q. *J. Power Sources* **2010**, *195*, 1091-1094.
52. Yao, C. F.; Zhuang, L.; Cao, Y. L.; Ai, X. P.; Yang, H. X. *Int. J. Hydrogen Energy* **2008**, *33*, 2462-2467.
53. Dai, H.-B.; Gao, L.-L.; Liang, Y.; Kang, X.-D.; Wang, P. *J. Power Sources* **2010**, *195*, 307-312.
54. Durap, F.; ZahmakIran, M.; Özkar, S. *Appl. Catal., A* **2009**, *369*, 53-59.
55. Erdogan, H.; Metin, O.; Ozkar, S. *Phys. Chem. Chem. Phys.* **2009**, *11*, 10519-10525.
56. Kalidindi, S. B.; Indirani, M.; Jagirdar, B. R. *Inorg. Chem.* **2008**, *47*, 7424-7429.

57. Kalidindi, S. B.; Sanyal, U.; Jagirdar, B. R. *Phys. Chem. Chem. Phys.* **2008**, *10*, 5870-5874.
58. Kalidindi, S. B.; Vernekar, A. A.; Jagirdar, B. R. *Phys. Chem. Chem. Phys.* **2009**, *11*, 770-775.
59. Park, J.-H.; Kim, H.-S.; Kim, H.-J.; Han, M.-K.; Shul, Y.-G. *Res. Chem. Intermed.* **2008**, *34*, 709-715.
60. Simagina, V. I.; Storozhenko, P. A.; Netskina, O. V.; Komova, O. V.; Odegova, G. V.; Larichev, Y. V.; Ishchenko, A. V.; Ozerova, A. M. *Catal. Today* **2008**, *138*, 253-259.
61. Umegaki, T.; Yan, J.-M.; Zhang, X.-B.; Shioyama, H.; Kuriyama, N.; Xu, Q. *Int. J. Hydrogen Energy* **2009**, *34*, 3816-3822.
62. Umegaki, T.; Yan, J.-M.; Zhang, X.-B.; Shioyama, H.; Kuriyama, N.; Xu, Q. *J. Power Sources* **2009**, *191*, 209-216.
63. Yan, J.-M.; Zhang, X.-B.; Han, S.; Shioyama, H.; Xu, Q. *Angew. Chem. Int. Ed.* **2008**, *47*, 2287-2289.
64. Yang, X.; Cheng, F.; Liang, J.; Tao, Z.; Chen, J. *Int. J. Hydrogen Energy* **2009**, *34*, 8785-8791.
65. Baitalow, F.; Baumann, J.; Wolf, G.; Jaenicke-Roessler, K.; Leitner, G. *Thermochim. Acta* **2002**, *391*, 159-168.
66. Hausdorf, S.; Baitalow, F.; Wolf, G.; Mertens, F. O. R. L. *Int. J. Hydrogen Energy* **2008**, *33*, 608-614.
67. Neiner, D.; Karkamkar, A.; Linehan, J. C.; Arey, B.; Autrey, T.; Kauzlarich, S. *M. J. Phys. Chem. C* **2008**, *113*, 1098-1103.

68. Stowe, A. C.; Shaw, W. J.; Linehan, J. C.; Schmid, B.; Autrey, T. *Phys. Chem. Chem. Phys.* **2007**, *9*, 1831-1836 and references therein.
69. Hu, M. G.; Geanangel, R. A.; Wendlandt, W. W. *Thermochim. Acta* **1978**, *23*, 249-255.
70. Komm, R.; Geanangel, R. A.; Liepins, R. *Inorg. Chem.* **1983**, *22*, 1684-1686.
71. Onak, T. P.; Shapiro, I. *J. Chem. Phys.* **1960**, *32*, 952.
72. Fazen, P. J.; Beck, J. S.; Lynch, A. T.; Remsen, E. E.; Sneddon, L. G. *Chem. Mater.* **1990**, *2*, 96-97.
73. Fazen, P. J.; Remsen, E. E.; Beck, J. S.; Carroll, P. J.; McGhie, A. R.; Sneddon, L. G. *Chem. Mater.* **1995**, *7*, 1942-1956.
74. Gervais, C.; Framery, E.; Duriez, C.; Maquet, J.; Vaultier, M.; Babonneau, F. *J. Eur. Ceram. Soc.* **2005**, *25*, 129-135.
75. Denis, J. M.; Forintos, H.; Szelke, H.; Toupet, L.; Pham, T. N.; Madec, P. J.; Gaumont, A. C. *Chem. Comm.* **2003**, 54-55.
76. Jaska, C. A.; Temple, K.; Lough, A. J.; Manners, I. *J. Am. Chem. Soc.* **2003**, *125*, 9424-9434.
77. Stephens, F. H.; Baker, R. T.; Matus, M. H.; Grant, D. J.; Dixon, D. A. *Angew. Chem. Int. Ed.* **2007**, *46*, 746-749.
78. Jaska, C. A.; Temple, K.; Lough, A. J.; Manners, I. *Chem. Comm.* **2001**, 962-963.
79. Jaska, C. A.; Manners, I. *J. Am. Chem. Soc.* **2004**, *126*, 2698-2699.
80. Clark, T. J.; Lee, K.; Manners, I. *Chem. Eur. J.* **2006**, *12*, 8634-8648.
81. Clark, T. J.; Russell, C. A.; Manners, I. *J. Am. Chem. Soc.* **2006**, *128*, 9582-9583.

82. Fulton, J. L.; Linehan, J. C.; Autrey, T.; Balasubramanian, M.; Chen, Y.; Scymczak, N. K. *J. Am. Chem. Soc.* **2007**, *129*, 11936-11949.
83. Chen, Y.; Fulton, J. L.; Linehan, J. C.; Autrey, T. *J. Am. Chem. Soc.* **2005**, *127*, 3254-3255.
84. Cheng, F.; Ma, H.; Li, Y.; Chen, J. *Inorg. Chem.* **2007**, *46*, 788-794.
85. Shrestha, R. P.; Diyabalanage, H. V. K.; Semelsberger, T. A.; Ott, K. C.; Burrell, A. K. *Int. J. Hydrogen Energy* **2009**, *34*, 2616-2621.
86. Zhang, X.-B.; Yan, J.-M.; Han, S.; Shioyama, H.; Xu, Q. *J. Am. Chem. Soc.* **2009**, *131*, 2778-2779.
87. Denney, M. C.; Pons, V.; Hebden, T. J.; Heinekey, D. M.; Goldberg, K. I. *J. Am. Chem. Soc.* **2006**, *128*, 12048-12049.
88. Dietrich, B. L.; Goldberg, K. I.; Heinekey, D. M.; Autrey, T.; Linehan, J. C. *Inorg. Chem.* **2008**, *47*, 8583-8585.
89. Paul, A.; Musgrave, C. B. *Angew. Chem. Int. Ed.* **2007**, *46*, 8153-8156.
90. Pons, V.; Baker, R. T.; Szymczak, N. K.; Heldebrant, D. J.; Linehan, J. C.; Matus, M. H.; Grant, D. J.; Dixon, D. A. *Chem. Comm.* **2008**, 6597-6599.
91. Keaton, R. J.; Blacquiere, J. M.; Baker, R. T. *J. Am. Chem. Soc.* **2007**, *129*, 1844-1845.
92. Zimmerman, P. M.; Paul, A.; Musgrave, C. B. *Inorg. Chem.* **2009**, *48*, 5418-5433.
93. Zimmerman, Paul M.; Paul, A.; Zhang, Z.; Musgrave, Charles B. *Angew. Chem. Int. Ed.* **2009**, *48*, 2201-2205.
94. Yang, X.; Hall, M. B. *J. Organomet. Chem.* **2009**, *694*, 2831-2838.
95. Pun, D.; Lobkovsky, E.; Chirik, P. J. *Chem. Comm.* **2007**, 3297-3299.

96. Staubitz, A.; Soto, A. P.; Manners, I. *Angew. Chem. Int. Ed.* **2008**, *47*, 6212-6215.
97. Hebden, T. J.; Denney, M. C.; Pons, V.; Piccoli, P. M. B.; Koetzle, T. F.; Schultz, A. J.; Kaminsky, W.; Goldberg, K. I.; Heinekey, D. M. *J. Am. Chem. Soc.* **2008**, *130*, 10812-10820.
98. Pons, V.; Denney, M. C.; Goldberg, K. I.; Heinekey, D. M. in *230th ACS National Meeting*, Washington, DC, 2005, FUEL-051.
99. Yang, X.; Hall, M. B. *J. Am. Chem. Soc.* **2008**, *130*, 1798-1799.
100. Luo, Y.; Ohno, K. *Organometallics* **2007**, *26*, 3597-3600.
101. Yan, J.-M.; Zhang, X.-B.; Han, S.; Shioyama, H.; Xu, Q. *Inorg. Chem.* **2009**, *48*, 7389-7393.
102. Ramachandran, P. V.; Gagare, P. D. *Inorg. Chem.* **2007**, *46*, 7810-7817.
103. Heldebrant, D. J.; Karkamkar, A.; Linehan, J. C.; Autrey, T. *Energy Environ. Sci.* **2008**, *1*, 156-160.
104. Davis, B. L.; Dixon, D. A.; Garner, E. B.; Gordon, J. C.; Matus, M. H.; Scott, B.; Stephens, F. H. *Angew. Chem. Int. Ed.* **2009**, *48*, DOI: 10.1002 and references therein.
105. Sutton, A. D.; Davis, B. L.; Bhattacharyya, K. X.; Ellis, B. D.; Gordon, J. C.; Power, P. P. *Chem. Comm.* **2010**, *46*, 148-149.
106. Mock, M. T.; Potter, R. G.; Camaioni, D. M.; Li, J.; Dougherty, W. G.; Kassel, W. S.; Twamley, B.; DuBois, D. L. *J. Am. Chem. Soc.* **2009**, *131*, 14454-14465.

## Chapter 2

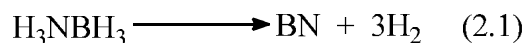
### Ammonia Borane Hydrogen Release in Ionic Liquids

#### Summary

Ionic liquids were found to promote the rate and extent of H<sub>2</sub>-release from ammonia borane (AB), a promising, high capacity hydrogen storage material. For example, AB reactions at 85 °C in 1-butyl-3-methylimidazolium chloride (bmimCl) (50:50-wt%) exhibited no induction period and released 1.0 H<sub>2</sub>-equiv. in 67 min and 2.2 H<sub>2</sub>-equiv. in 330 min at 85 °C, whereas comparable solid-state AB reactions had a 180 min induction period and required 360 min to release ~0.8 H<sub>2</sub>-equiv. at 85 °C, with the release of only another ~0.1 H<sub>2</sub>-equiv. at longer times. Significant rate enhancements for the ionic-liquid mixtures were obtained with only moderate increases in temperature, with, for example, a 50:50-wt% AB/bmimCl mixture releasing 1.0 H<sub>2</sub>-equiv. in 5 min and 2.2 H<sub>2</sub>-equiv. in only 20 min at 110 °C. Increasing the AB/bmimCl ratio to 80:20 still gave enhanced H<sub>2</sub>-release rates compared to the solid-state, and produced a system that achieved 11.4 materials-weight percent H<sub>2</sub>-release. Solid-state and solution <sup>11</sup>B NMR studies of AB H<sub>2</sub>-release reactions in progress support a mechanistic pathway involving: (1) ionic-liquid promoted conversion of AB into its more reactive ionic diammoniate of diborane (DADB) form, (2) further intermolecular dehydrocoupling reactions between hydridic B-H hydrogens and protonic N-H hydrogens on DADB and/or AB to form neutral polyaminoborane polymers and (3) polyaminoborane dehydrogenation to unsaturated cross-linked polyborazylene materials.

## 2.1 Introduction

The requirement for efficient and safe methods for hydrogen storage is a major hurdle that must be overcome to enable the use of hydrogen as an alternative energy carrier.<sup>1,2</sup> Owing to its high hydrogen content, ammonia borane (AB) has been identified as one of the leading candidates for chemical hydrogen storage, potentially releasing 19.6 wt% H<sub>2</sub> according to **Equation 2.1**.<sup>3</sup>



As discussed in **Chapter 1**, partial dehydrogenation of ammonia borane can be thermally induced in the solid-state,<sup>4,5</sup> but to be useful for hydrogen storage, milder conditions and more controllable reactions still need to be developed. Such reactions could, in principle, be attained in solution, but practical applications of chemical hydrogen storage would require a replacement for the volatile organic solvents that have traditionally been employed for reactions of molecular chemical hydrides. The work reported in this **Chapter** demonstrates that ionic liquids provide advantageous media for ammonia borane dehydrogenation in which both the extent and rate of hydrogen release are significantly increased. Solid-state and *in situ* <sup>11</sup>B NMR studies of reactions in progress are also presented that provide insight into the intermediates and mechanistic steps involved in ionic-liquid promoted AB H<sub>2</sub>-release.

## 2.2 Experimental Section

### 2.2.1 Materials

All manipulations were carried out using standard high-vacuum or inert-atmosphere techniques as described by Shriver.<sup>6</sup> Ammonia borane (Aviabor 97% minimum purity) was ground into a free flowing powder using a commercial coffee grinder. The diammoniate of diborane (DADB) was synthesized by the literature method.<sup>7</sup> The 1-butyl-3-methylimidazolium iodide (bmimI) was synthesized sonochemically from 1-iodobutane and 1-methyl-imidazole according to literature methods.<sup>8</sup> All ionic liquids, including 1-butyl-2,3-dimethylimidazolium chloride (bmmimCl) (EMD), 1-butyl-3-methylimidazolium tetrafluoroborate (bmimBF<sub>4</sub>), 1-butyl-3-methylimidazolium chloride (bmimCl), 1-butyl-3-methylimidazolium triflate (bmimOTf), 1-butyl-3-methylimidazolium hexafluorophosphate (bmimPF<sub>6</sub>), 1-ethyl-2,3-dimethylimidazolium ethylsulfate (emmimEtSO<sub>4</sub>), 1-ethyl-2,3-dimethylimidazolium triflate (emmimOTf), 1,3-dimethylimidazolium methylsulfate (mmimMeSO<sub>4</sub>) and 1-propyl-2,3-dimethylimidazolium triflate (pmmimTf<sub>3</sub>C) (Aldrich) were dried by toluene azeotropic distillation to remove any moisture. Tetraethylene glycol dimethyl ether (Sigma 99%) (tetraglyme) and ethylene glycol dimethyl ether (Sigma 99%) (glyme) were distilled from sodium under vacuum with heating.

### 2.2.2 Physical Measurements

#### 2.2.2.1 H<sub>2</sub>-Release Measured On a Toepler Pump

The Toepler pump system used for hydrogen measurements was similar to that described by Shriver.<sup>6</sup> The Toepler pump (**Figure 2.1**) system also enabled the trapping



of any volatile dehydrogenation products. This method of measuring H<sub>2</sub>-release worked best for reactions with slow H<sub>2</sub>-release rates, since the Toepler pump requires several minutes to make each measurement. The released gases from the reaction vessel were first passed through a liquid nitrogen trap before continuing on to the Toepler pump (700 mL). The released H<sub>2</sub> was then pumped into a series of calibrated volumes with the final pressure of the collected H<sub>2</sub> gas measured ( $\pm 0.5$  mm) with the aid of a U-tube manometer. After the H<sub>2</sub> measurement was completed, the in-line liquid nitrogen trap was warmed to room temperature and the amount of any volatiles that had been trapped were then also measured using the Toepler pump.

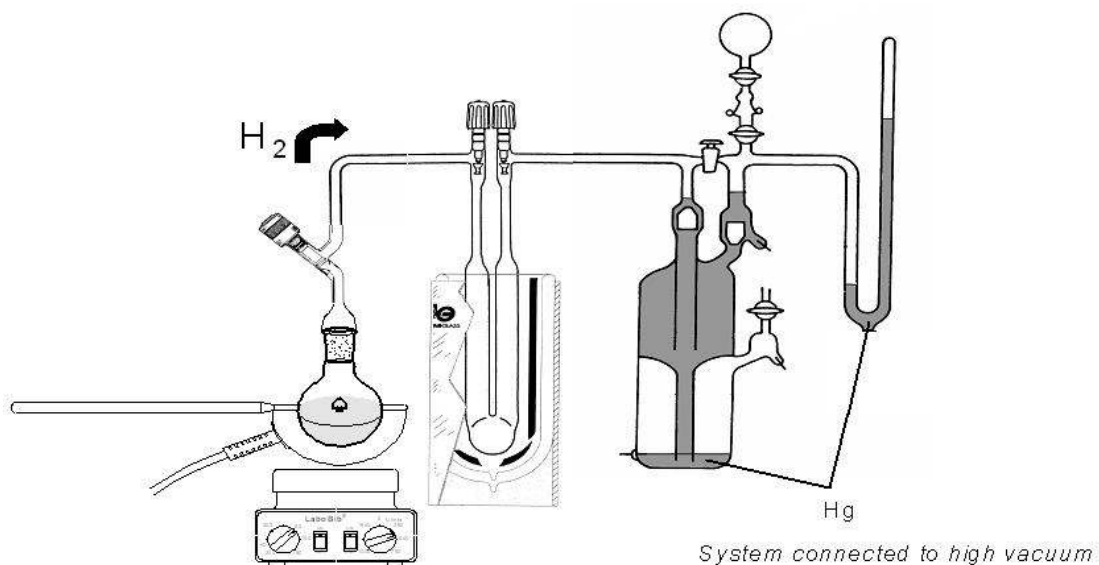


**Figure 2.1** Toepler pump system used for H<sub>2</sub>-release measurements.

#### 2.2.2.2 H<sub>2</sub>-Release Measured On an Automated Gas Burette

For reactions with faster rates, an automated gas burette was employed for H<sub>2</sub>-release measurements. The automated gas burette (**Figure 2.2**) was based on a design

reported by Zheng et al.,<sup>9</sup> but employed all glass connections with a cold trap (-78 °C) inserted between the reaction flask and burette to allow trapping of any volatiles that might have been produced during the reaction. The gas burette enabled rapid data collection of H<sub>2</sub>-release at short time ranges.

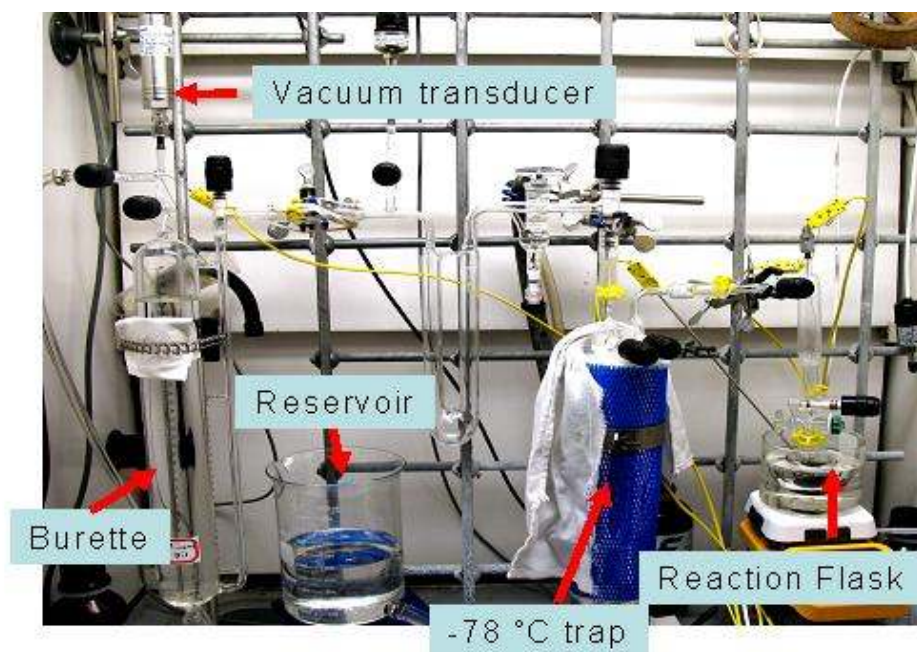


**Figure 2.2** Automated gas burette used for H<sub>2</sub>-release measurements.

Unlike the Toepler pump reactions, which were run under vacuum, reactions carried out with the burette were run under inert gas at atmospheric pressure to mimic real-world conditions. As shown in **Figure 2.2**, the reactions were carried out in the volume-calibrated flask on the right, which was plunged into a pre-heated oil bath to start the reaction. On top of the reaction flask was an air condenser to keep most of the volatiles in the reaction flask. The H<sub>2</sub> stream, along with any additional volatiles, passed through the -78 °C trap and flowed into the bottom of the oil-filled burette. As H<sub>2</sub>

collected at the top of the burette, the oil flowed into a reservoir kept at atmospheric pressure (measured with pressure gauge). The pressure difference in the burette was tracked with a vacuum transducer and the temperature was tracked at multiple locations with thermocouples. All data were collected and processed on a program written in LabVIEW 8.5 by Zheng et al.<sup>9</sup>

A typical data set collected with the automated gas burette is shown in **Table 2.1** where the data in columns one and two run from page 6 to 24, then begin again in columns 3 and 4. The data set is plotted in **Figure 2.4** plot B. The number of seconds per data point was set from 1 point per second up to 10 or more seconds per point depending on the rate of the reaction and length of reaction. The example is from the measurement of the H<sub>2</sub>-release from a solid-state AB sample at 85 °C for ~400 minutes with 1 point every 10 seconds. The flask was plunged into the oil bath at time point 0.73698 min after the computer program had time to equilibrate. Since this was a solid-state reaction, the time between plunging the flask into the oil bath and the onset of H<sub>2</sub>-release corresponds to the AB induction period. The fluctuations in the baseline before the onset of H<sub>2</sub>-release are just due to signal noise. H<sub>2</sub>-release began at the bolded time point 170.203 min on page 20 and essentially stopped at the bolded point 376.604 min on page 22. Control experiments conducted without AB showed negligible pressure change, corresponding to less than <0.01 gas equivalents, when a helium filled reaction flask connected to the gas burette was heated up to 120 °C. Clearly, a large amount of data can be collected with this setup. The rest of the data sets for the gas burette graphs presented in **Chapter 2** are available on a CD submitted with the paper copy of this

dissertation and electronically in the supplementary files submitted with the electronic copy of this dissertation.

**Table 2.1. AB H<sub>2</sub>-Release Data Collected on the Automated Gas Burette from the H<sub>2</sub>-Release Reaction of a Solid-State AB Sample at 85 °C**

Equiv.	Time	Equiv.	Time	Equiv.	Time	Equiv.	Time
0	0.33698	0.02658	98.337	0.0856	196.47	0.66494	294.603
-0.001	0.47031	0.02712	98.4701	0.08554	196.604	0.66583	294.737
-0.0028	0.60365	0.02562	98.6034	0.08685	196.737	0.6648	294.87
-0.0009	0.73698	0.025	98.737	0.08798	196.87	0.66334	295.003
0.00396	0.87031	0.0242	98.8703	0.08789	197.003	0.66541	295.137
0.11409	1.00365	0.02481	99.0036	0.08893	197.137	0.66588	295.27
0.04792	1.13672	0.02395	99.137	0.08952	197.27	0.66595	295.403
0.03474	1.27005	0.02207	99.2703	0.08984	197.403	0.66779	295.537
0.02714	1.40365	0.0235	99.4036	0.09402	197.537	0.66859	295.67
0.01239	1.53672	0.02249	99.537	0.09007	197.67	0.66852	295.803
0.0034	1.67005	0.02169	99.6701	0.09194	197.803	0.66792	295.937
-0.0033	1.80339	0.02341	99.8036	0.09225	197.937	0.6691	296.07
-0.0058	1.93672	0.02322	99.937	0.09327	198.07	0.66914	296.203
-0.0004	2.07005	0.02372	100.07	0.09267	198.203	0.66912	296.337
-0.0061	2.20339	0.02417	100.203	0.09316	198.337	0.66991	296.47
-0.0086	2.33672	0.02417	100.337	0.09308	198.47	0.67269	296.603
-0.0027	2.47005	0.02336	100.47	0.09507	198.604	0.67334	296.737
-0.0059	2.60365	0.02339	100.604	0.09856	198.737	0.67406	296.87
-0.0079	2.73698	0.02378	100.737	0.09568	198.87	0.6737	297.003
0.00052	2.87031	0.02494	100.87	0.09653	199.003	0.6729	297.137
-0.0082	3.00365	0.02403	101.004	0.096	199.137	0.67458	297.27
-0.0082	3.13698	0.02175	101.137	0.09687	199.27	0.67574	297.403
-0.0094	3.27005	0.01951	101.27	0.10136	199.403	0.67612	297.537
-0.0083	3.40339	0.02296	101.403	0.09723	199.537	0.67767	297.67
-0.009	3.53672	0.02577	101.537	0.09853	199.67	0.67786	297.803
-0.0092	3.67005	0.02668	101.67	0.09974	199.803	0.67661	297.937
-0.0096	3.80339	0.0232	101.804	0.09993	199.937	0.67861	298.07
-0.0086	3.93672	0.02046	101.937	0.10082	200.07	0.67827	298.204
-0.0081	4.07005	0.02377	102.07	0.10217	200.204	0.67904	298.337
-0.0093	4.20365	0.02235	102.203	0.10229	200.337	0.68326	298.47
-0.0078	4.33698	0.02219	102.337	0.10306	200.47	0.67994	298.603

-0.0072	4.47031	0.0219	102.47	0.10432	200.604	0.68089	298.737
-0.0116	4.60365	0.02299	102.603	0.10474	200.737	0.68135	298.87
-0.0102	4.73698	0.02317	102.737	0.10441	200.87	0.68121	299.003
-0.0113	4.87031	0.02508	102.87	0.10529	201.004	0.68326	299.137
-0.0102	5.00339	0.02422	103.003	0.1057	201.137	0.68312	299.27
-0.0096	5.13672	0.02233	103.137	0.10689	201.27	0.68413	299.403
-0.0079	5.27031	0.02144	103.27	0.10769	201.403	0.6847	299.537
-0.0087	5.40365	0.0234	103.403	0.10678	201.537	0.68473	299.67
-0.0079	5.53672	0.02223	103.537	0.10657	201.67	0.68436	299.803
-0.0068	5.67005	0.0223	103.67	0.109	201.803	0.68641	299.937
-0.0079	5.80339	0.02298	103.803	0.10806	201.937	0.68577	300.07
-0.0082	5.93672	0.02354	103.937	0.10802	202.07	0.68527	300.204
-0.0068	6.07005	0.02253	104.07	0.10857	202.204	0.69099	300.337
-0.008	6.20339	0.02204	104.204	0.10881	202.337	0.68879	300.47
-0.006	6.33672	0.02254	104.337	0.10884	202.47	0.68815	300.603
-0.0065	6.47005	0.0234	104.47	0.11114	202.603	0.68872	300.737
-0.0077	6.60365	0.021	104.604	0.11099	202.737	0.69124	300.87
-0.0075	6.73672	0.02026	104.737	0.11133	202.87	0.68864	301.004
-0.0074	6.87005	0.0209	104.87	0.11186	203.003	0.68754	301.137
-0.0072	7.00365	0.02104	105.003	0.11276	203.137	0.69084	301.27
-0.0068	7.13698	0.02005	105.137	0.11234	203.27	0.68952	301.403
-0.0062	7.27031	0.02162	105.27	0.11355	203.403	0.68689	301.537
-0.0053	7.40365	0.02308	105.403	0.11429	203.537	0.68979	301.67
-0.0073	7.53698	0.02474	105.537	0.11815	203.67	0.69288	301.803
-0.0063	7.67031	0.02237	105.67	0.11391	203.803	0.69166	301.937
-0.005	7.80339	0.02222	105.803	0.114	203.937	0.69201	302.07
-0.0039	7.93698	0.02366	105.937	0.1164	204.07	0.69404	302.204
-0.0037	8.07005	0.02226	106.07	0.11704	204.203	0.69321	302.337
-0.0032	8.20339	0.01967	106.204	0.11797	204.337	0.6927	302.47
-0.0018	8.33672	0.01915	106.337	0.11787	204.47	0.69365	302.603
-0.0014	8.47005	0.02022	106.47	0.11874	204.603	0.69462	302.737
-0.0017	8.60339	0.02004	106.604	0.11848	204.737	0.69368	302.87
-0.0017	8.73672	0.01944	106.737	0.1184	204.87	0.69443	303.003
-0.0032	8.87005	0.01986	106.87	0.12355	205.003	0.69587	303.137
-0.0016	9.00365	0.02008	107.003	0.11887	205.137	0.69438	303.27
-0.0024	9.13698	0.01945	107.137	0.12503	205.27	0.69531	303.403
-0.003	9.27031	0.02125	107.27	0.11891	205.403	0.70269	303.537
-0.0027	9.40365	0.02048	107.403	0.12618	205.537	0.69627	303.67
-0.0037	9.53672	0.02135	107.537	0.12141	205.67	0.69645	303.803
-0.0035	9.67005	0.02216	107.67	0.12214	205.803	0.6978	303.937

-0.0059	9.80339	0.0209	107.803	0.12438	205.937	0.69712	304.07
-0.0045	9.93672	0.02211	107.937	0.12426	206.07	0.69896	304.203
-0.0061	10.0701	0.02264	108.07	0.12478	206.203	0.69983	304.337
-0.0072	10.2034	0.02195	108.203	0.12379	206.337	0.6995	304.47
-0.0053	10.337	0.02318	108.337	0.12542	206.47	0.70035	304.604
-0.0047	10.4703	0.0223	108.47	0.1249	206.604	0.69854	304.737
-0.003	10.6034	0.02209	108.604	0.1262	206.737	0.70157	304.87
-0.0035	10.7367	0.02101	108.737	0.12519	206.87	0.70017	305.003
-0.0022	10.8701	0.02324	108.87	0.12987	207.004	0.69967	305.137
-0.0025	11.0034	0.01943	109.003	0.12795	207.137	0.70263	305.27
-0.0059	11.1367	0.0189	109.137	0.12902	207.27	0.70049	305.403
-0.0037	11.2701	0.01892	109.27	0.12921	207.403	0.70037	305.537
-0.0032	11.4034	0.01946	109.403	0.13117	207.537	0.70161	305.67
-0.0014	11.5367	0.01958	109.537	0.13647	207.67	0.70326	305.804
-0.0013	11.6703	0.02033	109.67	0.13124	207.803	0.70205	305.937
-0.002	11.8036	0.0206	109.804	0.13229	207.937	0.70777	306.07
-0.001	11.937	0.0176	109.937	0.13364	208.07	0.70465	306.203
-0.0013	12.0703	0.0189	110.07	0.13245	208.203	0.70565	306.337
-0.001	12.2034	0.01988	110.203	0.13491	208.337	0.70484	306.47
0.00017	12.3367	0.01989	110.337	0.13572	208.47	0.70463	306.603
-0.0016	12.4701	0.02006	110.47	0.13521	208.604	0.70603	306.737
-3E-05	12.6034	0.02108	110.603	0.13579	208.737	0.70855	306.87
-0.0008	12.7367	0.02192	110.737	0.13622	208.87	0.70911	307.003
-0.0015	12.8701	0.02093	110.87	0.13762	209.003	0.70957	307.137
-0.001	13.0034	0.02105	111.003	0.13761	209.137	0.70839	307.27
-0.0015	13.1367	0.02027	111.137	0.13718	209.27	0.70805	307.404
-0.0034	13.2701	0.01836	111.27	0.1384	209.403	0.7096	307.537
-0.0022	13.4034	0.01941	111.404	0.13909	209.537	0.70909	307.67
-0.002	13.537	0.01964	111.537	0.14142	209.67	0.71002	307.803
-0.0008	13.6701	0.01894	111.67	0.1402	209.803	0.71072	307.937
-0.0015	13.8034	0.02002	111.804	0.1424	209.937	0.71083	308.07
-0.0012	13.9367	0.01848	111.937	0.14255	210.07	0.7088	308.203
-0.0023	14.0703	0.01885	112.07	0.14904	210.203	0.71038	308.337
-0.0003	14.2036	0.02013	112.204	0.14438	210.337	0.71131	308.47
0.00251	14.337	0.01886	112.337	0.14477	210.47	0.71075	308.603
0.00019	14.4701	0.02203	112.47	0.14527	210.603	0.71343	308.737
0.00033	14.6034	0.01827	112.604	0.1455	210.737	0.71753	308.87
0.00107	14.7367	0.01653	112.737	0.14654	210.87	0.71378	309.004
6.2E-05	14.8701	0.01661	112.87	0.14708	211.003	0.71479	309.137
-0.0011	15.0034	0.01998	113.003	0.14995	211.137	0.7142	309.27

-0.0009	15.1367	0.01948	113.137	0.14777	211.27	0.71503	309.403
-0.0018	15.2701	0.01859	113.27	0.14778	211.403	0.71451	309.537
-0.0009	15.4034	0.01893	113.404	0.15098	211.537	0.71584	309.67
-0.0015	15.5367	0.02005	113.537	0.15044	211.67	0.71626	309.803
-0.0008	15.6701	0.0175	113.67	0.15234	211.803	0.7173	309.937
0.00051	15.8034	0.01682	113.804	0.15354	211.937	0.71778	310.07
-0.0003	15.9367	0.01658	113.937	0.15294	212.07	0.71751	310.203
0.00095	16.0701	0.01625	114.07	0.15189	212.203	0.71713	310.337
0.00142	16.2034	0.01796	114.203	0.15813	212.337	0.71665	310.47
0.00253	16.3367	0.01859	114.337	0.15274	212.47	0.71799	310.603
0.00324	16.4701	0.01771	114.47	0.15374	212.603	0.718	310.737
0.00279	16.6036	0.0171	114.603	0.15557	212.737	0.71944	310.87
0.00204	16.737	0.0173	114.737	0.15648	212.87	0.72001	311.003
0.00364	16.8703	0.01574	114.87	0.15685	213.003	0.72053	311.137
0.00345	17.0034	0.01238	115.004	0.15804	213.137	0.72059	311.27
0.00343	17.1367	0.0101	115.137	0.15841	213.27	0.72031	311.403
0.00302	17.2701	0.01301	115.27	0.15994	213.403	0.71998	311.537
0.00253	17.4034	0.01563	115.403	0.16098	213.537	0.72049	311.67
0.00348	17.5367	0.0196	115.537	0.1615	213.67	0.72124	311.803
0.002	17.6701	0.01852	115.67	0.16079	213.803	0.72156	311.937
0.00404	17.8034	0.01831	115.803	0.16267	213.937	0.72197	312.07
0.00173	17.9367	0.02023	115.937	0.16326	214.07	0.72255	312.204
0.0024	18.0701	0.01766	116.07	0.16836	214.203	0.72173	312.337
0.00254	18.2034	0.01904	116.203	0.16268	214.337	0.72353	312.47
0.00141	18.3367	0.01896	116.337	0.16574	214.47	0.72379	312.604
0.00126	18.4701	0.01705	116.47	0.16587	214.603	0.72455	312.737
0.00152	18.6034	0.01702	116.603	0.16666	214.737	0.72391	312.87
0.00218	18.7367	0.01585	116.737	0.16628	214.87	0.72493	313.003
0.00475	18.8701	0.01737	116.87	0.16753	215.003	0.72504	313.137
0.0036	19.0034	0.01707	117.004	0.16989	215.137	0.72668	313.27
0.00313	19.1367	0.01748	117.137	0.16946	215.27	0.72588	313.403
0.00458	19.2701	0.0186	117.27	0.17057	215.403	0.72731	313.537
0.00403	19.4034	0.01763	117.403	0.16991	215.537	0.72665	313.67
0.00272	19.5367	0.01812	117.537	0.17193	215.67	0.72953	313.803
0.00395	19.6701	0.01827	117.67	0.17121	215.803	0.72875	313.937
0.00456	19.8034	0.01858	117.803	0.17135	215.937	0.72842	314.07
0.00274	19.937	0.01673	117.937	0.17144	216.07	0.72875	314.203
0.00404	20.0703	0.01947	118.07	0.17298	216.203	0.72953	314.337
0.00284	20.2036	0.01828	118.203	0.17502	216.337	0.73029	314.47
0.00351	20.3367	0.01941	118.337	0.17453	216.47	0.73036	314.603

0.00251	20.4701	0.01912	118.47	0.17324	216.603	0.73095	314.737
0.00368	20.6036	0.01974	118.604	0.17767	216.737	0.73115	314.87
0.004	20.737	0.01945	118.737	0.17612	216.87	0.73149	315.003
0.00335	20.8703	0.0186	118.87	0.17559	217.003	0.73046	315.137
0.00125	21.0034	0.01985	119.004	0.17749	217.137	0.73183	315.27
0.00198	21.1367	0.01979	119.137	0.17708	217.27	0.73362	315.403
0.00338	21.2701	0.02022	119.27	0.17884	217.403	0.73284	315.537
0.00489	21.4034	0.01893	119.403	0.177	217.537	0.73225	315.67
0.00465	21.5367	0.01982	119.537	0.17966	217.67	0.73408	315.804
0.00545	21.6701	0.01905	119.67	0.17913	217.804	0.7327	315.937
0.00455	21.8034	0.01972	119.804	0.17926	217.937	0.7321	316.07
0.00234	21.9367	0.01925	119.937	0.18457	218.07	0.73446	316.203
0.00016	22.0703	0.01931	120.07	0.17977	218.203	0.73413	316.337
0.00311	22.2034	0.01929	120.204	0.17935	218.337	0.7348	316.47
0.00186	22.3367	0.01635	120.337	0.1807	218.47	0.73592	316.603
0.00112	22.4703	0.01829	120.47	0.18418	218.603	0.73401	316.737
0.00354	22.6036	0.01785	120.603	0.1852	218.737	0.73571	316.87
0.00341	22.737	0.01784	120.737	0.18374	218.87	0.73558	317.003
0.00449	22.8701	0.01974	120.87	0.18576	219.003	0.73626	317.137
0.00434	23.0034	0.0183	121.003	0.18614	219.137	0.73645	317.27
0.00619	23.1367	0.01661	121.137	0.18615	219.27	0.7367	317.403
0.00414	23.2701	0.01608	121.27	0.18765	219.403	0.7367	317.537
0.00643	23.4036	0.01758	121.403	0.18645	219.537	0.73661	317.67
0.00292	23.5367	0.01789	121.537	0.19185	219.67	0.73483	317.803
0.00531	23.6701	0.01662	121.67	0.18642	219.803	0.73805	317.937
0.00287	23.8034	0.01736	121.803	0.18755	219.937	0.738	318.07
0.00337	23.9367	0.01797	121.937	0.18809	220.07	0.7378	318.203
0.00527	24.0703	0.01843	122.07	0.19024	220.203	0.74415	318.337
0.00594	24.2036	0.01653	122.203	0.19127	220.337	0.7387	318.47
0.00479	24.337	0.01668	122.337	0.1918	220.47	0.7391	318.603
0.00306	24.4701	0.01761	122.47	0.19236	220.603	0.73806	318.737
0.00463	24.6034	0.01853	122.603	0.1914	220.737	0.73781	318.87
0.00416	24.7367	0.01806	122.737	0.19569	220.87	0.74008	319.003
0.00367	24.8701	0.01851	122.87	0.19453	221.004	0.73815	319.137
0.00492	25.0036	0.01683	123.004	0.19406	221.137	0.73981	319.27
0.00625	25.1367	0.0175	123.137	0.1975	221.27	0.74066	319.404
0.0065	25.2701	0.01658	123.27	0.19701	221.404	0.74088	319.537
0.00885	25.4036	0.0162	123.403	0.19644	221.537	0.74161	319.67
0.0072	25.537	0.01605	123.537	0.19916	221.67	0.74172	319.804
0.00715	25.6703	0.01585	123.67	0.19787	221.803	0.74118	319.937



0.00868	25.8034	0.01674	123.804	0.19755	221.937	0.74092	320.07
0.00503	25.9367	0.0176	123.937	0.19918	222.07	0.74133	320.203
0.00513	26.0701	0.01698	124.07	0.20076	222.203	0.74273	320.337
0.00727	26.2036	0.01664	124.204	0.19998	222.337	0.74404	320.47
0.00794	26.3367	0.01653	124.337	0.2007	222.47	0.74427	320.603
0.00544	26.4703	0.01741	124.47	0.20406	222.604	0.74424	320.737
0.00526	26.6034	0.01705	124.603	0.2036	222.737	0.74329	320.87
0.00525	26.7367	0.01587	124.737	0.20339	222.87	0.74638	321.003
0.00448	26.8701	0.01661	124.87	0.20083	223.003	0.74531	321.137
0.00433	27.0036	0.01716	125.003	0.1981	223.137	0.74537	321.27
0.00493	27.137	0.01597	125.137	0.2023	223.27	0.74573	321.403
0.00525	27.2701	0.01704	125.27	0.21148	223.403	0.74518	321.537
0.00637	27.4036	0.01761	125.403	0.20251	223.537	0.74617	321.67
0.00543	27.537	0.0167	125.537	0.19912	223.67	0.74684	321.803
0.00763	27.6703	0.01747	125.67	0.20233	223.803	0.74594	321.937
0.00576	27.8036	0.01726	125.803	0.20432	223.937	0.75148	322.07
0.00588	27.937	0.01591	125.937	0.20174	224.07	0.74688	322.203
0.0062	28.0703	0.01505	126.07	0.20244	224.203	0.74865	322.337
0.00751	28.2034	0.0157	126.204	0.20458	224.337	0.74892	322.47
0.00728	28.3367	0.01596	126.337	0.20479	224.47	0.7486	322.603
0.00679	28.4701	0.01703	126.47	0.20189	224.603	0.74989	322.737
0.0076	28.6034	0.01717	126.604	0.20553	224.737	0.74987	322.87
0.00887	28.7367	0.01814	126.737	0.20561	224.87	0.75018	323.004
0.00665	28.8701	0.01647	126.87	0.20405	225.003	0.75001	323.137
0.00825	29.0034	0.01438	127.003	0.20587	225.137	0.75101	323.27
0.00605	29.1367	0.01686	127.137	0.20791	225.27	0.75217	323.403
0.00654	29.2701	0.0158	127.27	0.20829	225.403	0.75086	323.537
0.00577	29.4036	0.01712	127.403	0.20707	225.537	0.75092	323.67
0.00559	29.537	0.01658	127.537	0.21074	225.67	0.75087	323.804
0.00621	29.6701	0.01545	127.67	0.21619	225.803	0.75186	323.937
0.00639	29.8034	0.01575	127.804	0.21122	225.937	0.75277	324.07
0.00892	29.9367	0.01496	127.937	0.21213	226.07	0.75351	324.203
0.00675	30.0701	0.01665	128.07	0.21173	226.203	0.7523	324.337
0.00854	30.2034	0.01666	128.204	0.21214	226.337	0.75194	324.47
0.00738	30.3367	0.01878	128.337	0.21494	226.47	0.75252	324.604
0.006	30.4701	0.01564	128.47	0.21455	226.603	0.75326	324.737
0.00525	30.6034	0.01869	128.603	0.22146	226.737	0.75391	324.87
0.00663	30.7367	0.01835	128.737	0.21374	226.87	0.75883	325.003
0.00786	30.8701	0.01633	128.87	0.21781	227.003	0.75636	325.137
0.00832	31.0034	0.01615	129.003	0.21589	227.137	0.7561	325.27

0.00861	31.1367	0.01885	129.137	0.22215	227.27	0.75428	325.403
0.00918	31.2701	0.01593	129.27	0.22167	227.403	0.75576	325.537
0.0079	31.4034	0.01708	129.404	0.21928	227.537	0.75542	325.67
0.00735	31.537	0.01845	129.537	0.21859	227.67	0.75559	325.803
0.00746	31.6703	0.0166	129.67	0.22591	227.803	0.75531	325.937
0.00762	31.8036	0.01745	129.803	0.22361	227.937	0.75595	326.07
0.00917	31.937	0.01729	129.937	0.22243	228.07	0.7575	326.203
0.00923	32.0703	0.01705	130.07	0.22575	228.203	0.75686	326.337
0.00951	32.2034	0.01797	130.203	0.23037	228.337	0.75712	326.47
0.01125	32.337	0.0168	130.337	0.22597	228.47	0.75651	326.603
0.01144	32.4701	0.01663	130.47	0.22881	228.603	0.75652	326.737
0.00982	32.6034	0.01779	130.604	0.22784	228.737	0.75763	326.87
0.01375	32.7367	0.01785	130.737	0.23594	228.87	0.75839	327.004
0.01255	32.8701	0.01792	130.87	0.22948	229.004	0.75769	327.137
0.01096	33.0034	0.01906	131.004	0.23248	229.137	0.7583	327.27
0.01038	33.1367	0.01505	131.137	0.23137	229.27	0.75826	327.403
0.01106	33.2701	0.0172	131.27	0.23326	229.403	0.7596	327.537
0.01134	33.4034	0.01823	131.403	0.23528	229.537	0.75857	327.67
0.01033	33.5367	0.01921	131.537	0.23367	229.67	0.75744	327.803
0.0115	33.6701	0.01748	131.67	0.2359	229.803	0.75769	327.937
0.01077	33.8034	0.01632	131.804	0.24432	229.937	0.75861	328.07
0.00996	33.937	0.01729	131.937	0.23796	230.07	0.75796	328.203
0.00856	34.0701	0.01715	132.07	0.23752	230.203	0.76135	328.337
0.00938	34.2036	0.01672	132.203	0.24026	230.337	0.75874	328.47
0.00968	34.3367	0.01889	132.337	0.2472	230.47	0.75863	328.604
0.00813	34.4701	0.01772	132.47	0.24133	230.604	0.76074	328.737
0.00864	34.6034	0.01798	132.603	0.24268	230.737	0.75954	328.87
0.00964	34.7367	0.01742	132.737	0.24552	230.87	0.7606	329.004
0.00958	34.8701	0.01602	132.87	0.24588	231.004	0.76095	329.137
0.009	35.0034	0.01548	133.003	0.24501	231.137	0.76094	329.27
0.00827	35.1367	0.01538	133.137	0.24775	231.27	0.75979	329.403
0.0098	35.2701	0.0163	133.27	0.25521	231.404	0.75996	329.537
0.01	35.4034	0.01638	133.403	0.24844	231.537	0.76145	329.67
0.01102	35.5367	0.01646	133.537	0.24987	231.67	0.76305	329.804
0.01215	35.6701	0.01671	133.67	0.25177	231.803	0.76255	329.937
0.01005	35.8034	0.0163	133.803	0.25197	231.937	0.76356	330.07
0.01112	35.9367	0.01571	133.937	0.25299	232.07	0.76287	330.203
0.01147	36.0701	0.01493	134.07	0.25406	232.204	0.76319	330.337
0.01112	36.2034	0.0162	134.203	0.26005	232.337	0.76336	330.47
0.01119	36.3367	0.01696	134.337	0.25476	232.47	0.76322	330.603

0.01033	36.4701	0.01588	134.47	0.25412	232.603	0.76473	330.737
0.0099	36.6034	0.01672	134.603	0.26367	232.737	0.76381	330.87
0.01064	36.737	0.01556	134.737	0.25695	232.87	0.76317	331.004
0.01167	36.8703	0.01631	134.87	0.25737	233.003	0.76474	331.137
0.01087	37.0036	0.01576	135.003	0.26074	233.137	0.76559	331.27
0.01132	37.1367	0.01595	135.137	0.26125	233.27	0.76427	331.403
0.01091	37.2701	0.01438	135.27	0.26118	233.403	0.76952	331.537
0.01103	37.4034	0.01605	135.403	0.26164	233.537	0.76629	331.67
0.0102	37.5367	0.01608	135.537	0.26281	233.67	0.76554	331.803
0.01062	37.6701	0.01461	135.67	0.26627	233.803	0.76573	331.937
0.01029	37.8034	0.0166	135.803	0.26478	233.937	0.76738	332.07
0.01093	37.9367	0.01766	135.937	0.26582	234.07	0.76638	332.203
0.01063	38.0701	0.01502	136.07	0.2668	234.203	0.76713	332.337
0.01251	38.2034	0.01333	136.203	0.26734	234.337	0.76788	332.47
0.01051	38.3367	0.01392	136.337	0.27272	234.47	0.76774	332.603
0.00974	38.4701	0.01589	136.47	0.26924	234.603	0.76666	332.737
0.01074	38.6036	0.01462	136.603	0.26928	234.737	0.76649	332.87
0.00993	38.7367	0.01359	136.737	0.27109	234.87	0.76577	333.004
0.01233	38.8701	0.01583	136.87	0.27189	235.003	0.76658	333.137
0.01247	39.0034	0.01598	137.003	0.2721	235.137	0.76613	333.27
0.01271	39.1367	0.01543	137.137	0.27201	235.27	0.76639	333.404
0.01225	39.2703	0.01758	137.27	0.27429	235.403	0.76724	333.537
0.01248	39.4036	0.01419	137.403	0.27409	235.537	0.76828	333.67
0.01225	39.537	0.01471	137.537	0.2748	235.67	0.76803	333.803
0.01293	39.6701	0.01616	137.67	0.27575	235.803	0.77098	333.937
0.0125	39.8034	0.01349	137.803	0.27788	235.937	0.76964	334.07
0.01501	39.9367	0.01395	137.937	0.27925	236.07	0.7699	334.203
0.01482	40.0701	0.01435	138.07	0.28146	236.203	0.7704	334.337
0.01317	40.2036	0.01563	138.203	0.27942	236.337	0.76959	334.47
0.01146	40.337	0.01594	138.337	0.28057	236.47	0.76959	334.603
0.0119	40.4701	0.0145	138.47	0.28459	236.604	0.77076	334.737
0.0119	40.6036	0.01667	138.603	0.2828	236.737	0.7716	334.87
0.01225	40.737	0.01533	138.737	0.2831	236.87	0.77092	335.004
0.0118	40.8703	0.0145	138.87	0.28977	237.003	0.7715	335.137
0.0139	41.0036	0.0165	139.004	0.28448	237.137	0.77208	335.27
0.01251	41.137	0.01481	139.137	0.28525	237.27	0.77235	335.404
0.01268	41.2703	0.01605	139.27	0.28634	237.403	0.77255	335.537
0.01202	41.4036	0.01538	139.403	0.29191	237.537	0.77171	335.67
0.01221	41.537	0.01505	139.537	0.28972	237.67	0.77325	335.803
0.01071	41.6701	0.01684	139.67	0.2896	237.803	0.773	335.937

0.01182	41.8034	0.01654	139.804	0.28931	237.937	0.7728	336.07
0.0134	41.937	0.01618	139.937	0.29006	238.07	0.77413	336.203
0.01369	42.0701	0.01742	140.07	0.2996	238.203	0.77443	336.337
0.01485	42.2034	0.01714	140.204	0.29191	238.337	0.77279	336.47
0.01474	42.3367	0.01708	140.337	0.29192	238.47	0.77433	336.603
0.01628	42.4701	0.01539	140.47	0.29505	238.603	0.77475	336.737
0.01578	42.6034	0.0149	140.604	0.29603	238.737	0.77602	336.87
0.01307	42.7367	0.01772	140.737	0.29484	238.87	0.77631	337.003
0.01235	42.8701	0.01556	140.87	0.29922	239.003	0.775	337.137
0.01287	43.0034	0.01528	141.004	0.29856	239.137	0.778	337.27
0.01253	43.1367	0.01747	141.137	0.29726	239.27	0.77733	337.403
0.0112	43.2703	0.01747	141.27	0.29762	239.404	0.77581	337.537
0.01078	43.4036	0.01612	141.403	0.30059	239.537	0.77741	337.67
0.01272	43.537	0.01506	141.537	0.30214	239.67	0.77675	337.803
0.0119	43.6703	0.01653	141.67	0.30382	239.803	0.7789	337.937
0.01181	43.8034	0.01609	141.804	0.30496	239.937	0.77927	338.07
0.01151	43.937	0.01639	141.937	0.30435	240.07	0.77831	338.203
0.01366	44.0703	0.0156	142.07	0.30497	240.203	0.77924	338.337
0.01314	44.2034	0.01357	142.203	0.30675	240.337	0.77878	338.47
0.01363	44.3367	0.01643	142.337	0.30745	240.47	0.7779	338.604
0.01288	44.4701	0.01624	142.47	0.30886	240.604	0.77918	338.737
0.01248	44.6034	0.01561	142.604	0.31022	240.737	0.77934	338.87
0.01348	44.737	0.01505	142.737	0.31413	240.87	0.77867	339.003
0.01338	44.8703	0.0156	142.87	0.31215	241.003	0.77799	339.137
0.01455	45.0036	0.01449	143.003	0.31396	241.137	0.78019	339.27
0.01308	45.1367	0.01288	143.137	0.313	241.27	0.77799	339.403
0.01312	45.2701	0.01642	143.27	0.31602	241.403	0.77837	339.537
0.0149	45.4034	0.01413	143.403	0.31621	241.537	0.78061	339.67
0.01527	45.5367	0.01436	143.537	0.32103	241.67	0.77905	339.804
0.01457	45.6701	0.01371	143.67	0.31795	241.804	0.77756	339.937
0.01408	45.8034	0.01488	143.803	0.31841	241.937	0.78134	340.07
0.01357	45.937	0.01229	143.937	0.32117	242.07	0.7806	340.203
0.01454	46.0701	0.01362	144.07	0.32172	242.203	0.77961	340.337
0.01651	46.2036	0.01784	144.204	0.32192	242.337	0.78104	340.47
0.01662	46.337	0.01501	144.337	0.32514	242.47	0.78115	340.603
0.01469	46.4703	0.01603	144.47	0.3256	242.603	0.7802	340.737
0.01619	46.6034	0.01836	144.603	0.3255	242.737	0.78144	340.87
0.01555	46.737	0.0139	144.737	0.32563	242.87	0.78467	341.003
0.01516	46.8703	0.01575	144.87	0.32835	243.003	0.78258	341.137
0.01649	47.0034	0.01641	145.003	0.33463	243.137	0.78212	341.27

0.01655	47.1367	0.01357	145.137	0.33083	243.27	0.78062	341.403
0.01779	47.2701	0.01367	145.27	0.33031	243.403	0.78241	341.537
0.01558	47.4034	0.01766	145.403	0.3318	243.537	0.78226	341.67
0.016	47.5367	0.01737	145.537	0.33323	243.67	0.78332	341.804
0.0145	47.6701	0.01521	145.67	0.3326	243.804	0.78251	341.937
0.01407	47.8036	0.01599	145.803	0.33613	243.937	0.78118	342.07
0.01553	47.937	0.01794	145.937	0.33723	244.07	0.78246	342.203
0.01357	48.0703	0.01516	146.07	0.33708	244.203	0.78257	342.337
0.01488	48.2036	0.01574	146.203	0.34056	244.337	0.78842	342.47
0.01492	48.3367	0.01664	146.337	0.34	244.47	0.78392	342.604
0.01682	48.4701	0.01496	146.47	0.34176	244.603	0.78189	342.737
0.01807	48.6034	0.01326	146.603	0.34314	244.737	0.78894	342.87
0.01664	48.7367	0.01611	146.737	0.34272	244.87	0.78639	343.003
0.01816	48.8701	0.0156	146.87	0.34358	245.003	0.78394	343.137
0.01799	49.0034	0.01344	147.004	0.35025	245.137	0.78635	343.27
0.01656	49.1367	0.01359	147.137	0.34672	245.27	0.78875	343.403
0.01672	49.2701	0.01666	147.27	0.34677	245.403	0.78518	343.537
0.01739	49.4034	0.01554	147.403	0.34805	245.537	0.78451	343.67
0.01694	49.5367	0.01349	147.537	0.34934	245.67	0.78614	343.803
0.01723	49.6701	0.01563	147.67	0.34982	245.804	0.78759	343.937
0.01832	49.8034	0.01562	147.803	0.35284	245.937	0.7858	344.07
0.01751	49.937	0.01403	147.937	0.35391	246.07	0.78702	344.203
0.0164	50.0703	0.0151	148.07	0.3536	246.203	0.78834	344.337
0.01708	50.2036	0.0163	148.204	0.35415	246.337	0.78822	344.47
0.01755	50.337	0.01506	148.337	0.35587	246.47	0.78735	344.603
0.01708	50.4703	0.01562	148.47	0.35674	246.603	0.78781	344.737
0.01817	50.6034	0.01752	148.603	0.35606	246.737	0.78932	344.87
0.0185	50.7367	0.01442	148.737	0.35787	246.87	0.78965	345.003
0.01652	50.8701	0.01458	148.87	0.35847	247.003	0.78908	345.137
0.01505	51.0034	0.017	149.003	0.36021	247.137	0.78958	345.27
0.01604	51.1367	0.01458	149.137	0.36107	247.27	0.78883	345.403
0.01881	51.2703	0.01527	149.27	0.36273	247.404	0.78843	345.537
0.01745	51.4036	0.01496	149.403	0.36451	247.537	0.78718	345.67
0.01606	51.537	0.01242	149.537	0.36425	247.67	0.79001	345.803
0.01789	51.6703	0.01311	149.67	0.36508	247.803	0.78804	345.937
0.01829	51.8036	0.01702	149.803	0.36709	247.937	0.78957	346.07
0.01751	51.937	0.0154	149.937	0.3668	248.07	0.79122	346.203
0.01803	52.0703	0.01523	150.07	0.36682	248.203	0.79059	346.337
0.01751	52.2036	0.01349	150.204	0.36903	248.337	0.7912	346.47
0.01697	52.337	0.01349	150.337	0.36955	248.47	0.79305	346.603

0.01714	52.4701	0.01759	150.47	0.37353	248.603	0.79027	346.737
0.01721	52.6034	0.01537	150.604	0.37158	248.737	0.79073	346.87
0.01713	52.7367	0.01456	150.737	0.37317	248.87	0.79096	347.003
0.01675	52.8701	0.01464	150.87	0.37139	249.003	0.79103	347.137
0.01713	53.0034	0.01637	151.003	0.37484	249.137	0.79039	347.27
0.01587	53.1367	0.01353	151.137	0.37646	249.27	0.79246	347.403
0.01637	53.2703	0.01495	151.27	0.37647	249.403	0.79452	347.537
0.01937	53.4034	0.01518	151.404	0.37968	249.537	0.79289	347.67
0.01847	53.5367	0.01606	151.537	0.37726	249.67	0.7943	347.804
0.01875	53.6701	0.01495	151.67	0.37852	249.803	0.79358	347.937
0.01804	53.8036	0.01379	151.803	0.37845	249.937	0.79305	348.07
0.0205	53.937	0.01401	151.937	0.37994	250.07	0.7936	348.204
0.01917	54.0701	0.01493	152.07	0.38148	250.203	0.79427	348.337
0.0183	54.2034	0.01338	152.203	0.38208	250.337	0.79318	348.47
0.01831	54.3367	0.0146	152.337	0.38368	250.47	0.79226	348.603
0.01696	54.4701	0.01499	152.47	0.38272	250.603	0.79415	348.737
0.01743	54.6034	0.01464	152.603	0.38425	250.737	0.79354	348.87
0.01718	54.7367	0.01448	152.737	0.38873	250.87	0.7922	349.003
0.01799	54.8703	0.01586	152.87	0.38637	251.003	0.79498	349.137
0.01816	55.0036	0.01587	153.003	0.3872	251.137	0.79464	349.27
0.01879	55.137	0.01428	153.137	0.3886	251.27	0.79405	349.403
0.01819	55.2701	0.01523	153.27	0.38847	251.403	0.79563	349.537
0.01646	55.4034	0.01562	153.403	0.39125	251.537	0.79667	349.67
0.01907	55.5367	0.01562	153.537	0.39293	251.67	0.79582	349.803
0.01797	55.6701	0.01668	153.67	0.39499	251.803	0.79745	349.937
0.01846	55.8034	0.01421	153.803	0.39399	251.937	0.79763	350.07
0.01824	55.9367	0.01401	153.937	0.39524	252.07	0.79512	350.203
0.01907	56.0701	0.01461	154.07	0.39573	252.203	0.79492	350.337
0.02033	56.2034	0.01328	154.203	0.39654	252.337	0.79746	350.47
0.01978	56.3367	0.01465	154.337	0.39857	252.47	0.79711	350.603
0.01754	56.4701	0.01568	154.47	0.40621	252.603	0.79514	350.737
0.01691	56.6036	0.01469	154.603	0.39987	252.737	0.79654	350.87
0.01863	56.7367	0.01497	154.737	0.4016	252.87	0.79668	351.004
0.01782	56.8701	0.01527	154.87	0.40278	253.003	0.79636	351.137
0.01776	57.0034	0.01499	155.003	0.40173	253.137	0.79664	351.27
0.01935	57.1367	0.01669	155.137	0.40286	253.27	0.79852	351.403
0.01919	57.2703	0.0168	155.27	0.40593	253.403	0.79961	351.537
0.01841	57.4034	0.01536	155.403	0.40693	253.537	0.79778	351.67
0.01937	57.5367	0.01602	155.537	0.4078	253.67	0.79999	351.804
0.01926	57.6701	0.01619	155.67	0.40728	253.803	0.8001	351.937

0.01901	57.8034	0.0157	155.804	0.40994	253.937	0.79789	352.07
0.01812	57.9367	0.01591	155.937	0.41098	254.07	0.79789	352.204
0.0191	58.0701	0.01475	156.07	0.41187	254.203	0.80043	352.337
0.01939	58.2034	0.0131	156.203	0.41439	254.337	0.79895	352.47
0.02047	58.3367	0.01427	156.337	0.41541	254.47	0.79965	352.604
0.01994	58.4703	0.01324	156.47	0.41661	254.603	0.79892	352.737
0.01973	58.6036	0.01359	156.603	0.41668	254.737	0.80071	352.87
0.02066	58.7367	0.01217	156.737	0.41706	254.87	0.79954	353.003
0.02149	58.8701	0.01272	156.87	0.41704	255.003	0.79921	353.137
0.02074	59.0034	0.013	157.003	0.41945	255.137	0.79888	353.27
0.02021	59.137	0.01285	157.137	0.42014	255.27	0.79825	353.404
0.02031	59.2701	0.01362	157.27	0.42102	255.404	0.8006	353.537
0.02007	59.4034	0.01524	157.403	0.42188	255.537	0.79858	353.67
0.01897	59.5367	0.01305	157.537	0.42247	255.67	0.79932	353.803
0.02072	59.6701	0.014	157.67	0.4221	255.804	0.79891	353.937
0.02041	59.8034	0.01363	157.803	0.42427	255.937	0.79917	354.07
0.01996	59.9367	0.01465	157.937	0.42557	256.07	0.80015	354.203
0.0201	60.0701	0.01471	158.07	0.42671	256.203	0.79912	354.337
0.01974	60.2034	0.01524	158.204	0.42861	256.337	0.79866	354.47
0.0203	60.3367	0.01485	158.337	0.43521	256.47	0.7991	354.603
0.01981	60.4703	0.01233	158.47	0.43036	256.604	0.80036	354.737
0.02049	60.6036	0.01412	158.603	0.43071	256.737	0.80186	354.87
0.02101	60.737	0.01386	158.737	0.43564	256.87	0.80102	355.003
0.02082	60.8701	0.01379	158.87	0.43342	257.003	0.80013	355.137
0.0215	61.0034	0.01348	159.003	0.43371	257.137	0.80172	355.27
0.02083	61.1367	0.01457	159.137	0.433	257.27	0.80201	355.403
0.02109	61.2701	0.01404	159.27	0.43729	257.404	0.80238	355.537
0.02031	61.4034	0.01518	159.404	0.43585	257.537	0.80488	355.67
0.02049	61.5367	0.01448	159.537	0.4367	257.67	0.80249	355.803
0.02171	61.6701	0.01341	159.67	0.44046	257.803	0.80392	355.937
0.02234	61.8034	0.01437	159.803	0.44033	257.937	0.80571	356.07
0.02322	61.937	0.01407	159.937	0.44138	258.07	0.8027	356.203
0.02169	62.0703	0.01398	160.07	0.44117	258.203	0.80306	356.337
0.02189	62.2034	0.01387	160.203	0.44551	258.337	0.80225	356.47
0.02182	62.3367	0.01353	160.337	0.44454	258.47	0.80125	356.603
0.0199	62.4703	0.0149	160.47	0.44389	258.603	0.80108	356.737
0.02127	62.6034	0.01477	160.603	0.44587	258.737	0.80338	356.87
0.01981	62.7367	0.01388	160.737	0.44651	258.87	0.80485	357.003
0.02162	62.8701	0.01379	160.87	0.44856	259.003	0.8047	357.137
0.02048	63.0036	0.01416	161.003	0.44921	259.137	0.80584	357.27

0.02056	63.137	0.01565	161.137	0.44965	259.27	0.8045	357.403
0.02252	63.2703	0.01512	161.27	0.45028	259.403	0.80426	357.537
0.02123	63.4034	0.01666	161.404	0.45073	259.537	0.80479	357.67
0.02326	63.5367	0.01513	161.537	0.45326	259.67	0.80495	357.803
0.0222	63.6701	0.01622	161.67	0.45152	259.803	0.80623	357.937
0.02337	63.8036	0.01545	161.804	0.4544	259.937	0.80648	358.07
0.02193	63.9367	0.01592	161.937	0.45406	260.07	0.80608	358.204
0.02118	64.0701	0.01548	162.07	0.45451	260.203	0.80409	358.337
0.02086	64.2034	0.01491	162.203	0.45711	260.337	0.80642	358.47
0.02274	64.3367	0.01195	162.337	0.45609	260.47	0.80629	358.603
0.02125	64.4703	0.01224	162.47	0.4601	260.603	0.80536	358.737
0.02304	64.6034	0.01538	162.603	0.45956	260.737	0.80513	358.87
0.02126	64.7367	0.0143	162.737	0.45987	260.87	0.80605	359.003
0.02292	64.8701	0.01277	162.87	0.46165	261.003	0.80434	359.137
0.02137	65.0034	0.01648	163.003	0.46142	261.137	0.80667	359.27
0.02302	65.1367	0.01934	163.137	0.46403	261.27	0.80607	359.403
0.0227	65.2701	0.01991	163.27	0.46503	261.403	0.8054	359.537
0.02421	65.4034	0.02293	163.403	0.4725	261.537	0.80818	359.67
0.0234	65.537	0.02569	163.537	0.47026	261.67	0.80836	359.804
0.02229	65.6703	0.02582	163.67	0.46879	261.803	0.80727	359.937
0.02356	65.8036	0.02666	163.803	0.47054	261.937	0.80751	360.07
0.02158	65.9367	0.02477	163.937	0.46999	262.07	0.80993	360.203
0.02092	66.0701	0.02332	164.07	0.47248	262.203	0.80875	360.337
0.02036	66.2034	0.02488	164.203	0.47329	262.337	0.80919	360.47
0.02224	66.3367	0.02533	164.337	0.47252	262.47	0.80961	360.603
0.02156	66.4701	0.02348	164.47	0.4821	262.603	0.80871	360.737
0.01976	66.6034	0.02639	164.603	0.47617	262.737	0.80848	360.87
0.02266	66.737	0.02734	164.737	0.47694	262.87	0.80914	361.003
0.02301	66.8703	0.02423	164.87	0.47857	263.003	0.81036	361.137
0.02286	67.0036	0.02359	165.003	0.47999	263.137	0.80886	361.27
0.02537	67.1367	0.02329	165.137	0.48166	263.27	0.81027	361.403
0.02254	67.2701	0.02231	165.27	0.48282	263.403	0.8097	361.537
0.02206	67.4034	0.02182	165.403	0.48474	263.537	0.80938	361.67
0.02287	67.5367	0.02206	165.537	0.48489	263.67	0.80962	361.804
0.0217	67.6703	0.02338	165.67	0.48512	263.803	0.81108	361.937
0.02314	67.8036	0.0234	165.803	0.48616	263.937	0.80833	362.07
0.02331	67.9367	0.02298	165.937	0.49005	264.07	0.80962	362.204
0.02166	68.0701	0.02268	166.07	0.48927	264.203	0.81104	362.337
0.0224	68.2036	0.02429	166.203	0.48963	264.337	0.8113	362.47
0.02194	68.3367	0.02267	166.337	0.49026	264.47	0.81024	362.603



0.0212	68.4703	0.02306	166.47	0.49531	264.603	0.81008	362.737
0.02134	68.6034	0.02224	166.603	0.49359	264.737	0.81031	362.87
0.02336	68.7367	0.0223	166.737	0.49389	264.87	0.81131	363.004
0.02337	68.8701	0.0232	166.87	0.49499	265.004	0.81097	363.137
0.02324	69.0034	0.02298	167.003	0.50176	265.137	0.81243	363.27
0.02293	69.1367	0.02096	167.137	0.4979	265.27	0.81109	363.404
0.02318	69.2701	0.0229	167.27	0.49865	265.404	0.81288	363.537
0.02172	69.4034	0.02354	167.403	0.49925	265.537	0.81432	363.67
0.02444	69.5367	0.02236	167.537	0.49939	265.67	0.81198	363.803
0.024	69.6701	0.02243	167.67	0.50155	265.803	0.81169	363.937
0.0229	69.8034	0.02168	167.803	0.50198	265.937	0.81363	364.07
0.02233	69.9367	0.02232	167.937	0.50225	266.07	0.81279	364.203
0.02325	70.0701	0.02081	168.07	0.50322	266.203	0.81087	364.337
0.0243	70.2034	0.02221	168.203	0.50404	266.337	0.81264	364.47
0.02419	70.3367	0.02187	168.337	0.50571	266.47	0.81407	364.603
0.02376	70.4701	0.02029	168.47	0.50761	266.603	0.8151	364.737
0.02448	70.6034	0.02123	168.603	0.51045	266.737	0.81326	364.87
0.02418	70.7367	0.02099	168.737	0.50722	266.87	0.81454	365.004
0.02487	70.8701	0.02286	168.87	0.50943	267.003	0.81604	365.137
0.02516	71.0034	0.02246	169.003	0.5089	267.137	0.81277	365.27
0.02439	71.1367	0.02175	169.137	0.51084	267.27	0.81443	365.404
0.02564	71.2703	0.02046	169.27	0.51269	267.403	0.81645	365.537
0.02363	71.4034	0.02345	169.403	0.51253	267.537	0.81384	365.67
0.0229	71.5367	0.02219	169.537	0.51783	267.67	0.81441	365.803
0.02415	71.6701	0.02176	169.67	0.51531	267.803	0.81716	365.937
0.02416	71.8034	0.02372	169.803	0.51481	267.937	0.81486	366.07
0.02279	71.937	0.02689	169.937	0.51602	268.07	0.81529	366.203
0.0245	72.0703	0.02597	170.07	0.5166	268.204	0.81723	366.337
0.0241	72.2036	<b>0.02348</b>	<b>170.203</b>	0.51783	268.337	0.81649	366.47
0.02292	72.337	0.02438	170.337	0.51859	268.47	0.81454	366.603
0.02378	72.4703	0.0265	170.47	0.51865	268.604	0.81823	366.737
0.02418	72.6034	0.02564	170.603	0.52165	268.737	0.8218	366.87
0.02526	72.7367	0.02585	170.737	0.52142	268.87	0.81549	367.003
0.02408	72.8701	0.02586	170.87	0.52272	269.004	0.81792	367.137
0.02526	73.0034	0.0252	171.004	0.52473	269.137	0.81804	367.27
0.02581	73.1367	0.02485	171.137	0.52415	269.27	0.81703	367.404
0.02596	73.2701	0.0262	171.27	0.52561	269.404	0.8169	367.537
0.02611	73.4036	0.02715	171.403	0.53133	269.537	0.81975	367.67
0.02746	73.537	0.02612	171.537	0.52828	269.67	0.81777	367.803
0.02923	73.6701	0.02671	171.67	0.52796	269.804	0.81652	367.937

0.02496	73.8034	0.0294	171.803	0.52901	269.937	0.81869	368.07
0.02535	73.9367	0.02749	171.937	0.53232	270.07	0.82142	368.204
0.02489	74.0703	0.02927	172.07	0.53136	270.204	0.81888	368.337
0.02495	74.2034	0.02872	172.203	0.53271	270.337	0.81925	368.47
0.02394	74.3367	0.02895	172.337	0.53237	270.47	0.82035	368.603
0.02486	74.4701	0.02855	172.47	0.53941	270.604	0.81918	368.737
0.02504	74.6034	0.02955	172.603	0.53279	270.737	0.81892	368.87
0.02513	74.737	0.03051	172.737	0.5335	270.87	0.82239	369.003
0.02549	74.8703	0.0269	172.87	0.53473	271.004	0.82199	369.137
0.02691	75.0036	0.03041	173.003	0.53523	271.137	0.82174	369.27
0.02617	75.137	0.03107	173.137	0.5384	271.27	0.82308	369.403
0.02518	75.2703	0.03198	173.27	0.53841	271.403	0.8204	369.537
0.02589	75.4036	0.03321	173.403	0.53781	271.537	0.81985	369.67
0.02548	75.5367	0.03011	173.537	0.53824	271.67	0.82109	369.803
0.02452	75.6701	0.03231	173.67	0.54087	271.803	0.82139	369.937
0.0239	75.8034	0.03173	173.803	0.54676	271.937	0.82086	370.07
0.02389	75.937	0.03228	173.937	0.54299	272.07	0.82249	370.203
0.02421	76.0701	0.03283	174.07	0.54387	272.204	0.82282	370.337
0.02526	76.2036	0.03401	174.203	0.54528	272.337	0.82097	370.47
0.02516	76.3367	0.03318	174.337	0.54593	272.47	0.82184	370.604
0.02499	76.4701	0.03159	174.47	0.55111	272.604	0.82386	370.737
0.02757	76.6034	0.03156	174.603	0.54819	272.737	0.82277	370.87
0.02499	76.737	0.03165	174.737	0.54844	272.87	0.8227	371.004
0.02421	76.8703	0.03239	174.87	0.54934	273.004	0.82342	371.137
0.02482	77.0036	0.03493	175.003	0.54855	273.137	0.82364	371.27
0.02634	77.1367	0.03502	175.137	0.55097	273.27	0.8219	371.403
0.02597	77.2703	0.0357	175.27	0.55229	273.404	0.82345	371.537
0.02612	77.4034	0.03702	175.403	0.55267	273.537	0.82388	371.67
0.02778	77.5367	0.03535	175.537	0.5537	273.67	0.82157	371.803
0.02434	77.6701	0.03572	175.67	0.55422	273.804	0.82389	371.937
0.02515	77.8034	0.03506	175.803	0.55649	273.937	0.82214	372.07
0.0243	77.9367	0.03548	175.937	0.55833	274.07	0.82172	372.203
0.02762	78.0701	0.0349	176.07	0.55915	274.203	0.82275	372.337
0.02691	78.2036	0.03548	176.204	0.56053	274.337	0.8248	372.47
0.02588	78.337	0.03688	176.337	0.56127	274.47	0.823	372.603
0.02599	78.4703	0.03785	176.47	0.56145	274.603	0.82524	372.737
0.02571	78.6034	0.03647	176.604	0.56343	274.737	0.82583	372.87
0.02571	78.7367	0.03681	176.737	0.56396	274.87	0.82434	373.003
0.02523	78.8701	0.03808	176.87	0.564	275.003	0.82539	373.137
0.02567	79.0034	0.03773	177.003	0.57099	275.137	0.82612	373.27

0.02388	79.137	0.03813	177.137	0.56701	275.27	0.82556	373.403
0.02455	79.2701	0.03786	177.27	0.56842	275.403	0.82641	373.537
0.02645	79.4036	0.0382	177.403	0.56689	275.537	0.82514	373.67
0.02715	79.537	0.03833	177.537	0.5703	275.67	0.82718	373.803
0.02705	79.6703	0.0384	177.67	0.57091	275.803	0.827	373.937
0.02633	79.8034	0.03992	177.804	0.57069	275.937	0.82694	374.07
0.02737	79.937	0.0397	177.937	0.57202	276.07	0.82625	374.203
0.02817	80.0703	0.03901	178.07	0.57339	276.203	0.82683	374.337
0.02676	80.2036	0.03937	178.203	0.57433	276.337	0.82574	374.47
0.02645	80.337	0.04068	178.337	0.57582	276.47	0.82751	374.604
0.02734	80.4703	0.03986	178.47	0.5752	276.603	0.82661	374.737
0.02582	80.6036	0.04087	178.604	0.57766	276.737	0.82575	374.87
0.02681	80.737	0.04121	178.737	0.57805	276.87	0.82753	375.004
0.02422	80.8701	0.04068	178.87	0.57876	277.003	0.82712	375.137
0.02476	81.0036	0.03988	179.003	0.58632	277.137	0.8267	375.27
0.02633	81.137	0.04163	179.137	0.58028	277.27	0.82879	375.403
0.02594	81.2701	0.04145	179.27	0.58129	277.403	0.83004	375.537
0.02676	81.4034	0.04153	179.403	0.58173	277.537	0.82571	375.67
0.02637	81.537	0.04149	179.537	0.58378	277.67	0.82978	375.803
0.02634	81.6703	0.04238	179.67	0.58565	277.803	0.83081	375.937
0.02698	81.8034	0.0428	179.803	0.58485	277.937	0.83328	376.07
0.02665	81.9367	0.04224	179.937	0.58618	278.07	0.83614	376.203
0.02757	82.0701	0.04342	180.07	0.58611	278.203	0.834	376.337
0.02713	82.2034	0.04281	180.203	0.58651	278.337	0.83449	376.47
0.02907	82.337	0.04389	180.337	0.58772	278.47	<b>0.83546</b>	<b>376.604</b>
0.02698	82.4701	0.0444	180.47	0.58891	278.603	0.8337	376.737
0.02625	82.6036	0.04395	180.603	0.58876	278.737	0.83477	376.87
0.0275	82.737	0.0462	180.737	0.5894	278.87	0.83538	377.003
0.02984	82.8703	0.04599	180.87	0.59048	279.003	0.83394	377.137
0.0292	83.0036	0.04533	181.003	0.59104	279.137	0.83551	377.27
0.0296	83.137	0.0477	181.137	0.59146	279.27	0.83597	377.403
0.03006	83.2701	0.04584	181.27	0.5925	279.403	0.83505	377.537
0.02745	83.4034	0.04723	181.403	0.59502	279.537	0.83528	377.67
0.02788	83.5367	0.0465	181.537	0.5949	279.67	0.8344	377.803
0.02715	83.6701	0.04611	181.67	0.59533	279.803	0.8344	377.937
0.02822	83.8034	0.04763	181.804	0.5966	279.937	0.8333	378.07
0.02781	83.9367	0.04652	181.937	0.59634	280.07	0.8335	378.203
0.02787	84.0701	0.04756	182.07	0.59781	280.203	0.83245	378.337
0.02848	84.2034	0.04839	182.203	0.6017	280.337	0.83545	378.47
0.02938	84.3367	0.04906	182.337	0.59756	280.47	0.8352	378.604

0.02669	84.4701	0.04852	182.47	0.60039	280.603	0.8364	378.737
0.02648	84.6036	0.04901	182.603	0.59881	280.737	0.83593	378.87
0.02643	84.7367	0.04878	182.737	0.60649	280.87	0.83688	379.003
0.0249	84.8701	0.04895	182.87	0.60057	281.003	0.83414	379.137
0.02593	85.0034	0.05004	183.003	0.60268	281.137	0.83267	379.27
0.02654	85.137	0.04916	183.137	0.60365	281.27	0.8358	379.403
0.02735	85.2701	0.04968	183.27	0.60629	281.403	0.83384	379.537
0.02736	85.4034	0.04904	183.403	0.60632	281.537	0.83142	379.67
0.02757	85.5367	0.0491	183.537	0.60559	281.67	0.83054	379.803
0.02917	85.6703	0.05196	183.67	0.60585	281.803	0.83336	379.937
0.02793	85.8036	0.05261	183.803	0.60634	281.937	0.83359	380.07
0.0278	85.9367	0.05142	183.937	0.60748	282.07	0.83303	380.203
0.02728	86.0703	0.05134	184.07	0.60441	282.203	0.83248	380.337
0.02671	86.2034	0.05492	184.203	0.6036	282.337	0.83359	380.47
0.02563	86.3367	0.05345	184.337	0.60588	282.47	0.83319	380.604
0.02719	86.4703	0.05502	184.47	0.60608	282.603	0.83358	380.737
0.02524	86.6034	0.05421	184.604	0.6076	282.737	0.83313	380.87
0.02711	86.7367	0.05535	184.737	0.60644	282.87	0.8325	381.003
0.02598	86.8701	0.05587	184.87	0.60559	283.003	0.83185	381.137
0.02743	87.0036	0.05707	185.003	0.60754	283.137	0.83264	381.27
0.02571	87.137	0.05489	185.137	0.60881	283.27	0.83396	381.403
0.02737	87.2703	0.05632	185.27	0.60871	283.403	0.83533	381.537
0.02704	87.4034	0.05674	185.403	0.60948	283.537	0.83502	381.67
0.02397	87.537	0.05667	185.537	0.61101	283.67	0.83362	381.803
0.02593	87.6703	0.05575	185.67	0.61041	283.803	0.83468	381.937
0.02925	87.8036	0.057	185.804	0.61282	283.937	0.83476	382.07
0.03361	87.937	0.05849	185.937	0.61355	284.07	0.83329	382.203
0.03328	88.0701	0.05732	186.07	0.61397	284.203	0.83447	382.337
0.03642	88.2034	0.05662	186.203	0.61686	284.337	0.83321	382.47
0.03566	88.3367	0.05671	186.337	0.61653	284.47	0.8342	382.604
0.03335	88.4701	0.0584	186.47	0.61661	284.603	0.83336	382.737
0.0299	88.6034	0.05897	186.603	0.61512	284.737	0.83539	382.87
0.02689	88.7367	0.05782	186.737	0.61667	284.87	0.83436	383.004
0.02685	88.8701	0.05904	186.87	0.61815	285.004	0.8358	383.137
0.02642	89.0036	0.06007	187.003	0.62341	285.137	0.83544	383.27
0.02651	89.1367	0.05967	187.137	0.61767	285.27	0.83487	383.404
0.0266	89.2701	0.05979	187.27	0.62119	285.403	0.83526	383.537
0.02635	89.4034	0.06057	187.404	0.6222	285.537	0.83596	383.67
0.02698	89.5367	0.05984	187.537	0.62301	285.67	0.83405	383.803
0.02821	89.6701	0.06034	187.67	0.62687	285.804	0.83539	383.937

0.02875	89.8034	0.06167	187.803	0.62423	285.937	0.83511	384.07
0.0279	89.9367	0.06087	187.937	0.62279	286.07	0.83472	384.203
0.02679	90.0703	0.06177	188.07	0.62435	286.204	0.8356	384.337
0.02611	90.2034	0.062	188.203	0.62474	286.337	0.8352	384.47
0.02642	90.3367	0.06232	188.337	0.62692	286.47	0.83632	384.604
0.02672	90.4701	0.06301	188.47	0.62708	286.603	0.8341	384.737
0.02631	90.6034	0.0633	188.603	0.63053	286.737	0.83519	384.87
0.02509	90.737	0.06268	188.737	0.62854	286.87	0.83497	385.004
0.0257	90.8703	0.06293	188.87	0.62995	287.004	0.83512	385.137
0.0242	91.0034	0.06499	189.004	0.63022	287.137	0.83466	385.27
0.0244	91.1367	0.06486	189.137	0.63101	287.27	0.83535	385.403
0.02519	91.2701	0.06369	189.27	0.63131	287.403	0.83451	385.537
0.0276	91.4034	0.06457	189.403	0.63198	287.537	0.83496	385.67
0.03193	91.5367	0.06453	189.537	0.63293	287.67	0.8344	385.804
0.03321	91.6701	0.06628	189.67	0.63412	287.803	0.83389	385.937
0.03269	91.8034	0.0664	189.803	0.63457	287.937	0.83596	386.07
0.03618	91.9367	0.06608	189.937	0.63688	288.07	0.83765	386.204
0.03636	92.0703	0.06522	190.07	0.63643	288.203	0.83533	386.337
0.03546	92.2036	0.06684	190.203	0.63529	288.337	0.83643	386.47
0.03555	92.337	0.06942	190.337	0.63755	288.47	0.8354	386.603
0.03628	92.4703	0.06967	190.47	0.63747	288.603	0.83637	386.737
0.03721	92.6034	0.06824	190.603	0.63886	288.737	0.83482	386.87
0.03595	92.7367	0.069	190.737	0.63972	288.87	0.83624	387.003
0.03675	92.8701	0.06868	190.87	0.64299	289.003	0.83685	387.137
0.03554	93.0034	0.06821	191.003	0.63943	289.137	0.8361	387.27
0.03349	93.137	0.07229	191.137	0.64154	289.27	0.83728	387.403
0.03374	93.2703	0.06932	191.27	0.6416	289.403	0.8363	387.537
0.03428	93.4034	0.06965	191.403	0.64139	289.537	0.83749	387.67
0.03123	93.5367	0.07113	191.537	0.64422	289.67	0.83595	387.803
0.03256	93.6701	0.07104	191.67	0.64474	289.803	0.83862	387.937
0.03173	93.8034	0.07258	191.803	0.64409	289.937	0.83855	388.07
0.03131	93.9367	0.07221	191.937	0.64489	290.07	0.83742	388.203
0.0289	94.0701	0.07319	192.07	0.64746	290.203	0.83841	388.337
0.0294	94.2034	0.07108	192.203	0.648	290.337	0.83864	388.47
0.02792	94.337	0.07308	192.337	0.64756	290.47	0.83886	388.603
0.02876	94.4701	0.07758	192.47	0.64779	290.603	0.83818	388.737
0.02891	94.6034	0.07404	192.604	0.6492	290.737	0.83743	388.87
0.03024	94.7367	0.0745	192.737	0.65159	290.87	0.83833	389.003
0.02907	94.8703	0.07379	192.87	0.65009	291.004	0.83933	389.137
0.02675	95.0036	0.07402	193.003	0.64998	291.137	0.83911	389.27

0.02885	95.137	0.07573	193.137	0.6502	291.27	0.83848	389.403
0.02919	95.2701	0.07671	193.27	0.65106	291.404	0.83941	389.537
0.02837	95.4034	0.07747	193.403	0.65115	291.537	0.83907	389.67
0.02827	95.537	0.07684	193.537	0.64884	291.67	0.84017	389.803
0.02923	95.6703	0.07675	193.67	0.65295	291.803	0.8374	389.937
0.02697	95.8036	0.07689	193.804	0.65412	291.937	0.83862	390.07
0.0262	95.9367	0.07713	193.937	0.65346	292.07	0.83662	390.203
0.02727	96.0701	0.07755	194.07	0.65379	292.203	0.83965	390.337
0.02695	96.2034	0.07688	194.203	0.65496	292.337	0.83905	390.47
0.02732	96.3367	0.07879	194.337	0.65496	292.47	0.83906	390.603
0.02757	96.4703	0.07964	194.47	0.65506	292.603	0.83804	390.737
0.02636	96.6036	0.07889	194.604	0.65569	292.737	0.83695	390.87
0.02367	96.737	0.07949	194.737	0.65518	292.87	0.83595	391.003
0.02275	96.8701	0.08009	194.87	0.65752	293.003	0.83506	391.137
0.02472	97.0034	0.0798	195.003	0.66055	293.137	0.83562	391.27
0.02785	97.1367	0.08054	195.137	0.65795	293.27	0.83515	391.403
0.02915	97.2701	0.0812	195.27	0.65961	293.404	0.83634	391.537
0.0293	97.4034	0.08093	195.403	0.66112	293.537	0.83609	391.67
0.02899	97.5367	0.08691	195.537	0.65897	293.67	0.83518	391.803
0.0288	97.6701	0.08252	195.67	0.6622	293.803	0.83562	391.937
0.02797	97.8034	0.08722	195.803	0.66218	293.937	0.83516	392.07
0.0294	97.9367	0.08396	195.937	0.66136	294.07	0.83695	392.204
0.0264	98.0701	0.0855	196.07	0.66316	294.203	0.83592	392.337
0.0259	98.2036	0.08495	196.204	0.6631	294.337	0.83729	392.47
		0.08652	196.337	0.66309	294.47	0.83919	392.604

### 2.2.2.3 Procedures for $^{11}\text{B}$ NMR Studies of Reaction Products

Solid-state and ionic liquid reactions carried out using either the Toepler pump or gas burette measurements were extracted with pyridine at various points in the reactions. The reaction flask was removed from the oil bath and cooled to room temperature, then dry pyridine was added to the reaction flask under  $\text{N}_2$  flow. The pyridine solution was extracted by syringe and then the  $^{11}\text{B}$  NMR was taken.

While bmimCl is a liquid at 85 °C, it is a solid at room temperature; therefore, solid-state  $^{11}\text{B}$  NMR analyses (at Pacific Northwest National Laboratories: 240 MHz machine spun at 10 kHz) were used to monitor the products of reactions carried out in bmimCl. All solid-state  $^{11}\text{B}$  chemical shifts were measured relative to external  $\text{NaBH}_4$  (-41 ppm) and then referenced to  $\text{BF}_3\cdot\text{O}(\text{C}_2\text{H}_5)_2$  (0.0 ppm).

The solution  $^{11}\text{B}$  NMR (128.4 MHz Bruker DMX-400) studies in the room temperature ionic-liquid bmimOTf were carried out by heating reaction mixtures composed of 50 mg of AB (1.6 mmol) or 50 mg of DADB (0.8 mmol) and 450 mg of ionic liquid at 85 °C in a sealed NMR tube, with the tube periodically removed from the heating bath to collect  $^{11}\text{B}$  NMR spectra of the reaction mixture (recorded at 25 °C).

All solid-state and solution  $^{11}\text{B}$  NMR chemical shifts are referenced to external  $\text{BF}_3\cdot\text{O}(\text{C}_2\text{H}_5)_2$  (0.0 ppm) with a negative sign indicating an upfield shift.

## 2.3 Results and Discussion

Utilization of waste heat from a PEM fuel cell can provide for AB H<sub>2</sub>-release reaction temperatures near 85 °C.<sup>5</sup> However, as described in **Chapter 1**, at 85 °C, H<sub>2</sub>-release from solid-state AB has been shown to exhibit an induction period of up to 3 h. After hydrogen release begins, only the release of ~0.9 equiv. of H<sub>2</sub> can be achieved, rather than the 3 equiv. predicted by **Equation 2.1**, even with prolonged heating at 85 °C.<sup>4,5</sup> As a result, a number of approaches are now being explored to induce efficient AB H<sub>2</sub>-release, including, for example, activation by transition metal catalysts,<sup>10-25</sup> acid catalysts,<sup>26</sup> base catalysts<sup>27</sup> and nano and meso-porous scaffolds.<sup>28-30</sup> Most of these additives use organic solvents either as the reaction medium or as the AB transport and loading method. The use of organic solvents is not desirable due to their high volatility which would result in loss to the environment. In addition, using organic solvents would also reduce petroleum based feedstock needed for synthesis. An alternative solvent system is necessary.

### 2.3.1 Why Use Ionic Liquids?

Ionic liquids are generally defined as salts that are relatively low viscosity liquids at temperatures below 100 °C. These salts have a number of unique properties that make them attractive substitutes for traditional organic solvents in hydrogen storage systems, including: (1) negligible vapor pressures, (2) stability to elevated temperatures, (3) the ability to dissolve a wide range of compounds and (4) a polar reaction medium that can stabilize ionic transition states and intermediates. The low volatility of these systems makes them superior to organic solvents and they have been used in a broad range of



applications.<sup>31-34</sup> Their ability to stabilize ionic intermediates is critical to AB dehydropolymerization initiation as discussed in section **2.3.7**.

Another promising application in ionic liquid technology is in transition-metal catalyst immobilization. Many industrial processes use heterogeneous catalysts despite more efficient, cheaper homogenous catalysts being available due to separation issues. Ionic liquids promise to become an immobilizing solvent system for catalysis where the catalyst is solubilized in the ionic liquid while the reagents and products are held in the organic layer (biphasic system) and can therefore be easily separated. Other uses for ionic liquids include solvation for radical polymerization and catalytic cracking of polyethylene as well as electrochemical reactions.<sup>31</sup> Ionic liquids are often air and moisture stable though many are hygroscopic, needing drying before use in reactions. Traditional synthetic methods for ionic liquids require long, high temperature reaction conditions whereas new methods utilize sonication and significantly shorter reaction times.<sup>35</sup>

Some of the most common ionic liquids are composed of inorganic anions,  $X^-$ ,  $BF_4^-$ ,  $PF_6^-$ , and nitrogen-containing organic cations, such as RN,R'N-imidazolium or RN-pyridinium. **Figure 2.3** shows the structures, acronyms, and melting points of the variety of ionic liquids used in these studies. The ionic liquids are sectioned into solid and liquid (at room temperature). The two position of the imidazolium ring in ionic liquids is susceptible to attack, since the hydrogen at this position is acidic. Reactions at this hydrogen can lead to solvent degradation and/or the formation of carbene borane adducts (most often during transition-metal catalyzed reactions). Replacing the hydrogen

with a methyl group eliminates this issue and these ionic liquids are termed ‘protected.’ The protected ionic liquids can be obtained as either solids or liquids.

Solid ionic liquids have the advantage of easily being measured and have a wider variety of protected imidazolium rings. Liquids, as discussed in section **2.3.6**, are useful for running *in situ*  $^{11}\text{B}$  NMR such as bmimI, bmimOTf, and mmimMeSO<sub>4</sub>. The main ionic liquid used in my work was 1-butyl-3-methylimidazolium chloride, bmimCl, since it showed good activity and was inexpensive and easy to handle. BmimCl’s melting point is above room temperature, but it forms a stirrable liquid at room temperature when mixed with AB.

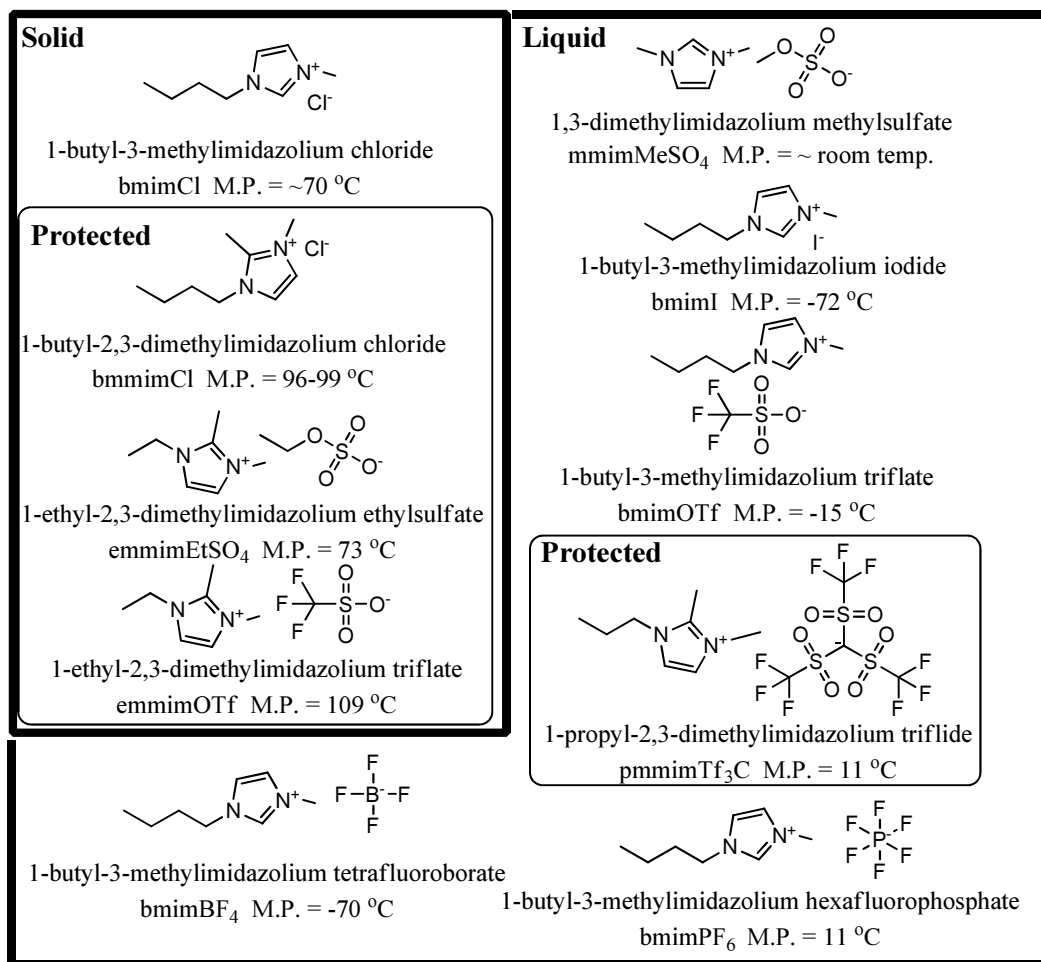


**Figure 2.3** Structures of ionic liquids used in these studies.

### 2.3.2 Procedures for AB H<sub>2</sub>-release reactions

For the experiments where the released H<sub>2</sub> was measured with the Toepler pump, the AB (250 mg, 8.1 mmol) was loaded under N<sub>2</sub> into ~100 mL single neck round bottom flasks with the ionic liquid (250 mg) given in **Tables 2.5-2.6**. The flasks were then evacuated, sealed, and placed in a hot oil bath preheated to the desired temperature. The flasks were opened at the indicated times and the released H<sub>2</sub> was quantified using the

Toepler pump system. Post reaction, the flasks were evacuated for 30 min through the cold trap to remove any volatile products from the reaction residue. The product residues and volatiles in the cold trap were extracted with dry glyme and analyzed by  $^{11}\text{B}$  NMR.

For reactions using the automated gas burette, the AB (150 mg, 4.87 mmol) samples were loaded into ~100 mL flasks with calibrated volumes, along with the ionic liquid (150 mg) or tetraglyme (0.15 mL) solvents. Under a flow of helium, the flask was attached to the burette system. The system was evacuated for 30 min for reactions with the ionic liquid solutions, and for 5 min for tetraglyme solutions. The system was then backfilled with helium and allowed to equilibrate to atmospheric pressure for ~30 min. Once the system pressure equalized, the data collection program was started and the flask was immersed in the preheated oil bath. The data are reported from the point where the flask was initially plunged into the oil bath, but  $\text{H}_2$ -release was not observed until the ionic-liquid/AB mixture melted. Data were recorded at 2-5 second intervals depending on the speed of the reaction. The product residues were extracted with dry glyme and analyzed by  $^{11}\text{B}$  NMR.

### 2.3.3 Solid-State vs. Ionic Liquid $\text{H}_2$ -Release

Earlier reported<sup>4</sup> AB  $\text{H}_2$ -release measurements from our lab for solid-state  $\text{H}_2$ -release were periodic values obtained using a Toepler pump, but the new studies reported herein use the automated gas burette.<sup>36</sup> This method has provided both more precise and continuous release data for these reactions. A comparison of the 85 °C  $\text{H}_2$ -release data, measured with the automated gas burette, obtained from solid-state AB versus AB dissolved in the 1-butyl-3-methyl-imidazolium chloride (bmimCl) ionic liquid (50:50- wt%) is presented in **Figure 2.4**. For the solid-state AB reaction, there was

negligible hydrogen production after 180 min and only 0.81 equivalents of H<sub>2</sub> after 360 min. Other samples heated for longer times (67 h) showed that a total of only 0.9 H<sub>2</sub>-equivalents could ultimately be obtained from the solid-state AB reactions at 85 °C. In contrast, the AB/bmimCl mixture exhibited no induction period, with H<sub>2</sub>-release beginning immediately after the solution melted, to give release of 1.0 H<sub>2</sub>-equiv. in 67 min and 2.2 H<sub>2</sub>-equiv. in 330 min. The released H<sub>2</sub> was passed through a -78 °C trap before entering the gas burette. When the reaction was complete, the contents of the trap were extracted with glyme solvent, but <sup>11</sup>B NMR analyses of the solution showed only trace amounts of borazine.

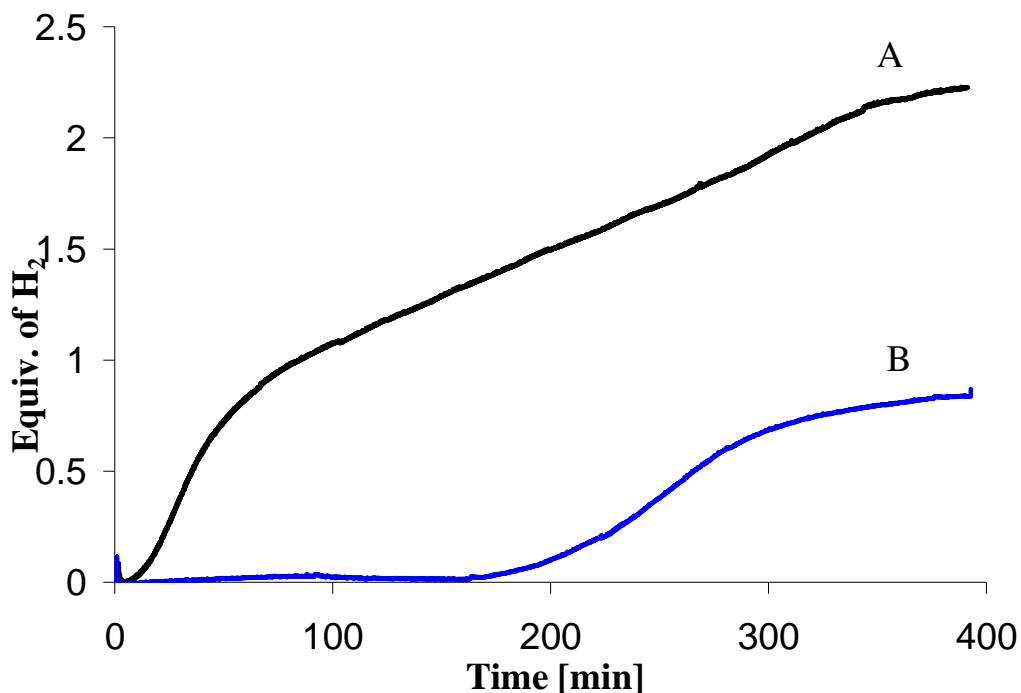


**Figure 2.4** H<sub>2</sub>-release measurements (gas burette) at 85 °C of: (A) 50-wt% AB (150 mg) in bmimCl (150 mg,) and (B) solid-state AB (150 mg).

The AB/bmimCl H<sub>2</sub>-release plot in **Figure 2.4** also clearly shows that release appears to occur in at least two steps with the release rate for the 2<sup>nd</sup> H<sub>2</sub>-equiv. being significantly slower than for the 1<sup>st</sup> equiv. Dramatic increases (**Figure 2.5**) in the rate of H<sub>2</sub>-release of the 50:50-wt% AB/bmimCl mixture for both H<sub>2</sub>-equivalents were observed as the temperature was increased with the release of 1.0 H<sub>2</sub>-equiv. in 37 min and 2.2 H<sub>2</sub>-equiv. in 161 min at 95 °C, 1.0 H<sub>2</sub>-equiv. in 9 min and 2.2 H<sub>2</sub>-equiv. in 45 min at 105 °C, and 1.0 H<sub>2</sub>-equiv. in 5 min and 2.2 H<sub>2</sub>-equiv. in 20 min at 110 °C . The 75 °C reaction did not reach 2 H<sub>2</sub>-equiv.

**Table 2.2 Times to Selected Equivalent Points of H<sub>2</sub>-Release (Gas Burette) of Ionic Liquid and Solid-State Reactions at 85 °C**

(A)		(B)	
H <sub>2</sub> -Equiv.	Minutes	H <sub>2</sub> -Equiv.	Minutes
0.25	24	0.25	231
0.5	35	0.5	265
0.75	52	0.75	323
1	84	0.84	385
1.25	142	-	-
1.5	200	-	-
1.75	263	-	-
2	316	-	-

(A) 50-wt% AB (150 mg) in bmimCl (150 mg,) and (B) solid-state AB (150 mg).

(Reaction (B) stopped at 0.84 equivalents).

As discussed in **Chapter 1**, the U.S. Department of Energy (DOE) has set a 2015 gravimetric total-system target for H<sub>2</sub>-storage of 9.0 total-system-wt%.<sup>37,38</sup> The release of 2.2 H<sub>2</sub>-equiv. from a 50:50 AB/bmimCl mixture corresponds to a release of 7.2 mat-wt% H<sub>2</sub> [mat-wt% H<sub>2</sub> = H<sub>2</sub>-wt/(AB+bmimCl-wts)]. In order for an AB/ionic-liquid

system to attain the DOE total-system targets, an increase in the mat-wt% by reduction of the weight of the ionic-liquid component is necessary. As can be seen in **Figure 2.6**, it was found that significantly enhanced H<sub>2</sub>-release rates compared to the solid-state could still be obtained when employing as little as 20.2-wt% bmimCl. Thus, 2.0 H<sub>2</sub>-equiv. were released from 80:20 AB/bmimCl solutions in only 52 min and 157 min at 120 °C and 110 °C, respectively, with both solutions then ultimately giving 2.2 H<sub>2</sub>-equiv. at longer times. The final release observed for these mixtures corresponds to an 11.4 mat-wt% H<sub>2</sub>-release.

The 85 °C H<sub>2</sub>-release data (Toepler pump measurements) in **Table 2.5** and **Figure 2.7** show that AB H<sub>2</sub>-release is activated in a variety of 50:50-wt% AB/ionic-liquid mixtures, but that these mixtures exhibit a range of H<sub>2</sub>-release extents and rates. The biggest differences were observed for the release of the 2<sup>nd</sup> equivalent. The bmimCl, bmmimCl, bmimBF<sub>4</sub>, mmimMeSO<sub>4</sub> and emmimEtSO<sub>4</sub> (refer to **Figure 2.3** for structures) mixtures all yielded over 2 H<sub>2</sub>-equiv. at reasonably comparable rates, while the other mixtures showed greatly decreased release rates beyond the 1<sup>st</sup> equiv. For the pmmimTf<sub>3</sub>C mixture, H<sub>2</sub>-release stopped, as was observed for the AB solid-state reactions at 85 °C, after only ~0.9 H<sub>2</sub>-equiv. As shown in **Table 2.6** and **Figure 2.8**, the H<sub>2</sub>-release rates were significantly decreased upon lowering the temperature with the mmimMeSO<sub>4</sub> and emmimEtSO<sub>4</sub> mixtures being the most active. At 45 °C, bmimCl and bmmimCl showed little activity.

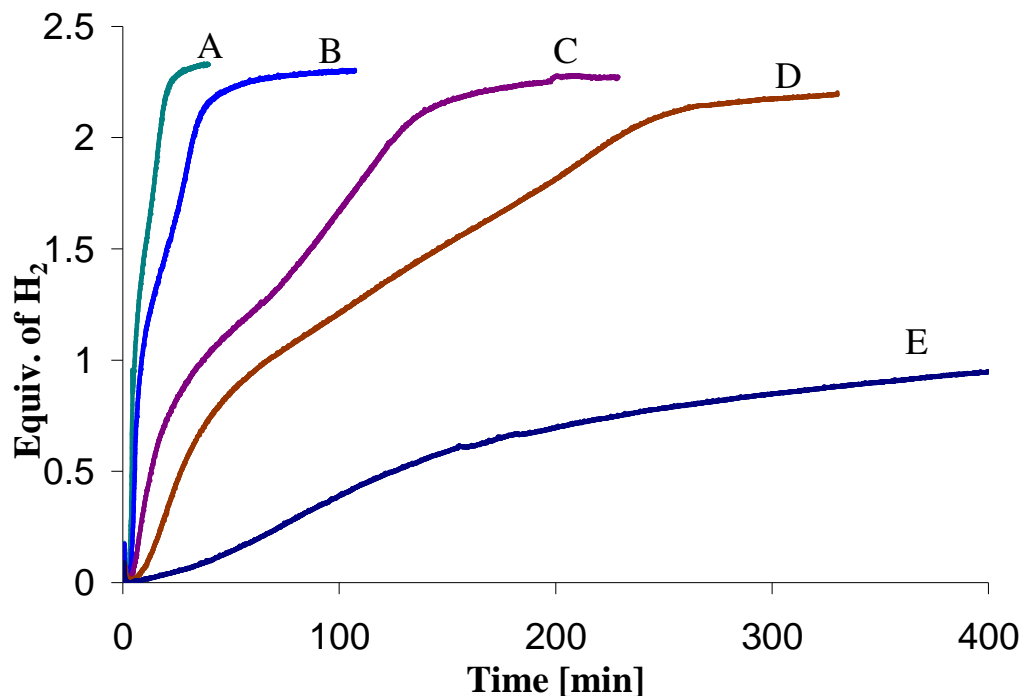


**Figure 2.5** H<sub>2</sub>-release measurements (gas burette) of 50-wt% AB (150 mg) in bmimCl (150 mg) at: (A) 110 °C, (B) 105 °C, (C) 95 °C, (D) 85 °C and (E) 75 °C.

**Table 2.3 Times to Selected Equivalent Points of H<sub>2</sub>-Release (Gas Burette) of 50-wt% AB (150 mg) in BmimCl (150 mg) at Different Temperatures**

(A)		(B)		(C)		(D)	
H <sub>2</sub> -Equiv.	Minutes	H <sub>2</sub> -Equiv.	Minutes	H <sub>2</sub> -Equiv.	Minutes	H <sub>2</sub> -Equiv.	Minutes
0.25	3	0.25	5	0.25	8	0.25	18
0.5	4	0.5	5	0.5	13	0.5	27
0.75	4	0.75	6	0.75	21	0.75	40
1	5	1	9	1	37	1	67
1.25	7	1.25	13	1.25	63	1.25	106
1.5	10	1.5	20	1.5	87	1.5	146
1.75	14	1.75	27	1.75	106	1.75	190
2	17	2	32	2	126	2	228

(A) 110 °C, (B) 105 °C, (C) 95 °C, (D) 85 °C and (E) 75 °C.



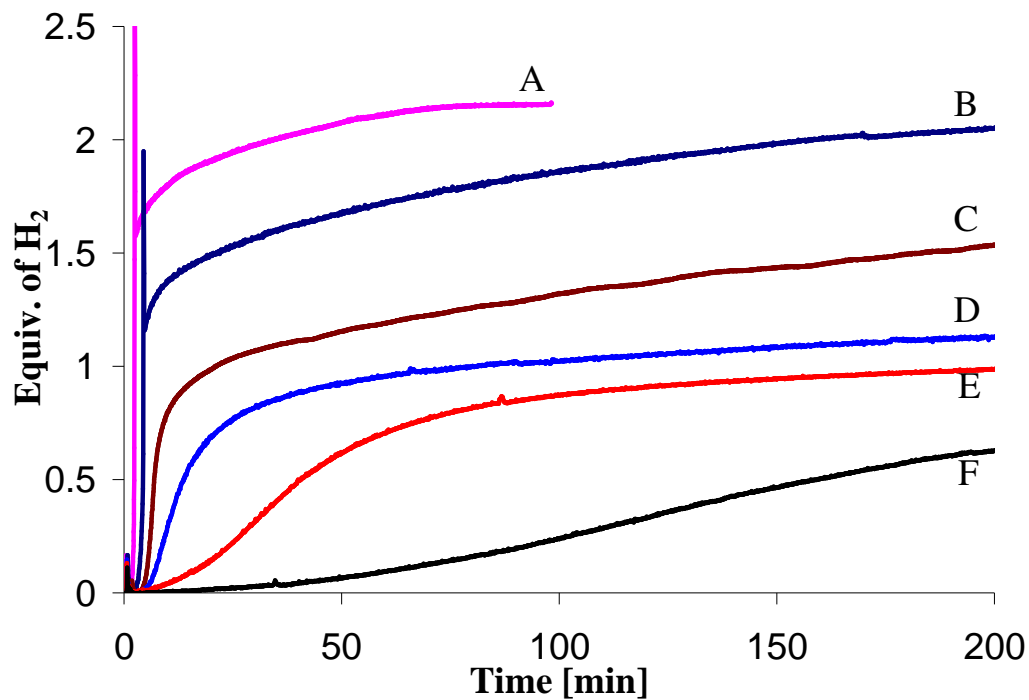


**Figure 2.6** H<sub>2</sub>-release measurements (gas burette) of AB (150 mg) in 20.2-wt% bmimCl (38 mg): (A) 120 °C, (B) 110 °C, (C) 105 °C, (D) 95 °C, (E) 85 °C and (F) 75 °C. (The early spike in the data is caused by the initial delay of the burette to respond to H<sub>2</sub>-release)

**Table 2.4 Times to Selected Equivalent Points of H<sub>2</sub>-Release (Gas Burette) of AB (150 mg) in 20.2-wt% BmimCl (38 mg) at Different Temperatures**

(A)		(B)		(C)		(D)	
H <sub>2</sub> -Equiv.	Minutes	H <sub>2</sub> -Equiv.	Minutes	H <sub>2</sub> -Equiv.	Minutes	H <sub>2</sub> -Equiv.	Minutes
0.25	2	0.25	4	0.25	6	0.25	9
0.5	2	0.5	4	0.5	7	0.5	14
0.75	2	0.75	4	0.75	9	0.75	24
1	2	1	4	1	21	1	80
1.25	2	1.25	6	1.25	77	1.25	331
1.5	2	1.5	21	1.5	183	1.5	753
1.75	7	1.75	67	1.75	374	1.75	1278
2	34	2	158	2	767	-	-

(A) 120 °C, (B) 110 °C, (C) 105 °C, (D) 95 °C, (E) 85 °C and (F) 75 °C (Reaction (B) stopped at 0.84 equivalents).

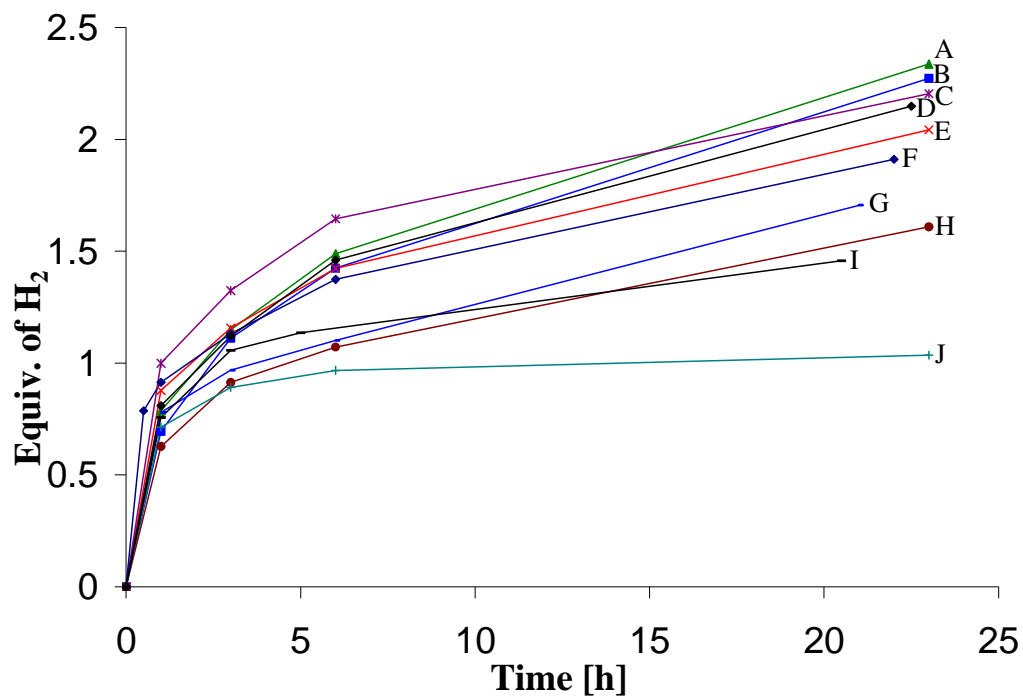


**Figure 2.7** H<sub>2</sub>-release measurements (Toepler pump) of the reaction of 50-wt% AB (250 mg) at 85 °C in 250 mg of: (A) bmmimCl, (B) bmimCl, (C) emmimEtSO<sub>4</sub>, (D) bmimBF<sub>4</sub>, (E) mmimMeSO<sub>4</sub>, (F) bmimOTf, (G) emmimOTf, (H) bmimI, (I) bmimPF<sub>6</sub> and (J) pmmimTf<sub>3</sub>C.

**Table 2.5** H<sub>2</sub>-Release Data (Toepler pump) for AB/Ionic-Liquid (50-wt%) Reactions at 85 °C

Ionic Liquid	Time [h]	H <sub>2</sub> -Released	
		equiv.	mmol
bmimCl	1	0.70	5.63
	3	1.11	9.00
	6	1.42	11.5
	23	2.20	17.8
bmmimCl	1	0.79	6.37

	3	1.15	9.31
	6	1.49	12.1
	23	2.34	18.9
bmimI	1	0.63	5.08
	3	0.91	7.40
	6	1.07	8.68
	23	1.61	13.0
bmimBF <sub>4</sub>	1	0.81	6.56
	3	1.12	9.07
	6	1.46	11.8
	23	2.15	17.03
bmimPF <sub>6</sub>	1	0.76	6.13
	3	1.06	8.56
	6	1.14	9.20
	23	1.46	11.8
mmimMeSO <sub>4</sub>	1	0.88	7.11
	3	1.16	9.37
	6	1.42	11.5
	23	2.04	16.5
emmimEtSO <sub>4</sub>	1	1.00	8.09
	3	1.32	10.7
	6	1.64	13.3
	23	2.20	17.8
bmimOTf	1	0.91	7.40
	3	1.13	9.16
	6	1.37	11.1
	23	1.91	15.5
emmimOTf	1	0.78	6.31
	3	0.97	7.84
	6	1.10	8.91
	23	1.71	13.8
pmmimTf <sub>3</sub> C	1	0.71	5.79
	3	0.89	7.22
	6	0.97	7.83
	23	1.04	8.39

250 mg (8.1 mmol) of AB and 250 mg of the ionic-liquid were used in all experiments.

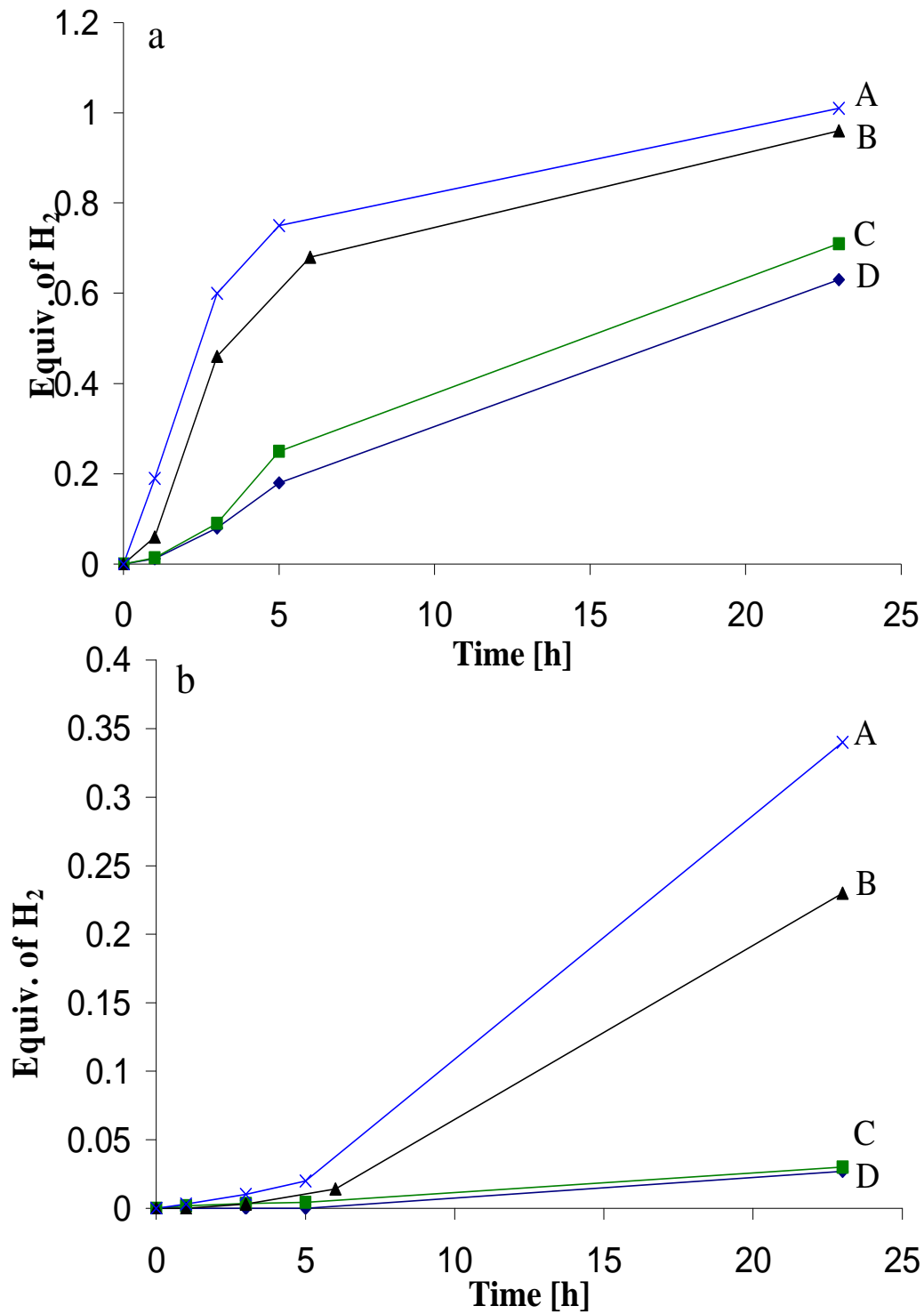


**Figure 2.8** H<sub>2</sub>-release measurements (Toepler pump) of the reaction of 50-wt% AB (250 mg) in 250 mg of: (A) emmimEtSO<sub>4</sub>, (B) mmimMeSO<sub>4</sub>, (C) bmmimCl and (D) bmimCl at (a) 65 °C and (b) 45 °C.

**Table 2.6 H<sub>2</sub>-Release Data (Toepler pump) for AB/Ionic-Liquid (50-wt%) Reactions at 65 and 45 °C**

Time [h]	Temp [°C]	Hydrogen Released equiv.	mmol
bmimCl			
1	65°	0.012	0.097
3	65°	0.08	0.67
5	65°	0.18	1.46
23	65°	0.63	5.07
1	45°	-	-
3	45°	-	-
5	45°	-	-
23	45°	0.027	0.23
bmmimCl			
1	65°	0.014	0.11
3	65°	0.09	0.75
5	65°	0.25	2.03
23	65°	0.71	5.73
1	45°	0.0017	0.014
3	45°	0.0034	0.028
5	45°	0.0043	0.034
23	45°	0.03	0.26
mmimMeSO <sub>4</sub>			
1	65°	0.06	0.47
3	65°	0.46	3.71
6	65°	0.68	5.53
23	65°	0.96	7.76
1	45°	-	-
3	45°	0.003	0.028
6	45°	0.014	0.11
23	45°	0.23	1.90
emmimEtSO <sub>4</sub>			
1	65°	0.19	1.51
3	65°	0.60	4.87
5	65°	0.75	6.08
23	65°	1.01	8.19
1	45°	0.003	0.028

3	45°	0.01	0.083
5	45°	0.02	0.19
23	45°	0.34	2.77

---

250 mg (8.1 mmol) of AB and 250 mg of the ionic-liquid were used in all experiments.

### 2.3.4 $^{11}\text{B}$ NMR Characterization of Reaction Products and Pathways

The bmimCl ionic liquid is a solid at room temperature, but the 50:50-wt% AB/bmimCl mixtures formed a viscous, stirrable room temperature liquid. However, as the  $\text{H}_2$ -release reaction began, the mixture foamed. As the  $\text{H}_2$ -release neared the loss of  $\sim 1$   $\text{H}_2$ -equiv., the foam began to convert to a white solid. The entire AB/bmimCl mixture ultimately became solid as the reaction reached over 2  $\text{H}_2$ -equiv. Similar behavior was seen for the other 50:50-wt% AB/ionic-liquid mixtures, but with some differences in their liquid ranges. On the other hand, the 80:20-wt% AB/bmimCl mixtures formed a moist paste at room temperature. Upon initial heating, this paste melted, but then rapidly solidified after the onset of  $\text{H}_2$ -release. Solid formation was likewise observed in  $\text{H}_2$ -release reactions of 50:50-wt% AB/tetraglyme systems (discussed later) to produce a final two-phase liquid/solid mixture.

#### 2.3.4.1 $^{11}\text{B}$ NMR of Pyridine Extracts from Reaction Products

The  $^{11}\text{B}$  NMR spectra of the pyridine soluble products produced at different stages in the AB solid-state and AB/bmimCl reactions are compared in **Figure 2.9**. Consistent with the observed absence of  $\text{H}_2$ -loss, the spectrum (**Figure 2.9a**) of the residue of the 1 h solid-state AB reaction showed only unreacted AB (quartet,  $-22.3$  ppm<sup>37</sup>), whereas the spectrum (**Figure 2.9c**) of the 1 h AB/bmimCl mixture clearly showed multiple resonances indicating a significant reaction that was consistent with its measured 0.52 equiv. of  $\text{H}_2$ -release. As shown in **Figures 2.9b** and **2.9d**, the spectra of the pyridine soluble residues of the AB solid-state and AB/bmimCl reactions obtained after the reactions had released 0.83 and 0.95  $\text{H}_2$ -equiv., respectively, were similar, each showing that the AB



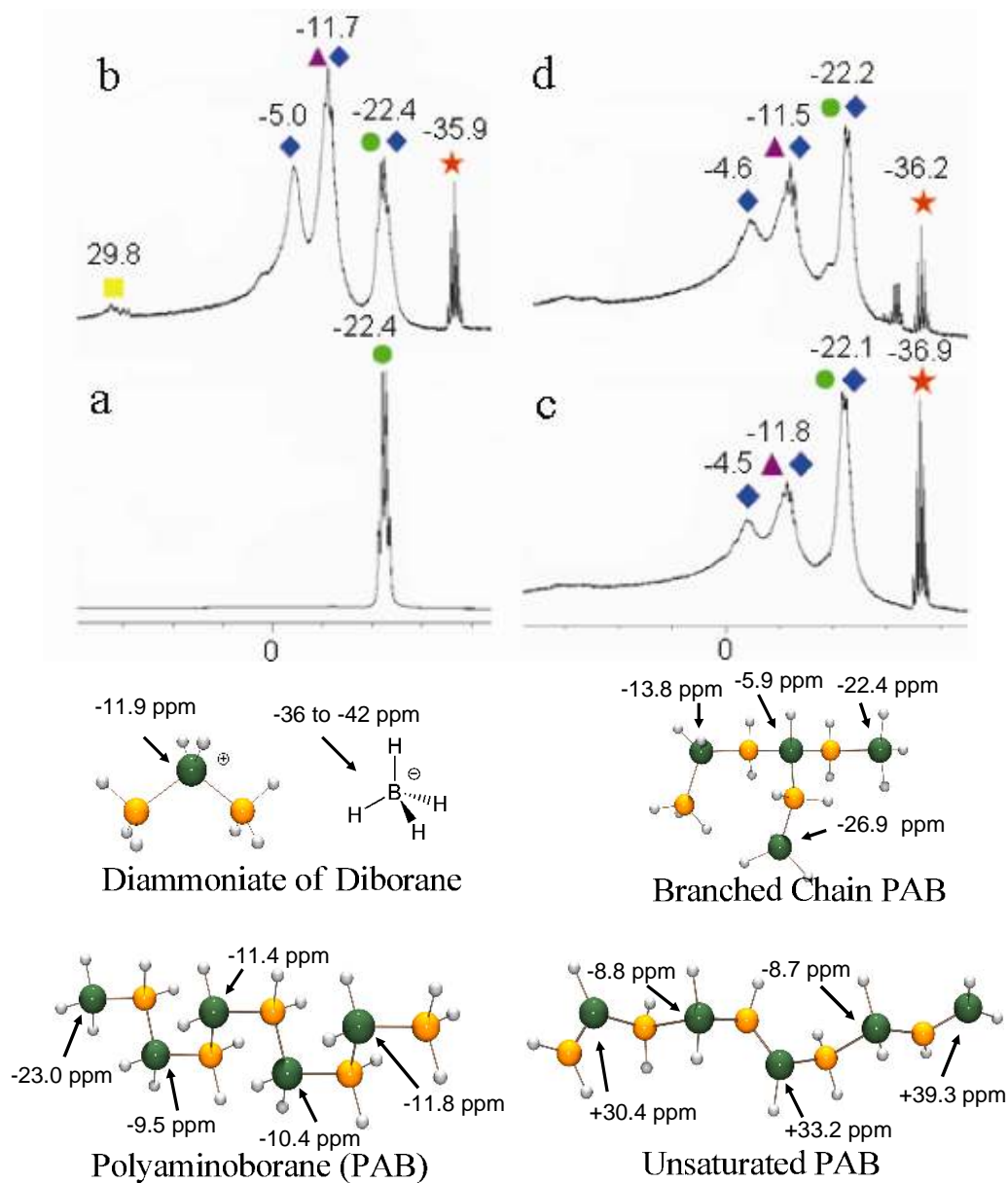


**Figure 2.9** Above: Solution  $^{11}\text{B}$  NMR (128.4 MHz) spectra of the residues (extracted in pyridine) of the 85 °C reaction of: **(Left)** solid-state AB (250 mg) after  $\text{H}_2$ -release of: (a) 0.04 equiv. and (b) 0.83 equiv. **(Right)** 50-wt% AB (250 mg) in bmimCl (250 mg) after  $\text{H}_2$ -release of: (c) 0.52 equiv. and (d) 0.95 equiv. AB ●, DADB (★  $\text{BH}_4^-$  ▲  $\text{BH}_2^+$ ), PAB ◆, B=N ■. Below: Select  $^{11}\text{B}$  NMR calculated shifts.

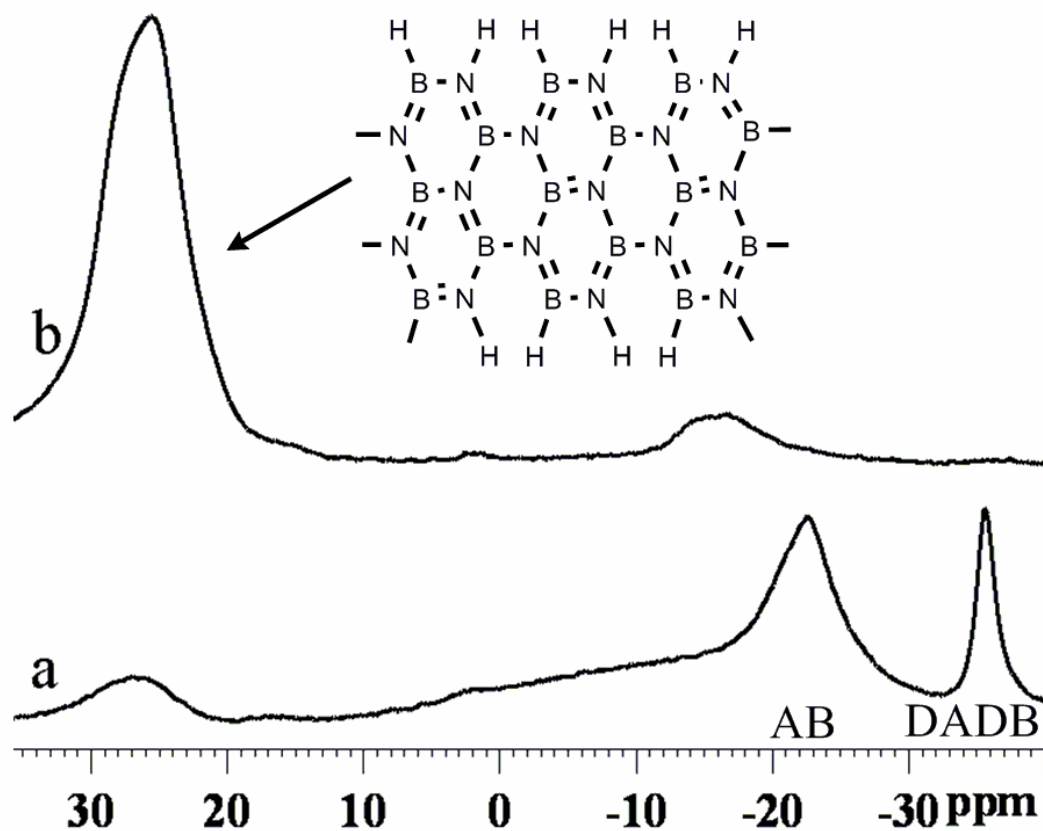


**Figure 2.10** Solid-state  $^{11}\text{B}$  NMR (240 MHz) spectra recorded at 25 °C of the reaction of 50-wt% AB (150 mg) in bmimCl (150 mg) at 110 °C after the release of: (a) 1 equiv. and (b) 2 equiv.

resonance had decreased and the growth of new resonances arising from the diammoniate of diborane (which forms without the loss of  $\text{H}_2$ ),  $[(\text{NH}_3)_2\text{BH}_2]^+\text{BH}_4^-$ , (DADB) (-13.3 (overlapped) and -37.6 ppm)<sup>7,39</sup> and branched-chain polyaminoborane polymers (PAB) (-7, -13.3 and -25.1 ppm).<sup>4</sup> As dehydrogenation progressed past 1 equivalent, only a

small amount of material was pyridine soluble; therefore, solid-state NMR was also used to analyze these materials.

#### 2.3.4.2 Solid-State $^{11}\text{B}$ NMR Studies

Consistent with both the  $\text{H}_2$ -release measurements and the  $^{11}\text{B}$  NMR analyses of the pyridine extracts, the solid-state  $^{11}\text{B}$  spectrum (**Figure 2.10**) of the reaction of a 50:50-wt% bmimCl/AB mixture heated at 110 °C also showed the presence of DADB after 1.0 equiv. of  $\text{H}_2$ -release. The solid-state  $^{11}\text{B}$  NMR spectrum of the final product after the release of 2  $\text{H}_2$ -equiv. showed a broad downfield resonance characteristic of the  $\text{sp}^2$  boron-nitrogen framework of cross-linked polyborazylene structures,<sup>40-42</sup> indicating that AB dehydrogenation ultimately produced B=N unsaturated products. NMR studies of the dehydrogenated products of AB  $\text{H}_2$ -release promoted by solid-state thermal reactions<sup>5,41</sup> have likewise shown the formation of B=N unsaturated final products after the release of more than 2  $\text{H}_2$ -equiv.

#### 2.3.4.3 *In Situ* $^{11}\text{B}$ NMR Studies in Ionic Liquids

*In situ*  $^{11}\text{B}$  NMR studies (**Figure 2.11**) of AB  $\text{H}_2$ -release at 85 °C in a solution of the room temperature ionic liquid bmimOTf (10:90 AB/bmimOTf mixture) exhibited features similar to those observed in the solid-state NMR spectra of the more concentrated AB/bmimCl reactions. Initially, only the AB resonance was present, but the appearance, after 10 min, of the well resolved quintet resonance near -38 ppm indicated significant AB conversion to DADB. After 30 min, 0.5  $\text{H}_2$ -equiv. had been released, but the NMR spectrum (**Figure 2.11c**) indicated that the AB was completely consumed to produce a mixture of DADB and PAB polymer. Once the reaction reached the release of 0.9  $\text{H}_2$ -equiv., the spectrum (**Figure 2.11d**) of the mixture showed a decrease in the

DADB resonance along with a corresponding increase in the PAB resonances. The spectrum taken after the release of 1.5 H<sub>2</sub>-equiv. (**Figure 2.11e**) showed that the DADB had been almost completely consumed and a new downfield resonance near 16 ppm had appeared. This 16 ppm resonance continued (**Figure 2.11f**) to grow and the PAB resonances continued to decrease as the reaction achieved the release of 2.0 H<sub>2</sub>-equiv.

The solid-state <sup>11</sup>B NMR spectrum, discussed earlier (**Figure 2.10**), of the product of the AB/bmimCl reaction after the release of 2 H<sub>2</sub>-equiv. showed the broad downfield resonance near 30 ppm that is characteristic of unsaturated sp<sup>2</sup> boron-nitrogen frameworks. On the other hand, the *in situ* NMR studies of the AB/bmimOTf reactions, as well as similar NMR studies of the 85 °C H<sub>2</sub>-release from AB/mmimMeSO<sub>4</sub> and AB/bmimI reactions, showed the growth of a 16 ppm resonance after the release of 2 H<sub>2</sub>-equiv. The 16 ppm resonance in these ionic liquid reactions is thus shifted almost 14 ppm upfield relative to that normally found for polyborazylene<sup>40-42</sup> or borazine.<sup>43</sup> This suggests that if either of these unsaturated species were formed in these solutions, the observed chemical shift change could result from interactions with the ionic liquid solvent.

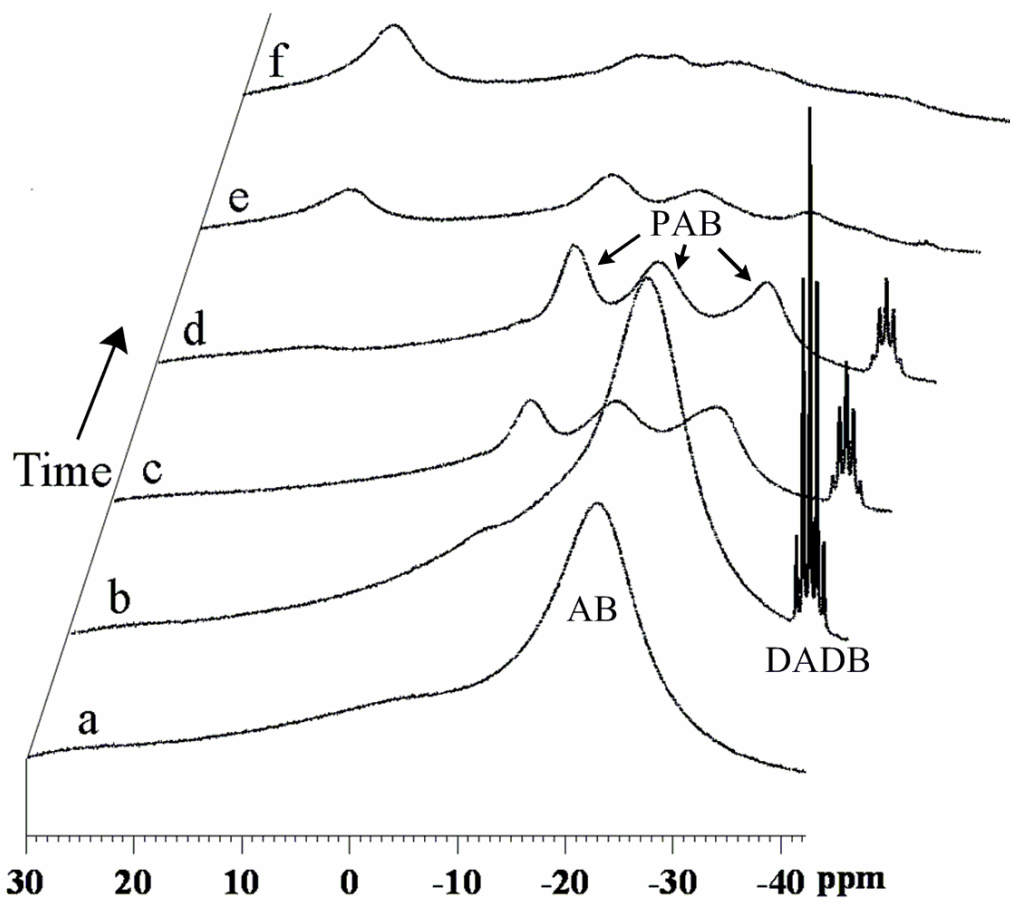


**Figure 2.11** Solution  $^{11}\text{B}$  NMR (128.4 MHz) spectra recorded at 25 °C of the reaction of 10-wt% AB (50 mg) in bmimOTf (450 mg) at 85 °C after the release of: (a) 0.0 equiv. (0 min), (b) 0.1 equiv. (10 min), (c) 0.5 equiv. (30 min), (d) 0.9 equiv. (60 min), (e) 1.5 equiv. (180 min) and (f) 2.0 equiv. (360 min). (The broad DADB resonance at -13 ppm is obscured by the AB and PAB resonances)

Given both their polar compositions and planar aromatic like structures and properties, a variety of ionic liquid interactions would be possible for borazine and polyborazylene, including the formation of ionic liquid hydrogen-bonded and/or

clathrated<sup>44-49</sup> species. Holbrey et al. have shown that ionic liquids can clathrate aromatic species such as benzene, toluene, and *o*- *m*- *p*- xylene. In the ionic liquid 1,3-dimethylimidazolium hexafluorophosphate, crystals were grown from these clathrates and X-ray data were collected showing the benzene does actually form layered complexes with the imidazolium rings. The aromatic is encapsulated in a cation-anion cage with the cation imidazolium methyl groups having strong  $\pi$ -interactions with the aromatic.<sup>47</sup> These interactions are shown in **Figure 2.12**.

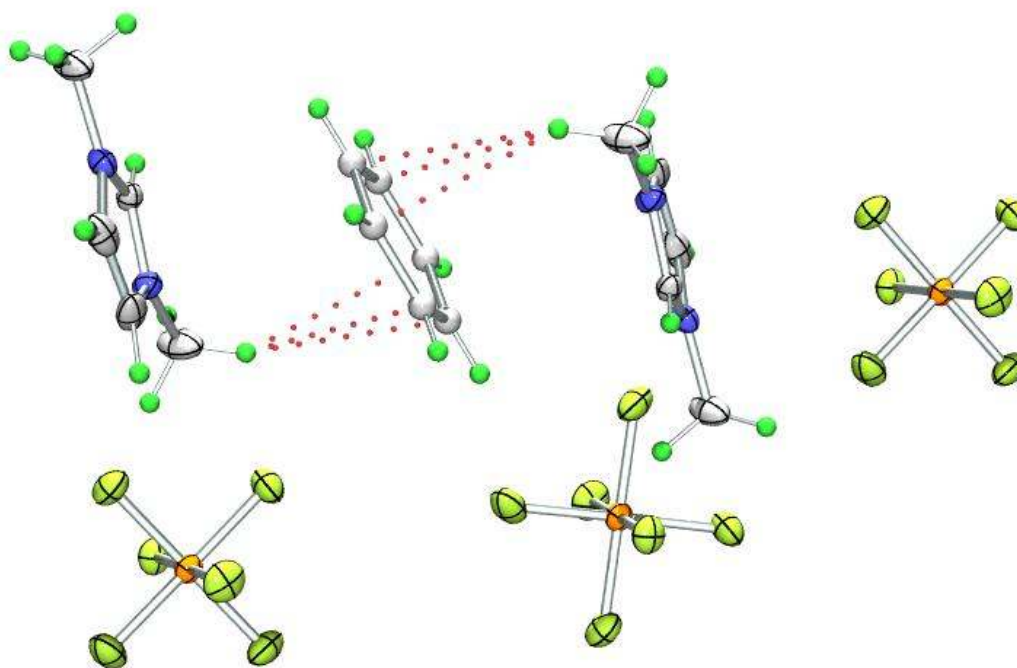


**Figure 2.12** 1,3-dimethylimidazolium hexafluorophosphate with 0.5 mol benzene included as a clathrate. Three closest benzene carbons are shown interacting with methyl hydrogen: distances are 3.07 Å, 3.03 Å, and 3.22 Å.<sup>47</sup>

Similar interactions would be expected to occur in the isoelectronic BN analogue borazine. Several  $^{11}\text{B}$  NMR studies specifically probing this phenomenon showed interactions like that found by Holbrey and others. These interactions are expected to decrease as the temperature is increased and, as shown in the  $^{11}\text{B}$  NMR spectra in **Figure 2.13**, it was found that upon recording the NMR spectrum of the final AB/bmimOTf sample with the NMR probe heated at 100 °C instead of 27 °C, the resonance at 16 ppm disappeared and was replaced by a resonance in the more normal 30 ppm region of borazine. It was likewise found that when glyme (1:10 glyme) was added to an AB/bmimOTf reaction sample exhibiting a 16 ppm resonance, this resonance disappeared and was replaced by a 30 ppm resonance. Additional evidence that borazine could give rise to a shift in this region in ionic liquid solutions was obtained by recording the spectra of a pure sample of borazine dissolved in 90 wt% bmimI. The initial spectrum showed only a broad downfield peak (**Figure 2.14a**), but this resonance then shifted to 16 ppm after the solution was heated at 85 °C (**Figure 2.14b**). The borazine could then be recovered from the bmimI solution by extraction with toluene (**Figure 2.14c**). These results are thus all consistent with a significant interaction between borazine and the ionic liquids. Some ionic liquids required initial heating to form these interactions, whereas the less viscous ionic liquids formed them at room temperature. Such interactions may play a key role in retarding the loss of borazine, a likely fuel cell catalyst poison, during AB  $\text{H}_2$ -release.

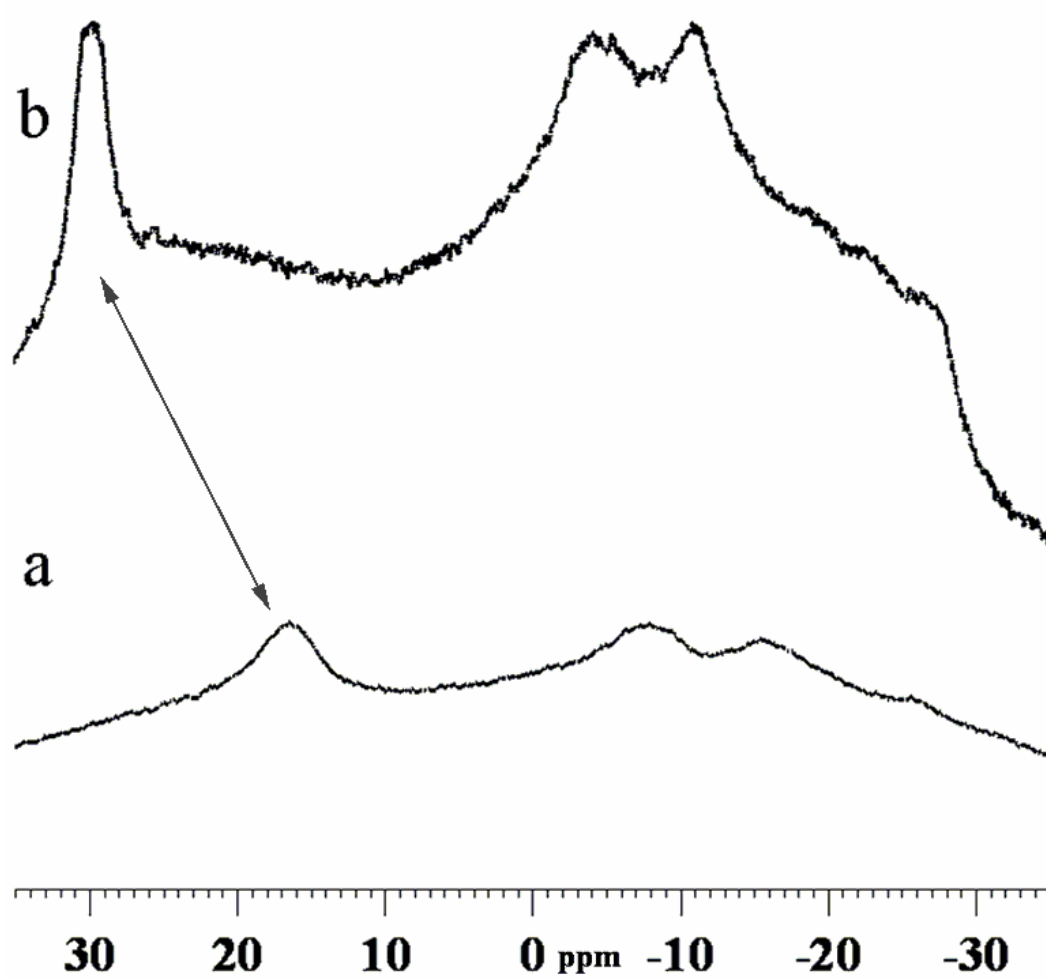


**Figure 2.13** Solution  $^{11}\text{B}$  NMR (128.4 MHz) of the reaction of 10-wt% AB (50 mg) in bmimOTf (450 mg) at 85 °C for 6 h: (a) NMR probe at 27 °C and (b) NMR probe at 100 °C.



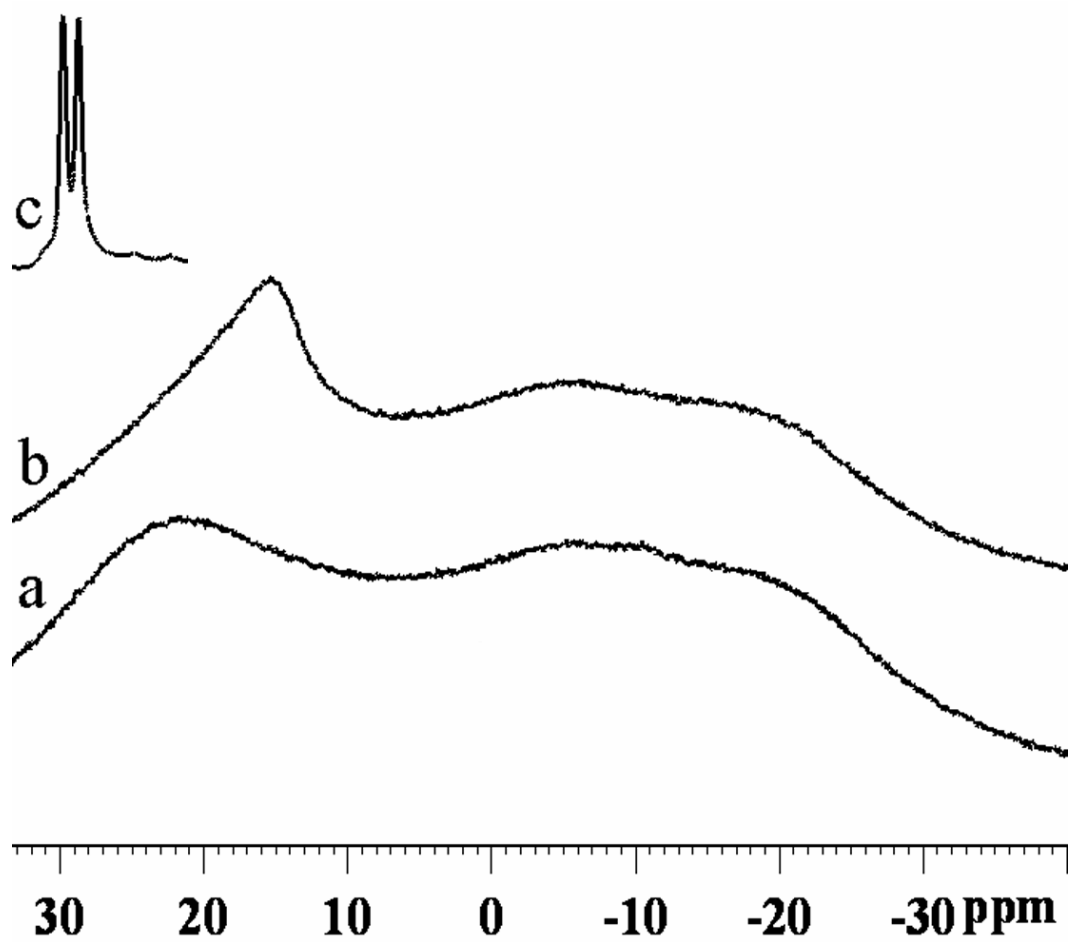
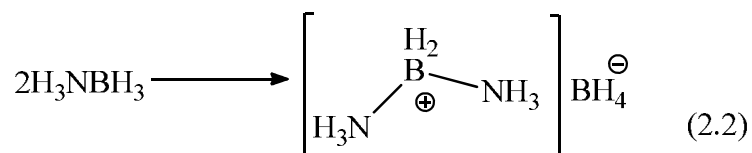


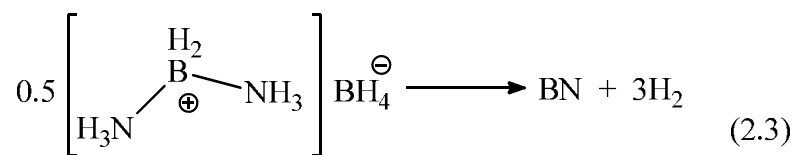
**Figure 2.14** Solution  $^{11}\text{B}$  NMR (128.4 MHz) spectra recorded at 25 °C of 10-wt% borazine (50 mg) in bmimI (450 mg) after: (a) initial mixing at 25 °C, (b) 19 h at 85 °C and (c) the toluene extraction after heating.

### 2.3.6 Why do Ionic Liquids Accelerate AB H<sub>2</sub>-release? What is the Role of DADB?

The <sup>11</sup>B NMR spectra of the pyridine extracts (**Figure 2.9**) of both solid-state and ionic liquid H<sub>2</sub>-release reactions at different times and the *in situ* NMR experiments in ionic liquids (**Figure 2.11**) clearly showed the initial formation of diammoniate of diborane (DADB) (**Equation 2.2**) resulting from the reaction of two equivalents (without H<sub>2</sub>-loss) of AB.



The fact that the DADB is a precursor to the formation of the polyaminoboranes, rather than just a side reaction, was demonstrated by H<sub>2</sub>-release and <sup>11</sup>B NMR studies of DADB reactivity in ionic liquids. These studies showed that the 85 °C reaction of a pre-synthesized<sup>7,39</sup> pure sample of DADB dissolved in bmimOTf (10-wt% DADB) yielded the same type of polyaminoborane products, but with faster H<sub>2</sub>-release rates, as those found in the AB/bmimOTf reactions.



The theoretical DADB H<sub>2</sub>-release reaction in terms of AB equiv. is given by **Equation 2.3**. The H<sub>2</sub>-release rates for separate 10 wt% DADB and AB samples in bmimOTf are compared in **Figure 2.15**, where the faster rate of the DADB reaction is clearly apparent. While AB/bmimOTf required 96 min to release 1.0 H<sub>2</sub>-equiv. and 274 min for 1.5 H<sub>2</sub>-equiv., the DADB required only 28 min for 1.0 H<sub>2</sub>-equiv. and 94 min for 1.5

H<sub>2</sub>-equiv. At 400 min, the DADB/bmimOTf reaction had already released 2.09 H<sub>2</sub>-equiv., while the AB/bmimCl reaction was still at 1.76 H<sub>2</sub>-equiv. These rates are also faster than DADB H<sub>2</sub>-release from the solid state.<sup>50</sup> As can be seen in the NMR studies in **Figure 2.16**, the initial <sup>11</sup>B NMR spectrum obtained from a 10-wt% DADB/bmimOTf sample showed only the broad resonances expected for the DADB (NH<sub>3</sub>)<sub>2</sub>BH<sub>2</sub><sup>+</sup> (-13.3 ppm) and BH<sub>4</sub><sup>-</sup> (-37.6 ppm) components. However, after heating for only 10 min at 85 °C, most of the DADB had been converted to PAB. At 30 min, 0.9 H<sub>2</sub>-equiv. had been released and the <sup>11</sup>B NMR spectrum at this point (**Figure 2.16c**) showed that the DADB had been completely consumed. As the reaction proceeded beyond the release of 1 H<sub>2</sub>-equiv., a new resonance grew in that was also at the 16 ppm shift observed in the AB/bmimOTf reactions (**Figure 2.16d-f**).

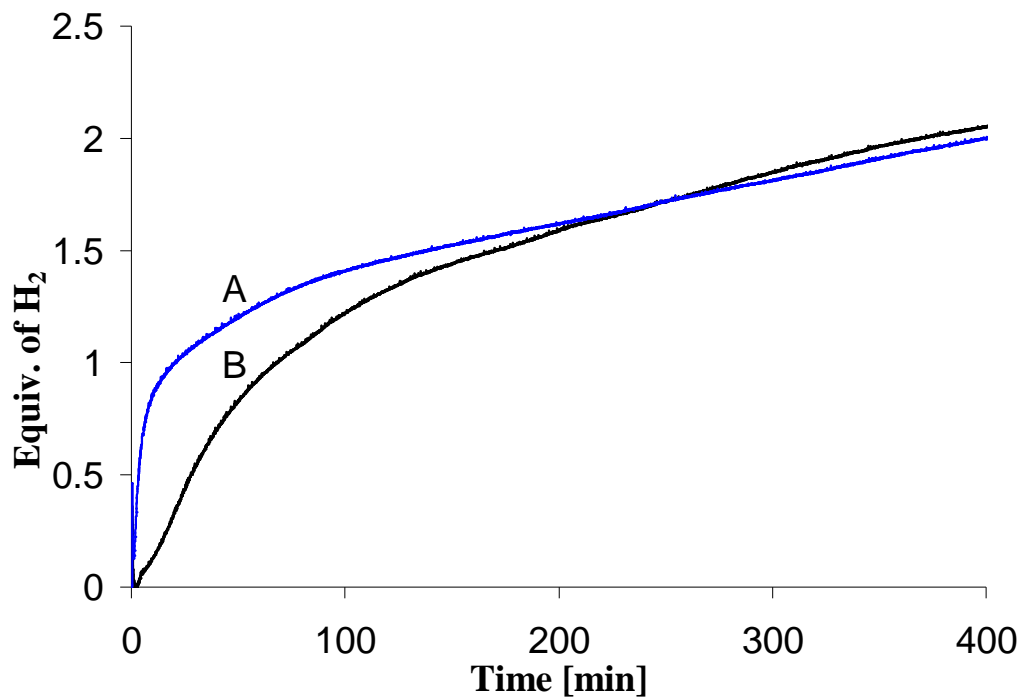


**Figure 2.15** H<sub>2</sub>-release measurements (gas burette) of bmimOTf (450 mg) and 10-wt% (50 mg) of: (A) DADB and (B) AB.

**Table 2.7** Times to Selected Equivalent Points of H<sub>2</sub>-Release (Gas Burette) of bmimOTf (450 mg) and 10-wt% (50 mg) each of: (A) DADB and (B) AB at 85 °C

(A)		(B)	
H <sub>2</sub> -Equiv.	Minutes	H <sub>2</sub> -Equiv.	Minutes
0.25	2	0.25	17
0.5	3	0.5	28
0.75	6	0.75	43
1	20	1	68
1.25	58	1.25	105
1.5	137	1.5	170
1.75	265	1.75	262
2	398	2	367

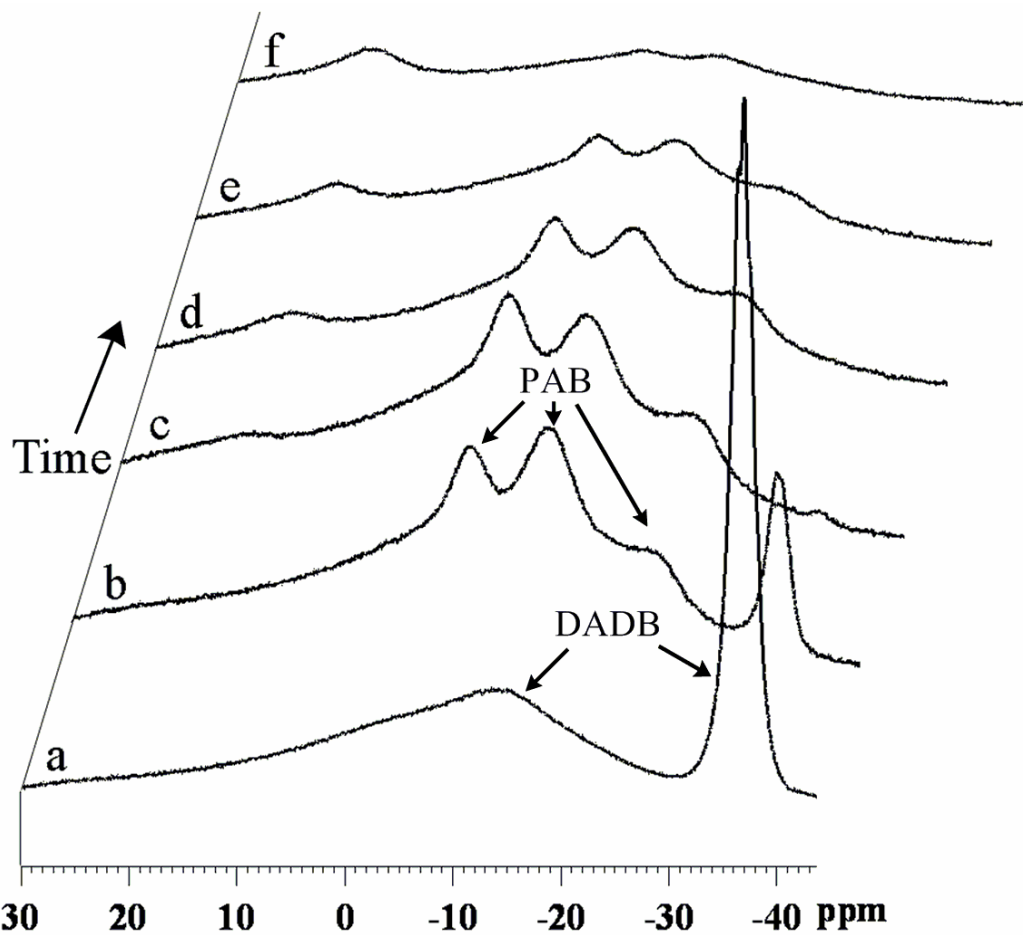


**Figure 2.16** Solution  $^{11}\text{B}$  NMR (128.4 MHz) spectra recorded at 25 °C of the reaction of 10-wt% DADB (50 mg) in bmimOTf (450 mg) at 85 °C after the release of: (a) 0.0 equiv. (0 min), (b) 0.9 equiv. (10 min), (c) 1.1 equiv. (30 min), (d) 1.3 equiv. (60 min), (e) 1.6 equiv. (180 min) and (f) 1.9 equiv. (360 min).

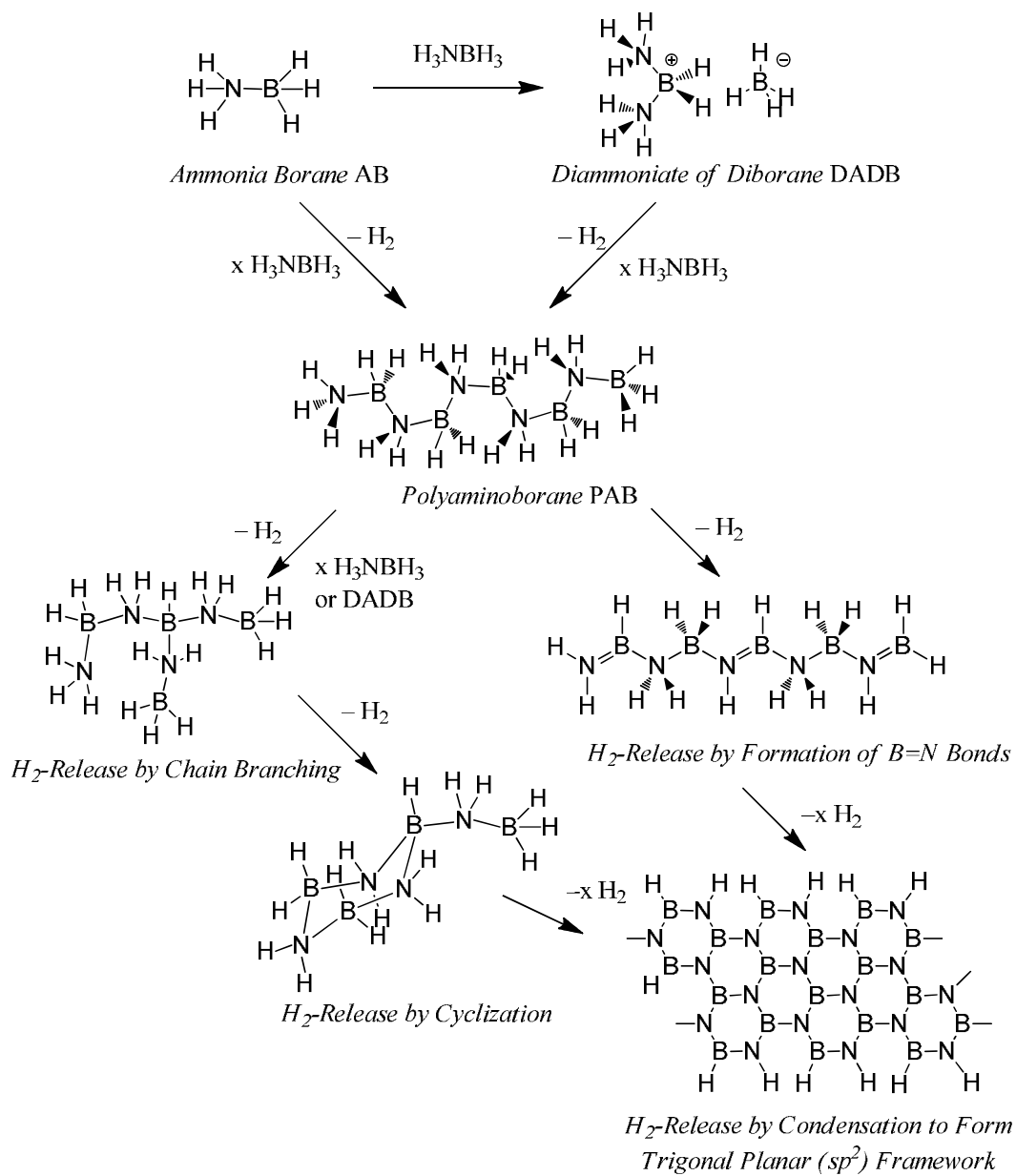


**Figure 2.17** Possible pathway for ionic-liquid promoted  $H_2$ -release from AB.

The combined solid-state and solution  $^{11}B$  NMR studies of AB/ionic-liquid and DADB/ionic-liquid  $H_2$ -release reactions in progress support a AB dehydrogenation pathway in ionic liquids (**Figure 2.17**) involving: (1) ionic-liquid promoted conversion of

AB into its more reactive ionic DADB form, (2) further intermolecular dehydrocoupling reactions between hydridic B-H hydrogens and protonic N-H hydrogens on DADB and/or AB to form polyaminoborane polymers and (3) polyaminoborane dehydrogenation to unsaturated cross-linked polyborazylene materials. The initial formation of DADB has also been proposed as a key step in thermally-induced AB H<sub>2</sub>-release reactions in the solid state<sup>50,51</sup> and in organic solvents,<sup>52</sup> but the highly polar medium provided by ionic liquids promotes DADB formation and appears to be the key activating feature of these ionic liquid reactions.

### 2.3.7 H<sub>2</sub>-Release Reactions in Tetraglyme

The AB H<sub>2</sub>-release observed in the ionic liquid solvents was also compared with that obtained for the conventional polar organic solvent, tetraglyme. The H<sub>2</sub>-release data for a 50:50 wt% ratio AB/tetraglyme mixture showed that both the extent and rate of H<sub>2</sub>-release were comparable to that of the AB/bmimCl reactions (**Figure 2.18**). However, the <sup>11</sup>B NMR spectra of the AB/tetraglyme reactions showed that, unlike in the ionic liquids, there was little evidence of PAB formation, with the major product being instead borazine (30.1 ppm)<sup>43</sup> along with smaller amounts of BH<sub>4</sub><sup>-</sup> (-36.8 ppm)<sup>43</sup> and μ-aminodiborane (-27.5 ppm)<sup>43</sup> (**Figure 2.19**). Thus, ionic liquid solvents are favored for AB H<sub>2</sub>-release since they suppress or retard the formation of these undesired products.

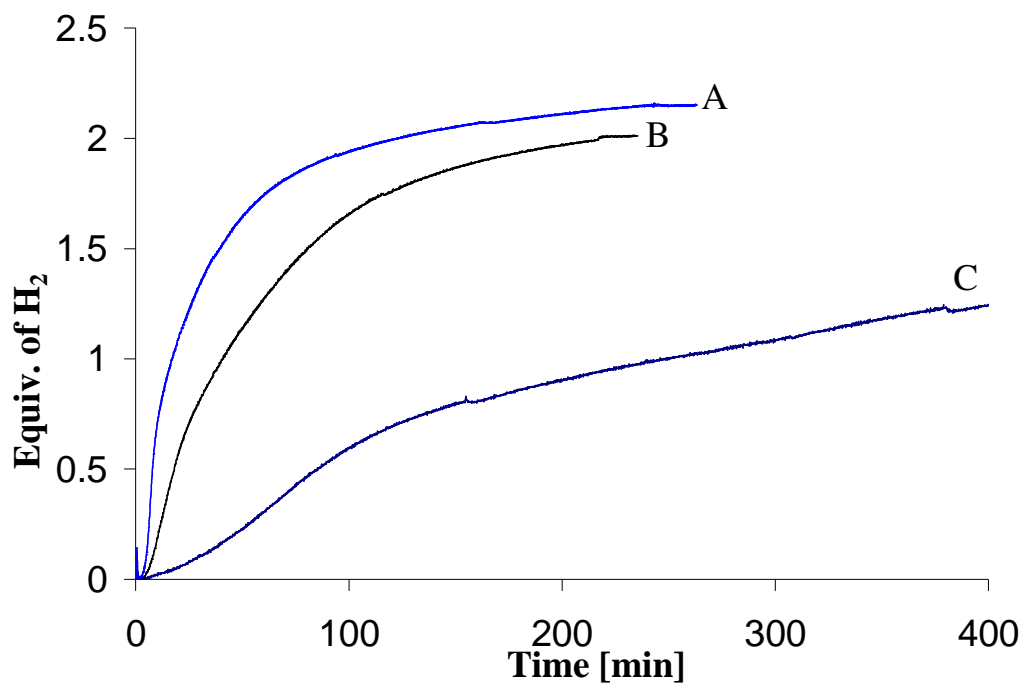


**Figure 2.18** H<sub>2</sub>-release measurements (gas burette) of 50-wt% AB (150 mg) in tetraglyme (150 mg) at: (A) 95 °C, (B) 85 °C and (C) 75 °C.

**Table 2.8 Times to Selected Equivalent Points of H<sub>2</sub>-Release (Gas Burette) of 50-wt% AB (150 mg) in Tetraglyme (150 mg) at Different Temperatures**

(A)		(B)		(C)	
H <sub>2</sub> -Equiv.	Minutes	H <sub>2</sub> -Equiv.	Minutes	H <sub>2</sub> -Equiv.	Minutes
0.25	6	0.25	12	0.25	53
0.5	8	0.5	18	0.5	85
0.75	11	0.75	27	0.75	135
1	17	1	41	1	246
1.25	26	1.25	58	1.25	403
1.5	39	1.5	80	1.5	585
1.75	60	1.75	118	1.75	816
2	122	2	217	2	1130

(A) 95 °C, (B) 85 °C and (C) 75 °C.



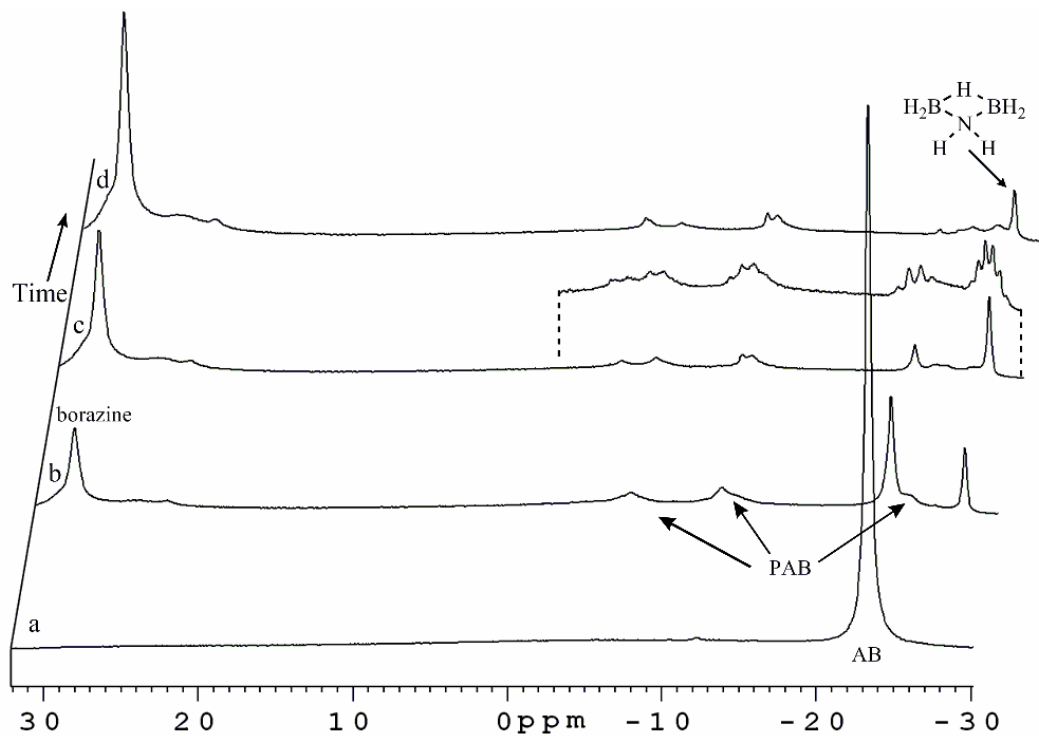


**Figure 2.19** Solution  $^{11}\text{B}\{^1\text{H}\}$  NMR (128 MHz) spectra recorded at 80 °C of the reaction of 10-wt% AB (50 mg) in tetraglyme (450 mg) at 85 °C after: (a) 1.1 equiv. (60 min), (b) 1.7 equiv. (180 min) and (c) 1.9 equiv. (360 min). Inset shows  $^1\text{H}$  coupled spectra.

## 2.4 Conclusions

The results described in this **Chapter** have demonstrated that ionic liquids have an activating effect on ammonia borane H<sub>2</sub>-release. Unlike the solid-state H<sub>2</sub>-release reactions, AB H<sub>2</sub>-release reactions in ionic liquids do not exhibit an induction period. <sup>11</sup>B NMR and H<sub>2</sub>-release studies showed that DADB is the active intermediate in AB dehydropolymerization and that ionic liquids induce the formation of DADB from AB. By increasing the speed of formation of DADB, ionic liquids dramatically improve the H<sub>2</sub>-release rate from AB. The high extent of their H<sub>2</sub>-release, the tunability of both their H<sub>2</sub>-materials weight percents and release rates, and their product control that is attained by either trapping or suppressing unwanted volatile side products make AB/ionic-liquid based systems attractive candidates for chemical hydrogen storage applications.

## 2.5 References

1. Graetz, J. *Chem. Soc. Rev.* **2009**, 38, 73-82.
2. Hamilton, C. W.; Baker, R. T.; Staubitz, A.; Manners, I. *Chem. Soc. Rev.* **2009**, 38, 279-293.
3. Stephens, F. H.; Pons, V.; Baker, R. T. *Dalton Trans.* **2007**, 25, 2613-2626.
4. Bluhm, M. E.; Bradley, M. G.; Butterick III, R.; Kusari, U.; Sneddon, L. G. *J. Am. Chem. Soc.* **2006**, 128, 7748-7749 and references therein.
5. Stowe, A. C.; Shaw, W. J.; Linehan, J. C.; Schmid, B.; Autrey, T. *Phys. Chem. Chem. Phys.* **2007**, 9, 1831-1836 and references therein.
6. Shriver, D. F.; Drezdson, M. A., *Manipulation of Air Sensitive Compounds*. 2 ed.; Wiley: New York, 1986.
7. Shore, S. G.; Parry, R. W. *J. Am. Chem. Soc.* **1958**, 80, 20-24 and preceding papers in this issue.
8. Namboodiri, V. V.; Varma, R. S. *Org. Lett.* **2002**, 4, 3161-3163.
9. Zheng, F.; Rassat, S. D.; Helderandt, D. J.; Caldwell, D. D.; Aardahl, C. L.; Autrey, T.; Linehan, J. C.; Rappe, K. G. *Rev. Sci. Instrum.* **2008**, 79, 084103-1 - 084103-5.
10. Jaska, C. A.; Temple, K.; Lough, A. J.; Manners, I. *Chem. Comm.* **2001**, 962-963.
11. Jaska, C. A.; Temple, K.; Lough, A. J.; Manners, I. *J. Am. Chem. Soc.* **2003**, 125, 9424-9434.
12. Jaska, C. A.; Manners, I. *J. Am. Chem. Soc.* **2004**, 126, 2698-2699.
13. Clark, T. J.; Lee, K.; Manners, I. *Chem. Eur. J.* **2006**, 12, 8634-8648.
14. Clark, T. J.; Russell, C. A.; Manners, I. *J. Am. Chem. Soc.* **2006**, 128, 9582-9583.

15. Denney, M. C.; Pons, V.; Hebden, T. J.; Heinekey, D. M.; Goldberg, K. I. *J. Am. Chem. Soc.* **2006**, *128*, 12048-12049.
16. Fulton, J. L.; Linehan, J. C.; Autrey, T.; Balasubramanian, M.; Chen, Y.; Szymczak, N. K. *J. Am. Chem. Soc.* **2007**, *129*, 11936-11949.
17. Jiang, Y.; Berke, H. *Chem. Comm.* **2007**, 3571-3573.
18. Keaton, R. J.; Blacquiere, J. M.; Baker, R. T. *J. Am. Chem. Soc.* **2007**, *129*, 1844-1845.
19. Paul, A.; Musgrave, C. B. *Angew. Chem., Int. Ed.* **2007**, *46*, 8153-8156.
20. Pun, D.; Lobkovsky, E.; Chirik, P. J. *Chem. Comm.* **2007**, 3297-3299.
21. Blacquiere, N.; Diallo-Garcia, S.; Gorelsky, S. I.; Black, D. A.; Fagnou, K. *J. Am. Chem. Soc.* **2008**, *130*, 14034-14035.
22. Douglas, T. M.; Chaplin, A. B.; Weller, A. S. *J. Am. Chem. Soc.* **2008**, *130*, 14432-14433.
23. Staubitz, A.; Soto, A. P.; Manners, I. *Angew. Chem., Int. Ed.* **2008**, *47*, 6212-6215.
24. Yang, X.; Hall, M. B. *J. Am. Chem. Soc.* **2008**, *130*, 1798-1799.
25. Forster, T. D.; Tuononen, H. M.; Parvez, M.; Roesler, R. *J. Am. Chem. Soc.* **2009**, *131*, 6689-6691.
26. Stephens, F. H.; Baker, R. T.; Matus, M. H.; Grant, D. J.; Dixon, D. A. *Angew. Chem., Int. Ed.* **2007**, *46*, 746-749.
27. Himmelberger, D. W.; Bluhm, M. E.; Sneddon, L. G. *Prepr. Symp. - Am. Chem. Soc., Div. Fuel Chem.* **2008**, *53*, 666-667.

28. Gutowska, A.; Li, L.; Shin, Y.; Wang, C. M.; Li, X. S.; Linehan, J. C.; Smith, R. S.; Kay, B. D.; Schmid, B.; Shaw, W.; Gutowski, M.; Autrey, T. *Angew. Chem., Int. Ed.* **2005**, *44*, 3578-3582.
29. Sepehri, S.; Feaver, A.; Shaw, W. J.; Howard, C. J.; Zhang, Q.; Autrey, T.; Cao J. *Phys. Chem. B* **2007**, *111*, 14285-14289.
30. Paolone, A.; Palumbo, O.; Rispoli, P.; Cantelli, R.; Autrey, T.; Karkamkar, A. J. *Phys. Chem. C* **2009**, *113*, 10319-10321.
31. Dupont, J.; de Souza, R. F.; Suarez, P. A. Z. *Chem. Rev.* **2002**, *102*, 3667-3692.
32. Dyson, P. J. *Appl. Oragnomet. Chem.* **2002**, *16*, 495-500.
33. Wasserscheid, P.; Keim, W. *Angew. Chem., Int. Ed.* **2002**, *39*, 3772-3789.
34. Zhao, H.; Malhotra, S. V. *Aldrich Chimica Acta* **2002**, *35*, 75-83.
35. Namboodiri, V. V.; Varma, R. S. *Org. Lett.* **2002**, *4*, 3161-3163.
36. Zheng, F.; Rassat, S. D.; Helderandt, D. J.; Caldwell, D. D.; Aardahl, C. L.; Autrey, T.; Linehan, J. C.; Rappe, K. G. *Rev. Sci. Instrum.* **2008**, *79*, 084103.
37. Satyapal, S. *2007 DOE Hydrogen Program Review*.  
[http://www.hydrogen.energy.gov/pdfs/review07/st\\_0\\_satyapal.pdf](http://www.hydrogen.energy.gov/pdfs/review07/st_0_satyapal.pdf).
38. Dillich, S. *2009 DOE Hydrogen Program & Vehicle Technologies Program*  
[http://www.hydrogen.energy.gov/pdfs/review09/st\\_0\\_dillich.pdf](http://www.hydrogen.energy.gov/pdfs/review09/st_0_dillich.pdf). DOE has recently lowered the 2015 gravimetric total system target to only 5.5 total system weight %.
39. Onak, T. P.; Shapiro, I. *J. Chem. Phys.* **1960**, *32*, 952.
40. Fazen, P. J.; Beck, J. S.; Lynch, A. T.; Remsen, E. E.; Sneddon, L. G. *Chem. Mater.* **1990**, *2*, 96-97.

41. Fazen, P. J.; Remsen, E. E.; Beck, J. S.; Carroll, P. J.; McGhie, A. R.; Sneddon, L. *G. Chem. Mater.* **1995**, *7*, 1942-1956.
42. Gervais, C.; Framery, E.; Duriez, C.; Maquet, J.; Vaultier, M.; Babonneau, F. *J. Eur. Ceram. Soc.* **2005**, *25*, 129-135.
43. Nöth, H.; Wrackmeyer, B., In *Nuclear Magnetic Resonance Spectroscopy of Boron Compounds*, Springer-Verlag: New York, 1978; pp 188, 265, 394-395.
44. Christie, S.; Dubois, R. H.; Rogers, R. D.; White, P. S.; Zaworotko, M. J. *J. Inclusion Phenom.* **1991**, *11*, 103-114.
45. Coleman, A. W.; Means, C. M.; Bott, S. G.; Atwood, J. L. *J. Chem. Crystallogr.* **1990**, *20*, 199-201.
46. Gaudet, M. V.; Peterson, D. C.; Zaworotko, M. J. *J. Inclusion Phenom.* **1988**, *6*, 425-428.
47. Holbrey, J. D.; Reichert, W. M.; Nieuwenhuyzen, M.; Sheppard, O.; Hardacre, C.; Rogers, R. D. *Chem. Comm.* **2003**, 476-477.
48. Pickett, C. J. *Chem. Comm.* **1985**, 323-326.
49. Surette, J. K. D.; Green, L.; Singer, R. D. *Chem. Comm.* **1996**, 2753-2754.
50. Heldebrant, D. J.; Karkamkar, A.; Hess, N. J.; Bowden, M.; Rassat, S.; Zheng, F.; Rappe, K.; Autrey, T. *Chem. Mater.* **2008**, *20*, 5332-5336.
51. Stowe, A. C.; Shaw, W. J.; Linehan, J. C.; Schmid, B.; Autrey, T. *Phys. Chem. Chem. Phys.* **2007**, *9*, 1831-1836 and references therein.
52. Shaw, W. J.; Linehan, J. C.; Szymczak, N. K.; Helderand, D. J.; Yonker, C.; Camaioni, D. M.; Baker, R. T.; Autrey, T. *Angew. Chem. Int. Ed.* **2008**, *47*, 7493-7496.

## Chapter 3

### Base Promoted Ammonia Borane Hydrogen Release

#### Summary

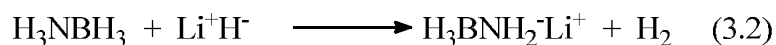
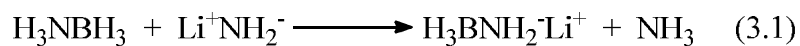
The strong non-nucleophilic base, bis(dimethylamino)naphthalene, (Proton Sponge, PS) has been found to promote the rate and extent of H<sub>2</sub>-release from ammonia borane (AB) in both the solid state and in ionic-liquid and tetraglyme solutions. For example, AB reactions in 1-butyl-3-methylimidazolium chloride (bmimCl) containing 5.3 mol% PS released 2 equivalents of H<sub>2</sub> in 171 min at 85 °C and only 9 min at 110 °C, whereas comparable reactions without PS required 316 min at 85 °C and 20 min at 110 °C. Ionic liquid solvents proved more favorable than tetraglyme since they reduced the formation of undesirable products, such as borazine. Solid-state and solution <sup>11</sup>B NMR studies of PS-promoted reactions in progress support a reaction pathway involving initial AB deprotonation to form the H<sub>3</sub>BNH<sub>2</sub><sup>-</sup> anion. This anion can then initiate AB dehydropolymerization to form branched-chain polyaminoborane polymers. Subsequent chain-branching and dehydrogenation reactions lead ultimately to a cross-linked polyborazylene-type product. Model studies of the reactions of [Et<sub>3</sub>BNH<sub>2</sub>BH<sub>3</sub>]<sup>-</sup>Li<sup>+</sup> with AB show evidence of chain-growth,<sup>1</sup> providing additional support for a PS-promoted AB anionic dehydropolymerization H<sub>2</sub>-release process.

### 3.1 Introduction

In the preceding **Chapter**, it was shown that the addition of ionic liquids to ammonia borane dramatically increased the extent and rate of H<sub>2</sub>-release and eliminated the induction period that had been observed in solid-state reactions. These studies showed that DADB is the active intermediate in AB dehydropolymerization and that ionic liquids induce the formation of DADB from AB.

The Ionic-liquid based systems described in **Chapter 2** can be tuned to achieve a range of H<sub>2</sub>-release rates. But it was also found that the H<sub>2</sub>-release rate dramatically slowed after the first equivalent was released. Clearly there is room for other methods for improving the rate and extent of H<sub>2</sub>-release from AB. In addition to ionic liquids a number of other approaches are now being explored by others to induce AB H<sub>2</sub>-release, such as the use of transition metal catalysts,<sup>6-21</sup> acid catalysts,<sup>2</sup> nano and meso-porous scaffolds.<sup>3-5</sup> In this **Chapter**, the activating effect of base additives will be described for reactions in the solid-state, ionic liquids, and tetraglyme and it will be shown that they enhance H<sub>2</sub>-release of the second AB equivalent.

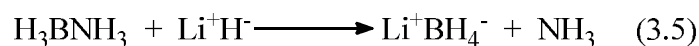
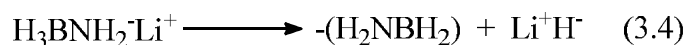
Earlier work showed<sup>6,7</sup> that the addition of small amounts of either LiH or LiNH<sub>2</sub> to AB in the solid state eliminated the induction period and increased both the rate and extent of H<sub>2</sub>-release at 85 °C. As outlined in **Equations 3.1** and **3.2**, the initial step in these reactions was proposed to be AB deprotonation to produce the H<sub>3</sub>BNH<sub>2</sub><sup>-</sup> anion, with this anion then inducing anionic dehydropolymerization of AB to produce a growing polyaminoborane polymer (**Equation 3.3**).







Unfortunately, these reactions stopped after the release of ~1.5 H<sub>2</sub>-equivalents due at least in part to the formation of the LiBH<sub>4</sub> side-product via the reactions in **Equations 3.4** and **3.5**. Since LiBH<sub>4</sub> does not decompose until >350 °C, its formation reduces the extent of AB H<sub>2</sub>-release at 85 °C.<sup>8</sup>



In order to avoid the formation of stable alkali-metal borohydrides, we investigated the use of alternative nitrogen-based deprotonating agents to induce AB polymerization. This **Chapter** reports that the strong (pka ~12), non-nucleophilic base, bis(dimethylamino)naphthalene (Proton Sponge, PS),<sup>9</sup> can also induce AB H<sub>2</sub>-release via an anionic dehydropolymerization mechanism with the advantage that the formation of a stable BH<sub>4</sub><sup>-</sup> salt is avoided.

## 3.2 Experimental Section

### 3.2.1 Materials

All manipulations were carried out using standard high vacuum or inert atmosphere techniques, as described by Shriver.<sup>10</sup> Ammonia borane (AB) (Aviabor, 97% minimum purity) was ground into a free flowing powder using a commercial coffee grinder. The 1-butyl-3-methylimidazolium chloride (bmimCl), 1,3-dimethylimidazolium methylsulfate (mmimMeSO<sub>4</sub>), 1-butyl-2,3-dimethylimidazolium chloride (bdmimCl), and 1-ethyl-2,3-dimethylimidazolium ethylsulfate (edmimEtSO<sub>4</sub>) ionic liquids (Fluka) were dried by toluene azeotropic distillation. Tetraethylene glycol dimethyl ether (Sigma 99%) (tetraglyme) and ethylene glycol dimethyl ether (Sigma 99%) (glyme) were vacuum distilled from sodium with heating. Aldrich bis(dimethylamino)naphthalene (Proton Sponge, PS) was sublimed and stored under inert atmosphere and light free conditions.

### 3.2.2 Physical Measurements

The Toepler pump system used for hydrogen measurements was similar to that described by Shriver<sup>10</sup> and was diagramed in **Figure 2.1** of **Chapter 2**. The released gases from the reaction vessel were first passed through a liquid nitrogen trap before continuing on to the Toepler pump (700 mL). The released H<sub>2</sub> was then pumped into a series of calibrated volumes with the final pressure of the collected H<sub>2</sub>-gas measured ( $\pm 0.5$  mm) with the aid of a U-tube manometer. After the H<sub>2</sub>-measurement was completed, the in-line liquid nitrogen trap was warmed to room temperature and the amount of any volatiles that had been trapped was then also measured using the Toepler pump.

The automated gas burette **Figure 2.2** of **Chapter 2** was based on the design reported by Zheng et al.,<sup>11</sup> but employed all glass connections with a cold trap (-78 °C) inserted between the reaction flask and burette to allow trapping of any volatiles that might have been produced during the reaction. A more complete description of both the Toepler pump and automated gas burette is available in **Chapter 2**.

Differential scanning calorimetry was carried out on a Setaram C80 calorimeter at Pacific Northwest National Laboratories. Samples containing 50 mg of AB and 50 mg of bmimCl, without and with 5 mol% (18 mg) of PS were loaded into the cells under a N<sub>2</sub> atmosphere. The ramp rate was 1 °C/min and samples were taken to either 85 °C or 110 °C.

Solid-state reactions carried out with the Toepler pump were extracted with pyridine at various points in the reactions and monitored by <sup>11</sup>B NMR. The reaction flask was removed from the oil bath and cooled to room temperature, then dry pyridine was added to the reaction flask under N<sub>2</sub> flow. The pyridine solution was extracted by syringe and then the <sup>11</sup>B NMR was taken.

While bmimCl is a liquid at 85 °C, it is a solid at room temperature; therefore, solid-state <sup>11</sup>B NMR analyses (at Pacific Northwest National Laboratories: 240 MHz machine spun at 10 kHz) were used to monitor the products of reactions carried out in bmimCl. All solid state <sup>11</sup>B chemical shifts were measured relative to external NaBH<sub>4</sub> (-41 ppm).

The solution <sup>11</sup>B NMR (128.4 MHz Bruker DMX-400) studies in the room temperature ionic liquid mmimMeSO<sub>4</sub> were carried out by heating the reaction mixtures in sealed NMR tubes at 85 °C for the indicated times with the spectra taken at 25 °C. The

$^{11}\text{B}$  NMR spectra of the reactions in tetraglyme were collected with the NMR probe heated at 80 °C.

All solid-state and solution  $^{11}\text{B}$  NMR chemical shifts are referenced to external  $\text{BF}_3\cdot\text{O}(\text{C}_2\text{H}_5)_2$  (0.0 ppm) with a negative sign indicating an upfield shift.

### 3.2.3 Procedures for AB H<sub>2</sub>-Release Reactions

For the experiments where the released H<sub>2</sub> was measured with the Toepler pump, the AB (250 mg, 8.1 mmol) was loaded into the reaction flasks under N<sub>2</sub>. The solid-state reactions of AB/PS mixtures were carried out in evacuated 500 mL break-seal flasks that were heated in an oven preheated to the desired temperature. The solids were initially crudely mixed, since upon heating the solid mixtures were found to form a melt before the onset of H<sub>2</sub>-release. Reactions in solution were loaded into ~100 mL flasks with the ionic liquid and PS in the amounts given in the tables. The flasks were then evacuated, sealed, and placed in a hot oil bath preheated to the desired temperature. The flasks were opened at the indicated times and the released hydrogen quantified using the Toepler pump system. Post reaction, the flasks were evacuated for 30 min through the cold trap to remove any volatile products from the reaction residue. The product residues and volatiles in the cold trap were extracted with dry glyme and analyzed by  $^{11}\text{B}$  NMR.

For reactions using the automated gas burette, the AB (150 mg, 4.87 mmol) samples were loaded into ~100 mL flasks with calibrated volumes, along with the ionic liquid (150 mg) or tetraglyme (0.15 mL) solvents and PS. Under a flow of helium, the flask was attached to the burette system. The system was evacuated 30 min for reactions with the ionic liquid solutions, and 5 min for tetraglyme solutions. The system was then backfilled with helium and allowed to equilibrate to atmospheric pressure for ~30 min.

Once the system pressure equalized, the data collection program was started and the flask was immersed in the preheated oil bath. The product residues were extracted with dry glyme and analyzed by  $^{11}\text{B}$  NMR. The data are reported from the point where the flask was initially plunged into the oil bath, but  $\text{H}_2$ -release was not observed until the ionic-liquid/AB mixture melted. Data were recorded at 2-5 second intervals depending on the speed of the reaction. An example data set is shown in **Table 2.1** in **Chapter 2** along with a more complete description of the automated gas burette. The rest of the data sets for the gas burette graphs presented in this **Chapter** are available on a CD submitted with the paper copy of this dissertation and electronically in the supplementary files submitted with the electronic copy of this dissertation.

Reactions of bmimCl and bmimCl/PS with partially dehydrogenated AB followed the procedures for the automated gas burette. Initially, two separate samples of neat AB (150 mg, 4.87 mmol) were heated for 23 h at 85 °C to release ~1 equivalent of  $\text{H}_2$ . The reaction flasks were removed from the gas burette system under a flow of helium and then taken into a glove box where bmimCl (150 mg, 50 wt%) was added to one sample and bmimCl (150 mg, 50 wt%) and PS (55 mg, 5 mol%) added to the second. After thorough mixing, the flasks were reattached to the gas burette system and heated again at 85 °C. Data were recorded on the gas burette system until  $\text{H}_2$ -release stopped.

### 3.2.4 Computational Methods

DFT/GIAO/NMR calculations were performed using the Gaussian 03 program.<sup>12</sup> Geometries were fully optimized at the B3LYP/6-31G(d) level without symmetry constraints. The  $^{11}\text{B}$  NMR chemical shifts were calculated at the B3LYP/6-311G(d) level using the GIAO option within Gaussian 03. The  $^{11}\text{B}$  NMR GIAO chemical shifts are

referenced to  $\text{BF}_3 \cdot \text{OEt}_2$  using an absolute shielding constant of 101.58, which was obtained from the GIAO NMR calculated shift of  $\text{BF}_3 \cdot \text{OEt}_2$  at the B3LYP/6-311G(d)//B3LYP/6-31G(d) level of theory. The Cartesian coordinates for the calculated species in **Figures 3.9** and **3.18** are listed below in **Tables 3.1-3.5**.

**Table 3.1 Cartesian Coordinates for  $[\text{H}_3\text{BNH}_2]^-$  (Figure 3.9A)**

	X	Y	Z
N	-0.773299	-0.000000	-0.134999
B	0.791599	-0.000000	0.012799
H	-1.135099	-0.804499	0.381400
H	-1.135099	0.804499	0.381400
H	1.259600	1.009599	-0.542400
H	1.259600	-1.009500	-0.542600
H	1.206199	-0.000100	1.203099

**Table 3.2 Cartesian Coordinates for Straight Chain**

**$[\text{H}_3\text{BNH}_2\text{BH}_2\text{NH}_2\text{BH}_2\text{NH}_2\text{BH}_2\text{NH}_2]^-$  (Figure 3.9B)**

	X	Y	Z
N	1.959700	0.758999	1.187400
B	2.540399	0.412200	-0.198300
N	1.293600	-0.033100	-1.148400
B	0.438000	-1.324199	-0.793400
N	-0.208900	-1.079400	0.647899
B	-1.770800	-0.859699	0.824700
N	-2.317500	0.158000	-0.263600
B	-1.968999	1.736400	-0.269600
H	2.621800	0.566400	1.930099
H	1.690000	1.733499	1.274600
H	3.295600	-0.544500	-0.124400
H	3.079500	1.353000	-0.788600
H	1.666900	-0.159100	-2.085399
H	0.660999	0.766799	-1.215500
H	1.179299	-2.286599	-0.761700
H	-0.431200	-1.475000	-1.641799
H	0.363400	-0.328299	1.081500
H	0.006900	-1.898000	1.208599

H	-2.009999	-0.428400	1.935800
H	-2.320700	-1.938300	0.636300
H	-3.330500	0.091499	-0.210599
H	-2.079099	-0.229699	-1.175400
H	-2.334400	2.210500	0.790599
H	-2.574799	2.233699	-1.213899
H	-0.765400	1.877400	-0.419700

**Table 3.3 Cartesian Coordinates for Branched Chain**

**$[(\text{NH}_2\text{BH}_3)_2\text{BHNH}_2\text{BH}_2\text{NH}_2]^-$  (Figure 3.9C)**

	X	Y	Z
N	0.936900	-1.183599	0.363600
N	-3.477799	0.052300	-0.022599
B	-2.135199	-0.649400	0.192800
N	-0.967499	0.439900	-0.199000
B	0.448600	-0.075100	-0.630100
N	1.511099	1.101200	-0.554800
B	1.424499	2.188700	0.643000
B	2.350199	-1.921000	0.066400
H	0.204500	-1.889200	0.394999
H	0.967599	-0.795899	1.306100
H	-3.907000	0.364899	0.842100
H	-4.148900	-0.556700	-0.475500
H	-1.892199	-0.982400	1.350600
H	-1.999500	-1.589500	-0.576400
H	-0.870600	1.111000	0.562499
H	-1.391400	0.972999	-0.955799
H	0.388799	-0.524300	-1.750799
H	1.519300	1.602100	-1.438399
H	2.418199	0.634999	-0.505100
H	0.455499	2.902500	0.431400
H	1.299700	1.582000	1.695699
H	2.453100	2.843799	0.631900
H	2.261599	-2.477400	-1.011600
H	3.231400	-1.069400	0.053500
H	2.550500	-2.713099	0.974099

**Table 3.4 Cartesian Coordinates for Branched Chain****[H<sub>3</sub>BNH<sub>2</sub>BH<sub>2</sub>(BH<sub>2</sub>NH<sub>3</sub>)NHBH<sub>2</sub>NH<sub>2</sub>]<sup>-</sup> (Figure 3.9D)**

	X	Y	Z
B	0.952800	1.127599	-0.632599
B	-3.608900	-0.082999	-0.197800
N	-2.090899	0.391100	0.108600
B	-0.943000	-0.681100	0.233600
N	0.470500	0.036699	0.461900
B	1.593199	-0.997600	0.780699
N	1.653900	-1.898799	-0.575000
N	1.751000	2.201099	0.111999
H	-0.009499	1.651199	-1.183400
H	-4.299799	0.933600	-0.234500
H	-3.970399	-0.817499	0.707500
H	-3.621200	-0.655200	-1.274800
H	-1.807799	1.056199	-0.608300
H	-2.124200	0.935900	0.968200
H	-0.910399	-1.311300	-0.815700
H	-1.180600	-1.407399	1.179100
H	0.390799	0.606400	1.304599
H	1.332799	-1.745900	1.699600
H	2.697300	-0.496499	0.891300
H	0.750399	-2.344899	-0.726400
H	1.785399	-1.215200	-1.331499
H	2.398799	-2.585799	-0.574399
H	1.818200	3.047100	-0.444999
H	2.704399	1.902899	0.300900
H	1.584100	0.505399	-1.529600

**Table 3.5 Cartesian Coordinates for [H<sub>3</sub>BNH<sub>2</sub>BH<sub>2</sub>NH<sub>2</sub>BEt<sub>3</sub>]<sup>-</sup> (Figure 3.18)**

	X	Y	Z
H	-1.973376	1.031556	0.884937
H	-2.201170	0.815859	-1.126664
H	-0.820510	-1.339560	0.655743
H	-0.852136	-1.250299	-0.957451
B	-2.066478	0.275274	-0.052926
B	0.836476	-0.192348	-0.092427
N	-0.768299	-0.670796	-0.118477
C	1.605095	-1.636615	-0.386310
H	1.200371	-2.068877	-1.323103



H	1.334269	-2.370456	0.397727
C	1.108688	0.872984	-1.310904
H	0.702173	0.466378	-2.255249
H	2.197316	0.926333	-1.485537
C	1.069508	0.408922	1.420464
H	0.321383	1.193611	1.605925
H	0.850119	-0.370906	2.175262
C	3.137576	-1.647815	-0.521249
H	3.631333	-1.364183	0.415665
H	3.529675	-2.638214	-0.802335
H	3.476580	-0.938600	-1.287172
C	0.592853	2.314007	-1.146182
H	0.839618	2.949048	-2.012247
H	-0.493703	2.336795	-1.019284
H	1.029156	2.795498	-0.260936
C	2.454242	0.997297	1.747594
H	2.482709	1.479006	2.737705
H	3.241083	0.232662	1.745465
H	2.750655	1.756872	1.012585
H	-3.347816	-1.408267	-0.518157
H	-3.215754	-1.163142	1.079698
H	-5.045222	0.442455	-0.884607
H	-5.589647	-0.981050	0.446384
H	-4.870481	0.792194	1.104587
N	-3.326438	-0.671772	0.190345
B	-4.834247	-0.038808	0.214854

### 3.3 Results and Discussion

#### 3.3.1 H<sub>2</sub>-Release from AB/PS Solid-State Reactions

As shown in **Figure 3.1a** and **Table 3.6**, initial H<sub>2</sub>-release measurements using the Toepler pump of the solid-state reactions of AB in the presence of 1.0 and 5.2 mol% PS at 85 °C clearly demonstrated the activating effect of PS on AB H<sub>2</sub>-release. While the reaction with 1.0 mol % PS still showed an induction period with no H<sub>2</sub>-released after 1 h, the extent of release was significantly increased at 3 h (0.65 equiv.) compared to that from pure AB at the same time (0.34 equiv.). The data for the 5.2 mol % PS reaction

indicated both a shortened induction period, with 0.35 equiv. already released at 1 h, and significantly increased amounts of H<sub>2</sub>-release at both 3 h (0.93 equiv.) and 20 h (1.12 equiv.) compared to those of either the pure AB or 1.0 mol% PS reactions. However, the solid-state AB/PS reactions stopped just after the release of ~1.1 H<sub>2</sub>-equivalents. More detailed H<sub>2</sub>-release data collected (**Table 3.7** and **Figure 3.1b**) for the 5.2 mol% PS reaction with the automated gas burette again clearly demonstrated that the induction period was shortened and that the rate of H<sub>2</sub>-release was increased upon the addition of 5.2 mol% PS.

The NMR spectra in **Figure 3.2** of the glyme-soluble residues from the solid-state AB/PS reactions showed features similar to those of the pure AB reactions. Thus, as the reaction progressed, the AB resonance (-23.5 ppm) decreased and was replaced by resonances arising from both the diammoniate of diborane, [(NH<sub>3</sub>)<sub>2</sub>BH<sub>2</sub>]<sup>+</sup>BH<sub>4</sub><sup>-</sup>, (DADB) (-13.3 (overlapped) and -37.6 ppm)<sup>13,14</sup> and branched-chain polyaminoborane polymers (-7, -13.3 and -25.1 ppm)<sup>15</sup> with the observed shift is in good agreement with the calculated shifts given in **Chapter 2, Figure 2.9**. Consistent with the faster H<sub>2</sub>-release found for the PS/AB mixtures, the spectra show that after 22 h the amount of unreacted AB was less in the PS/AB reactions than in that of the pure AB reaction.

The solid-state <sup>11</sup>B NMR spectra in **Figure 3.3** of the final products of the reactions showed an additional broad resonance centered near ~23 ppm that is characteristic of the sp<sup>2</sup> boron-framework of cross-linked polyborazylene structures,<sup>16-18</sup> thus indicating that AB dehydrogenation ultimately produces B=N unsaturated products. Consistent with this conclusion, the <sup>11</sup>B NMR spectra of the volatile products of the PS/AB reactions collected in the cold trap through which the released H<sub>2</sub> had been

passed, also indicated some borazine ( $B_3N_3H_6$ ) formation with the amount of the volatiles (ranging from 0.04 to 0.25 mmol depending upon the particular experiment) corresponding to less than 10% of the AB converting to borazine.

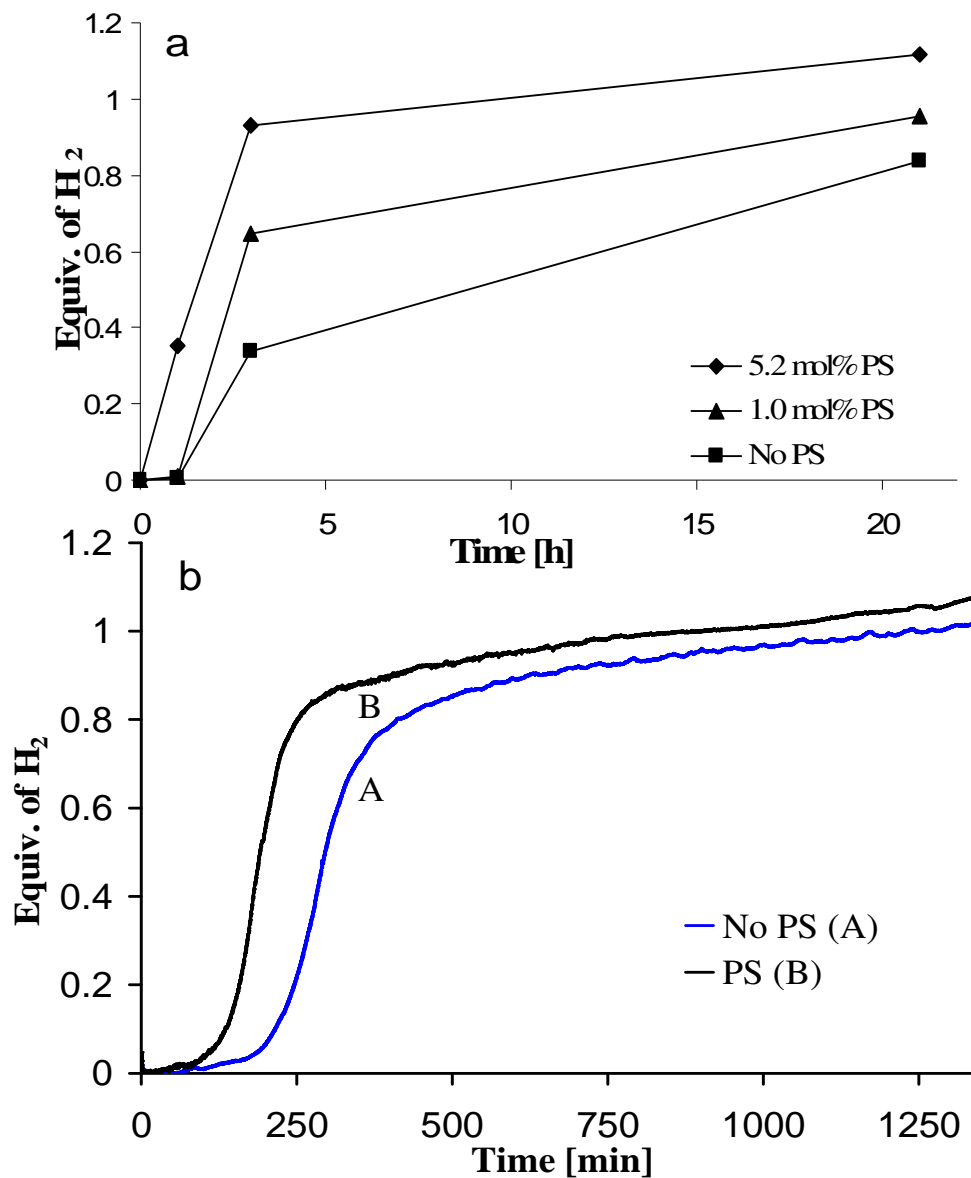


**Figure 3.1** H<sub>2</sub>-release measurements (a) (Toepler pump) for solid state AB (250 mg) reactions with 0, 1.0 and 5.2 mol% PS (18 and 91 mg) at 85 °C, (b) (gas burette) for solid state AB (150 mg) reactions with 0 and 5.2 mol% PS (55 mg) at 85 °C.

**Table 3.6 H<sub>2</sub>-Release Data (Toepler pump) for AB/PS Solid-State Reactions at 85****°C**

Time [h]	Amount of PS [mol%, mg, mmol]	Total wt [mg]	H <sub>2</sub> -Released	
			equiv.	mmol
1	-	250	-	0.02
3	-	250	0.34	2.74
21	-	250	0.84	6.79
1	<b>1.0, 18, 0.084</b>	268	-	0.08
3	<b>1.0, 18, 0.084</b>	268	0.65	5.23
21	<b>1.0, 18, 0.084</b>	268	0.95	7.73
1	<b>5.2, 91, 0.43</b>	341	0.35	2.86
3	<b>5.2, 91, 0.43</b>	341	0.92	7.52
21	<b>5.2, 91, 0.43</b>	341	1.12	9.04

250 mg NH<sub>3</sub>BH<sub>3</sub> (8.1 mmol) was used for all reactions.

**Table 3.7 H<sub>2</sub>-Release Data (gas burette) for AB/PS Solid-State Reactions at 85 °C**

Amount of PS [mol%, mg, mmol]	Total wt [mg]	Time to H <sub>2</sub> -equivalents (min)		
		0.5 equiv.	1 equiv.	Final (equiv.)
-	150	295	1264	1333 (1.02)
<b>5.3, 55, 0.26</b>	205	191	885	1334 (1.08)

150 mg NH<sub>3</sub>BH<sub>3</sub> (4.87 mmol) was used for all reactions.

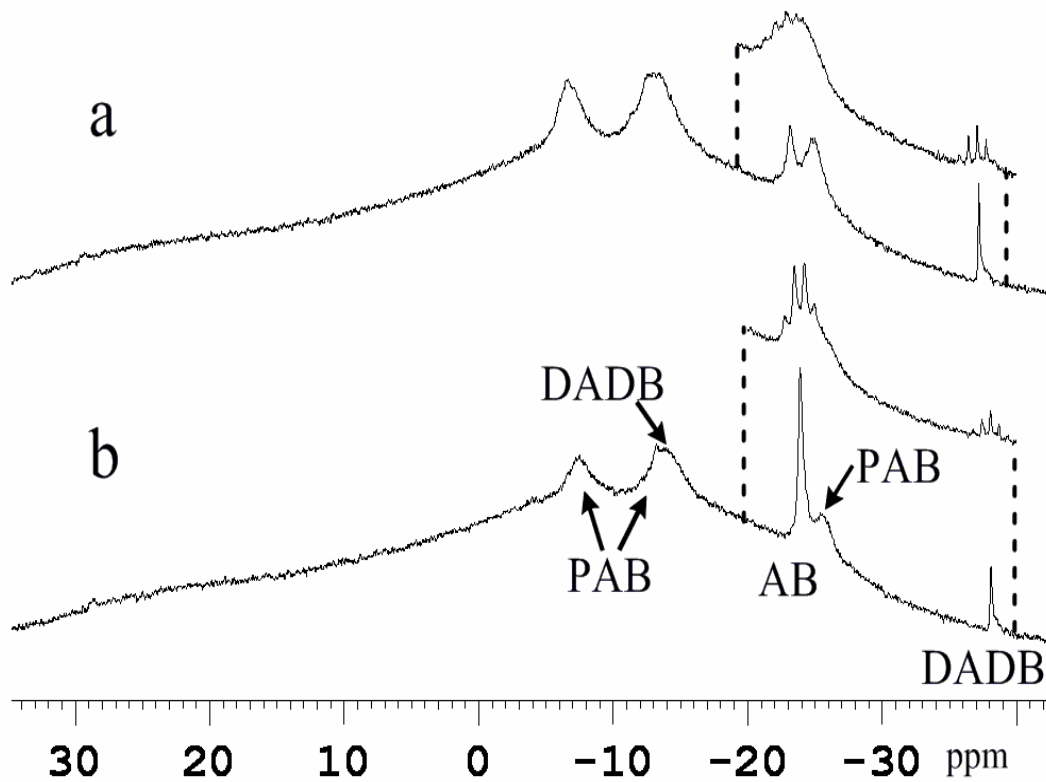


**Figure 3.2**  $^{11}\text{B}\{^1\text{H}\}$  NMR (128.4 MHz) spectra (insets show  $^1\text{H}$  coupled spectra) recorded at 25 °C of the glyme extract of the reaction of: (a) AB (150 mg) and 5.3 mol% PS (55 mg) at 85 °C for 22 h and (b) AB (150 mg) at 85 °C for 22 h. (The broad DADB resonance at -13 ppm is obscured by the PAB resonance)

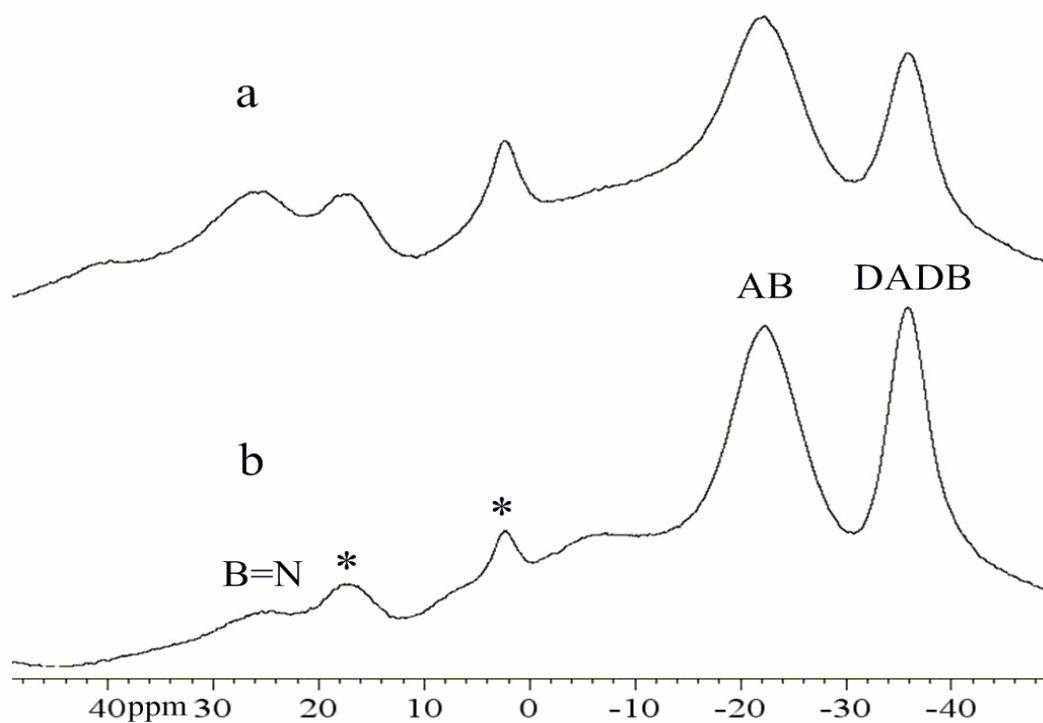


**Figure 3.3** Solid-state  $^{11}\text{B}$  NMR (240 MHz) spectra recorded at 25 °C of the reaction of: (a) AB (150 mg) and 5.3 mol% PS (55 mg) at 85 °C until 1  $\text{H}_2$ -equivalent was released and (b) AB (150 mg) at 85 °C until 1  $\text{H}_2$ -equivalent was released. (The broad DADB resonance at -13 ppm is obscured by the AB resonance) \*Borate resonances at 17 and 2 ppm result from exposure of sample to air.

### 3.3.2 H<sub>2</sub>-Release from AB/PS Solution Reactions

#### 3.3.2.1 Initial Reactions Measured with the Toepler Pump

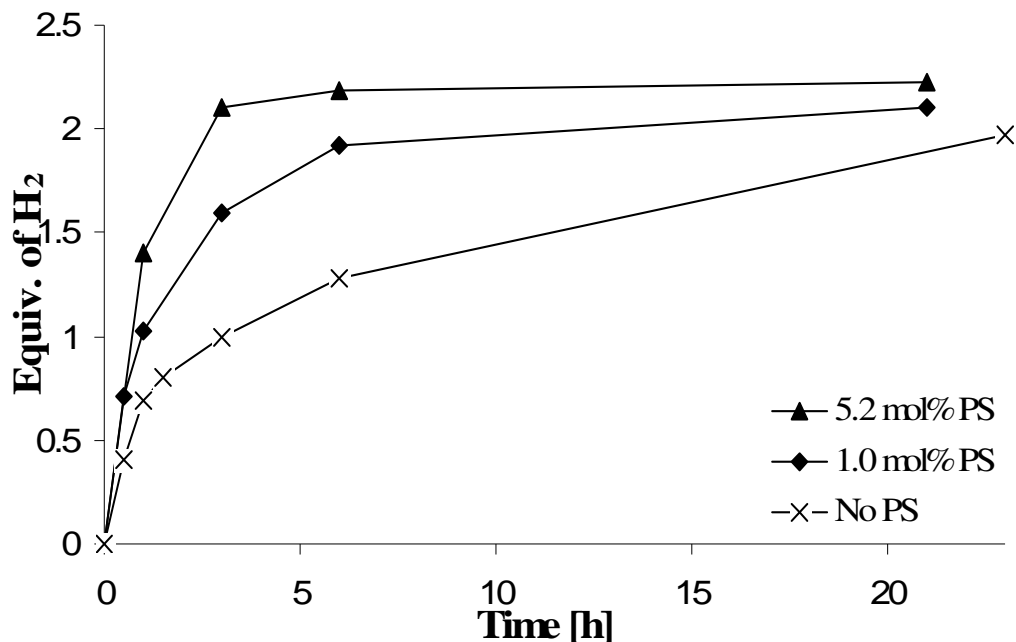


**Figure 3.4** H<sub>2</sub>-release measurements (Toepler pump) of the reaction of AB (250 mg) in bmimCl (250 mg) with 0, 1.0 and 5.2 mol% PS (18 and 91 mg) at 85 °C.

The work described in **Chapter 2** and elsewhere<sup>15</sup> showed that polar solvents, especially ionic liquids such as 1-butyl-3-methylimidazolium chloride (bmimCl), can activate H<sub>2</sub>-release from AB at 85 °C, with over 2 equivalents being produced in ~5 h from a 50/50 weight% AB/bmimCl mixture. Comparisons of the H<sub>2</sub>-release rates using Toepler pump measurements of AB dissolved in bmimCl with different amounts of added PS at 85 °C are summarized in **Table 3.8** and **Figure 3.4**. In the absence of PS, only 0.69, 1.00, 1.28 and 1.97 H<sub>2</sub>-equiv. were released at 1, 3, 6 and 23 h, respectively. In contrast, a similar reaction of AB in bmimCl containing 5.2 mol% PS showed a

significantly increased H<sub>2</sub>-release rate, with 1.40 H<sub>2</sub>-equiv. released by 1 h and 2.10 H<sub>2</sub>-equiv. released after only 3 h. Even when the amount of PS was decreased to only 0.5 mol% PS, there were still significant increases in the H<sub>2</sub>-release found at 1 h (0.83 equiv.), 3 h (1.65 equiv.) and 6 h (2.10 equiv.) compared to those of the reaction without PS.

The plots in **Figure 3.4** show that the biggest differences in the H<sub>2</sub>-release rates of the bmimCl reactions with and without PS occurred following the release of the first equivalent of H<sub>2</sub>. For the reaction without PS, the first equivalent was released in 3 h, and even after 23 h only 1.97 equiv was released. On the other hand, by 3 h the reactions with 5.2 and 1.0 mol% PS had already released 2.10 and 1.75 equiv., respectively, and at 6 h, 2.18 and 2.01 equiv. Thus, PS appears to have significantly enhanced the release rate of the second H<sub>2</sub>- equivalent from AB.

Differential scanning calorimetry measurements also support this conclusion. The black curve in **Figure 3.5a** shows a single well-defined exotherm for the release of the first H<sub>2</sub>-equivalent from the reaction of an AB/bmimCl mixture. The blue curve, which is from the reaction of a similar mixture containing 5.3 mol% of added PS, clearly exhibits a second exotherm indicating the release of additional H<sub>2</sub> by a different process. Consistent with the H<sub>2</sub>-release measurements that showed significant rate enhancements for the 2<sup>nd</sup> H<sub>2</sub>-equivalent as the temperature was raised, when the upper temperature of the DSC analysis was raised from 85 °C to 110 °C (**Figure 3.5b**), the second exotherm grew and shifted to shorter times such that it overlapped the first isotherm.



**Table 3.8 H<sub>2</sub>-Release Data (Toepler pump) for AB/BmimCl/PS Reactions at 85 °C**

Time [h]	Amount of PS [mol%, mg, mmol]	Total <sup>a</sup> wt [mg]	H <sub>2</sub> -Released	
			equiv.	mmol
1	-	500	0.69	5.62
3	-	500	1.00	8.10
6	-	500	1.28	10.36
23	-	500	1.97	15.94
1	<b>0.5</b> , 9, 0.04	509	0.83	6.70
3	<b>0.5</b> , 9, 0.04	509	1.65	13.37
6	<b>0.5</b> , 9, 0.04	509	2.10	17.04
22	<b>0.5</b> , 9, 0.04	509	2.23	18.04
1	<b>5.2</b> , 91, 0.43	591	1.40	11.33
3	<b>5.2</b> , 91, 0.43	591	2.10	17.02
6	<b>5.2</b> , 91, 0.43	591	2.18	17.67
21	<b>5.2</b> , 91, 0.43	591	2.23	18.04
1	<b>24.9</b> , 434, 2.03	934	0.79	6.37
3	<b>24.9</b> , 434, 2.03	934	1.75	14.14
6	<b>24.9</b> , 434, 2.03	934	2.01	16.28
22	<b>24.9</b> , 434, 2.03	934	2.13	17.23

250 mg NH<sub>3</sub>BH<sub>3</sub> (8.1 mmol) and 250 mg bmimCl were used for all reactions.

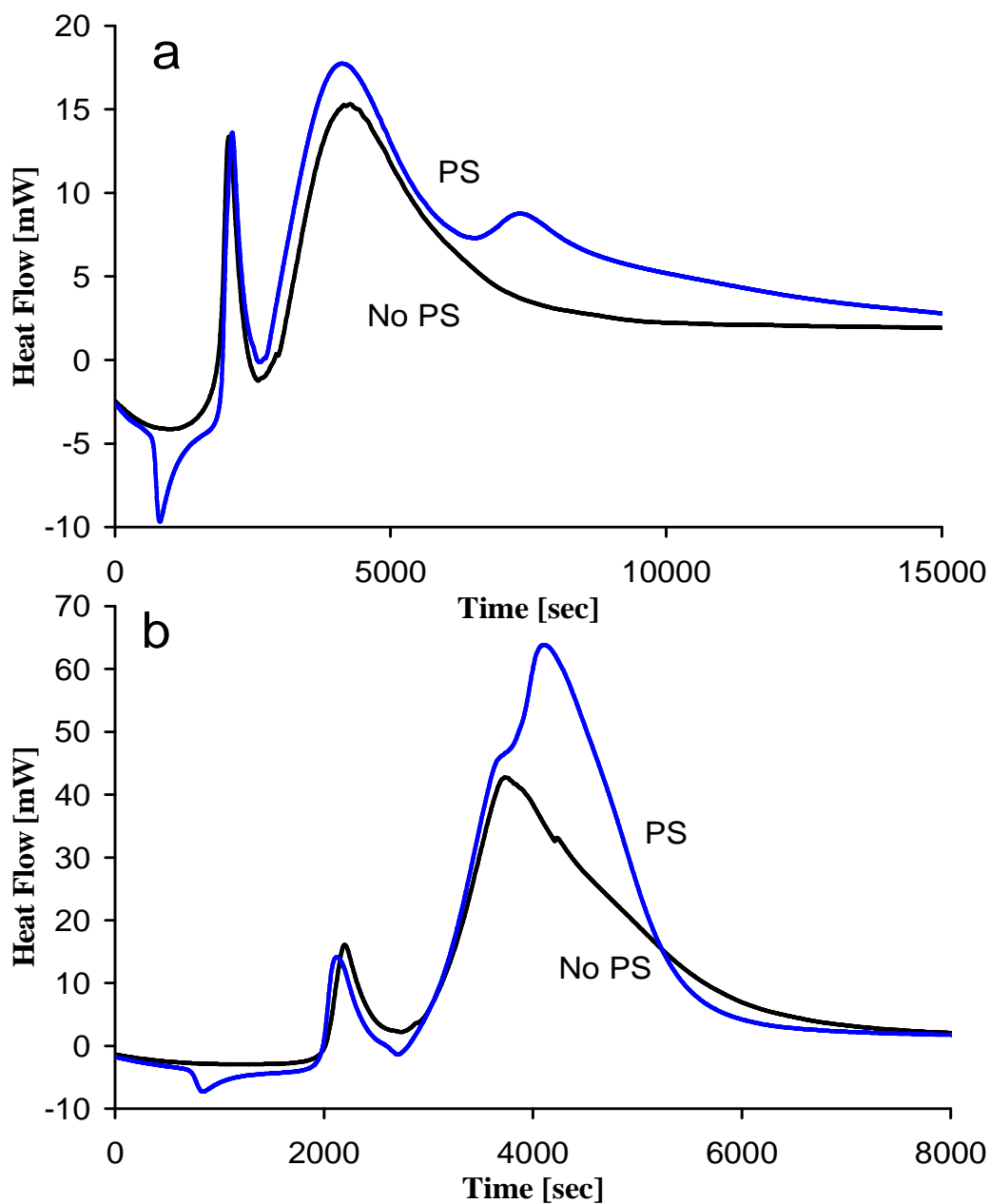


**Figure 3.5** Differential Scanning Calorimetry analyses of the reactions of AB (150 mg) in bmimCl (150 mg) with 5.3 mol% PS (55 mg) at: (a) 85 °C and (b) 110 °C. \*Initial exotherm is apparatus artifact.

### 3.3.2.2 H<sub>2</sub>-Release Reactions Measured with the Automated Gas Burette

In order to better quantify the effects of both PS-loading and temperature, more detailed H<sub>2</sub>-release data on a series of 50/50 wt% AB/bmimCl systems containing from 0 to 24.9 mol% PS at 75, 85, 95 and 110 °C were collected on the automated gas burette (**Table 3.9** and **Figure 3.6**). The rate of H<sub>2</sub>-release increased as the mol% of PS in the mixture was increased. For example, as shown in **Figure 3.6a**, while the reaction at 85 °C without PS required 84 min and 316 min to liberate the 1<sup>st</sup> and 2<sup>nd</sup> equivalents of H<sub>2</sub>, the reactions with 0.96 (1<sup>st</sup> 74, 2<sup>nd</sup> 179 min), 5.3 (1<sup>st</sup> 61, 2<sup>nd</sup> 171 min) and 24.9 (1<sup>st</sup> 41, 2<sup>nd</sup> 77 min) mol% PS were all significantly faster, with the fastest rate found for the highest loading. Substantial rate increases were observed for all reactions when the reaction temperature was increased. Thus, as illustrated in the plots in **Figure 3.6b**, at 110 °C the reaction without PS required only 7.4 min and 20 min to liberate the 1<sup>st</sup> and 2<sup>nd</sup> equivalents of H<sub>2</sub>, but the reactions with 0.96 (1<sup>st</sup> 5.9, 2<sup>nd</sup> 13 min), 5.3 (1<sup>st</sup> 4.3, 2<sup>nd</sup> 9 min) and 24.9 (1<sup>st</sup> 4.3, 2<sup>nd</sup> 7 min) mol% PS were all again significantly faster. It is also noteworthy that at 95 °C and 110 °C, unlike at 85 °C, the rate of H<sub>2</sub>-release for the 5.3 and 24.9 mol% PS reactions were similar; indicating that less PS is required to induce H<sub>2</sub>-release at higher temperatures.

The above studies all indicate that both bmimCl and PS promote the loss of more than one equivalent of H<sub>2</sub> with the combination of PS in bmimCl being the most effective. To further test this conclusion, two samples of neat AB were first heated at 85 °C for 23 h to produce a partially dehydrogenated material where only ~1.0 H<sub>2</sub>-equivalent had been released. To the first sample bmimCl was added and to the second sample both PS and bmimCl. The flasks were then reheated at 85 °C to produce liquid suspensions,

and any additional H<sub>2</sub>-release was measured. While the heating of AB in the solid state at 85 °C for more extended periods (~48 h) gave no further H<sub>2</sub>-release, both Toepler pump (**Table 3.10**) and gas burette measurements (**Figure 3.7**) showed that the addition of either bmimCl or bmimCl/PS to the partially dehydrogenated AB caused H<sub>2</sub>-release to resume, ultimately yielding an additional ~0.7 equivalent of H<sub>2</sub> from both samples, with the bmimCl/PS reaction exhibiting the fastest rate.

**Table 3.9 H<sub>2</sub>-Release Data (gas burette) for AB/bmimCl/PS Reactions**

Temp. °C	Amount of PS [mol%, mg, mmol]	Total <sup>a</sup> wt [mg]	Time to H <sub>2</sub> -equivalents (min)			
			0.75 equiv.	1 equiv.	1.5 equiv.	Final (equiv.)
75	-	300	228	459	-	1041 (1.43)
	<b>0.96</b> , 10, 0.047	310	205	320	665	1040 (2)
	<b>5.3</b> , 55, 0.26	355	161	215	342	723 (1.99)
	<b>24.9</b> , 260, 1.21	560	140	208	378	782 (1.98)
85	-	300	52	84	199	316 (2)
	<b>0.96</b> , 10, 0.047	310	50	74	118	179 (2)
	<b>5.3</b> , 55, 0.26	355	45	61	95	171 (2)
	<b>24.9</b> , 260, 1.21	560	35	41	55	77 (2)
95	-	300	21	37	87	126 (2)
	<b>0.96</b> , 10, 0.047	310	20	27	44	72 (2)
	<b>5.3</b> , 55, 0.26	355	17	21	31	52 (2)
	<b>24.9</b> , 260, 1.21	560	16.3	20.9	32	59 (1.91)
110	-	300	5.8	7.4	12	20 (2)
	<b>0.96</b> , 10, 0.047	310	4.9	5.9	8	13 (2)
	<b>5.3</b> , 55, 0.26	355	3.8	4.3	6	9 (2)
	<b>24.9</b> , 260, 1.21	560	4.0	4.3	5	7 (2)

150 mg NH<sub>3</sub>BH<sub>3</sub> (4.87 mmol) and 150 mg bmimCl were used for all reactions.

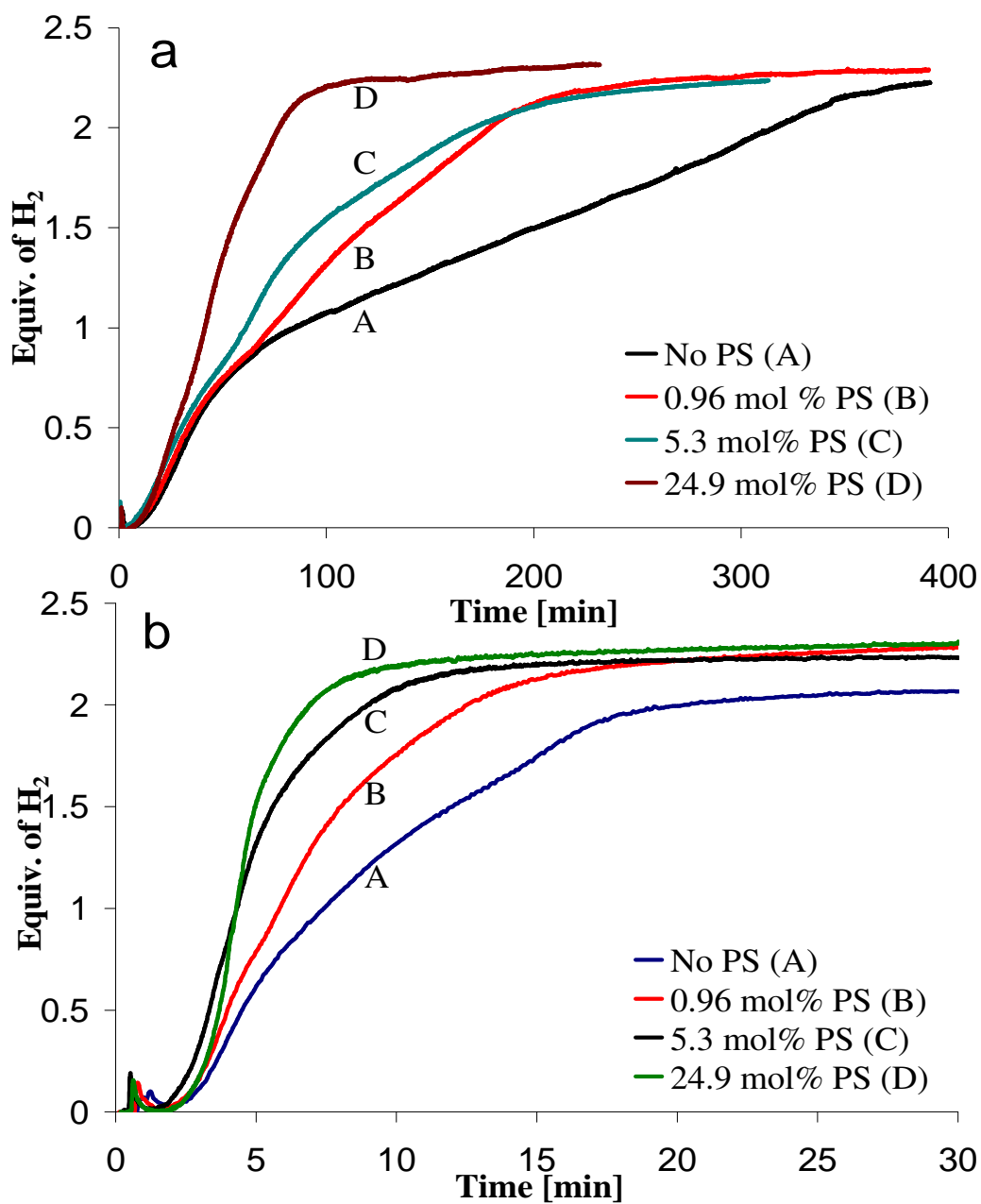


**Figure 3.6** H<sub>2</sub>-release measurements (gas burette) of the reaction of AB (150 mg) in bmimCl (150 mg) with 0, 0.96, 5.3 and 24.9 mol% PS (10, 55 and 260 mg) at: (a) 85 °C and (b) 110 °C.

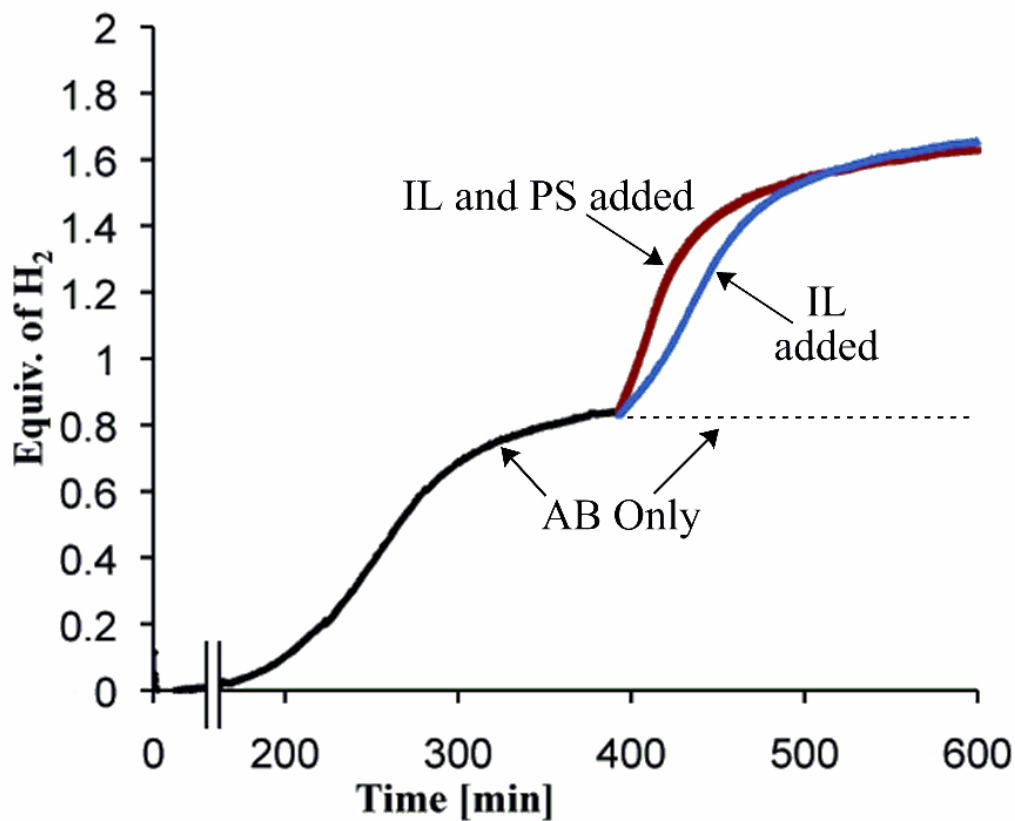


**Figure 3.7** H<sub>2</sub>-release measurements (gas burette) of partially dehydrogenated AB (150 mg) where 1 H<sub>2</sub>-equivalent was initially released at 85 °C, then bmimCl (150 mg) and bmimCl (150 mg)/PS (55 mg/5.2 mol%) were added to separate samples and heating resumed at 85 °C. The dashed line shows the observed AB H<sub>2</sub>-release when IL and/or PS are not added.

**Table 3.10 H<sub>2</sub>-Release (Toepler pump) Data for Partially Dehydrogenated AB**

Time [h]	Total <sup>a</sup> wt [mg]	H <sub>2</sub> -Released	
		equiv.	mmol
0	250	0.99	8.04
1 <sup>b</sup>	500	1.05	8.51
2 <sup>b</sup>	500	1.11	9.02
3 <sup>b</sup>	500	1.27	10.30
21 <sup>b</sup>	500	1.78	14.42
24 <sup>b</sup>	500	1.79	14.51
0	250	0.98	7.96
1 <sup>c</sup>	591	1.21	9.82
2 <sup>c</sup>	591	1.45	11.75
3 <sup>c</sup>	591	1.51	12.20
24 <sup>c</sup>	591	1.70	13.77

<sup>a</sup>250 mg NH<sub>3</sub>BH<sub>3</sub> (8.1 mmol) for all experiments. <sup>b</sup>250 mg bmimCl added post neat NH<sub>3</sub>BH<sub>3</sub> reaction. <sup>c</sup>250 mg bmimCl and 91 mg PS added post neat NH<sub>3</sub>BH<sub>3</sub> reaction.

### 3.3.3 $^{11}\text{B}$ NMR Studies of Reaction Pathways and Intermediates

#### 3.3.3.1 Solid-State $^{11}\text{B}$ NMR Studies

While bmimCl is a liquid at 85 °C, it is a solid at room temperature; therefore, solid-state NMR was used to monitor the bmimCl/AB/PS reactions at different stages by heating the liquid mixtures at 85 °C, then quenching the reactions at the indicated times by cooling to room temperature, with subsequent analyses of the resulting solid materials by solid-state  $^{11}\text{B}$  NMR. Consistent with the  $\text{H}_2$ -release measurements and  $^{11}\text{B}$  NMR studies of solid-state PS/AB reactions, the solid-state  $^{11}\text{B}$  spectrum of the reaction of a 50/50 wt% bmimCl/AB mixture containing 5.2 mol% PS showed after 0.5 equiv. of  $\text{H}_2$ -release, the resonances of both DADB<sup>13,14</sup> and branched chain polyaminoboranes (**Figure 3.8**).<sup>15</sup> The small signal (-21.2 ppm) that is apparent just downfield of the AB (-23.2 ppm) resonance has a chemical shift value consistent with that previously reported<sup>19-22</sup> for the  $\text{H}_3\text{BNH}_2^-$  anion (-21.49 ppm) and with its DFT/GIAO calculated value (-20.6 ppm) (**Figure 3.9**).

As the reaction continued, the resonances broadened and diminished and a new resonance centered at 25.9 ppm grew in that is characteristic of unsaturated  $\text{sp}^2$ -hybridized boron. As shown in the spectrum in **Figure 3.10**, after prolonged reaction (23 h) only the 25.9 ppm resonance remained, indicating that all final products had unsaturated  $\text{sp}^2$ -hybridized structures. NMR studies of the dehydrogenated products of AB  $\text{H}_2$ -release promoted by solid-state thermal reactions<sup>23</sup> have likewise shown the formation of similar types of B=N unsaturated final products after more than 2 equivalents of  $\text{H}_2$ -release.



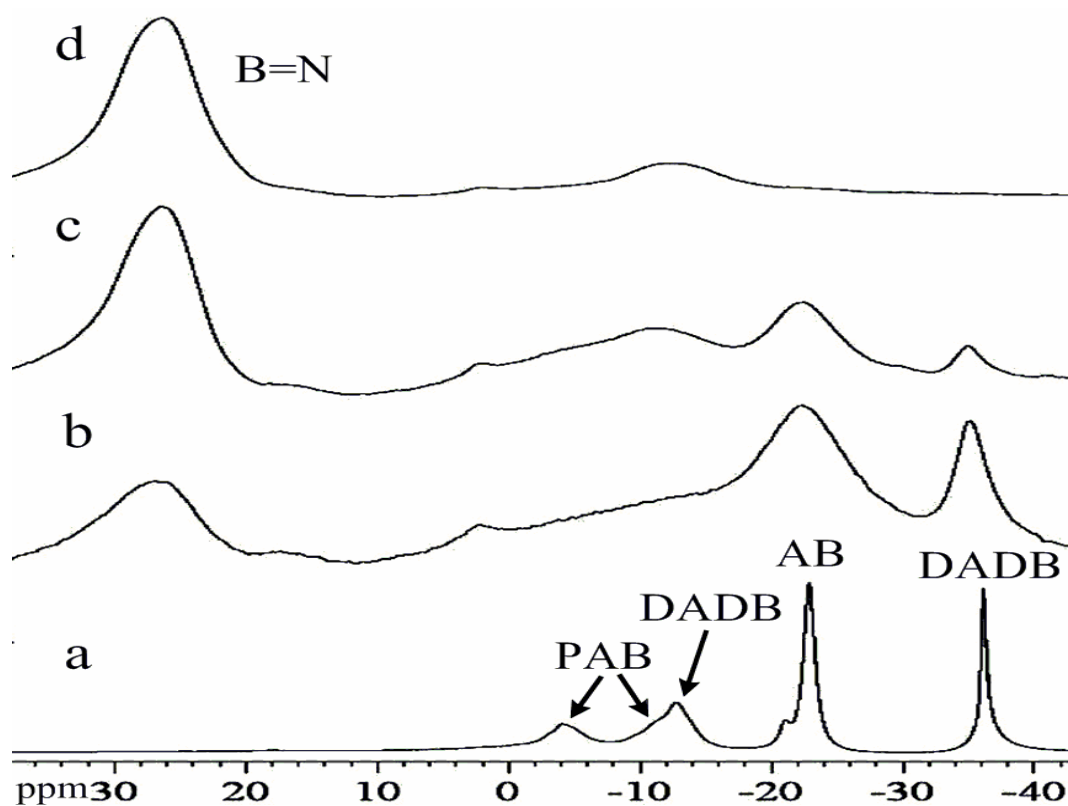


**Figure 3.8** Solid-state  $^{11}\text{B}$  NMR (240 MHz) spectra recorded at 25 °C of the reaction of AB (150 mg) and 5.3 mol% PS (55 mg) in bmimCl (150 mg) at 85 °C after the  $\text{H}_2$ -release of: (a) 0.5 equiv. (30 min), (b) 1 equiv. (61 min), (c) 1.5 equiv. (95 min) and (d) 2 equiv. (171 min). (The broad DADB resonance at -13 ppm is obscured by the AB and PAB resonances)

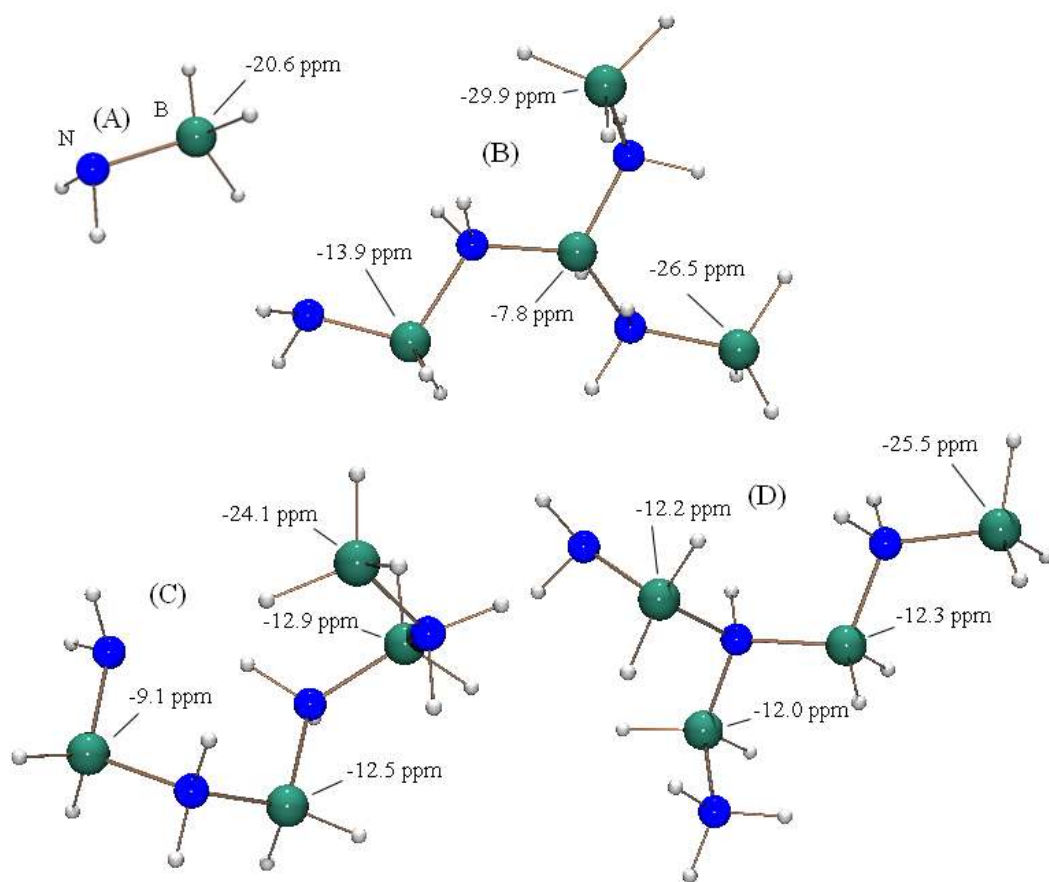


**Figure 3.9** DFT optimized geometries (B3LYP/6-31G(d)) and GIAO calculated (B3LYP/6-311G(d))  $^{11}\text{B}$  NMR chemical shifts. The shifts for the corresponding neutral species are given in **Chapter 2, Figure 9**.

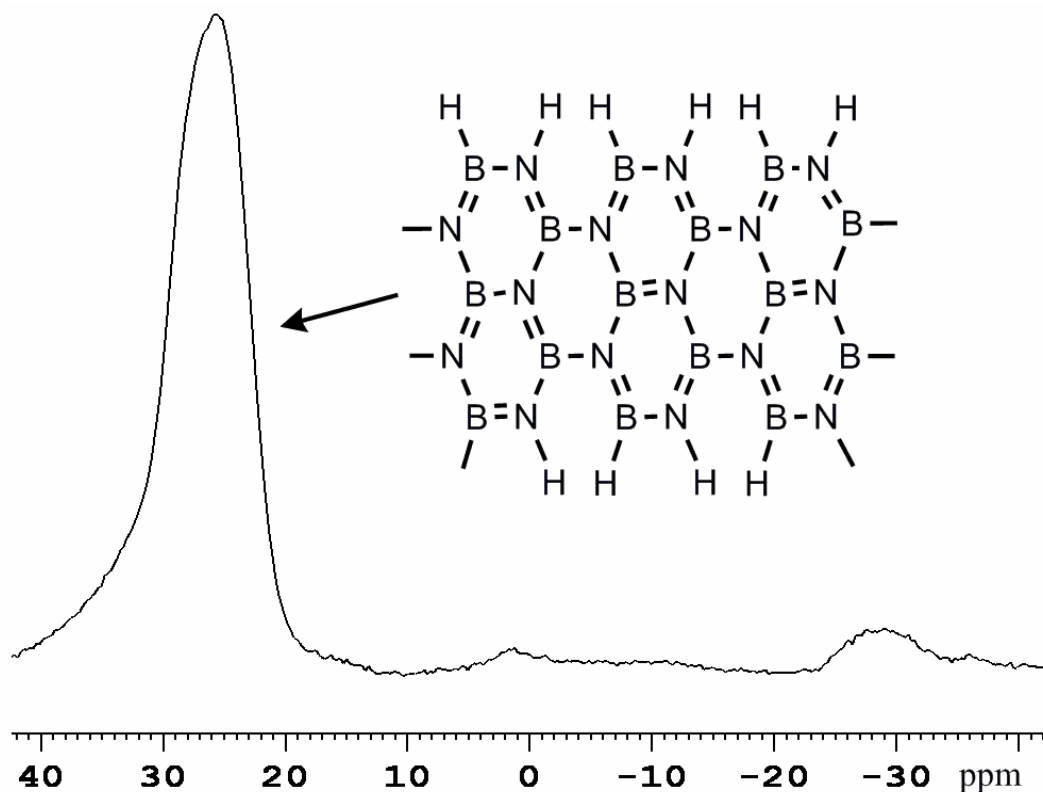


**Figure 3.10** Solid-state  $^{11}\text{B}$  NMR (240 MHz) spectrum recorded at 25 °C of the reaction of AB (250 mg) and 5.2 mol% PS (91 mg) in bmimCl (150 mg) at 85 °C for 23 h.

### 3.3.3.2 *In Situ* $^{11}\text{B}$ NMR Studies of Reaction Progress in Ionic Liquids

*In situ* solution  $^{11}\text{B}$  NMR studies of the PS promoted  $\text{H}_2$ -release from AB in the room temperature ionic liquid mmimMeSO<sub>4</sub> at 85 °C also exhibited features similar to those observed in the solid-state NMR spectra of the bmimCl reactions. It is also significant that the  $^{11}\text{B}$  NMR spectra of the reactions with and without PS in mmimMeSO<sub>4</sub> (**Figure 3.11**) showed the formation of similar types of products. In both reactions, DADB and polyaminoborane polymers were formed initially, then at the longer times where more  $\text{H}_2$  was released, the DADB and polyaminoborane resonances

decreased and insoluble materials formed. Only a small intensity resonance was observed near 25 ppm indicating that if unsaturated B=N products, such as borazine or polyborazylene, were formed they must have reacted rapidly to form the final insoluble product.

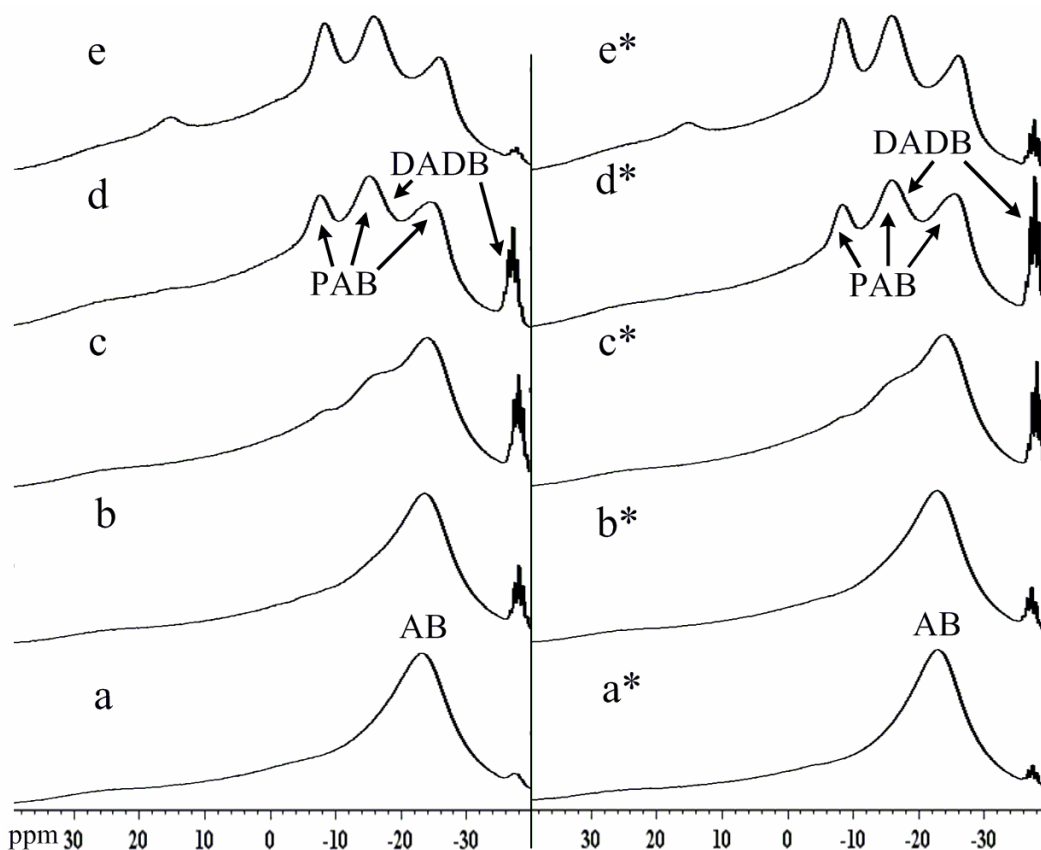


**Figure 3.11** Solution  $^{11}\text{B}$  NMR (128 MHz) spectra recorded at 25 °C of the reaction of AB (50 mg) in mmimMeSO<sub>4</sub> (450 mg) at 85 °C, (right) with 5.2 mol% PS (18 mg) after the release of: (a) 0.03 equiv., (b) 0.08 equiv., (c) 0.32 equiv., (d) 1.14 equiv. and (e) 1.63 equiv.; (left) without PS after the release of: (a\*) 0.03 equiv., (b\*) 0.08 equiv., (c\*) 0.29 equiv., (d\*) 1.07 equiv. and (e\*) 1.62 equiv. (The broad DADB resonance at -13 ppm is obscured by the AB and PAB resonances)

### 3.3.4 Proton Sponge Reduces Foaming During AB Thermolysis

One of the barriers to the utilization of AB H<sub>2</sub>-release for hydrogen storage, is that AB dehydrogenation in either the solid state or in solution normally produces considerable foaming.<sup>24</sup> However, as shown in the photographs in **Figure 3.12**, Proton Sponge, besides increasing both the rate and extent of H<sub>2</sub>-release, was found to have the unanticipated, but highly beneficial, effect of significantly reducing foaming during AB H<sub>2</sub>-release in the bmimCl/PS reactions.

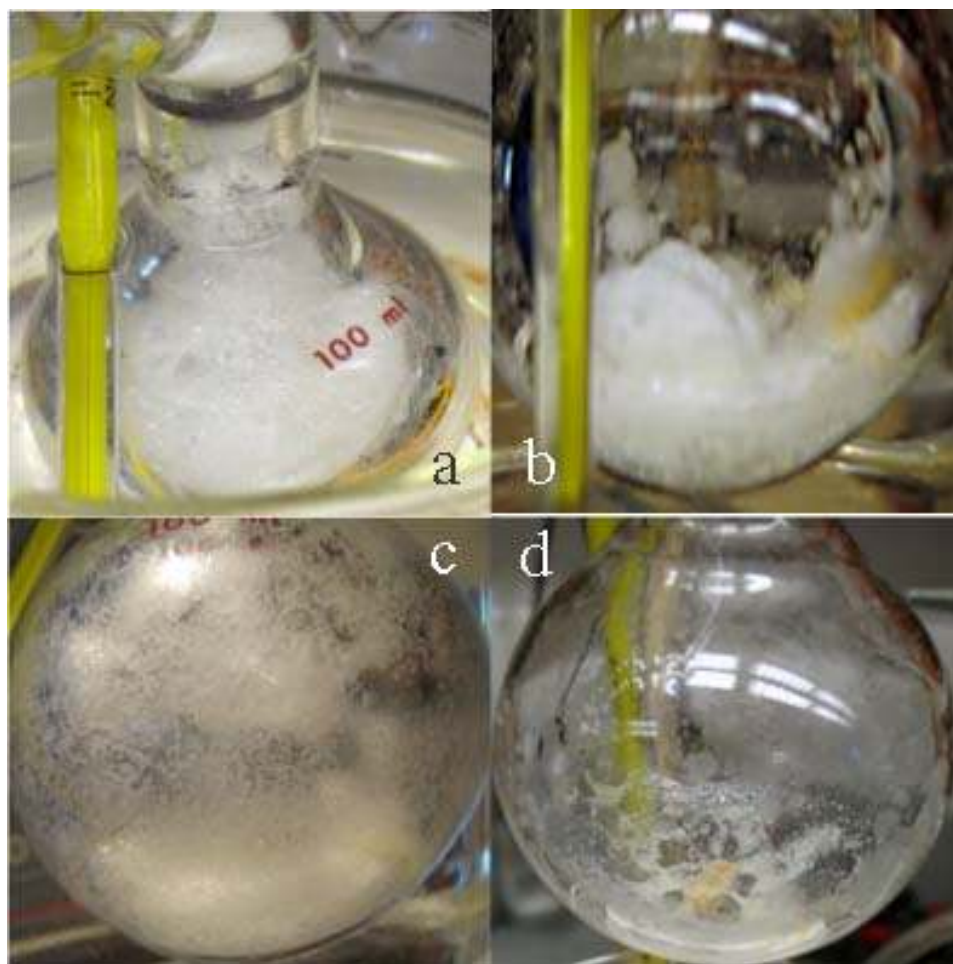


**Figure 3.12** Foaming resulting from the reaction of 250 mg AB in 250 mg bmimCl after 1 h at 100 °C: (a) without PS, (b) with 5.2 mol% PS (91 mg).

### 3.3.5 H<sub>2</sub>-Release in Other Ionic Liquids and Tetraglyme

PS was also found to increase AB H<sub>2</sub>-release in both other ionic liquids and tetraglyme, with both the extent and rate of H<sub>2</sub>-release comparable to that of the PS/bmimCl reactions (Table 3.11 and Figure 3.13). Gas burette data (Table 3.12) at 85 °C for the tetraglyme reactions showed that fast rates could be achieved with only 1 mol% of PS. The <sup>11</sup>B NMR spectra of the tetraglyme/PS reactions also showed evidence for the initial formation of the H<sub>3</sub>BNH<sub>2</sub><sup>-</sup> anion, followed by the appearance of the resonances for polyaminoborane polymers. However, at longer times, unlike in the ionic liquids, the major product was borazine (30.1 ppm)<sup>25</sup> along with smaller amounts of BH<sub>4</sub><sup>-</sup> (-36.8 ppm)<sup>25</sup> and  $\mu$ -aminodiborane (-27.5 ppm)<sup>25</sup> (Figure 3.14). Thus, ionic liquid solvents are favored for AB H<sub>2</sub>-release since they suppress or reduce the formation of these products.

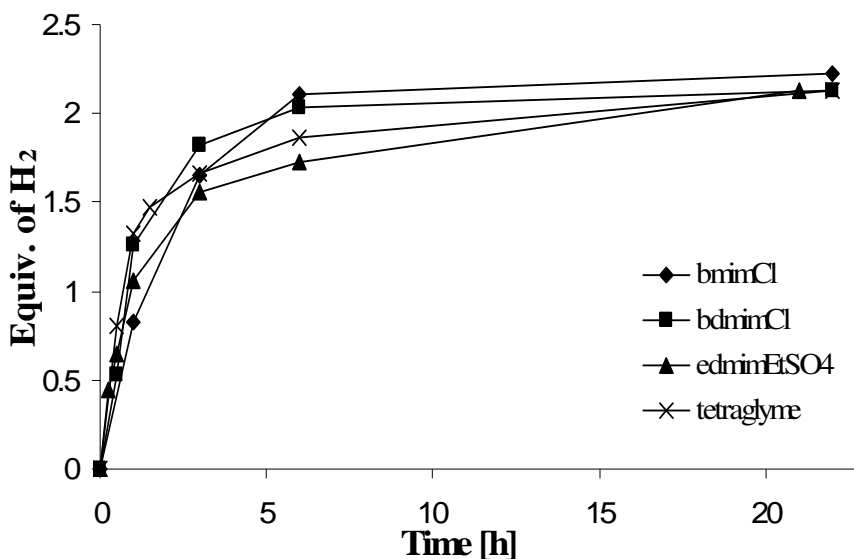


**Figure 3.13** H<sub>2</sub>-release measurements (Toepler pump) of the reaction of AB (250 mg) in ionic liquids or tetraglyme (250 mg) with 5.2 mol% PS (91 mg) at 85 °C.

**Table 3.11 H<sub>2</sub>-Release Data (Toepler pump) for AB/Ionic-Liquid/PS Reactions at 85 °C**

Solvent	Time [h]	Amount of PS [mol%, mg, mmol]	Total <sup>a</sup> wt [mg]	H <sub>2</sub> -Released equiv.	mmol
BDmimCl	1	-	500	0.68	5.52
	3	-	500	1.06	8.58
	6	-	500	1.31	10.61
	22	-	500	2.29	18.59
BDmimCl	1	<b>5.2</b> , 91, 0.43	591	1.26	10.19
	3	<b>5.2</b> , 91, 0.43	591	1.82	14.74
	6	<b>5.2</b> , 91, 0.43	591	2.03	16.47
	22	<b>5.2</b> , 91, 0.43	591	2.13	17.23
EDmimEtSO <sub>4</sub>	1	-	500	1.00	8.09
	3	-	500	1.32	10.7
	6	-	500	1.64	11.3
	22	-	500	2.20	17.8
EDmimEtSO <sub>4</sub>	1	<b>5.2</b> , 91, 0.43	591	1.52	12.33
	3	<b>5.2</b> , 91, 0.43	591	1.91	15.50
	6	<b>5.2</b> , 91, 0.43	591	2.04	16.51
	21.5	<b>5.2</b> , 91, 0.43	591	2.16	17.47
Tetraglyme	1	-	500	1.19	9.65
	3	-	500	1.80	14.57
	6	-	500	1.97	15.97
	22	-	500	2.12	17.20
Tetraglyme	1	<b>5.2</b> , 91, 0.43	591	1.32	10.73
	3	<b>5.2</b> , 91, 0.43	591	1.66	13.45
	6	<b>5.2</b> , 91, 0.43	591	1.86	15.10
	22	<b>5.2</b> , 91, 0.43	591	2.13	17.22

250 mg NH<sub>3</sub>BH<sub>3</sub> (8.1 mmol) and 250 mg ionic liquid or tetraglyme were used for all reactions.

**Table 3.12 H<sub>2</sub>-Release Data (gas burette) for AB/Tetraglyme/PS Reactions at 85 °C**

Temp °C	Amount of PS [mol%, mg, mmol]	Total <sup>a</sup> wt [mg]	Time to H <sub>2</sub> -equivalents (min)		
			1 equiv.	1.5 equiv.	Final (equiv.)
75	-	300	248	587	1126 (2)
	<b>0.96</b> , 10, 0.047	310	166	234	461 (2)
	<b>5.3</b> , 55, 0.26	355	164	263	886 (2)
	<b>24.9</b> , 260, 1.21	560	193	458	1238 (1.91)
85	-	300	40.7	80.4	211 (2)
	<b>0.96</b> , 10, 0.047	310	36.1	51.4	125 (2)
	<b>5.3</b> , 55, 0.26	355	27.8	51.6	253 (1.87)
	<b>24.9</b> , 260, 1.21	560	34.9	107	325 (1.76)
95	-	300	17.2	39.6	122 (2)
	<b>0.96</b> , 10, 0.047	310	14.4	22.9	77.1 (2)
	<b>5.3</b> , 55, 0.26	355	12.1	25.2	169 (2)
	<b>24.9</b> , 260, 1.21	560	18.5	87.2	369 (1.88)

150 mg NH<sub>3</sub>BH<sub>3</sub> (4.87 mmol) and 150 mg tetraglyme were used for all reactions.



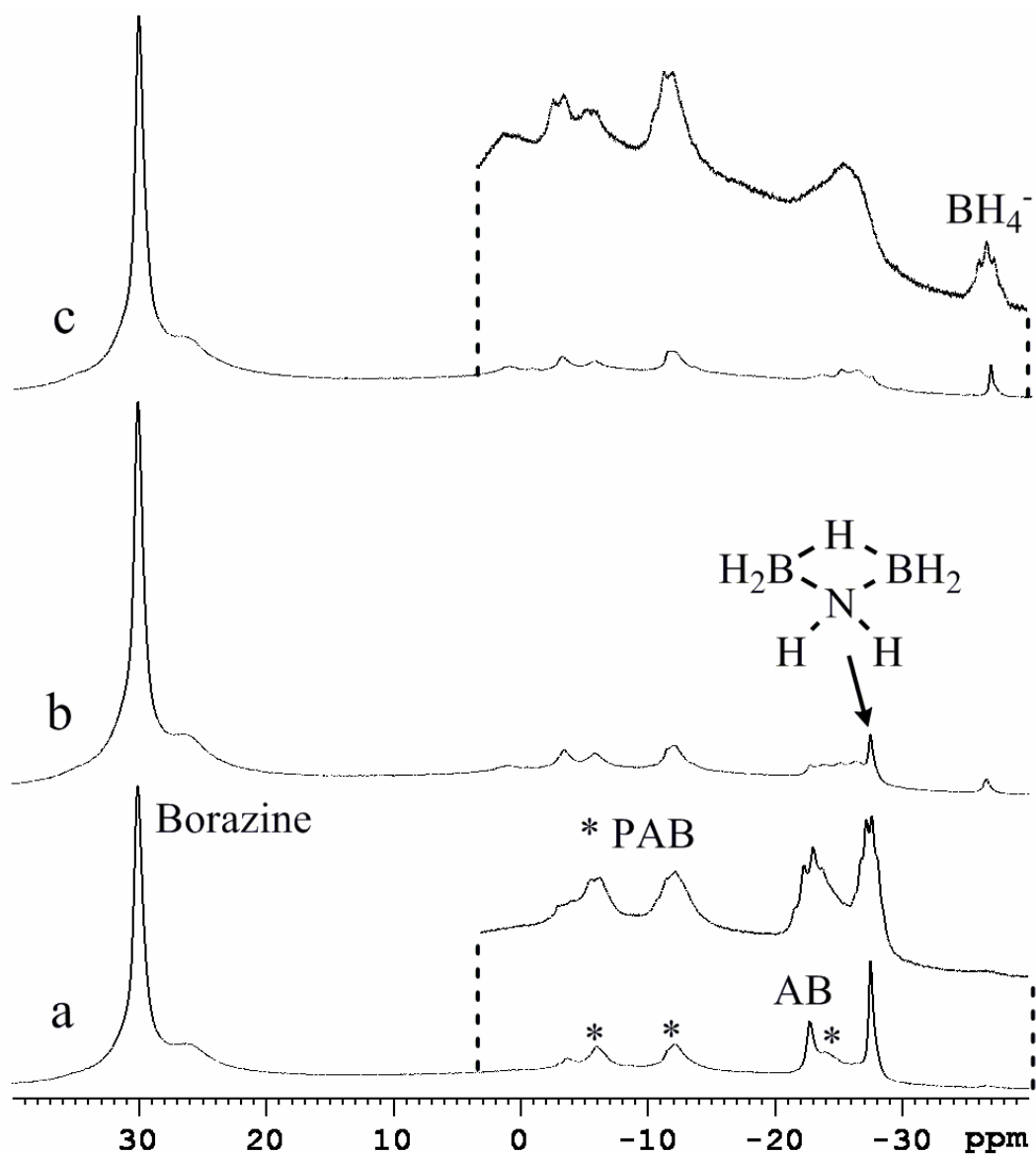
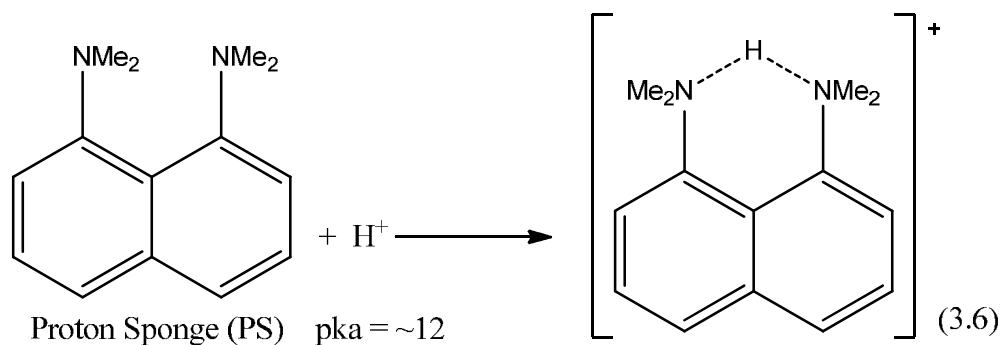


**Figure 3.14** Solution  $^{11}\text{B}\{^1\text{H}\}$  NMR (128 MHz) spectra (insets show  $^1\text{H}$  coupled spectra) recorded at  $80\text{ }^\circ\text{C}$  of the reaction of AB (50 mg) and 5.2 mol% PS (18 mg) in tetraglyme (450 mg) at  $85\text{ }^\circ\text{C}$  after: (a) 1 h, (b) 3 h, and (c) 6 h.

### 3.3.6 Why Does Proton Sponge Induce H<sub>2</sub>-Release from AB?

In **Chapter 2** and elsewhere,<sup>15</sup> it was proposed that the AB activation for H<sub>2</sub>-release that is observed in ionic liquids may occur by a mechanistic pathway (**Chapter 2, Figure 2.16**) involving: (1) ionic-liquid promoted conversion of AB into its more reactive ionic DADB form ([BH<sub>2</sub>(NH<sub>3</sub>)<sub>2</sub>]BH<sub>4</sub><sup>-</sup>), (2) further intermolecular dehydrocoupling reactions between hydridic B-H hydrogens and protonic N-H hydrogens on DADB and/or AB to form neutral polyaminoborane polymers and (3) polyaminoborane dehydrogenation to unsaturated cross-linked polyborazylene materials. The initial formation of DADB has also been proposed as a key step in thermally-induced AB H<sub>2</sub>-release reactions in the solid state and in organic solvents.<sup>23,26</sup> While a DADB pathway may contribute to the H<sub>2</sub>-release observed in the bmimCl/PS solutions, the observed rate enhancements and DSC properties of the Proton Sponge reactions suggest that there is also another mechanistic pathway for H<sub>2</sub>-release in these systems.



Proton Sponge is a strong base and because of its low nucleophilicity is frequently used as a deprotonating agent in organic and inorganic syntheses that can eliminate the undesirable side reactions often found with more coordinating bases.<sup>9</sup> Shown in **Equation 3.6**, PS gains its low nucleophilicity from the hindered lone pairs that are partially protected by a methyl group from the other nitrogen. A contributing factor to

the high basicity found in PS is the naphthalene backbone strain. Free PS has a strained naphthalene backbone due to the lone pair/lone pair repulsion and methyl group steric strain. The protonated form is less strained because the lone pairs swing into the naphthalene plane to bond making the PSH<sup>+</sup> more stable than would be expected without the strain relief.<sup>27</sup> The observation of a <sup>11</sup>B NMR signal near -21.0 ppm and a <sup>1</sup>H NMR signal at ~18.9 ppm, characteristic of AB deprotonation to form the H<sub>3</sub>BNH<sub>2</sub><sup>-</sup>PSH<sup>+</sup> ion, at the beginning stages of the reactions of AB with PS, strongly supports a PS-promoted AB H<sub>2</sub>-release reaction pathway.

Deprotonation of AB by bases is well-known. For example, the H<sub>3</sub>BNH<sub>2</sub><sup>-</sup>Li<sup>+</sup> salt has previously been prepared *in situ* from AB and n-BuLi at 0 °C.<sup>19</sup> More recently, ball milling<sup>20,22,28</sup> and solution<sup>29,30</sup> reactions of AB with metal hydrides have been used to generate H<sub>3</sub>BNH<sub>2</sub><sup>-</sup>M<sup>+</sup> (M = Li and Na) and (H<sub>3</sub>BNH<sub>2</sub><sup>-</sup>)<sub>2</sub>Ca<sup>2+</sup>. Work<sup>1</sup> by Chang Yoon in our lab showed that AB deprotonation could also be easily achieved by its reaction with either lithium or potassium triethylborohydride (**Equation 3.7**), but that in these cases, a Et<sub>3</sub>B-stabilized anion was formed, with the observed resonances in the <sup>11</sup>B NMR spectra of the Li<sup>+</sup> (-7.5 (s) and -23.8 (q) ppm) and K<sup>+</sup> (-7.8 (s) and -23.6 (q) ppm) compounds being assigned based on the DFT/GIAO calculations to the BEt<sub>3</sub><sup>-</sup> (calc -10.6) and terminal -BH<sub>3</sub> (calc -25.3) units in the anion.<sup>1</sup>



The structures of H<sub>3</sub>BNH<sub>2</sub><sup>-</sup>M<sup>+</sup> (M = Li and Na) and (H<sub>3</sub>BNH<sub>2</sub><sup>-</sup>)<sub>2</sub>Ca<sup>2+</sup> have recently been established from the analyses of their high resolution powder diffraction data,<sup>28,30</sup> and that of (H<sub>3</sub>BNH<sub>2</sub><sup>-</sup>)<sub>2</sub>Ca<sup>2+</sup>•2THF by a single-crystal X-ray determination.<sup>29</sup> The crystallographic determination of the [Et<sub>3</sub>BNH<sub>2</sub>BH<sub>3</sub>]<sup>-</sup>K<sup>+</sup>•18-crown-6 complex in

**Figure 15,**<sup>1</sup> confirmed that following AB nitrogen-deprotonation by the triethylborohydride, the Lewis-acidic triethylborane group coordinated at the nitrogen.

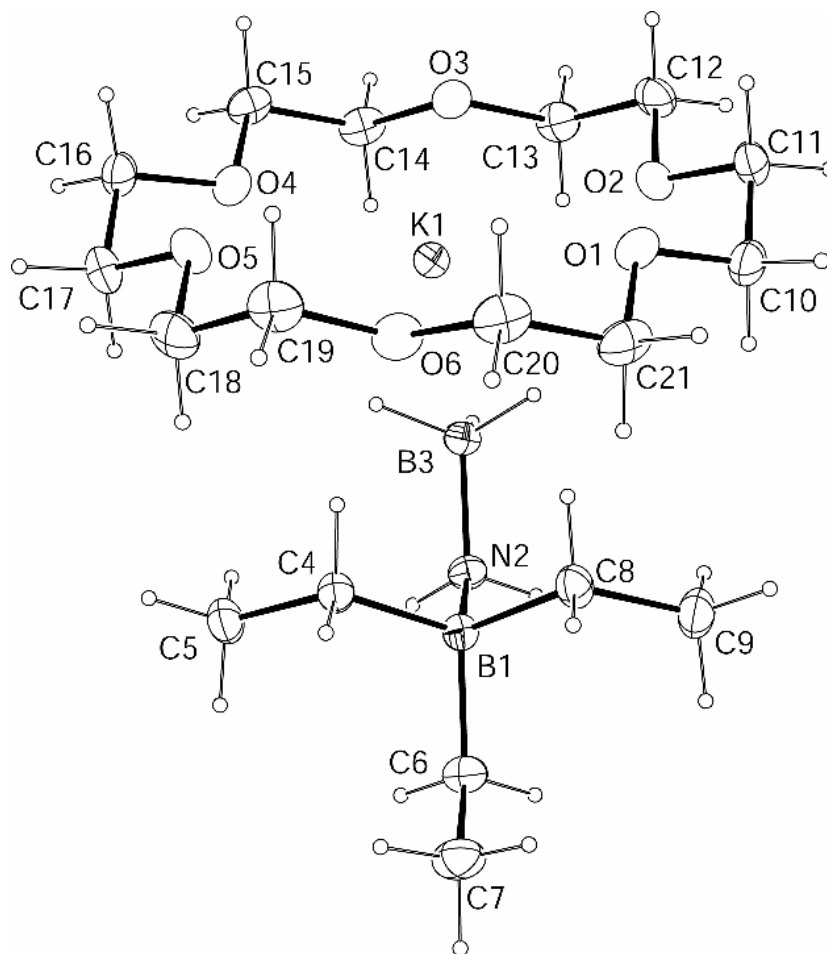


**Figure 3.15** Selected bond distances (Å) and angles (°) for [Et<sub>3</sub>BNH<sub>2</sub>BH<sub>3</sub>]<sup>-</sup>

K<sup>+</sup>•18-crown-6: B3-N2, 1.594(2); B1-N2, 1.630(2); B1-C4, 1.622(2); B1-C6 1.637(2);  
 B1-C8, 1.629(2); B3-H3a, 1.13(2); B3-H3b, 1.14(2); B3-H3c, 1.13(2); N2-H2a, 0.94(2);  
 N2-H2b, 0.91(2); K1-H3a, 2.85(2); K1-H3c, 2.76(2); B1-N2-B3, 122.05(10); N2-B1-C4,  
 108.75(11); N2-B1-C6, 105.17(10); N2-B1-C8, 108.43(11); B1-N2-H2a, 107.0(11);  
 B1-N2-H2b, 107.6(10); H2a-N2-H2b, 106(2).<sup>1</sup>

Electronic structure calculations on  $[\text{H}_2\text{NBH}_3]^- \text{M}^+$  have predicted<sup>28,30</sup> that the B-H hydrogens in these complexes will be much more negatively charged and, as a result, have a higher basicity than in AB. This increases the ability of these anions to release  $\text{H}_2$  by the intermolecular reaction of their hydridic B-H hydrogens with an N-H proton on an adjacent complex. Thus, the most likely second step in PS-promoted AB  $\text{H}_2$ -release is the intermolecular dehydrocoupling of one of the hydridic B-H hydrogens of  $[\text{H}_2\text{NBH}_3]^- \text{PSH}^+$  with a  $\text{H}_3\text{NBH}_3$  to produce, as shown in **Figure 3.16**, a growing anionic polyaminoborane polymer. DFT/GIAO calculations of model anionic polymers showed that their  $^{11}\text{B}$  NMR chemical shifts (**Figure 3.9**) would be indistinguishable from those of the corresponding neutral polyaminoborane polymers,<sup>15</sup> thus explaining the similarity of the spectra for the reactions with and without PS in **Figure 3.11**.

The expected decreased acidity of the internal  $\text{NH}_2$  hydrogens of a polyaminoborane polymer relative to those on terminal  $\text{NH}_3$  units should result in the  $\text{NH}_2$  protons being less reactive for dehydrocoupling reactions that could liberate more than one-equivalent of  $\text{H}_2$ . Thus, the increased release-rate for the second equivalent of  $\text{H}_2$  observed for the PS-induced reactions of AB may result from the greater ability of the more basic B-H hydrogens of an *anionic* polyaminoborane to induce  $\text{H}_2$ -elimination reactions with the protons at these  $\text{NH}_2$  sites.

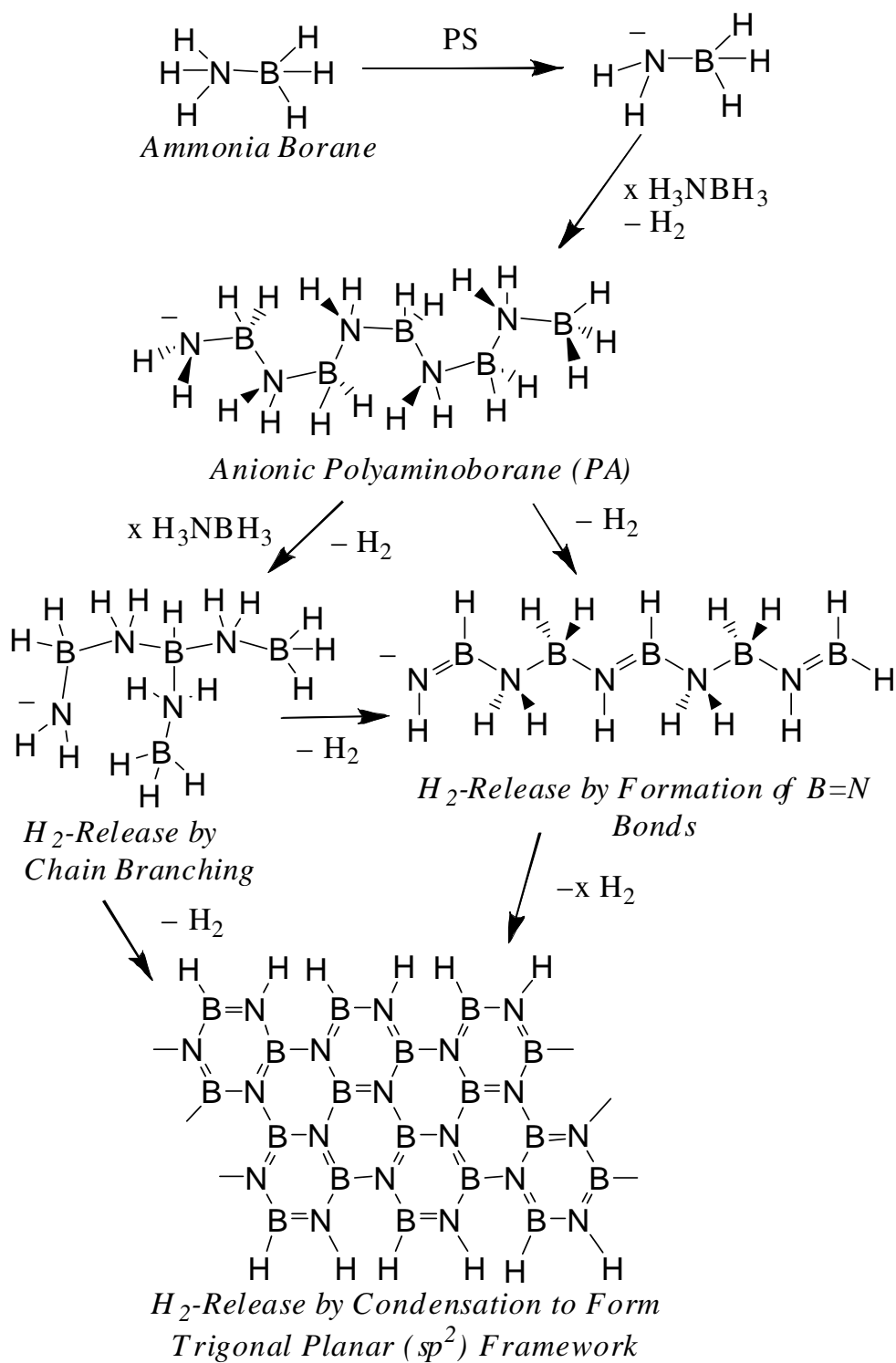


**Figure 3.16** Possible anionic polymerization pathway for PS-promoted  $\text{H}_2$ -release from AB.

Support for the proposed anionic polymerization pathway for the AB/PS reaction was obtained from the Chang Yoon studies of the reaction (**Equation 3.8**) of  $[\text{Et}_3\text{BNH}_2\text{BH}_3]^- \text{Li}^+$  with AB.<sup>1</sup> The higher Lewis acidity of the  $\text{BH}_3$  group compared to the  $\text{Et}_3\text{B}$  unit should significantly increase the nucleophilic character of the boron-hydrogens and enhance the ability of this anion to undergo dehydropolymerization with AB. In agreement with this expectation, Toepler pump measurements confirmed the loss of  $\text{H}_2$  during the reaction of equal equivalents of  $\text{NH}_3\text{BH}_3$  with  $[\text{Et}_3\text{BNH}_2\text{BH}_3]^- \text{Li}^+$  at 23 °C and an electrospray mass spectrum indicated formation of  $\text{Et}_3\text{BNH}_2\text{BH}_2\text{NH}_2\text{BH}_3^-$ . The  $^{11}\text{B}$  NMR spectra was in good agreement with the calculated  $^{11}\text{B}$  NMR shifts for the DFT optimized geometry of the chain growth product  $\text{Et}_3\text{BNH}_2\text{BH}_2\text{NH}_2\text{BH}_3^-$  given in **Figure 3.17**.



These results provide additional strong support for a PS-induced  $\text{H}_2$ -release mechanism involving an intermolecular anionic dehydropolymerization pathway initiated by the  $\text{NH}_2\text{BH}_3^-$  anion.

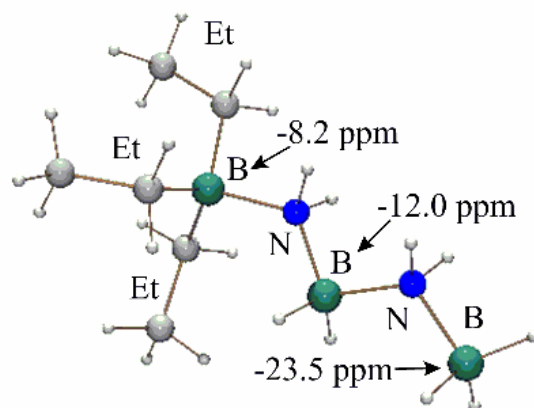


**Figure 3.17** DFT (B3LYP/6-31G(d)) optimized geometry and GIAO

(B3LYP/6-311G(d)) calculated <sup>11</sup>B NMR shifts for [Et<sub>3</sub>BNH<sub>2</sub>BH<sub>2</sub>NH<sub>2</sub>BH<sub>3</sub>]<sup>-</sup>.



### 3.4 Conclusions

In summary, the work described in this **Chapter** demonstrated base-activation by Proton Sponge of AB H<sub>2</sub>-release in solid-state and in ionic-liquid and tetraglyme solution reactions. My experimental observations and model study contributions by Chang Yoon support an anionic dehydropolymerization mechanism initiated by the H<sub>3</sub>BNH<sub>2</sub><sup>-</sup> anion. For the bmimCl/PS reactions, significantly increased rates of AB H<sub>2</sub>-release, yielding over 2 equivalents of H<sub>2</sub>, were achieved with as little as 1 mol% Proton Sponge. PS was also found to have the unanticipated effect of significantly reducing reaction foaming. These studies further demonstrate that H<sub>2</sub>-release from chemical hydrides can occur by a number of different mechanistic pathways and strongly suggest that optimal chemical-hydride based H<sub>2</sub>-release systems may require the use of synergistic dehydrogenation methods to induce H<sub>2</sub>-loss from chemically different intermediates formed during release reactions.

### 3.5 References

1. Himmelberger, D. W.; Yoon, C. W.; Bluhm, M. E.; Carroll, P. J.; Sneddon, L. G. *J. Am. Chem. Soc.* **2009**, *131*, 14101-14110.
2. Stephens, F. H.; Baker, R. T.; Matus, M. H.; Grant, D. J.; Dixon, D. A. *Angew. Chem., Int. Ed.* **2007**, *46*, 746-749.
3. Gutowska, A.; Li, L.; Shin, Y.; Wang, C. M.; Li, X. S.; Linehan, J. C.; Smith, R. S.; Kay, B. D.; Schmid, B.; Shaw, W. J.; Gutowski, M.; Autrey, T. *Angew. Chem. Int. Ed.* **2005**, *44*, 3578-3582.
4. Paolone, A.; Palumbo, O.; Rispoli, P.; Cantelli, R.; Autrey, T.; Karkamkar, A. *J. Phys. Chem. C* **2009**, *113*, 10319-10321.
5. Sepehri, S.; Feaver, A.; Shaw, W. J.; Howard, C. J.; Zhang, Q.; Autrey, T.; Cao, G. *J. Phys. Chem. B* **2007**, *111*, 14285-14289.
6. Sneddon, L. G. *2007 DOE Hydrogen Program Review*.  
[http://www.hydrogen.energy.gov/pdfs/review07/st\\_27\\_sneddon.pdf](http://www.hydrogen.energy.gov/pdfs/review07/st_27_sneddon.pdf).
7. Bluhm, M. E.; Bradley, M. G.; Sneddon, L. G. *Prepr. Symp. - Am. Chem. Soc., Div. Fuel Chem.* **2006**, *51*, 571-572.
8. Fang, Z. Z.; Wang, P.; Rufford, T. E.; Kang, X. D.; Lu, G. Q.; Cheng, H. M. *Acta Mater.* **2008**, *56*, 6257-6263.
9. Alder, R. W. *Chem. Rev.* **1989**, *89*, 1215-1223.
10. Shriver, D. F.; Drezdson, M. A., *Manipulation of Air Sensitive Compounds*. 2 ed.; Wiley: New York, 1986.

11. Zheng, F.; Rassat, S. D.; Helderandt, D. J.; Caldwell, D. D.; Aardahl, C. L.; Autrey, T.; Linehan, J. C.; Rappe, K. G. *Rev. Sci. Instrum.* **2008**, *79*, 084103-1 - 084103-5.
12. Frisch, M. J. *et al.* *Gaussian 03*, Revision B.05; Gaussian, Inc.: Pittsburgh, PA, **2003**.
13. Onak, T. P.; Shapiro, I. *J. Chem. Phys.* **1960**, *32*, 952.
14. Shore, S. G.; Parry, R. W. *J. Am. Chem. Soc.* **1958**, *80*, 20-24 and preceding papers in this issue.
15. Bluhm, M. E.; Bradley, M. G.; Butterick III, R.; Kusari, U.; Sneddon, L. G. *J. Am. Chem. Soc.* **2006**, *128*, 7748-7749 and references therein.
16. Fazen, P. J.; Beck, J. S.; Lynch, A. T.; Remsen, E. E.; Sneddon, L. G. *Chem. Mater.* **1990**, *2*, 96-97.
17. Fazen, P. J.; Remsen, E. E.; Beck, J. S.; Carroll, P. J.; McGhie, A. R.; Sneddon, L. G. *Chem. Mater.* **1995**, *7*, 1942-1956.
18. Gervais, C.; Framery, E.; Duriez, C.; Maquet, J.; Vaultier, M.; Babonneau, F. *J. Eur. Ceram. Soc.* **2005**, *25*, 129-135.
19. Myers, A. G.; Yang, B. H.; David, K. J. *Tetrahedron Lett.* **1996**, *37*, 3623-3626.
20. Kang, X.; Fang, Z.; Kong, L.; Cheng, H.; Yao, X.; Lu, G.; Wang, P. *Adv. Mater.* **2008**, *20*, 2756-2759.
21. Xiong, Z.; Chua, Y. S.; Wu, G.; Xu, W.; Chen, P.; Shaw, W.; Karkamkar, A.; Linehan, J.; Smurthwaite, T.; Autrey, T. *Chem. Comm.* **2008**, 5595-5597.

22. Xiong, Z.; Yong, C. K.; Wu, G.; Chen, P.; Shaw, W.; Karkamkar, A.; Autrey, T.; Jones, M. O.; Johnson, S. R.; Edwards, P. P.; David, W. I. F. *Nat. Mater.* **2008**, *7*, 138-141.
23. Stowe, A. C.; Shaw, W. J.; Linehan, J. C.; Schmid, B.; Autrey, T. *Phys. Chem. Chem. Phys.* **2007**, *9*, 1831-1836 and references therein.
24. Aardahl, C. L. *2008 DOE Hydrogen Program Review*.  
[http://www.hydrogen.energy.gov/pdfs/review08/st\\_5\\_aardahl.pdf](http://www.hydrogen.energy.gov/pdfs/review08/st_5_aardahl.pdf).
25. Nöth, H.; Wrackmeyer, B., In *Nuclear Magnetic Resonance Spectroscopy of Boron Compounds*, Springer-Verlag: New York, 1978; pp 188, 265, 394-395.
26. Shaw, W. J.; Linehan, J. C.; Szymczak, N. K.; Heldebrant, D. J.; Yonker, C.; Camaioni, D. M.; Baker, R. T.; Autrey, T. *Angew. Chem., Int. Ed.* **2008**, *47*, 7493-7496.
27. Alder, R. W. *Chem. Rev.* **1989**, *89*, 1215-1223.
28. Ramzan, M.; Silveary, F.; Blomqvist, A.; Scheicher, R. H.; Lebegue, S.; Ahuja, R. *Phys. Rev. B: Condens. Matter Mater. Phys.* **2009**, *79*, 132102-4.
29. Diyabalanage, H. V. K.; Shrestha, R. P.; Semelsberger, T. A.; Scott, B. L.; Bowden, M. E.; Davis, B. L.; Burrell, A. K. *Angew. Chem., Int. Ed.* **2007**, *46*, 8995-8997.
30. Wu, H.; Zhou, W.; Yildirim, T. *J. Am. Chem. Soc.* **2008**, *130*, 14834-14839.